



University
of Glasgow

Bracken, Hazel (2015) *Investigating the properties of translational arrest motifs: interactions between the nascent chain and the ribosome.*
PhD thesis.

<http://theses.gla.ac.uk/6150/>

Copyright and moral rights for this thesis are retained by the author

A copy can be downloaded for personal non-commercial research or study, without prior permission or charge

This thesis cannot be reproduced or quoted extensively from without first obtaining permission in writing from the Author

The content must not be changed in any way or sold commercially in any format or medium without the formal permission of the Author

When referring to this work, full bibliographic details including the author, title, awarding institution and date of the thesis must be given

**Investigating the properties of translational
arrest motifs; interactions between the nascent
chain and the ribosome**

Hazel Bracken

MSci

Submitted in fulfilment of the requirements
for the Degree of Doctor of Philosophy

Institute of Molecular, Cell and Systems Biology
College of Medical, Veterinary and Life Sciences

University of Glasgow

2015

Abstract

Ribosomes are responsible for the synthesis of all cellular proteins. It was initially believed that translating nascent chains would not interact with the ribosome exit tunnel, however, a small but increasing number of proteins have been identified that interact with the exit tunnel to induce translational arrest. *Escherichia coli* (*E.coli*) secretion monitor (SecM) is one such stalling peptide. SecM monitors the SecYEG translocon export activity through its own translocation to the periplasm and upregulates translation of SecA, an ATPase involved in the SecYEG translocation machinery, when translocation is reduced. How stalling peptides interact with the ribosome exit tunnel is not fully understood, however, a key feature required is an essential amino acid arrest motif at their C-terminus, and additionally some peptides, including SecM, undergo compaction of the nascent chain within the exit tunnel upon stalling.

In this study analysis of SecM peptides with both alanine and conservative mutations of key arrest motif residues were investigated. This identified three conservative mutants that can retain a degree of stalling; and this level of stalling is further increased when coupled with mutation of a non-essential arrest motif residue P153A. Further analysis of these mutants by pegylation assays indicates that this increase in stalling ability is due to the ability of the P153A mutation to reintroduce compaction of the nascent chain within the exit tunnel, possibly due to the improved flexibility of the nascent chain provided by the removal of the restrictive proline residue. These methods highlight the significance of the interactions between the nascent chain and the exit tunnel, which contribute to translation arrest.

This study also examines the ability of stalling peptides to undergo translation arrest in ribosomes of alternative domains, investigating in particular the ability of *E.coli* SecM and TnaC and fungal *Neurospora crassa* (*N.crassa*) AAP to arrest in eukaryotic Wheat Germ and prokaryotic *E.coli* ribosomes. This study concludes that stalling peptides only induce translation arrest in ribosomes of the same domain. In addition, it also revealed the ability of inducible stalling peptides to undergo translational pausing, prior to the commitment to full translation arrest, a process that does not appear to occur in intrinsic stalling peptides.

Contents

ABSTRACT	2
CONTENTS	3
LIST OF TABLES	8
LIST OF FIGURES	9
ACKNOWLEDGEMENTS	12
AUTHOR’S DECLARATION	13
DEFINITIONS/ABBREVIATIONS	14
1 INTRODUCTION	19
1.1 THE RIBOSOME	19
<i>1.1.1 General Introduction</i>	19
<i>1.1.2 Ribosome Structure</i>	19
<i>1.1.3 Ribosome Function</i>	23
1.1.3.1 Overview of translation	23
1.1.3.2 Formation of the translation initiation complex	23
1.1.3.2 Translation Elongation Cycle	25
1.1.3.3 Translation Termination	28
1.1.3.4 Differences in eukaryotic translation	30
<i>1.1.3.4.1 Eukaryotic translation initiation</i>	30
<i>1.1.3.4.2 Eukaryotic translation termination and ribosome recycling</i>	32
1.1.3.5 Translational recoding	32
1.1.4.1 Structure and properties of the ribosome exit tunnel	34
1.1.4.2 Nascent chain folding within the ribosome exit tunnel	36
1.1.4.3 Nascent chain interactions with the ribosome exit tunnel	37
1.2 TRANSLATIONAL ARREST PEPTIDES	39
<i>1.2.1 General overview of stalling peptides</i>	39
<i>1.2.2 SecM – Secretion monitor</i>	44
<i>1.2.3 TnaC</i>	47
<i>1.2.4 AAP – Arginine Attenuator Peptide</i>	52
<i>1.2.5 Comparison of SecM, TnaC and AAP interactions with the ribosome exit tunnel</i>	54
<i>1.2.6 Other translation arrest peptides</i>	54

1.2.6.1 Antibiotic-induced stalling peptides	54
1.2.6.2 Experimentally obtained stalling peptides.....	57
1.2.6.3 Mammalian uORFs encoding stalling peptides.....	59
1.2.6.4 Summary of translation arrest peptides	60
1.3 PROJECT AIMS	61
2 MATERIALS AND METHODS	62
2.1 GENERAL REAGENTS	62
2.2 GENERAL BUFFERS AND SOLUTIONS	65
2.3 ESCHERICHIA COLI STRAINS AND PLASMID VECTORS.....	68
2.3.1 <i>ESCHERICHIA COLI</i> STRAINS.....	68
2.3.2 PLASMID VECTORS.....	69
2.4 GENERAL MOLECULAR BIOLOGY METHODS.....	71
2.4.1 <i>Preparation of LB plates</i>	71
2.4.2 <i>Preparation of competent bacterial cells</i>	71
2.4.3 <i>Transformation of competent bacteria</i>	71
2.4.4 <i>Small-scale preparation of plasmid DNA (mini-prep)</i>	72
2.4.5 <i>Polymerase chain reaction</i>	72
2.4.5.1 DNA amplification by Polymerase Chain Reaction (PCR).....	72
2.4.5.2 Site-directed mutagenesis PCR.....	73
2.4.5.2.1 <i>Single point mutations</i>	73
2.4.5.2.2 <i>Multiple point mutations</i>	75
2.4.6 <i>Purification of PCR products</i>	76
2.4.7 <i>DNA agarose gel electrophoresis</i>	76
2.4.8 <i>DNA purification from agarose gels</i>	77
2.4.9 <i>Restriction endonuclease digestion</i>	77
2.4.10 <i>Ligation of DNA</i>	78
2.4.11 <i>DNA sequencing</i>	78
2.4.12 <i>In vitro transcription</i>	78
2.5 IN VITRO TRANSLATION METHODS.....	80
2.5.1 <i>S-30 bacterial cell extract preparation</i>	80
2.5.2 <i>Translation reactions</i>	80
2.5.2.1 <i>E.coli in vitro</i> transcription-translation reactions	80
2.5.2.2 Wheat Germ translation reactions	81
2.5.3 <i>CTABr precipitation assays</i>	82

2.5.3.1 <i>SecM</i> constructs.....	82
2.5.3.2 <i>AAP</i> and <i>TnaC</i> constructs.....	82
2.5.4 <i>Pegylation assays</i>	82
2.5.4.1 <i>Pegylation assay as a test for nascent chain compaction in the exit tunnel</i>	82
2.5.4.2 <i>Pegylation RNaseA assay to test for nascent chain structure formation and cysteine protection.</i>	83
2.5.5 <i>Puromycin release assays</i>	84
2.5.6 <i>Ribosome nascent chain (RNC) stability assays</i>	84
2.6 GENERAL BIOCHEMICAL METHODS AND ANALYSIS.....	85
2.6.1 <i>Gel Electrophoresis</i>	85
2.6.2 <i>Autoradiography</i>	85
2.6.3 <i>Image J analysis</i>	85
3 SEQUENCE SPECIFICITY OF THE SECM ARREST MOTIF.....	86
3.1 INTRODUCTION	86
3.2 RESULTS.....	91
3.3 CONCLUSION.....	103
4. COMPACTION OF THE SECM NASCENT CHAIN UPON TRANSLATION ARREST	108
4.1 INTRODUCTION	108
4.2 RESULTS.....	112
4.2.1 <i>Pegylation as an assay to study SecM compaction upon translation arrest</i>	112
4.2.2 <i>Pegylation of compacted and extended SecM peptides stalled on the ribosome</i>	116
4.2.3 <i>Analysis of compaction of selected single SecM mutants</i>	122
4.2.4 <i>Analysis of compaction of selected conservative SecM mutations coupled with P153A</i>	127
4.3 CONCLUSION.....	134
4.3.1 <i>Analysing SecM stalling and compaction by cysteine pegylation</i>	134
4.3.2 <i>Influence of single conservative mutations on compaction of SecM nascent chain</i>	135
4.3.3 <i>Influence of additional flexibility of the nascent chain resulting from P153A mutation on compaction of SecM mutants</i>	138
4.4.4 <i>Overall conclusions and scope for future investigations</i>	139

5. SPECIFICITY OF TRANSLATION ARREST MOTIFS IN NON-NATIVE RIBOSOMES (PROKARYOTIC VS. EUKARYOTIC).....	140
5.1 INTRODUCTION	140
5.2 RESULTS.....	148
5.2.1 <i>SecM</i>	148
5.2.2 <i>TnaC and TnaC+4</i>	149
5.2.2.1 <i>TnaC and TnaC+4 stalling in prokaryotic <i>E.coli</i> ribosomes</i>	149
5.2.2.2 <i>TnaC and TnaC+4 stalling in eukaryotic Wheat Germ ribosomes....</i>	152
5.2.3 <i>AAP and AAP+4</i>	155
5.2.3.1 <i>AAP and AAP+4 stalling in eukaryotic Wheat Germ ribosomes.....</i>	155
5.2.3.2 <i>AAP and AAP+4 stalling in prokaryotic <i>E.coli</i> ribosomes.....</i>	157
5.2.4 <i>Summary</i>	159
5.3 CONCLUSION.....	160
5.3.1 <i>Inducible translation arrest peptides can undergo translational pausing, but not arrest, in alternative ribosome systems</i>	160
5.3.2 <i>Translation arrest in alternative ribosome systems</i>	162
5.3.3 <i>Influence of additional +4 C-terminus residues</i>	164
5.3.4 <i>Overall conclusions</i>	165
6 FINAL DISCUSSION.....	166
6.1 STALLING PEPTIDE NASCENT CHAIN INTERACTIONS WITH THE RIBOSOME EXIT TUNNEL.....	166
6.2 SPECIFICITY OF TRANSLATION ARREST PEPTIDES IN NON-NATIVE RIBOSOMES	169
6.3 FUTURE DIRECTIONS.....	172
APPENDIX 1: APPLYING SECM STALLING TO GENERATE RIBOSOME-NASCENT CHAIN COMPLEXES TO STUDY THE FOLDING OF PROTEINS OF INTEREST ARRESTED ON THE RIBOSOME	175
APPENDIX 2: TABLE OF CONSTRUCTS	182
A2.1 CHAPTER 3 CONSTRUCTS.....	182
A2.2 CHAPTER 4 CONSTRUCTS.....	185
A2.3 CHAPTER 5 CONSTRUCTS.....	187
A2.4 APPENDIX 1 CONSTRUCTS.....	188
APPENDIX 3: GENERATION OF PLASMID CONSTRUCTS	189
A3.1 pTRC-SECM	189

A3.2 PGEM-SECM	189
A3.3 PTRC-SECM-AAP AND PTRC-SECM-AAP+4	189
A3.4 PGEM-SECM-AAP AND PGEM-SECM-AAP+4	189
A3.5 PTRC-SECM-TNAC AND PTRC-SECM-TNAC+4	190
A3.6 PGEM-SECM-TNAC AND PGEM-SECM-TNAC+4	190
A3.7 PTRC-B2M-SECM CONSTRUCTS	190
REFERENCES	192

List of Tables

Table 1.1	Stalling motifs of selected translational arrest peptides as determined by mutational analysis.....	40
Table 3.1	Molecular structures of the amino acid residues that were altered in the SecM mutant constructs.....	90
Table 5.1.	Comparison of the C-terminus amino acid sequences of the translational stalling peptides SecM, TnaC and AAP.....	143
Table 5.2	Summary of SecM, TnaC and AAP stalling in alternative ribosome systems.....	159
Table A2.1	SecM single alanine mutants.....	182
Table A2.2	SecM alanine mutants with P153A double mutation.....	182
Table A2.3	SecM single conservative mutants.....	183
Table A2.4	SecM conservative mutants with P153A double mutation.....	183
Table A2.5	SecM conservative mutants with P146A and P153A double and triple mutations.....	184
Table A2.6	SecM single cysteine mutants.....	185
Table A2.7	SecM cysteine mutants with Q158P mutations.....	185
Table A2.8	SecM P153A and conservative mutants with cysteine mutations.....	186
Table A2.9	SecM conservative/P153A double mutants with cysteine mutations.....	186
Table A2.10	SecM methionine mutations.....	187

List of Figures

Figure 1.1	Structural overview of the prokaryotic 70S ribosome and the path of the mRNA between the ribosome subunits.....	21
Figure 1.2	Prokaryotic translation initiation.....	24
Figure 1.3	The path of an amino acid from the cytoplasm to the ribosome.....	26
Figure 1.4	Steps of translation elongation	27
Figure 1.5	The process of translocation.....	29
Figure 1.6	Overview of peptide bond formation.....	30
Figure 1.7	The mechanism of cap-dependent eukaryotic translation initiation.....	31
Figure 1.8	Structures of the 50S prokaryotic and 60S eukaryotic large ribosome subunits.....	35
Figure 1.9	Phylogenic tree highlighting the distribution of selected translation arrest peptides SecM, TnaC and MifM.....	43
Figure 1.10	Summary of SecM translation and translocation.....	45
Figure 1.11	SecM arrest upon tRNA-Gly ratcheting.....	48
Figure 1.12	Tryptophanase (<i>tna</i>) operon and SecM and TnaC peptides stalled on the ribosome.....	50
Figure 1.13	Comparison of cryo-EM data of AAP, TnaC and SecM peptides arrested within the ribosome exit tunnel.....	55
Figure 1.14	ErmBL in the ribosome exit tunnel.....	58
Figure 2.1	pTrc99A and pGEM-4Z plasmid maps.....	70
Figure 3.1	C-terminal 44 residues of SecM.....	87
Figure 3.2	MDFF modelling of the SecM nascent chain indicating its path through the ribosome exit tunnel.....	88
Figure 3.3	Stalling of single and double SecM alanine mutants.....	93
Figure 3.4	Summary of stalling of single and double SecM alanine mutants.....	94
Figure 3.5	Stalling of single and double SecM conservative mutants.....	96
Figure 3.6	Summary of stalling of single and double SecM alanine and conservative mutants.....	97

Figure 3.7	Stalling of selected SecM peptides in mutant ribosome exit tunnels.....	100
Figure 3.8	Stalling of double and triple SecM conservative mutants.....	101
Figure 3.9	Full summary of the stalling results of all the SecM mutants in this study.....	102
Figure 4.1	Pegylation as an assay for measuring nascent chain compaction within the ribosome exit tunnel.....	110
Figure 4.2	SecM cysteine mutants analysed by CTABr precipitation and initial test pegylation assay.....	113
Figure 4.3	RNaseA nascent chain release control.....	115
Figure 4.4	Pegylation assays of wild type SecM and SecM Q158P.....	117
Figure 4.5	Length of the nascent chain contained within the ribosome exit tunnel dependant on the level of compaction.....	119
Figure 4.6	Pegylation assays of truncated SecM constructs.....	121
Figure 4.7	Pegylation of SecM P153A and summary of extended and compacted SecM controls.....	123
Figure 4.8	Pegylation of conservative SecM F150Y mutant.....	125
Figure 4.9	Pegylation of conservative SecM I156L and G161S mutants.....	126
Figure 4.10	Analysis of pegylation and compaction of SecM F150Y and SecM F150Y/P153A mutants.....	128
Figure 4.11	Analysis of pegylation and compaction of SecM I156L and SecM I156L/P153A mutants.....	130
Figure 4.12	Analysis of pegylation and compaction of SecM G161S and SecM G161S/P153A mutants.....	131
Figure 4.13	Combined summary of translation arrest and degree of compaction for the selected conservative SecM mutants studied.....	133
Figure 5.1	Molecular structures of prokaryotic and eukaryotic large ribosomal subunits indicating the path of the exit tunnel.....	142
Figure 5.2	The generated AAP and TnaC constructs employed in this chapter.....	145
Figure 5.3	Summary of puromycin release assay.....	147

Figure 5.4	Stalling of <i>E.coli</i> SecM in prokaryotic <i>E.coli</i> and eukaryotic Wheat Germ translation systems.....	148
Figure 5.5	Stalling of SecM-TnaC and SecM-TnaC+4 in a prokaryotic <i>E.coli</i> translation system.....	150
Figure 5.6	Stalling of SecM-TnaC and SecM-TnaC+4 in an <i>E.coli</i> translation system with RNaseA incubation.....	151
Figure 5.7	Stalling of SecM-TnaC and SecM-TnaC+4 in eukaryotic Wheat Germ cell-free translation system with RNaseA incubation.....	153
Figure 5.8	SecM-TnaC stalling in prokaryotic <i>E.coli</i> and eukaryotic Wheat Germ translation system detected by Puromycin release assay.....	154
Figure 5.9	AAP stalling in eukaryotic Wheat Germ and prokaryotic <i>E.coli</i> translation systems.....	156
Figure 5.10	Stalling of SecM-AAP and SecM-AAP D12N in prokaryotic <i>E.coli</i> translation system detected by puromycin release assay.....	158
Figure 5.11	Comparison of tRNA positions within the PTC of prokaryotic and eukaryotic ribosomes.....	163
Figure 6.1	Representation of translational pausing.....	170
Figure A1.1	Structure of B2M and B2M-SecM constructs.....	176
Figure A1.2	B2M-SecM test translations.....	177
Figure A1.3	B2M-SecM stability time course with sucrose cushion assay.....	179
Figure A1.4	B2M-SecM stability time course with CTABr precipitation assay.....	180

Acknowledgements

Firstly I would like to thank my supervisor Dr. Cheryl Woolhead, her knowledge and input into this project has been invaluable to me. I would also like to thank the BBSRC for funding my PhD studentship.

A big thank you to all the members of the Woolhead lab both past and present, including Dr. Philip Robinson, Jon Cherry and Jane Findlay. Additionally, the members of the other groups in Lab 241 and Lab 310, especially Dr. Phoebe Sharp, your help, support and laughs along the way have kept me going.

I have always said I could never have made it through my PhD without the stress relief of taekwondo, so a huge thank you to my instructor Scott McMillan and also my fellow students, especially anyone I have ever kicked in the face and vice versa, best therapy ever.

To all my friends, thank you for always making me smile, having you guys there to turn to for support and a general moan about life means the world to me. Finally I would like to wish a huge thank you to my family who have supported me throughout my PhD, I honestly could not have done this without you.

Author's Declaration

I declare that the work presented in this thesis has been carried out by myself, unless otherwise stated. It is entirely of my own composition and has not been submitted, in whole or in part, for any other degree.

Hazel Bracken

February 2015

Definitions/Abbreviations

~	Approximately
°C	Degrees Celsius
Å	Angstroms
α -helix	Alpha Helix
AAP	Arginine Attenuator Peptide
AdoMetDC	S-Adenosyl-Methionine Decarboxylase
Ala	Alanine
APS	Ammonium Persulphate
Arg	Arginine
Asn	Asparagine
Asp	Aspartic Acid
ATP	Adenosine 5'-triphosphate
β -sheet	Beta Sheet
B2M	Beta-2 Microglobulin
bp	Base Pair
BSA	Bovine Serum Albumin
<i>B.subtilis</i>	<i>Bacillus subtilis</i>
CaCl ₂	Calcium Chloride
cAMP	Adenosine 3', 5'-cyclic Monophosphate
Ci	Curie
cryo-EM	Cryo-Electron Microscopy
CTABr	Cetyltrimethylammonium Bromide
Cys	Cysteine
Da	Dalton
ddH ₂ O	Double Distilled Water

DNA	Deoxyribonucleic Acid
dNTP	Deoxyribonucleotide Triphosphate
DTT	Dithiothreitol
<i>E. coli</i>	<i>Escherichia coli</i>
EDTA	Ethylenediaminetetracetic Acid
EF	Elongation Factor
ER	Endoplasmic Reticulum
FRET	Fluorescence Resonance Energy Transfer
g	Gram
Gly	Glycine
GTP	Guanosine-5'-Triphosphate
GDP	Guanosine Diphosphate
HCl	Hydrochloric Acid
hCMV	human cytomegalovirus
HEPES	2-[4-(2-Hydroxyethyl)-1-Piperazine] Ethanesulphonic Acid
IF	Initiation Factor
Ile	Isoleucine
IPTG	Isopropyl- β -D-thiogalactopyranoside
k	Kilo
kb	Kilo Base Pair
KCl	Potassium Chloride
kDa	Kilo Dalton
KGlu	Potassium Glutamate
KH ₂ PO ₄	Potassium Dihydrogen Orthophosphate
K ₂ HPO ₄	di-Potassium Hydrogen Phosphate
KOAc	Potassium Acetate
KOH	Potassium Hydroxide

L	Litre
LB	Lysogeny Broth
Lys	Lysine
μ	Micro
m	Milli
M	Molar
MDFF	Molecular-Dynamics Flexible Fitting
Met	Methionine
MgCl ₂	Magnesium Chloride
MgOAc	Magnesium Acetate
MgSO ₄	Magnesium Sulphate
mRNA	Messenger RNA
<i>M.succiniciproducens</i>	<i>Mannheimia succiniciproducens</i>
MW	Molecular Weight
MWCO	Molecular Weight Cut-off
n	Nano
NaCl	Sodium Chloride
Na ₂ HPO ₄	Disodium Hydrogen Orthophosphate
NaOAc	Sodium Acetate
<i>N.crassa</i>	<i>Neurospora crassa</i>
NH ₄ OAc	Ammonium Acetate
NMR	Nuclear Magnetic Resonance
OD	Optical Density
ORF	Open Reading Frame
p	Pico
PCR	Polymerase Chain Reaction
PEG-mal	Methoxypolyethylene Glycol Maleimide

Phe	Phenylalanine
PIC	Pre-Initiation Complex
PMSF	Phenylmethanesulphonyl Fluoride
Pro	Proline
psi	Pounds Per Square Inch
PTC	Peptidyl Transferase Centre
<i>P.vulgaris</i>	<i>Proteus vulgaris</i>
RNA	Ribonucleic Acid
RNaseA	Ribonuclease A
RNC	Ribosome-Nascent Chain
rNTP	Ribonucleotide Triphosphate
rpm	Rotations Per Minute
RF	Release Factor
RRF	Ribosome Recycling Factor
rRNA	Ribosomal RNA
s	Seconds
SD	Shine-Dalgarno
SDS	Sodium Dodecyl Sulphate
SDS-PAGE	Sodium Dodecyl Sulphate Polyacrylamide Gel Electrophoresis
SecM	Secretion Monitor
Ser	Serine
SOB	Super Optimal Broth
TAE	Tris Acetate EDTA
TCA	Trichloroacetic acid
TEMED	N,N,N',N'-Tetramethylethylenediamine
tmRNA	Transfer-messenger RNA
Tna	Tryptophanase

Tris	Tris(hydroxymethyl)aminoethane
tRNA	Transfer RNA
Trp	Tryptophan
Tyr	Tyrosine
uORF	Upstream Open Reading Frame
UTR	Untranslated Region
UV	Ultraviolet
Val	Valine
v/v	Volume to Volume ratio
WT	Wild Type
w/v	Weight to Volume Ratio

1 Introduction

1.1 The ribosome

1.1.1 General Introduction

The ribosome is the cellular machinery that synthesises proteins from the substrate amino acids and is the most complex ribozyme in the cell, composed of both protein and RNA it is the RNA moieties that are responsible for the catalytic activity. Genomic DNA is transcribed to messenger RNA (mRNA) by RNA polymerase, which is then in turn translated to the peptide sequence by the ribosome. The ribosome is responsible for a 2×10^7 -fold rate of enhancement in peptide bond formation, which is achieved through enabling the optimum positioning of substrates, (Sievers et al., 2004). It was initially believed that ribosomes were non-discriminating against the proteins they synthesised, in order to allow them to process such a huge number of different peptides. However, this is not the case and there is a small but increasing number of peptides that have been found to interact with the ribosome and stall their own translation. Ribosome stalling can have multiple functions including: to disrupt the secondary structure of the bound mRNA, thereby exposing downstream Shine-Dalgarno sequences; regulating transcription/translation of downstream genes; or enabling secondary functions such as *cis*-chaperoning.

1.1.2 Ribosome Structure

The ribosome consists of two separate subunits, the complete 70S prokaryotic ribosome has a large 50S and a small 30S subunit and has a total mass of ~2.3 MDa, whilst eukaryotic 80S ribosomes consist of 60S and 40S large and small subunits respectively, and can have a molecular weight up to 4.3 MDa (Melnikov et al., 2012). In bacteria the large ribosomal subunit is composed of 2 ribosomal RNAs (rRNA) (23S and 5S) and ~31 proteins, whilst the small ribosomal subunit is composed of one rRNA (16S) and ~21 proteins. In comparison, in eukaryotes the ribosome consists of 80 ribosomal proteins (79 in yeast) and four rRNA chains (28S, 5.8S, and 5S in the large subunit and 18S in the small subunit). These large and small subunits exist separately in the cytoplasm until they are brought together by initiation factors (IFs) to synthesise protein. X-ray crystallographic studies identified that the catalytic peptidyl transferase centre (PTC) was composed solely

of rRNA, with the nearest protein moiety at least 18 Å away (Nissen et al., 2000). This confirmed earlier suggestions that the ribosome functioned as a ribozyme (Noller et al., 1992). The detailed mechanism of peptide bond synthesis within the PTC will be explained in the following section, 1.1.3.

There are 3 transfer RNA (tRNA) binding sites at the interface between the large and small subunits at the PTC: the A (aminoacyl), P (peptidyl) and E (exit) sites, which are highlighted in Figure 1.1A and B (Ramakrishnan, 2002). The A site is responsible for accepting the incoming aminoacylated tRNA molecule carrying the next amino acid to be added to the peptide being synthesised; whilst the P site accommodates the tRNA molecule carrying the growing polypeptide chain; and the E site contains the deacylated tRNA molecule that has dissociated from the peptide chain prior to being ejected from the ribosome. During the translation process, mRNA enters from the side of the 30S subunit close to ribosomal proteins S11 and S7 and moves stepwise, one codon at a time, through the ribosome between the large and small subunits, see Figure 1.1C (Yusupova et al., 2001). The small subunit binds mRNA and the tRNA anticodon stem-loops, and is responsible for maintaining the accuracy of the translation process during mRNA codon and tRNA anti-codon base pairing. The large subunit contains the PTC and its role is to bind the acceptor arms of the tRNA molecules and catalyse the peptide bond formation between the incoming A site amino acid and P site peptide chain. As will be discussed further in later sections, the ribosome also relies on additional protein factors such as GTPases that are activated to promote translation.

Despite the differences in mass, the prokaryotic and eukaryotic ribosomes share an evolutionarily conserved core structure consisting of 34 conserved proteins (15 in the small and 19 in the large subunit) and ~4,400 RNA nucleotides (Lecompte et al., 2002; Melnikov et al., 2012). These conserved regions contain the main active sites of the ribosome including the decoding site, PTC and tRNA binding sites (Spahn et al., 2001). Outwith this conserved core, the ribosomes contain insertions and extensions to the core protein and rRNA segments, as well as additional domain-specific proteins. For instance the 70S prokaryotic ribosome contains 20 bacteria-specific proteins (6 in the 30S subunit and 14 in the 50S subunit), whilst the eukaryotic ribosome contains 46 proteins that have no bacterial homologs (18 in the 40S subunit and 28 in the 60S subunit) (Melnikov et al., 2012). The majority of these protein and rRNA extensions are located on the solvent-exposed surface

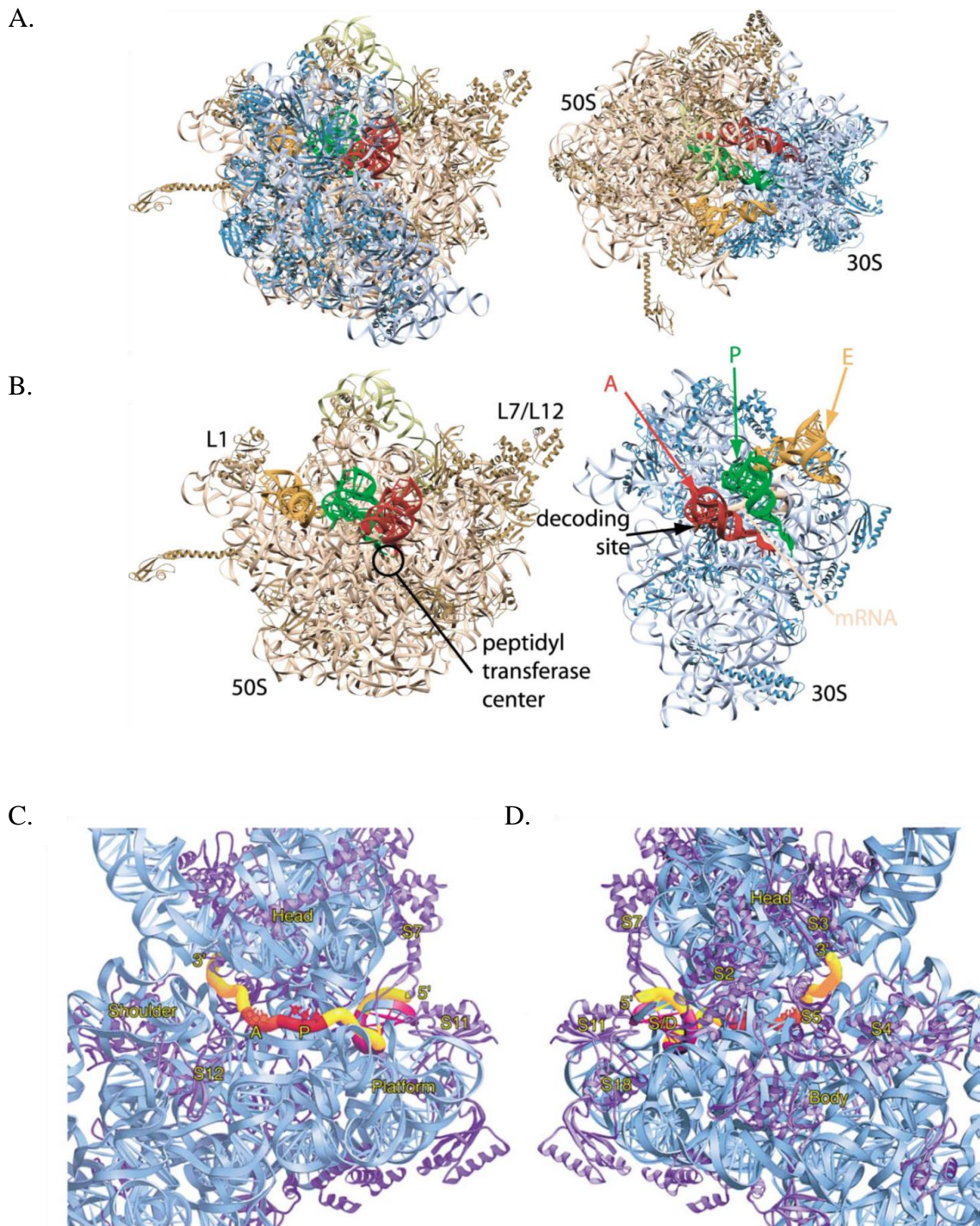


Figure 1.1 Structural overview of the prokaryotic 70S ribosome and the path of the mRNA between the ribosome subunits. A. An x-ray crystallographic structure of the complete 70S ribosome and B. Separated 50S and 30S subunits. The 50S subunit is illustrated in white and 30S in blue, with the A, P and E sites indicated in red, green and yellow respectively. Structure reproduced from Ramakrishnan (2002). C. The path of the mRNA through the 30S ribosomal subunit viewed from the subunit interface and D. from the solvent aspect. The mRNA enters at the back of the platform close to ribosomal proteins S11 and S7 and exits between the head and the shoulder regions of the ribosome. The A and P site codons are indicated in orange and red respectively and the ribosomal proteins are indicated in purple and 16S rRNA in light blue. Structure reproduced from Yusupova et al., (2001).

of the ribosome enabling them to be accessible to interacting partners such as translation factors and chaperones (Ben-Shem et al., 2011). The differences in complexity of prokaryotic and eukaryotic ribosomes are reflected in their assembly, with bacterial ribosome biogenesis requires relatively few non-ribosomal factors (Shajani et al., 2011), whilst eukaryotic ribosomes require the assistance of approximately 200 maturation factors (Panse and Johnson, 2010). In addition eukaryotic ribosome assembly is also compartmentalised, initially in the nucleolus before the pre-ribosomes are exported to the nucleoplasm and then finally to the cytoplasm upon final maturation (Panse and Johnson, 2010). Whilst sharing a conserved core there can also be variations in the composition of ribosomes within prokaryotes and eukaryotes, and also to a smaller degree within the same species under different growth and stress conditions. These differences occur through alterations in the length and sequence of, predominantly, the rRNA components of the ribosome, although sometimes it may be due to an additional, or one fewer, ribosomal proteins. The mass of eukaryotic ribosomes can vary by ~1 MDa, and this is predominantly due to insertions in eukaryotic-specific RNA expansion segments (Yusupova and Yusupov, 2014).

It should be noted that in eukaryotes, in addition to cytoplasmic ribosomes, mitochondria and chloroplasts also contain structurally distinct ribosomes. Both organelles originated from early endosymbiotic events between eubacteria and eukaryotes, with the closest relation of mitochondria being α -Proteobacteria, whilst chloroplasts are related to cyanobacteria (Gray, 1993). Through the course of evolution, mitochondrial ribosomes have become structurally diverse from both cytoplasmic and bacterial ribosomes, with the complete 55S mammalian mitochondrial ribosome composed of a large 39S subunit and the small 28S subunit. They have also evolved to synthesise only a small number of peptides with mammalian mitochondrial ribosomes responsible for synthesising only 13 membrane proteins that are involved in oxidative phosphorylation or ATP generation (Amunts et al., 2014; Greber et al., 2014; Kaushal et al., 2014). The 70S chloroplast ribosomes are similar to eubacteria, comprising a small 30S and a large 50S subunit, with few differences in rRNA and orthologs to 50 *Escherichia coli* (*E.coli*) ribosomal proteins, lacking only L25 and L30, whilst containing an additional six proteins termed Plastid-Specific Ribosomal Proteins (PSRPs) (Sharma et al., 2007). The chloroplast genome encodes approximately 120 genes, categorised into two main classes, those that encode constituents of the genetic system and those that encode systems of the photosynthetic system (Tiller and Bock, 2014).

1.1.3 Ribosome Function

1.1.3.1 Overview of translation

The primary function of the ribosome occurs at the PTC where, in comparison to substrates free in solution, the rate of peptide bond formation is enhanced by lowering the entropy of activation through the optimum positioning of substrates and/or water exclusion within the active site (Sievers et al., 2004). The PTC is well adapted for this role and can maintain efficient transfer of amino acids from A site aminoacyl tRNAs to the growing peptide chain attached to the P site peptidyl tRNA, despite the wide range in their size, structure and chemical properties. There are 3 key steps to translation: initiation, elongation and termination, which are subsequently followed by recycling of the separated components to begin a new cycle. The process of elongation is similar between prokaryotes and eukaryotes with the features of the ribosome involved in these processes such as the PTC and decoding centres highly conserved. However, the two systems differ greatly in the mechanism of initiation of translation, which involves greater complexity in eukaryotes and requires more accessory factors to proceed correctly. The following sub-sections are a description of prokaryotic translation with the differences between prokaryotic and eukaryotic translation highlighted after.

1.1.3.2 Formation of the translation initiation complex

Initiation of translation in prokaryotes requires the formation of an active initiation complex consisting of both ribosomal subunits (50S and 30S), formylated aminoacyl initiator tRNA (fMet-tRNA^{fMet}), the mRNA to be translated and the three initiation factors (IF1, IF2 and IF3) (Simonetti et al., 2008). The initiator tRNA contains formylated methionine, fMet-tRNA^{fMet}, which is produced by methionyl-tRNA transformylase (Guillon et al., 1992; Lee et al., 1991). Formylation distinguishes initiator tRNA from elongation Met-tRNAs, increasing binding to Initiation Factors and reducing affinity for Elongation Factors, and enabling the tRNA to enter directly into the ribosome P site (Seong and Rajbhandary, 1987a, b). X-ray crystallographic structures confirmed that IF1 binds to the 30S ribosomal A site, preventing tRNA binding to this site and ensuring that the initiator tRNA, fMet-tRNA^{fMet}, binds only to the P site (Carter et al., 2001). It also increases the affinity of IF2, a small GTPase, for the ribosome (Zucker and Hershey, 1986). The function of IF2·GTP is to bind fMet-tRNA^{fMet} and aid its binding to the 30S

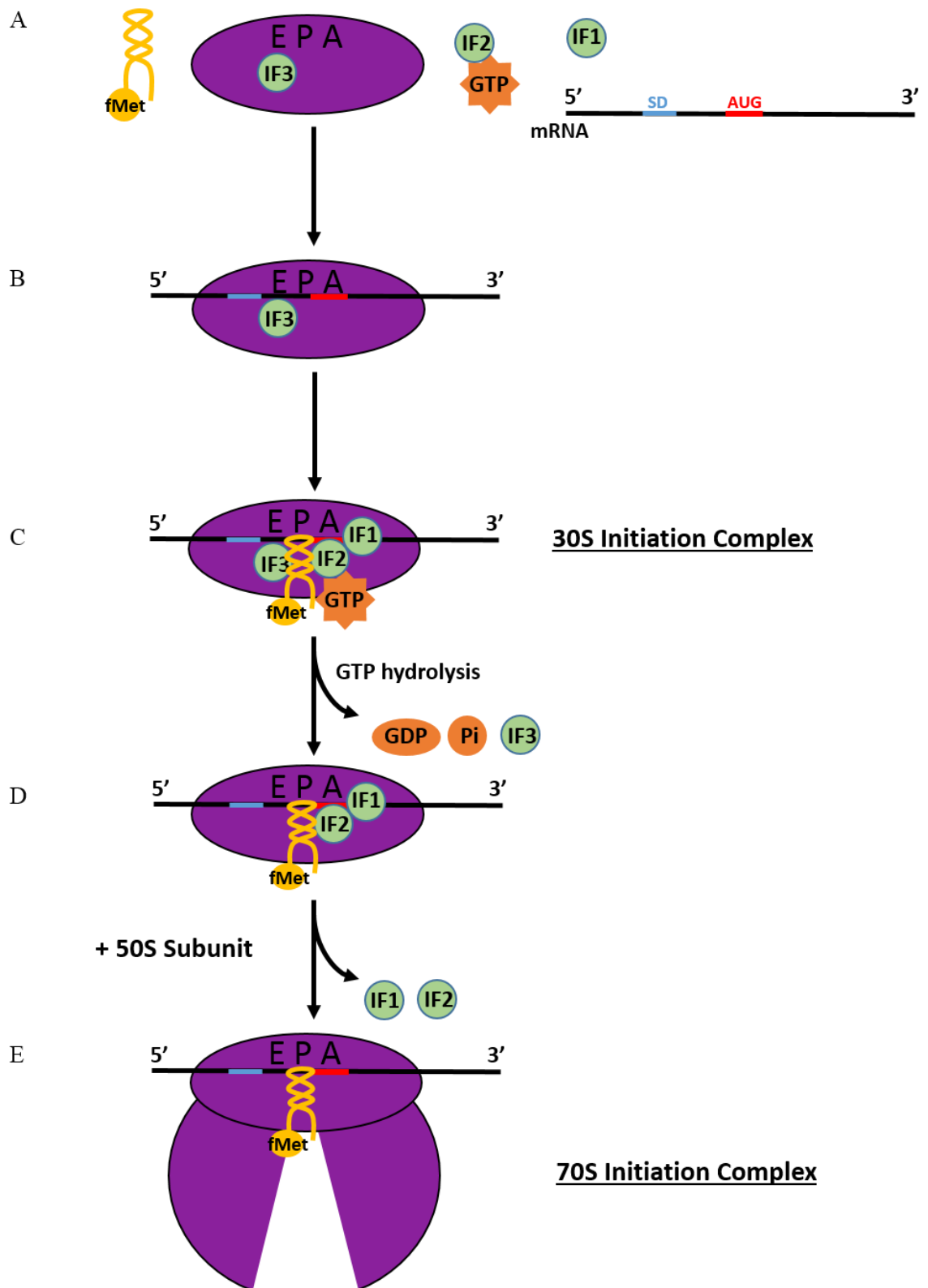


Figure 1.2 Prokaryotic translation initiation. A. Initiation Factor (IF) 3 binds to the 30S ribosomal subunit. B. The mRNA Shine-Dalgarno (SD) sequence interacts with and binds to the 30S subunit. C. This is followed by the binding of initiator fMet-tRNA^{fMet}, IF1 and IF2, constituting the 30S Initiation Complex. D. Hydrolysis of GTP by IF2 results in release of IF3 from the complex. E. Subsequent release of the remaining Initiation Factors IF1 and IF2 enables the binding of the 50S subunit. The process of protein synthesis then continues into the elongation, termination and recycling stages.

ribosomal subunit (Lockwood et al., 1971). The final initiation factor, IF3, binds to the E site of the 30S subunit (Dallas and Noller, 2001), preventing its association with the 50S subunit until after formation of the initiation complex (Subramanian and Davis, 1970). It also aids the selection of initiator tRNA, fMet-tRNA^{fMet}, through destabilising the binding of incorrect tRNAs at the ribosome P site (Hartz et al., 1990).

The initiation complex combines in a multi-step process that begins with the interaction of the 16S rRNA of the 30S ribosomal subunit, containing bound IF3 (Figure 1.2A), with the complimentary, purine-rich Shine-Dalgarno sequence of the mRNA (Figure 1.2B). The Shine-Dalgarno sequence contains up to 9 nucleotides (5'-ACCUCCUUA-3') and is located 5-9 bases upstream from the AUG initiation codon, and serves to recruit the ribosome subunits directly to the initiation site of the mRNA (Shine and Dalgarno, 1974). This is followed by binding of IF1, IF2 and initiator fMet-tRNA^{fMet} to form the 30S Initiation Complex (Figure 1.2C). IF2, a GTPase, promotes 50S subunit docking which subsequently induces GTP hydrolysis and results in the spontaneous release of IF3 (Figure 1.2D) (Antoun et al., 2006). Formation of the 70S ribosome is followed by release of IF1 and IF2, leaving fMet-tRNA^{fMet} situated in the P site in preparation for continuation into the peptide elongation cycle (Figure 1.2E) (Grigoriadou et al., 2007). As translation initiation is not restricted by the position of the AUG start site within the mRNA, prokaryotic mRNA can contain more than one open reading frame (ORF) with initiation able to occur at multiple sites within the mRNA (Laursen et al., 2005). In addition, as transcription and translation are coupled, translation is able to begin immediately upon synthesis of the 5' end of mRNA. It is also possible for multiple ribosomes to translate the same mRNA transcript creating chains of polyribosomes (polysomes).

1.1.3.2 Translation Elongation Cycle

The elongation cycle proceeds by the sequential addition of amino acids to the extending polypeptide chain. Firstly, the amino acids are paired with the correct tRNA in the cytoplasm by aminoacyl-tRNA synthetases. For each particular amino acid there is a specific aminoacyl-tRNA synthetase enzyme to catalyse their attachment to their corresponding tRNA. Aminoacylation of tRNA by aminoacyl-tRNA synthetases occurs through activation of the amino acids with ATP to generate aminoacyl-adenylates, followed by transfer of the amino acid to the relevant tRNA (Figure 1.3) (Ibba and Soll,

2000). The cell ensures the selection of the correct tRNA by subjecting aminoacyl-tRNA synthetases to kinetic proofreading, which is achieved by formation of a high energy intermediate during the aminoacylation steps (Guth and Francklyn, 2007). The high activation energy required to bind the correct tRNA and amino acid discriminates against erroneous pairings and results in an irreversible formation pathway. Following this, ternary complexes of aminoacyl tRNAs, elongation factor Tu (EF-Tu) and GTP are subsequently formed and directed to the ribosome by EF-Tu (Figure 1.4A) (Nissen et al., 1995). The sequence of the peptide is determined by complimentary base pairing between the mRNA codon situated in the A site and the anticodon of the tRNA carrying the amino acid. Once the tRNA-EF-Tu complex enters the ribosome A site (Figure 1.4B), if correct base pairing occurs, conformational changes occur within the ribosome. The ribosome is unable to pre-determine what tRNA will enter the A site and therefore correct base pairing is achieved by random sampling until the correct codon-anticodon match is achieved. This is recognised as it is kinetically more favourable and induces changes in the G domain of the EF-Tu (Rodnina et al., 1995), ultimately inducing hydrolysis of GTP by the GTPase EF-Tu (Figure 1.4C), followed by dissociation of EF-Tu-GDP enabling aminoacyl-tRNA to be accommodated in the A site (Figure 1.4D and 1.5B) (Pape et al., 1998; Rodnina et al., 1996). The interactions between the 16S rRNA and mRNA also have a role in tRNA selection and accuracy with correct tRNA binding inducing rearrangements in the 30S subunit at the conserved and essential 16S rRNA bases G530, A1492 and G530 of the 16S RNA that contact the codon-anticodon helix in the A site of the 30S subunit (Ogle et al., 2001).

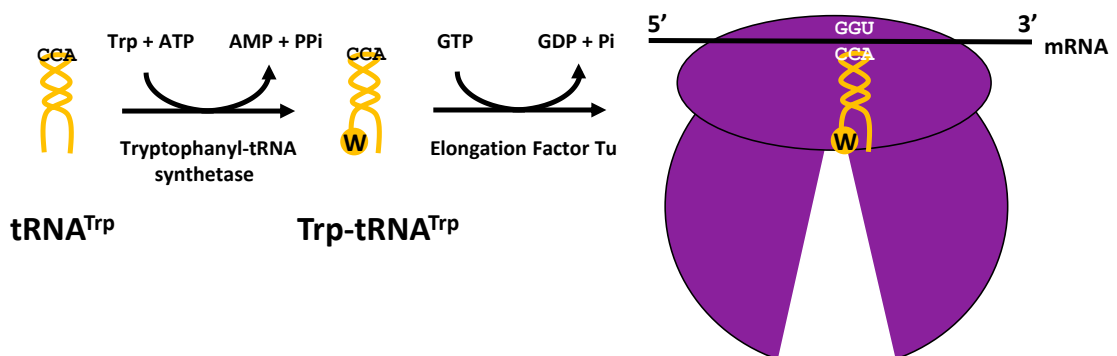


Figure 1.3 The path of an amino acid from the cytoplasm to the ribosome. The correct amino acid is attached to its corresponding tRNA by a specific aminoacyl-tRNA synthetase in an ATP dependent step. The aminoacyl-tRNA then interacts with EF-Tu and is delivered to the ribosome where the correct tRNA is selected through detection of the correct codon-anticodon pairing.

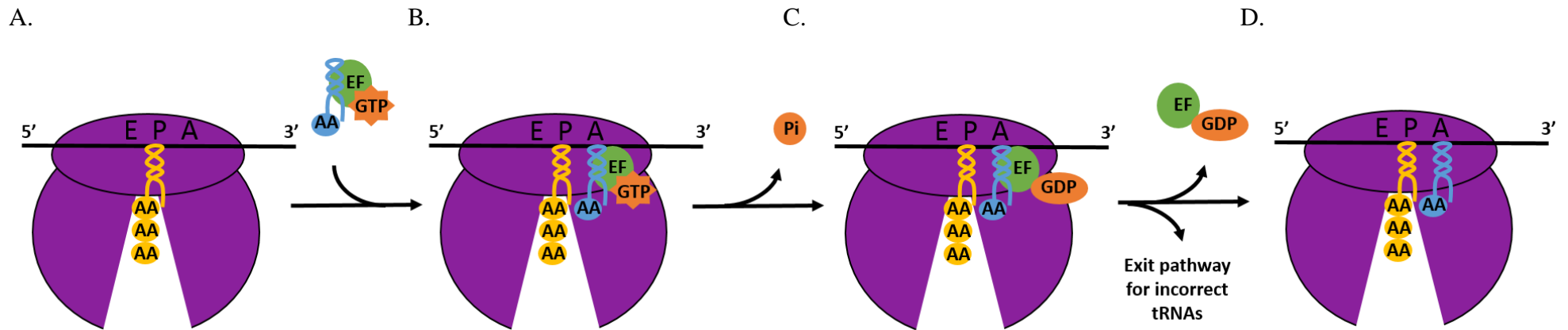


Figure 1.4 Steps of translation elongation. A. Elongating peptide resides in the ribosome exit tunnel with the associated tRNA situated in the ribosome P site. B. A complex of aminoacyl tRNA, elongation factor Tu (EF) and GTP enter the ribosome A site. C. Correct base pairing of the A site tRNA with the mRNA results in hydrolysis of GTP by EF-Tu. This is followed by dissociation of EF-Tu-GDP and accommodation of the aminoacyl-tRNA in the A site in preparation for peptide bond synthesis. D. Exit pathway for incorrect tRNAs.

Catalysis of peptide bond formation then occurs at the peptidyl transferase centre and involves the nucleophilic attack of the α -amino group of the aminoacyl-tRNA that is situated in the A site, on the peptidyl-tRNA located in the P site (Figure 1.5C and 1.6) (Beringer et al., 2005; Weinger et al., 2004). This creates a ribosome in the pre-translocational state whereby the peptide chain is transferred to the A site tRNA thus resulting in a deacylated tRNA in the P site (Figure 1.5D). The process of translocation involves the movement of tRNA molecules through the ribosome, concurrent with a shift in the mRNA reading frame of 3 nucleotides, exposing the next mRNA codon (Frank et al., 2007). This translocation is promoted through the ratcheting movement of the small and large subunits, during which the subunits move $\sim 6^\circ$ relative to each other (Agirrezabala et al., 2008; Frank and Agrawal, 2000; Julian et al., 2008). Single-molecule FRET experiments have demonstrated that this is a spontaneous rotational movement that fluctuates between the unratcheted and ratcheted states until binding of EF-G and movement of the deacylated P site tRNA into the 50S E site stabilises the rotated state (Blanchard et al., 2004; Cornish et al., 2008). Elongation factor G (EF-G), a GTPase, binds to the peptidyl-tRNA in the A site and facilitates its translocation to the P site whilst deacylated P site tRNA is translocated to the E site prior to its ejection from the ribosome (Figure 1.5E & F) (Moazed and Noller, 1989; Wilson and Noller, 1998). The movement of the tRNAs into the hybrid states are sequential, with the P/E tRNA hybrid first followed by the A/P switch (Munro et al., 2007; Pan et al., 2007). Following translocation the one amino acid residue extended peptidyl-tRNA is situated in the ribosome P site ready to repeat the elongation process until synthesis of the peptide is complete, at which point translation termination is undertaken as explained in the following section.

1.1.3.3 Translation Termination

The elongation process is repeated until an mRNA stop codon (UAA, UAG or UGA) enters the ribosome A site. This stop codon is recognised by Class I release factors, RF1 and RF2, which cleave the nascent polypeptide from the P site tRNA by hydrolysis of the ester bond as there is no amino acid to transfer to, thereby releasing the peptide from the ribosome. Both RF1 and RF2 recognise the UAA stop codon whilst UAG is only recognised by RF1 and UGA is recognised by only RF2 (Scolnick et al., 1968). RF3, a class II release factor is a GTPase and binds to RF1/2 on the ribosome and promotes their rapid dissociation (Freistroffer et al., 1997). Interaction of RF3 with RF1 or RF2 results in

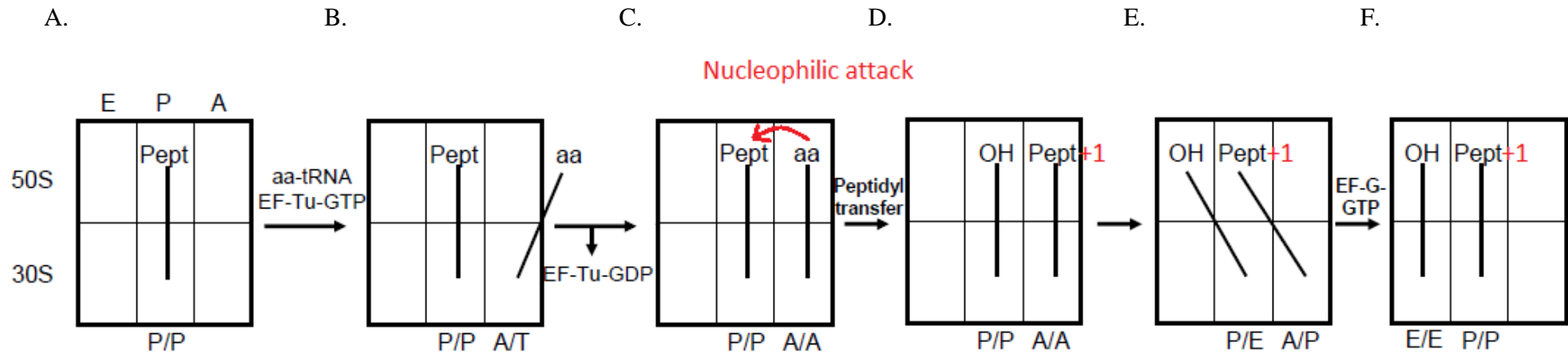


Figure 1.5 The process of translocation. A. Peptidyl-tRNA is situated in the P site; B. In complex with EF-Tu-GTP, aminoacyl-tRNA enters the A site and, in the event of correct base pairing, hydrolysis of GTP occurs and EF-Tu-GDP dissociates; C. The peptidyl-tRNA undergoes nucleophilic attack from the α -amino group of the aminoacyl-tRNA; D. The ribosome is in the pre-translocational state with peptidyl-tRNA in the A site and a deacylated tRNA in the P site; E. Upon subunit ratcheting the 3' end of the peptidyl-tRNA in the A site and the deacylated tRNA in the P site that are in contact with the 50S subunit spontaneously move to the P site and E site respectively, forming a hybrid state; F. Translocation is completed by the binding of EF-G-GTP which binds to the peptidyl-tRNA in the A site and facilitates its translocation to the P site, whilst deacylated P site tRNA is translocated to the E site prior to its ejection from the ribosome.

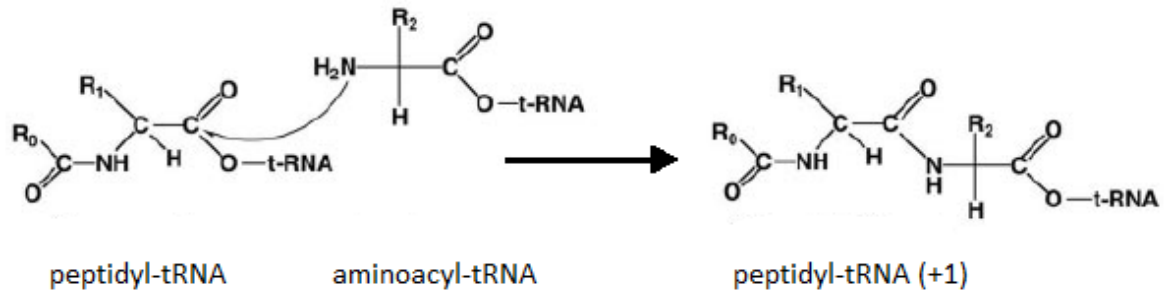


Figure 1.6 Overview of peptide bond formation. Nucleophilic attack of the peptidyl-tRNA in the P site by the α -amino group of the aminoacyl-tRNA in the A site results in peptide bond synthesis and extension of the peptide chain by one amino acid.

a rapid exchange of GDP for GTP, which is then subsequently hydrolysed to promote dissociation of RF3 (Zavialov et al., 2001). The ribosome is recycled for another round of translation in a GTP dependant step by the binding of ribosomal recycling factor (RRF) and EF-G, resulting in dissociation of the ribosome into separate 30S and 50S subunits. The bound mRNA and tRNA are released and the separate subunits bind initiation factor IF3 to prevent immediate and premature re-assembly (Peske et al., 2005; Zavialov et al., 2005).

1.1.3.4 Differences in eukaryotic translation

1.1.3.4.1 Eukaryotic translation initiation

As stated previously, the process of translation initiation is more complex in eukaryotes, with the following section briefly covering these differences. In prokaryotes, translation initiation requires only 3 initiation factors (IF1, IF2 and IF3) and it is the recognition of the Shine-Dalgarno sequence of the mRNA by the anti-Shine-Dalgarno sequence of the 16S rRNA that positions the start site codon at the ribosome P site. In eukaryotes this process requires at least 10 initiation factors, some of which are multi-subunit protein complexes (Jackson et al., 2010). Unlike the prokaryotic fMet-tRNA^{fMet}, the initiator tRNA (Met-tRNA_i) in the cytoplasm of eukaryotes is not formylated, instead, post-transcriptional modifications distinguish it from elongation Met-tRNA (Sonnenberg and Hinnebusch, 2009). Formylation of initiator Met-tRNA does, however, still occur in eukaryotic chloroplasts and mitochondria, which as stated previously evolved as a result of endosymbiosis with bacterium (Guillemaut and Weil, 1975; Smith and Marcker, 1968).

Unlike prokaryotes where the ribosome-initiation complex can bind at any point on the mRNA where the Shine-Dalgarno sequence is located at the start codon, eukaryotes locate the translation start site by scanning from the end of the mRNA in a 5' to 3' direction. Eukaryotic mRNAs undergo post-transcriptional modifications resulting in the addition of a 5' cap, consisting of a modified GTP (m7G) (Shatkin, 1976), and a 3' poly-A tail containing 150 or more adenine nucleotides (Sheets and Wickens, 1989). The poly-A tail functions to stabilise the mRNA and interact with the 5' end of the same mRNA, binding via eIF-4G, which binds both Poly-A Binding Protein (PABP) and eIF-4E, resulting in a closed-loop structure of the mRNA (Gallie, 1991; Wells et al., 1998) (Figure 1.7). The 5' cap is recognised by the small (40S) ribosomal subunit and assists in the formation of the pre-initiation complex (PIC) with eukaryotic initiation factors (eIFs) and Met-tRNA_i (Pestova and Kolupaeva, 2002). The eukaryotic pre-initiation complex begins scanning from the 5' untranslated region (5'UTR) of the mRNA until it reaches an AUG start codon located within a Kozak sequence, the consensus sequence of which is GCC(A/G)CCAUGG (Kozak, 1986, 1987). The start codon is identified by base pairing with the anti-codon of Met-tRNA_i (Cigan et al., 1988), and its recognition results in displacement of the Initiation Factors by the joining of the 60S subunit and the progression of translation initiation (Pestova et al., 2000).

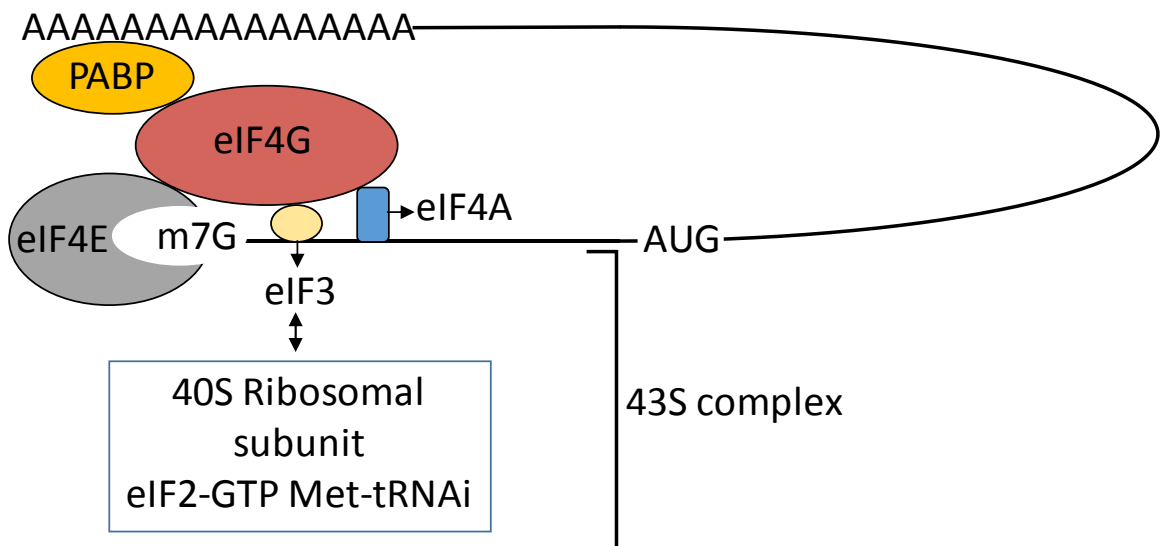


Figure 1.7 The mechanism of cap-dependent eukaryotic translation initiation. Eukaryotic mRNA exists in a closed-loop conformation due to the interactions of the 5' cap with the 3' poly-A tail via eIF4G binding to PABP and eIF4E. The 40S ribosome subunit is recruited via eIF3 interactions.

1.1.3.4.2 *Eukaryotic translation termination and ribosome recycling*

Eukaryotic translation termination also occurs in response to recognition of an mRNA stop codon (UAA, UAG or UGA) in the ribosome A site and requires two release factors, eRF1 and eRF3 (Zhouravleva et al., 1995). The Release Factors bind to the ribosome A site in a complex as eRF1/eRF3/GTP, with eRF1 responsible for recognition of the stop codon in the ribosome A site. Unlike prokaryotes that also contain RF2, in eukaryotes eRF1 is responsible for recognising all three potential stop codons. eRF3 is a GTPase and, after binding to the A site, causes hydrolysis of GTP, which in turn results in hydrolysis of the peptidyl-tRNA by eRF1 and release of the peptide chain from the ribosome (Alkalaeva et al., 2006). Ribosome recycling follows and is mediated by ABCE1, an ATPase and a member of the ATP-binding cassette (ABC) family of proteins, which dissociates the 60S subunit from the mRNA/tRNA/40S complex (Pisarev et al., 2010). Subsequent mRNA and tRNA release is mediated by initiation factors eIF3, eIF1, eIF1A and eIF3j, a loosely associated subunit of eIF3 (Pisarev et al., 2007).

1.1.3.5 **Translational recoding**

There are circumstances where exceptions can occur during the normal cycle of translation elongation and the ribosome can undergo programmed translational recoding caused by a ribosomal frameshift (Gesteland et al., 1992). Whilst the AUG start site determines the translational reading frame there are situations where this reading frame can be shifted by one base, either in the 5' (-1) or 3' (+1) direction, or in some circumstances, at translational hop sites, the ribosome may skip larger sections of nucleotides before continuing back into translation (Belew et al., 2014; Herbst et al., 1994; Plant et al., 2003). Although present in all domains of life, frameshifting is a method highly utilised by viruses to increase the coding capacity of their genomes (Miller et al., 1997). These occurrences require a translational pause during elongation in order to occur and are generally mRNA mediated, however, some are mediated by the peptide nascent chain.

Ribosomal frameshifting requires two key factors, a 'slippery site' on the mRNA where tRNA shift/mis-alignment is accommodated and a downstream mRNA stimulatory structure that functions to enable frameshifting to occur (Namy et al., 2004). This downstream structure may be an mRNA pseudoknot or a slowly translated region of

mRNA, the purpose of which is to provide an energetic barrier to elongation, resulting in the ribosome pausing over the slippery site and thus providing an opportunity for frameshifting to occur (Kontos et al., 2001). Examples of genes that undergo frameshifting are *prfB* in *E.coli*, which encodes Release Factor (Craigien and Caskey, 1986), and eukaryotic ornithine decarboxylase antizyme, Antizyme 1 (AZ1) (Matsufuji et al., 1995).

Translational hopping occurs when the ribosome bypasses larger regions of nucleotides before resuming translation, an example of which is gene product 60 (gp60) in bacteriophage T4. This is a single polypeptide that is encoded by a discontinuous reading frame that bypasses a 50 nucleotide non-coding region (Huang et al., 1988). The features that are necessary for gp60 translational hopping include glycine GGA codons flanking either side of the 50 nucleotide coding gap, a stop codon following the first glycine codon, mRNA stem-loop structure and a nascent peptide signal (Samatova et al., 2014; Wills et al., 2008). Translational hopping is not completely efficient as whilst nearly all ribosomes are able to disengage from the mRNA at the first glycine codon, only about 50% resume translation at the downstream open reading frame (Herr et al., 2000).

Finally, translational recoding can also take place on the same mRNA creating two different translational products within the same reading frame, an example of this is 2A peptides found in viruses. These 2A peptides undergo a 'stop-carry on' form of re-coding, whereby translation pauses at the final proline codon of the 2A peptide and recruits release factors to undergo stop codon-independent translation termination. The first peptide is released whilst translation reinitiates at the same codon, thus enabling two peptides to be produced from the same reading frame (Doronina et al., 2008; Luke et al., 2008). Numerous 2A peptides have been identified and whilst there appears to be high conservation in the C-terminus sequence there is a high degree of variability in the N-terminus, yet despite this mutagenesis studies indicate that all residues of the 2A peptide are important to stalling function (Sharma et al., 2012). These studies indicate that 2A nascent chain interactions with the ribosome are necessary to alter ribosomal conformation and promote translation termination in the absence of a stop codon (Sharma et al., 2012).

1.1.4 Ribosome Exit Tunnel

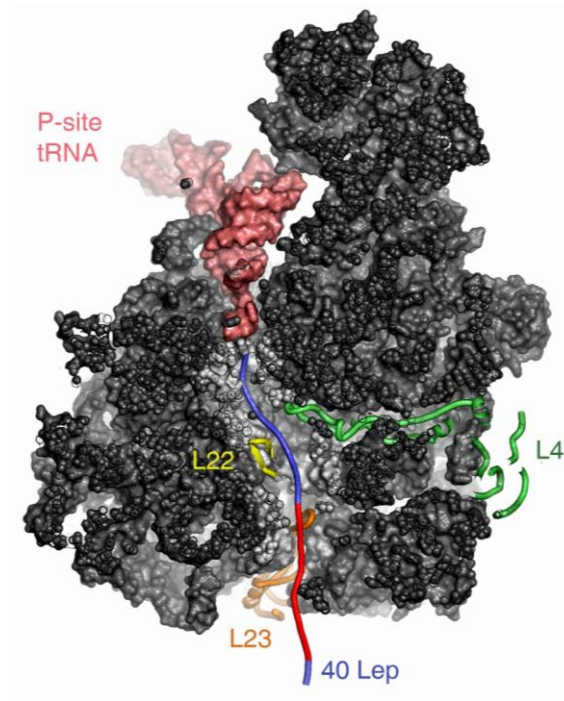
1.1.4.1 Structure and properties of the ribosome exit tunnel

During translation the growing polypeptides leave the ribosome via the exit tunnel that is ~100 Å in length and leads away from the PTC, through the large ribosomal subunit, exiting into the cytoplasm. Early evidence for the presence of the exit tunnel came from experiments that indicated 30 to 35 residues of the most recently synthesised part of the nascent chain were protected from proteolytic cleavage, indicating that these residues could still be contained within the ribosome (Malkin and Rich, 1967). Following this, the location of the exit tunnel opening at the opposite side of the large subunit from the PTC was detected by antibody binding to nascent peptides (Bernabeu and Lake, 1982). Later, visualization by cryo-Electron Microscopy (cryo-EM) confirmed the existence and location of ribosome exit tunnel (Frank et al., 1995), and more recently nascent polypeptides have even been visualized within the ribosome exit tunnel by cryo-EM (Becker et al., 2009; Bhushan et al., 2010a; Seidelt et al., 2009).

The tunnel walls are formed predominantly of hydrophilic residues of the 23S rRNA and it has an average diameter of ~20 Å. In addition, there are some protein contributions to the exit tunnel, with a constriction point 20-35 Å from the PTC formed by proteins L4 and L22 where the diameter narrows to ~10 Å. The role of the constriction site is not clear but it is speculated that it could have roles in sensing the nature of the polypeptide (Nakatogawa and Ito, 2002). Also located near to the exit tunnel opening is ribosomal protein L39e in eukaryotes, or equivalently an extension of L23 in prokaryotes (Ben-Shem et al., 2010; Harms et al., 2001; Schuwirth et al., 2005; Selmer et al., 2006), see Figure 1.8.

Overall the tunnel has an electronegative potential (Lu and Deutsch, 2008) and although there are still some hydrophobic residues lining the surface of the tunnel these are dispersed and there are no defined patches of hydrophobicity, which provides the tunnel with a relatively 'non-stick' nature (Nissen et al., 2000). Despite the initial belief of a passive role played by the ribosomal exit tunnel there is growing evidence indicating that interactions occur between the nascent chain and the ribosome exit tunnel to regulate translation of specific peptides, this will be discussed in Section 1.2.

A.



B.

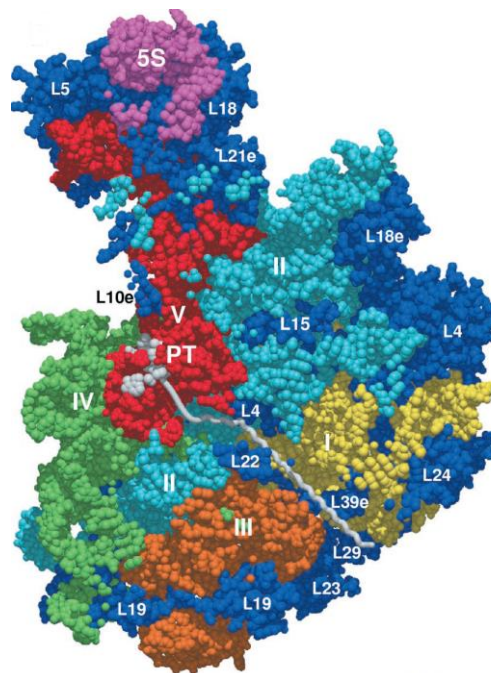


Figure 1.8 Structures of the 50S prokaryotic and 60S eukaryotic large ribosome subunits. A. Prokaryotic and B. Eukaryotic large ribosomal subunits, highlighting the path of the nascent chain through the exit tunnel. Note, proteins L4 and L22 which form the narrowest part of the exit tunnel at the constriction site. Also proteins L23 in prokaryotes and L39 in eukaryotes form contacts within the tunnel at the distal end near the exit tunnel opening. Structures reproduced from A. (Houben et al., 2005) and B. (Nissen et al., 2000).

1.1.4.2 Nascent chain folding within the ribosome exit tunnel

Early proteolytic digestion experiments of nascent chains within the ribosome indicated that between 30 and 35 amino acid residues are contained within the ribosome exit tunnel (Malkin and Rich, 1967). Whilst large-scale protein folding within the ribosome exit tunnel is not plausible due to the confines of the exit tunnel diameter, the dimensions are compatible with the formation of basic protein secondary structure such as alpha helices (Voss et al., 2006). Indeed through calculations and simulations it can be shown that alpha-helical structures are stabilised within the ribosome exit tunnel and nascent chains may in fact be entropically driven to form these structures (Ziv et al., 2005).

The ribosome exit tunnel does not have a uniform conformation throughout its length and experimental evidence indicates the existence of distinct 'folding zones' within the exit tunnel where formation of nascent chain secondary structure is favoured (Lu and Deutsch, 2005a). Protein tagging with methoxy-polyethylene glycol maleimide (PEG-mal) can be employed to assess when residues have traversed the ribosome exit tunnel, this method is known as pegylation. Pegylation studies were used to assess the folding of nascent chains with those that were engineered to contain segments of poly-alanines, which have a high propensity for alpha-helix formation, forming helical structures close to the PTC and also at the distal end of the exit tunnel (Lu and Deutsch, 2005a). Meanwhile, other pegylation studies have shown that native transmembrane segments form helices at lower points in the exit tunnel (Tu and Deutsch, 2010) and indeed analysis of peptides with regions of high alpha-helical propensity also showed helix formation only at the distal end of the exit tunnel (Bhushan et al., 2010a). None formed helical structures in the middle of the exit tunnel in the area coinciding with the constriction point. However, fluorescence resonance energy transfer (FRET) assays, which gave the first direct measure of secondary structure within the tunnel, indicated that a transmembrane sequence in a nascent membrane protein compacts into an alpha-helical structure close to the PTC and maintains this structure throughout the length of its passage through the exit tunnel (Woolhead et al., 2004). Although, as determined in the same study, this is not the case for all peptides as a secretory protein was shown to traverse the exit tunnel in an extended conformation (Woolhead et al., 2004).

Further to this, the formation of more complex tertiary structure was again prohibited in the confines further up the exit tunnel but could take place within the last 20 Å at the distal end, within an area termed the ‘folding vestibule’ (Kosolapov and Deutsch, 2009; Tu et al., 2014). These findings were also supported by computational simulation results which corroborated that tertiary structure formation can occur within the distal folding vestibule (O'Brien et al., 2010). This leads to the conclusion that it is a combination of factors between the environment of the exit tunnel and the nature of the nascent chain, including factors such as: hydrophobicity, length and helix propensity, which determines whether a nascent chain will form alpha-helical structures as it traverses the exit tunnel and also whether it maintains this structure.

1.1.4.3 Nascent chain interactions with the ribosome exit tunnel

There is a wide range of evidence indicating that the nascent chain can communicate with the ribosome on which it is being translated, through interactions with the ribosome exit tunnel. There appear to be many functions of this communication, both positive and negative, some of which will be discussed here. One function may be to recruit molecular chaperones and other auxiliary factors to the ribosome prior to release of the nascent chain. For instance, it has been demonstrated in *E.coli*, using leader peptidase (Lep) as a model inner membrane protein, that nascent chains that are too short to have exited the ribosome exit tunnel can still recruit SRP from within the tunnel. In this particular case, the signal is transferred from within the ribosome tunnel by inducing a conformational change in the ribosomal tunnel protein L23 (Bornemann et al., 2008). Further evidence has shown that this interaction coincides with transmembrane domain compaction in the *E.coli* exit tunnel (Robinson et al., 2012). Another example is the gating of the endoplasmic reticulum translocon pore in eukaryotes which is controlled by transmembrane proteins during their translation whilst they are still contained within the exit tunnel (Liao et al., 1997).

The nascent chain interactions with the exit tunnel can also function to cause translation arrest of the ribosome on which the peptide is being synthesised and stall its own translation. Translation arrest can be short or long term and can have several different functions. For instance, evidence has recently emerged of a post-initiation translational pausing, occurring at the 5th codon of mRNA, due to interactions between the first few amino acids translated and the ribosome exit tunnel. It is believed that the function of this

short term arrest is to enable the short nascent chain to sense the environment and ensure it correctly enters into the ribosome exit tunnel from the PTC prior to the ribosome committing to translation elongation (Han et al., 2014). Long term translational pausing due to interactions between the nascent chain and the ribosome exit tunnel functions to control the synthesis of downstream peptides within the same operon and is discussed in depth in the following Section 1.2.

1.2 Translational arrest peptides

1.2.1 General overview of stalling peptides

Contrary to initial belief of the ribosome exit tunnel being ‘non-stick’, not all peptides pass through the ribosome tunnel unhindered, some undergo translation arrest and ribosome stalling (Nakatogawa and Ito, 2002), and are termed translational arrest peptides. The function of this controlled ribosome stalling is to provide another level of cellular control to gene and protein expression, enabling regulation of transcription and translation of downstream genes on the same operon. Translation arrest is tightly controlled as aberrant ribosome stalling is detrimental to the cell. The downstream regulation as a result of translation arrest can be either positive or negative depending on the individual peptides, specific examples of which will be given in the following sections.

Peptides which undergo translational stalling contain essential amino acid residues or a series of essential residues, termed an arrest motif. It is these amino acid residues, not the mRNA sequence that encodes them that are responsible for regulating translation arrest through interactions with the ribosome exit tunnel. This is supported experimentally through studies in which silent base mutations were introduced into the mRNA codons that did not alter the amino acid sequence. This resulted in no effect on translation arrest, however, mutations of the same codons to sequences specifying alternative amino acids abolished arrest (Fang et al., 2000). Additionally ribosome mutations altering both 23S rRNA and L22 components of exit tunnel resulted in abolishment of the arrest function of stalling peptides such as SecM (Nakatogawa and Ito, 2002). A selection of stalling peptides and their essential residues are illustrated in Table 1.1. This table highlights the variability of amino acid arrest sequences indicating that the methods of stalling differ, to some degree, for each peptide. The interactions between the nascent chain and the ribosome exit tunnel mediate a *cis*-acting arrest signal and therefore stalling only occurs on the ribosome upon which the peptide is being synthesised. This stalling can occur at two points, either during translation elongation or termination. Stalling during translation elongation can itself occur at either the peptidyl transfer step whereby the peptidyl-tRNA remains stalled in the P site, examples of peptides undergoing stalling at this point include: SecM, MifM and ErmCL (Chiba and Ito, 2012; Muto et al., 2006; Vazquez-Laslop et al., 2008); or it can occur at the translocation step whereby the peptidyl-tRNA remains in the A site, as is the case for the CGS1 peptide (Onouchi et al., 2005). Peptides which undergo

Intrinsic																				P site	A site		
[1] SecM <i>E.coli</i>					F	x	x	x	x	W	I	x	x	x	x	G	I	R	A	G	P		
[2] SecM mutant					x	x	x	x	x	x	x	x	x	x	P	P	I	R	x	G	P		
[3] SecM <i>M.succiniciproducens</i>				x	x	x	x	x	x	x	x	x	x	H	A	P	I	R	G	S	P		
[4] Experimentally obtained												F	x	x	Y	x	I	W	P	P	P		
[5] MifM <i>B.subtilis</i>	R	I	x	x	W	I	x	x	x	x	x	M	N	x	x	x	x	x	x	x	x		
Inducible																				Inducer molecule			
[6] AAP <i>N.crassa</i>									D	Y	L	x	x	x	x	W	x	x	x	x	x	*	+ Arginine
[7] TnaC <i>E.coli</i>									W	x	x	x	D	x	x	I	x	x	x	x	P	*	+ Tryptophan
[8] TnaC <i>P.vulgaris</i>									W	x	x	x	D	x	x	L	x	x	x	x	P	x	+ Tryptophan
[9] ErmCL													M	x	x	x	x	I	F	V	I	x	+ Erythromycin
Distance from ribosome P site	-19	-18	-17	-16	-15	-14	-13	-12	-11	-10	-9	-8	-7	-6	-5	-4	-3	-2	-1	0	+1		

Table 1.1 Stalling motifs of selected translational arrest peptides as determined by mutational analysis. Only essential stalling residues are noted, non-essential residues are denoted by an 'x'. The residues occupying the ribosome A and P sites are shown on the right of the table. Some peptides stall with their respective stop codons in the ribosome A site and this is denoted in the table by an asterisk (*). Arrest sequences from [1] (Nakatogawa and Ito, 2002); [2] & [3] (Yap and Bernstein, 2009); [4] (Tanner et al., 2009); [5] (Chiba et al., 2009); [6] (Spevak et al., 2010); [7] (Cruz-Vera and Yanofsky, 2008); [8] (Cruz-Vera et al., 2009); [9] (Vazquez-Laslop et al., 2008).

translation termination arrest stall with a stop codon in the ribosome A site, examples of these stalling peptides include TnaC and AAP (Gong et al., 2001; Wang et al., 1998).

Translational arrest peptides can undergo one of two forms of translational arrest, either inducible or intrinsic. Inducible stalling peptides arrest only occurs when an effector molecule, such as an antibiotic or metabolite binds to the ribosome, for instance, ErmCL stalling in the presence of erythromycin (Vazquez-Laslop et al., 2008), or TnaC, which undergoes stalling when free tryptophan binds to the ribosome (Gong et al., 2001).

Alternatively stalling may be intrinsic, whereby arrest occurs without a cofactor and is only released upon interaction with other cellular components, such as in the case of SecM (Nakatogawa and Ito, 2002) or MifM (Chiba et al., 2009). In the case of these intrinsically stalled peptides they must be of sufficient length to traverse the exit tunnel to enable them to interact with extra-ribosomal factors to release stalling (Butkus et al., 2003).

In order to perform their function, translation arrest peptides must avoid detection by the intrinsic control mechanisms of the cell that are designed to sense and release stalled ribosomes. In bacteria, there are three different methods of rescuing stalled ribosomes, transfer messenger RNA (tmRNA) undertakes *trans*-translation to release stalling (Janssen and Hayes, 2012), whilst ArfA (YhdL) (Chadani et al., 2012) and ArfB (YaeJ) (Chadani et al., 2011; Gagnon et al., 2012) both induce peptidyl-tRNA hydrolysis by distinct mechanisms. Meanwhile in eukaryotes several mechanisms are used to sense stalled ribosomes and return normal function. These include ubiquitination, which tags peptides stalled during translation and targets them for degradation (Bengtson and Joazeiro, 2010), and also the three types of co-translational mRNA surveillance mechanisms: nonsense-mediated decay (NMD), no-go decay (NGD) and nonstop decay (NSD). NMD identifies mRNAs that contain a premature termination codon, whilst NSD identifies mRNAs without a termination codon and NGD targets mRNAs that contain sequences capable of potentially inducing ribosome stalling (Shoemaker and Green, 2012).

These methods rely on detecting stalled ribosomes with an empty A site occurring as a result of truncated mRNA or a shortage of amino acids or tRNA, however, many stalling peptides evade detection as the A site is occupied upon arrest (Garza-Sanchez et al., 2006; Muto et al., 2006; Onouchi et al., 2005). Whilst stalling peptides avoid detection under normal conditions, cells maintain control against overactive or prolonged stalling of arrest

peptides, as this is detrimental to the cell. For example, deliberate overexpression of SecM results in a sequestering of tRNA-Pro in the stalled SecM-Ribosome nascent chain (RNC) complexes. This depletion of tRNA-Pro results in a subset of stalled SecM-RNCs containing empty A sites and it is these that are targeted and released by tmRNA (Garza-Sanchez et al., 2006). Similarly, overexpression of *tnaC* results in depletion of tRNA-Pro (Gong et al., 2006), with this elevated stalling rescued by Ribosome Recycling Factor (RRF) and Release Factor 3 (RF3) (Gong et al., 2007). These examples indicate that whilst correctly functioning translation arrest peptides can operate in the cell, aberrant peptide stalling is not tolerated and is released.

In terms of evolution, translation arrest is a relatively recent adaptation with the stalling peptides established to date having limited phylogenetic distribution especially in comparison to the ribosome itself, which evolved very early and is therefore highly conserved across both prokaryotes and eukaryotes. Some examples of the limited distribution of stalling peptides are highlighted in Figure 1.9. For instance, SecM is only present in the orders *Enterobacteriales* and *Pasteurellales* (van der Sluis and Driessen, 2006), whilst TnaC occurs in the γ -proteobacterial orders *Enterobacteriales*, *Pasteurellales*, and also *Vibrionales* (Cruz-Vera and Yanofsky, 2008). Meanwhile MifM is further removed from these and is found in the *Firmicutes* phylum in the *Bacillales* order in the class *Bacilli* (Chiba et al., 2009). This restricted phylogenetic distribution may account for the species-specificity that has been demonstrated between some bacterial stalling peptides (Chiba et al., 2011). The situation in eukaryotes appears slightly broader but there are still no universal eukaryotic stalling peptides, for instance, the Upstream Open Reading Frames (uORFs) of CGS1, AAP and AdoMetDC are present within all plants, fungi and vertebrates respectively (Hood et al., 2007; Ito and Chiba, 2013). Due to the divergence between stalling peptides it is difficult to formulate a bioinformatical search to identify novel stalling peptides and as a consequence the list of stalling peptides remains incomplete.

The following sections contain a more detailed look at the three main translation arrest peptides investigated in this thesis: *E.coli* SecM, *E.coli* TnaC and *Neurospora crassa* (*N.crassa*) AAP; as well as a more general summary of some other stalling peptides of interest.

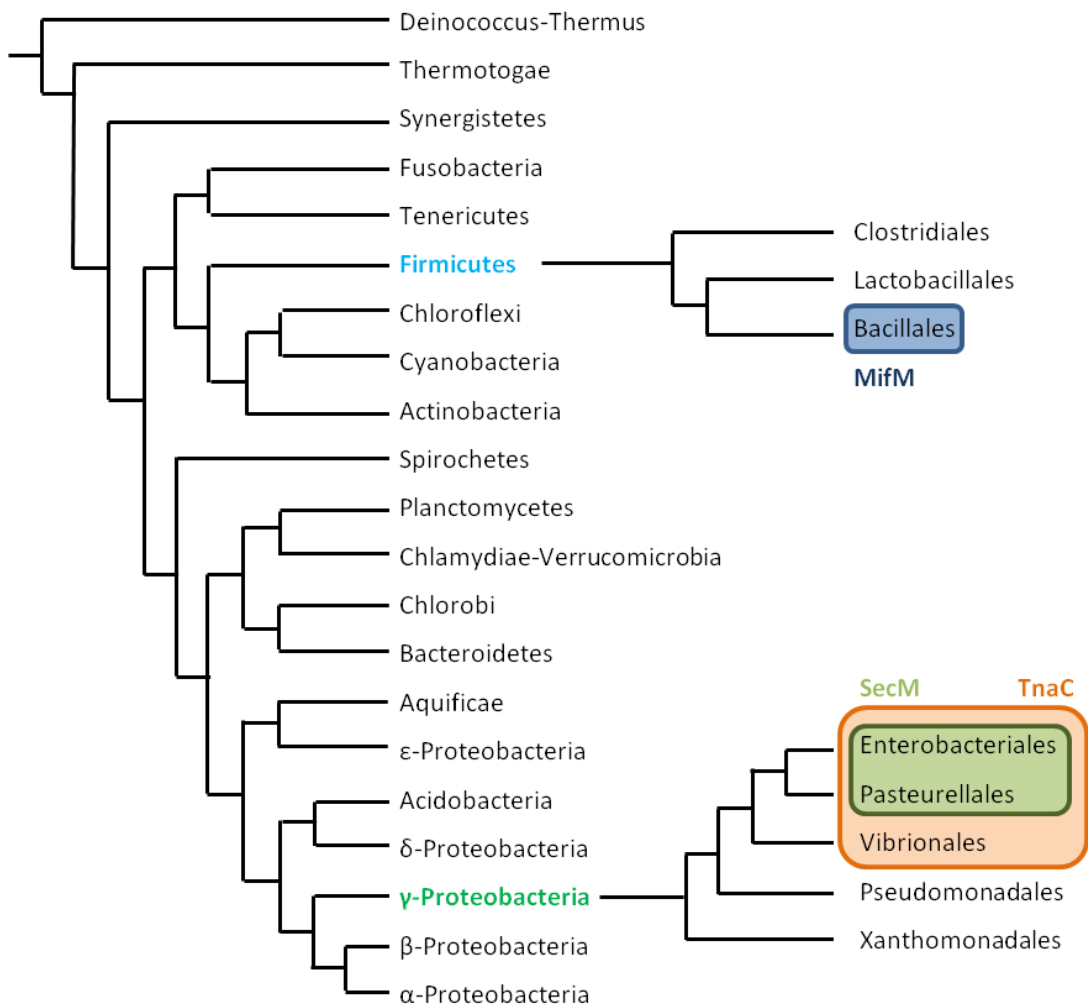


Figure 1.9 Phylogenetic tree highlighting the distribution of selected translation arrest peptides SecM, TnaC and MifM. MifM is found in the *Firmicutes* phylum in the *Bacillales* order in the class *Bacilli*, shown in blue. SecM (green) and TnaC (orange) occur in the γ -proteobacterial orders *Enterobacteriales*, *Pasteurellales*, and, additionally for TnaC, also *Vibrionales*. Diagram adapted from Ito and Chiba (2013).

1.2.2 *SecM* – *Secretion monitor*

Secretion Monitor (*SecM*) is a 170 amino acid peptide encoded upstream of the open reading frame (ORF) for *SecA*, an ATPase involved in the *SecYEG* translocation machinery. *SecM* monitors cell export activity through its own translocation to the periplasm and upregulates translation of *SecA* when translocation is reduced. Once exported to the cytoplasm the function of *SecM* is complete and it is rapidly degraded by tail-specific proteases (Nakatogawa and Ito, 2001). The *SecM* peptide contains a signal sequence in its N-terminal which co-translationally targets it to the *Sec* translocation machinery at the cell membrane (Nakatogawa et al., 2005), and an arrest motif in its C-terminal which interacts with the ribosome exit tunnel and induces elongation arrest at Pro-166 (Nakatogawa and Ito, 2002).

When the *SecM-SecA* mRNA is initially transcribed the *SecA* Shine-Dalgarno sequence is disguised by the mRNA secondary structure. Stalling of the ribosome translating *SecM* disrupts this mRNA hairpin exposing the Shine-Dalgarno sequence, thus enabling translation of *SecA* (McNicholas et al., 1997). Under normal conditions when the secretion status of the cell is sufficient, the stalling of *SecM* translation is transient, with a half-life of less than 1 minute, and the translation of *SecA* is basal (Nakatogawa and Ito, 2001). This transient stalling is released by the ‘pulling’ of the polypeptide through the *SecYEG* translocation machinery (Butkus et al., 2003). However, when cell secretion is impaired, this release of stalling does not occur and the Shine-Dalgarno sequence of *SecA* remains exposed, resulting in its upregulated translation and thus increased production of *SecA*. Additionally, *SecM* also functions as a *cis*-chaperone, its co-translational targeting to the membrane via its signal sequence results in the localisation of *SecA* production in the vicinity of the membrane and in doing so aids its efficient incorporation into the *Sec* translocation machinery where it functions (Nakatogawa et al., 2005). An outline of *SecM* translation in both secretion sufficient and secretion deficient conditions is shown in Figure 1.10.

Through a systematic process of alanine-scanning mutagenesis Nakatogawa and Ito (2002) identified the essential arrest motif of *SecM* to be: 150-FxxxxWlxxxxGIRAGP-166. Furthermore they identified that Pro-166 and Arg-163 residues are essential; Trp-155, Ile-156 and Gly-165 are important; and Phe-150, Gly-161, Ile-162 and Ala-164 are partially required for stalling. Translation is arrested 5 residues prior to the *SecM* stop codon at

Glycine-165, at this point tRNA-Pro166 is situated in the A site but is not incorporated into the peptide, however, it is still essential for stalling (Muto et al., 2006). Arrest is entirely *cis*-mediated by interactions occurring within the exit tunnel, as deletion of the N-terminal 122 residues, leaving only the last 44 residues which would still be contained within the ribosome exit tunnel, still allowed for arrest to occur, (Nakatogawa and Ito, 2002).

Since the elucidation of the key arrest motif residues, research has identified Arg-163 as the essential residue required for SecM stalling, with the exact positioning of this residue in the amino acid sequence essential for arrest (Yap and Bernstein, 2009). Molecular-dynamics flexible fitting (MDFF) modelling was used to visualise in atomic detail the structure of the stalled SecM nascent chain within the exit tunnel (Gumbart et al., 2012). This method enables atomic structures to be fitted into electron density maps by optimising the correlation of calculated and observed electron density maps thereby enabling high-resolution structures to be simulated (Trabuco et al., 2008). This has indicated that Arg-163 forms the key interactions with the ribosomal exit tunnel through interactions with 23S rRNA nucleotide A2062, whilst the other amino acid residues function to stabilise it

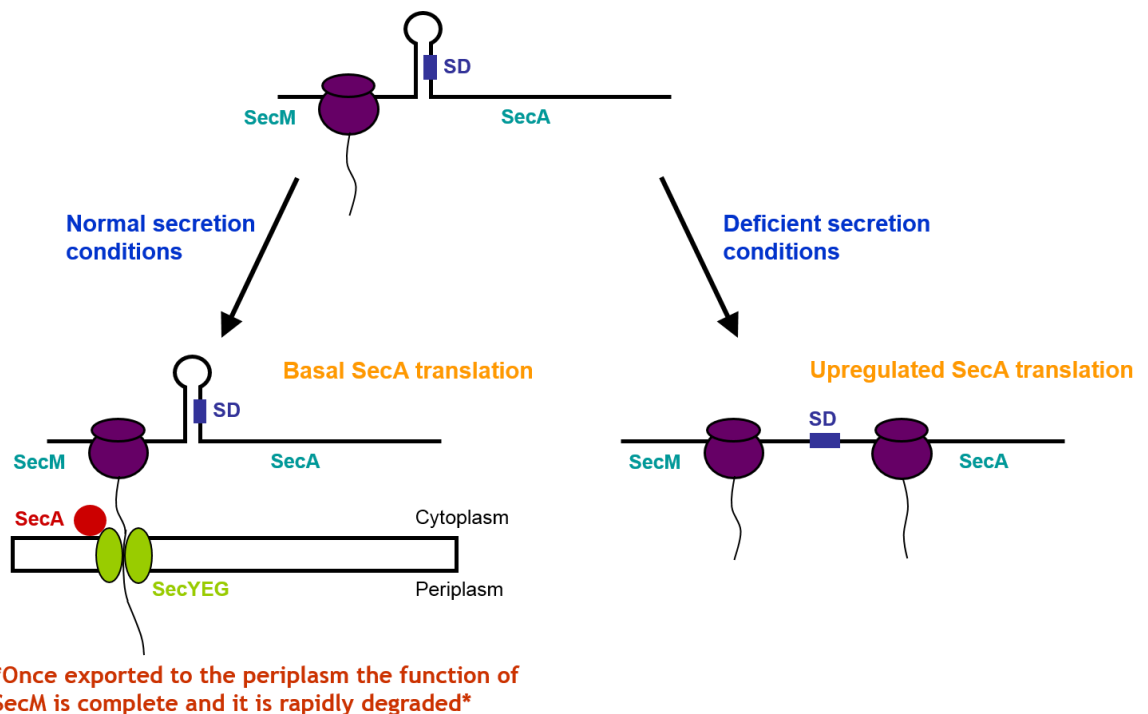


Figure 1.10 Summary of SecM translation and translocation. Under normal secretion conditions the stalling of SecM is transient as it is transported to the membrane and translocated through SecYEG, which releases stalling. In deficient secretion conditions, stalling of SecM is prolonged, the Shine-Dalgarno (SD) sequence of SecA is exposed and as a result SecA translation is upregulated.

through the correct positioning of the nascent chain within the exit tunnel. Indeed the mutation A2062U has been shown to abolish arrest of both SecM and ErmC stalling peptides (Vazquez-Laslop et al., 2010). Movement of the SecM nascent chain within the ribosome exit tunnel is key to its stalling, fluorescence resonance energy transfer (FRET) analysis has revealed that the C-terminus of SecM is in an extended conformation until synthesis of the arrest motif is complete, at which point the nascent chain undergoes compaction. This compaction is thought to be critical for the positioning of key residues, in particular Arg-163, within the exit tunnel, as mutations which prevent compaction, for instance mutation of non-essential amino acids 157-160 to proline, causes severe translation arrest defects. In support of this, in the same study, modification of Pro-153, a non-essential amino acid, to alanine was shown to restore translation arrest of wild type SecM in non-stalling L22-mutated ribosomes, by enabling increased freedom of movement of the nascent chain by removal of the restrictive proline residue (Woolhead et al., 2006). This increased freedom of movement is believed to allow the repositioning of the nascent chain within the exit tunnel which enables essential contacts to be formed.

Conformation of the SecM peptide within the ribosome exit tunnel was visualised by cryo-EM, with key interactions seen to take place in the upper tunnel between the SecM nascent chain and 23S rRNA nucleotides A2062, U2585 and U2609 and in the mid-tunnel with nucleotide A751 (Bhushan et al., 2011). A2062 is a highly flexible nucleotide (Fulle and Gohlke, 2009), which in the stalled SecM-RNC complex adopts a position flat against the ribosome exit tunnel wall, thought to be due to the constraints of the bulky SecM residues Arg-163 and also Ile-162. This restrained positioning of A2062, as a result of Arg-163, appears to be key to stalling as it has recently been shown that the orientation of A2062 initiates a relay signal through A2503 that results in PTC inactivation (Vazquez-Laslop et al., 2010). In addition to this key interaction, rRNA nucleotide U2585 also interacts with SecM in the vicinity of Ala-164, whilst U2609 interacts with the 3 amino acid region of 160-QAQ-158 of SecM. Furthermore, in the mid-tunnel the interaction between rRNA nucleotide A751 and SecM occurs in the proximity of Trp-155 and Ile-156 of SecM (Bhushan et al., 2011). Biochemical experimental approaches identified arrest suppressing mutations in the ribosome which coincide with the narrowest part of the ribosome tunnel, the constriction point, these key residues include A2058 and A749-A753 of 23S ribosomal RNA; Gly-91 and Ala-93 in L22 ribosomal protein (Nakatogawa and Ito, 2002); and also residues 82-84 of L22 (Woolhead et al., 2006).

The signal relayed to the PTC by interaction of Arg-163 with rRNA nucleotide A2062 was shown to result in a shift in the ester linkage of tRNA-Gly in the ribosome P site by approximately 2 Å (Bhushan et al., 2011) (Figure 1.11). Even slight increases in distance between the tRNA molecules in the PTC can affect the efficiency of peptidyl transfer at the PTC (Schmeing et al., 2005; Simonovic and Steitz, 2009), and therefore this ratcheting motion results in the A76 ester linkage shifting and preventing nucleophilic attack of the α -aminoacyl group of the A site tRNA-Pro, on the carbonyl carbon of the P site tRNA-Gly, and ultimately resulting in SecM translation arrest (Bhushan et al., 2011). This method of stalling is also aided by the presence of proline in the A site which naturally undergoes slower peptidyl transfer in comparison to other amino acids (Pavlov et al., 2009).

These studies reinforce the early findings that illustrated that the essential arrest residues, as elucidated by Nakatogawa and Ito (2002), were spaced apart at the C-terminus and not in a continual sequence, suggesting that it is not the detection of a continuous sequence but instead the positioning and recognition of individual residues of the nascent chain within the exit tunnel that enable arrest. Indeed, as discussed the current evidence indicates that the critical factors in SecM stalling are the positioning of Arg-163 to interact with rRNA nucleotide A2062 and the subsequent ratcheting of the ester linkage of tRNA-Gly.

1.2.3 *TnaC*

TnaC is the leader peptide of the tryptophanase (*tna*) operon and functions to induce ribosome stalling to control downstream gene expression, however, unlike SecM which undergoes translation elongation arrest, TnaC stalls by inhibiting translation termination. TnaC is located upstream of the *tnaA* and *tnaB* genes, which encode for tryptophanase and a tryptophan specific permease respectively (Gong and Yanofsky, 2002) (Figure 1.12A). The tryptophanase enzyme is important as it enables bacteria to degrade L-tryptophan to, pyruvate and ammonia allowing them to use tryptophan as a source of carbon, nitrogen and energy (Snell, 1975). Also as mentioned previously, TnaC is an inducible stalling peptide and only undergoes arrest in the presence of high concentrations of inducer molecule tryptophan (Gong et al., 2001). In contrast to the 170 amino acid SecM protein, at 24 amino acids in length TnaC is much shorter and remains fully contained within the ribosome exit tunnel throughout stalling (Figure 1.12B).

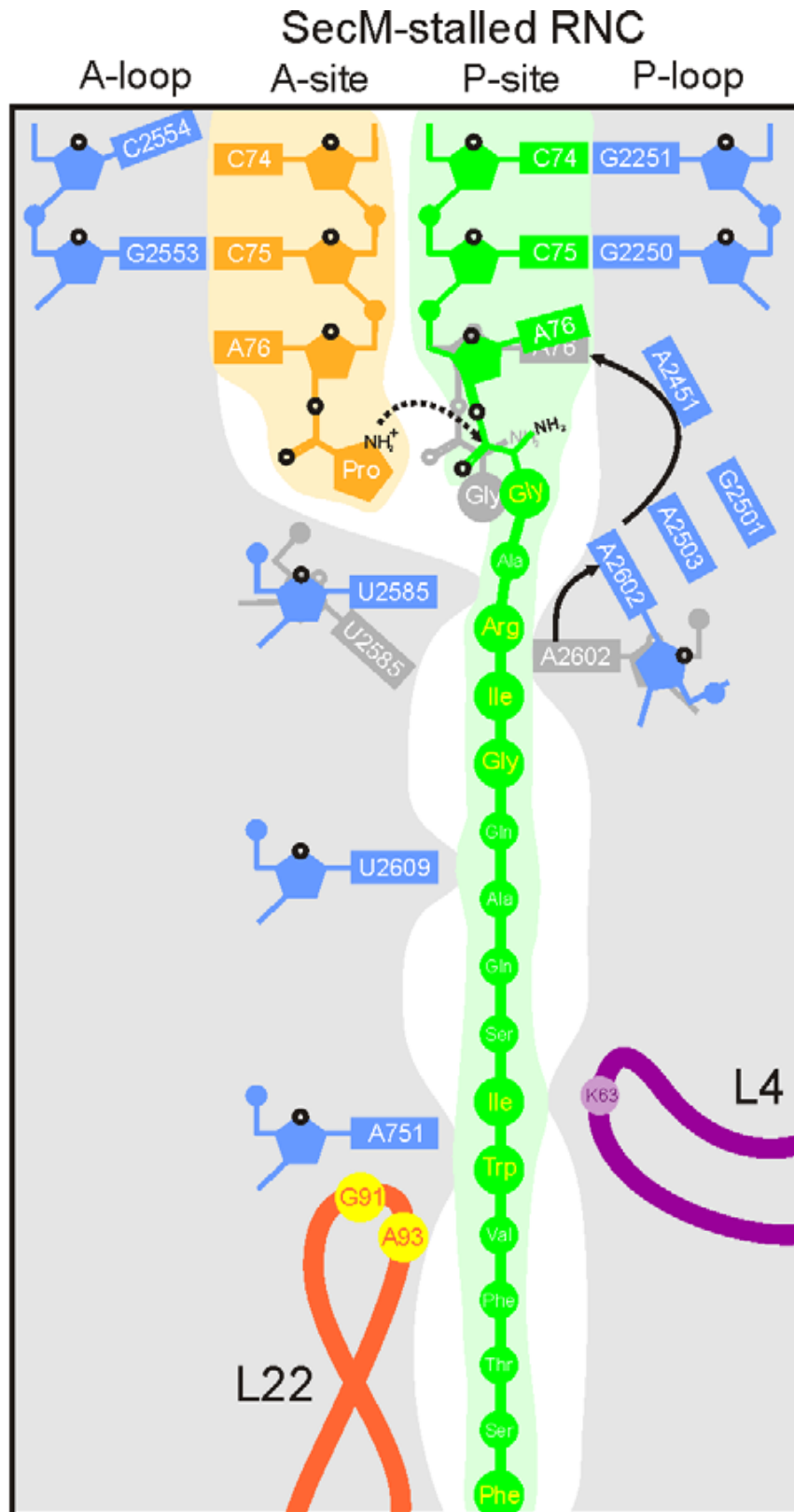


Figure 1.11 SecM arrest upon tRNA-Gly ratcheting. Schematic diagram of the interaction of the SecM nascent chain at selected points within the ribosome exit tunnel resulting in the optimal positioning of Arg-163. This residue interacts with 23S rRNA nucleotide A2062 to initiate a relay that ultimately results in the PTC inactivation through a ratcheting of the tRNA-Gly, preventing peptidyl transfer with the A site tRNA-Pro. Diagram reproduced from Bhushan et al., (2011).

The *tna* operon contains a 220-nucleotide spacer region separating the stop codon of *tnaC* from the downstream *tnaA* start codon, as shown in Figure 1.12A, which contains many Rho-dependant transcription termination binding sites (Stewart et al., 1986). If insufficient levels of free tryptophan are present then transcription is terminated in the leader region by the action of Rho factors, preventing the synthesis of the downstream *tnaA* and *tnaB* genes (Gong et al., 2001; Stewart et al., 1986). However, if sufficient levels of free tryptophan are present then TnaC will undergo inducible arrest upon reaching the *tnaC* stop codon. This is due to the bound tryptophan inhibiting Release Factor 2-mediated hydrolysis of the terminal peptidyl-tRNA^{Pro} and TnaC peptidyl transfer, resulting in the stalled ribosome remaining attached to the mRNA transcript. The stalled TnaC•70S complex blocks the Rho termination binding sites preventing downstream transcription termination and enabling *tnaA* and *tnaB* transcription to continue (Gong et al., 2001). This process results in reduction of the free tryptophan in the cytoplasm by the subsequent action of these enzymes and stalling therefore only continues until non-inducing levels of tryptophan are restored.

The exact position of tryptophan binding has not yet been confirmed, with cryo-EM structures of the TnaC-stalled ribosome that have so far been obtained lacking a bound tryptophan molecule (Seidelt et al., 2009). However, it is believed to bind close to the ribosome A site, as addition of tryptophanyl-tRNA^{Trp} as the terminal residue can substitute for free tryptophan binding in stalling (Gong and Yanofsky, 2002). Binding of tryptophan also blocks the methylation of 23S rRNA residue A2572 a nucleotide located in the peptidyl transferase centre indicating that it binds in this region (Cruz-Vera et al., 2006). More recent studies have suggested that the interaction of the TnaC residue Ile-19 with 23S rRNA nucleotide A2058 in the ribosome exit tunnel plays an important role in the sensing of the tryptophan molecule by the ribosome, although it was inconclusive if this was by directly creating a tryptophan binding site within the ribosome exit tunnel by or allosterically influencing tryptophan binding at the PTC (Martinez et al., 2014).

Mutational analysis identified the key arrest motif of the *E.coli tna* operon as: 12-WxxxDxxIxxxxP-24 (Cruz-Vera and Yanofsky, 2008). The terminal proline residue, Pro-24, is located in the ribosome P site whilst the Trp-12 residue is located near the L4/L22exit tunnel constriction, as determined by crosslinking of Lys-11 of TnaC-tRNA^{Pro} to A750 of 23S RNA (Cruz-Vera et al., 2005). These results have also subsequently been

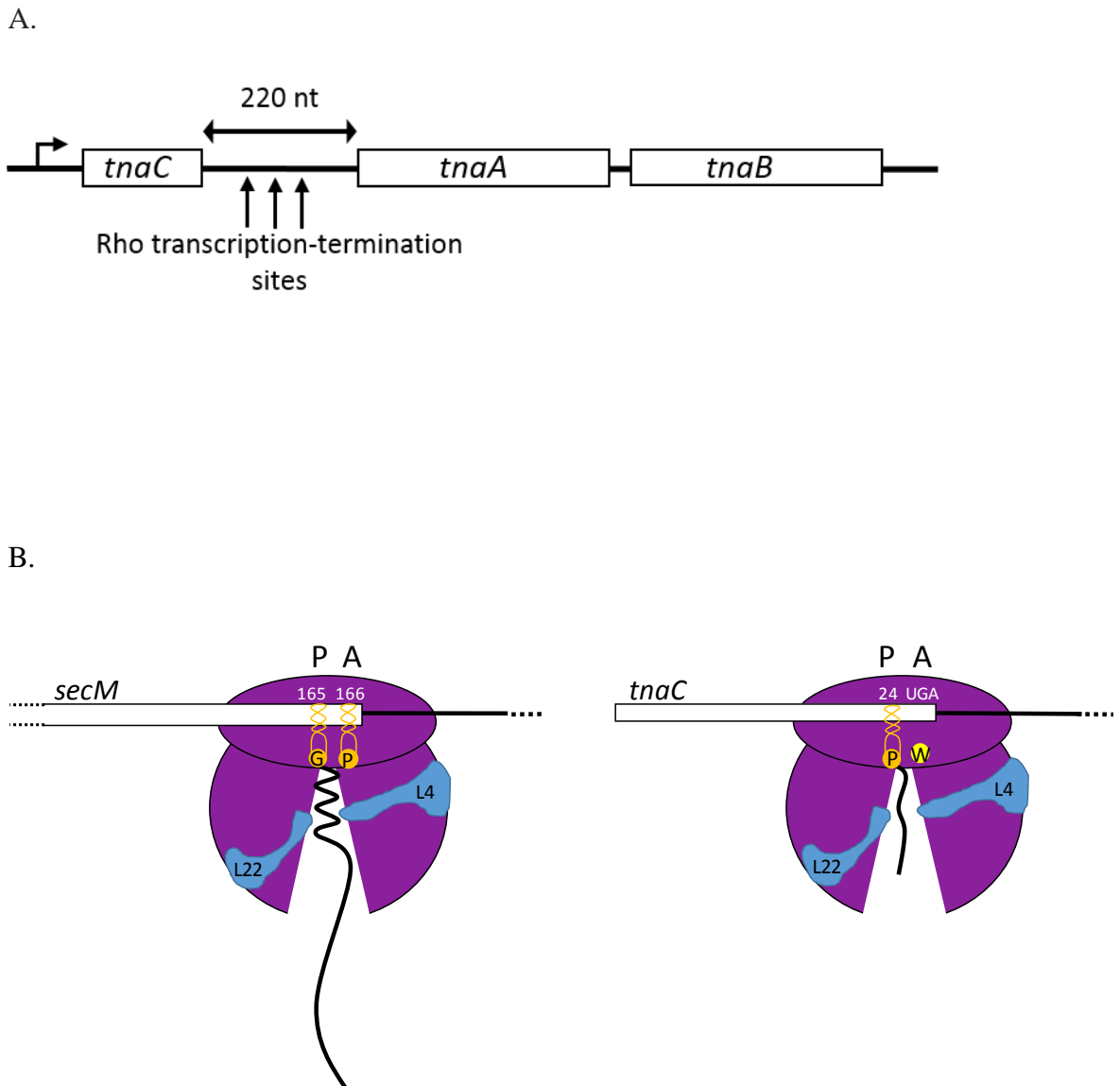


Figure 1.12 Tryptophanase (*tna*) operon and SecM and TnaC peptides stalled on the ribosome. A. Schematic representation of the tryptophanase operon indicating *tnaC* upstream of *tnaA* and *tnaB* on the mRNA, with the 220 nucleotide spacer region containing Rho transcription termination sites, separating them. B. Comparison of SecM and TnaC peptides stalled on the ribosome. Note SecM undergoes elongation arrest at residue Gly-165 with this amino acid in the P site and tRNA-Pro166 in the A site. Although a peptide bond is not formed, Pro-166 is still essential for stalling. TnaC undergoes arrest at Pro-24 only upon the binding of free tryptophan, the exact binding site of which is yet to be confirmed but is believed to be close to the ribosome A site (Gong and Yanofsky, 2002).

supported by the visualisation of the TnaC nascent chain stalled within the ribosome exit tunnel by cryo-EM (Seidelt et al., 2009). Trp-12 of TnaC-tRNA^{Pro} is responsible for inducing specific alterations in the ribosomal PTC that enables free tryptophan to bind, resulting in peptidyl transferase inhibition (Cruz-Vera et al., 2006). A key residue of the tunnel constriction point, A788, was also found to undergo reduced methylation in the presence of Trp12 of TnaC (Cruz-Vera et al., 2005).

Cryo-EM structures revealed interesting insights into the interactions between the TnaC nascent chain and the ribosome, highlighting the importance of specific rRNA nucleotides. In particular it has shown that 23S rRNA nucleotides A2602 and U2585, which are located close to the PTC, adopt distinct conformations in 70S·TnaC complex and that U2585 in particular shifts position to interact with the essential Pro-24 residue of TnaC (Seidelt et al., 2009). The positioning of A2602 and U2585 in the 70S·TnaC complex conflicts with any potential binding of release factors (Laurberg et al., 2008; Weixlbaumer et al., 2008), suggesting that even if the RFs bound, correct positioning of their GGQ motif within the PTC would be unable to occur, thereby preventing efficient hydrolysis and release of the nascent chain. Indeed, previous studies have highlighted the importance of A2602 in peptidyl-tRNA hydrolysis and nascent chain release from the ribosome (Polacek et al., 2003; Youngman et al., 2004), whilst other studies have revealed that mutation of the U2585 region of rRNA results in a reduction of the maximum level of tnaC operon induction (Yang et al., 2009).

Similarly to SecM, the positioning of the TnaC nascent chain within the ribosome exit tunnel is critical for stalling, with the exact spacing between amino acid residues, Pro-24 and Trp-12, shown to be essential for stalling (Gong and Yanofsky, 2002). Cryo-EM analysis of TnaC stalled RNC complexes indicate that, unlike SecM, the TnaC nascent chain remains in an extended conformation upon stalling (Seidelt et al., 2009). Within the ribosome exit tunnel the cryo-EM structures indicated proximity between rRNA nucleotides G2061 and A2062 with the TnaC residues Arg-23 and Asp-21 respectively. Also strong density existed between the Lys-18 residue of TnaC and the U2609 and A752 rRNA nucleotides within the tunnel wall, whilst the adjacent A751 residue is in close vicinity to Phe-13. In support of these being key contacts, previous experiments have shown that mutation of U2609 and insertions at A751 eliminate induction of stalling by tryptophan (Cruz-Vera et al., 2005). Also, as stated previously, interactions between Ile-19

of the TnaC nascent chain and 23S rRNA nucleotide A2058 have been shown to result in the creation of a tryptophan binding site within the ribosome (Martinez et al., 2014).

TnaC forms two substantial contacts with the β -hairpin of ribosomal protein L22, one at Arg-95 of the L22 protein with Thr-9 of TnaC, with the other at the tip of the L22 loop placing Lys-90 and Arg-92 in close proximity of the key residue Trp-12 of TnaC. Indeed Cruz-Vera *et al* (2005) also found that Lys-90 of ribosomal protein L22 and U2609 of 23S rRNA are essential for ribosome stalling, both of which are also located near the putative position of Trp-12 in the ribosome exit tunnel. It is interesting to note that Trp-155 of SecM is located 11 residues from the arrest point and is thought to occupy a similar position within the exit tunnel. These residues are located near the constriction point supporting the original views that this point in the tunnel acts as a ‘discriminating gate’ and is involved in key interactions with the nascent chain which influence stalling (Nakatogawa and Ito, 2002).

1.2.4 AAP – Arginine Attenuator Peptide

The fungal arginine attenuator peptide (AAP) is a eukaryotic regulatory stalling peptide located in an upstream open reading frame (uORF) of mRNA specifying the small subunit of arginine-specific carbamoyl phosphate synthetase (Werner et al., 1985). Like TnaC, it is an inducible stalling peptide and functions in response to high concentrations of arginine (Wang and Sachs, 1997). As a result of AAP-mediated translation arrest the ribosome stalls at the AAP termination codon, resulting in a blocking of the mRNA to additional ribosomes preventing them from scanning downstream to the initiation codon of the carbamoyl phosphatase synthetase, thereby reducing expression of this enzyme (Gaba et al., 2001; Wang and Sachs, 1997). This thesis focusses on *N.crassa* AAP, which modulates downstream expression of the *arg-2* gene, however, it is evolutionarily conserved amongst fungi, with AAP homologs encoded by all uORFs of genes specifying the carbamoyl phosphate synthetase enzymes that have thus far been characterised in fungi (Baek and Kenerley, 1998; Shen and Ebbolle, 1997; Werner et al., 1987). Additionally, *in vitro* translation assays have established that *N.crassa* AAP can initiate Arg-mediated stalling of fungal, plant and animal ribosomes highlighting the conservation between these ribosome systems (Fang et al., 2004).

N.crassa AAP is 24 amino acids in length, with residues 9-20 having been identified as the minimum domain required to confer stalling function with the essential amino acids determined as: 12-DYLxxxxW-19 (Spevak et al., 2010). In contrast to a lot of other stalling peptides, there was no strict requirement as to the identity of the amino acid in the P site of the ribosome upon translation arrest (see Table 1.1 for comparison). Further to this, whilst the length of AAP peptides is conserved across different fungal species, there is notable sequence divergence of the AAP C-terminus (Hood et al., 2007; Spevak et al., 2010). As with other stalling peptides, it has been confirmed that AAP stalling is dependent on the amino acid sequence and not the mRNA sequence encoding it (Fang et al., 2000).

It has been shown that binding of arginine induces AAP-mediated ribosome stalling through a change in conformation of the AAP nascent chain within the ribosome exit tunnel. This was established by site-specific crosslinking, which indicated that at high concentrations of arginine, a photo-reactive crosslinker positioned at Val-7 of AAP had reduced reactivity with ribosomal protein L17 (L22) and increased interaction with the L4 protein, than it did at low arginine concentrations (Wu et al., 2012). In support of this interaction, cryo-EM analysis has shown that residues 6 and 7 of AAP form a contact with the distal extension of the L4 protein (Bhushan et al., 2010b). The AAP nascent chain also appears to form a contact around residues 11 and 12 with ribosomal protein L17 (L22) and rRNA nucleotide A751 on one side of the tunnel and the proximal extension of L4 on the other. These are key residues of AAP, as their mutation results in abolishment of stalling (Freitag et al., 1996; Hood et al., 2007), indicating that these are important regions of contact. In addition to the interactions between AAP and the ribosomal proteins L17 (L22) and L4, cryo-EM analysis also identified the key interactions between the AAP nascent chain and specific rRNA nucleotides: U2585, A2062, A2058 and A751 (Bhushan et al., 2010b). As with the importance of the A2062 rRNA nucleotide contact in both SecM and TnaC translation arrest (Bhushan et al., 2011; Seidelt et al., 2009), the cryo-EM data for AAP also indicated a strong density in this region that may accommodate a specific orientation of this base (Bhushan et al., 2010b). The importance of this nucleotide in AAP-mediated ribosome stalling is also highlighted by the fact that mutation of Ala-24, which is located in its vicinity, and is most likely to interact with it, abolishes stalling (Wang and Sachs, 1997).

1.2.5 Comparison of SecM, TnaC and AAP interactions with the ribosome exit tunnel

The cryo-EM data for the three stalling peptides: SecM, TnaC and AAP highlight broad similarities between the main points of interaction with the rRNA and protein moieties of the ribosome exit tunnel, despite the lack of sequence conservation between the nascent chains themselves, see Figure 1.13 for an overview. A2062 in particular, appears to play a key role in the stalling function of many arrest peptides, possibly forming the link between the nascent chain within the ribosome exit tunnel and the transfer of the stalling signal to the PTC to undergo translation arrest. Other common regions of interaction appear to be 23S rRNA nucleotides: U2585, U2609 and A751, as well as the ribosomal proteins L4 and L22. The interactions between the nascent chain and the exit tunnel, despite being in similar regions, do not necessarily have the same degree of impact on the stalling function of the peptide. For instance, all 3 peptides interacted with rRNA nucleotide U2585, however, whilst mutations in this region significantly reduce TnaC stalling (Yang et al., 2009), they are shown to have a less notable effect on SecM stalling (Bhushan et al., 2011). Therefore despite the overall commonalities between the stalling peptides, it is believed that each undergoes a unique series of interactions with the ribosome exit tunnel to induce stalling.

1.2.6 Other translation arrest peptides

1.2.6.1 Antibiotic-induced stalling peptides

As well as the 3 stalling peptides focussed on in this thesis, there exists a growing number of other peptides which have been identified as undergoing translation arrest, all with various different functions and modes of arrest. For instance, there are a subset of bacterial stalling peptides which undergo arrest only in the presence of specific antibiotics (reviewed in (Ramu et al., 2009)). Translation arrest of these drug-dependent ribosome stalling peptides results in upregulation of antibiotic resistance genes. Of the antibiotic-dependant translation arrest peptides, the Erm-leader peptide class is one of the best characterised. Erythromycin and other macrolide antibiotics bind to the ribosome exit tunnel in close proximity to the PTC, inhibiting translation by constricting the tunnel and thus impeding the path of the nascent chain, ultimately resulting in peptidyl-tRNA drop-off (Menninger, 1985; Tenson et al., 2003). Erm methyltransferases, encoded by the *erm* gene, function by dimethylating the 23S rRNA nucleotide A2053, which is located at the

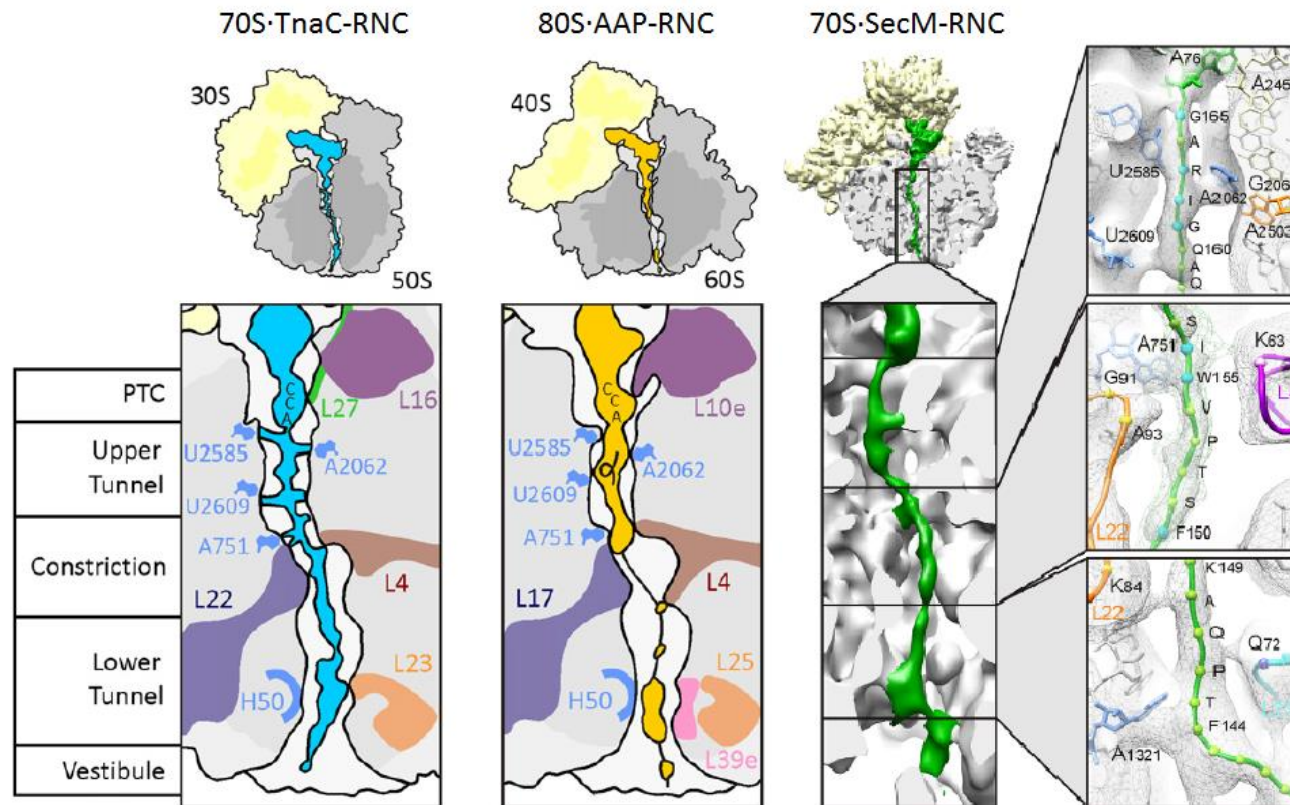


Figure 1.13 Comparison of cryo-EM data of AAP, TnaC and SecM peptides arrested within the ribosome exit tunnel. Highlighted are the regions of specific interactions between the nascent chain and the ribosome exit tunnel. Diagrams modified from Bhushan et al., (2010b) and Bhushan et al., (2011).

drug binding site, which in turn renders ribosomes resistant to macrolide binding (Skinner et al., 1983).

A well-defined Erm-leader peptide is ErmCL, a 19 amino acid leader peptide found in *Staphylococcus aureus* and other bacteria, which induces expression of the downstream *ermC* gene (Gryczan et al., 1980; Horinouchi and Weisblum, 1980). In the absence of erythromycin the full length ErmCL peptide is translated, whilst translation of *ermC* is attenuated as the Shine-Dalgarno sequence is masked by the mRNA secondary structure. The essential amino acid arrest motif of ErmCL has been shown to be composed of 6-IFVI-9, with Ile-9 situated in the ribosome P site upon arrest (Mayford and Weisblum, 1989). Stalling causes alteration of the mRNA secondary structure which exposes the Shine-Dalgarno sequence of *ermC* resulting in the activation of its expression. The N-terminal 5 amino acids can be mutated but cannot be deleted, indicating that they contribute essential, but non-specific, interactions within the exit tunnel (Vazquez-Laslop et al., 2008). Evidence of interactions within the exit tunnel is supported by the fact that deletion of Met-82 to Arg-84 in ribosomal protein L22 and mutation of rRNA residue A2062 alleviate the elongation arrest (Vazquez-Laslop et al., 2008).

The role of the antibiotic was initially believed to be relatively non-specific, serving only to act as a partial obstruction within the ribosome exit tunnel causing the nascent chain to subtly alter course, resulting in key interactions between the nascent chain and the exit tunnel to induce translation arrest. However, it now appears that it may play a dual role, both in modifying the path of the nascent chain but also in preparing the PTC for stalling through allosteric modification of key 23S rRNA nucleotides. Studies have shown that binding of the antibiotic to the ribosome exit tunnel results in repositioning of the rRNA nucleotides U2585 and A2602, even in the absence of contacts between the nascent chain and the antibiotic, indicating it is the antibiotic and not the nascent chain that predisposes the PTC for stalling (Sothiselvam et al., 2014). Studies previous to this had indicated that may be the case, for example studies on ErmCL revealed that the specific atomic structure of the antibiotic and the interactions it undertakes with either the nascent chain or the ribosome were essential for stalling (Vazquez-Laslop et al., 2011). Whilst the common peptide-sensing rRNA nucleotide A2062, as well as U1782, interact with the peptide, other rRNA nucleotides, C2610 and A2503, were found to be responsible for recognition of the

antibiotic. Successful translation arrest required generation of an arrest signal from both correct recognition of the antibiotic and the nascent chain (Vazquez-Laslop et al., 2011).

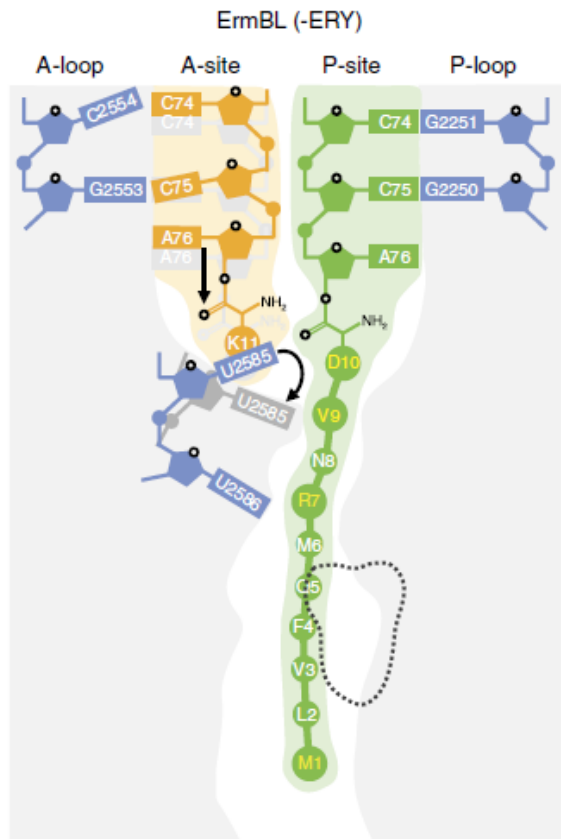
Cryo-EM structures of the antibiotic-induced leader peptide, ErmBL, stalled on the ribosome have recently been elucidated and support a role for antibiotic binding in altering the path of the nascent chain within the exit tunnel (Arenz et al., 2014) (see Figure 1.14). The amino acid sequence of this peptide varies considerably from ErmCL, as does its mechanism of action, for instance, whilst mutation of 23S rRNA nucleotides A2062 and A2503 abolishes stalling of ErmAL1 and ErmCL leader peptides, it has no influence on ErmBL and ErmDL arrest (Vazquez-Laslop et al., 2010). The cryo-EM study conclusively revealed binding of erythromycin created a constriction within the exit tunnel causing the path of the nascent chain to be altered. This in turn resulted in the nascent chain forming stable contacts with specific 23S rRNA nucleotides in the tunnel wall. In particular, Arg-7 interacts with U2586 whilst Val-9 and Asp-10 contact the PTC at U2585. This ultimately resulted in the stabilisation of the uninduced state of U2585, which in turn blocked accommodation of tRNA-Lys11 in the ribosome A site, thus preventing peptide bond formation and resulting in stalling of the ribosome (Arenz et al., 2014).

As more cryo-EM structures of translation arrest peptides are obtained it will be highly interesting to discover how the relay pathways they undergo to communicate between the nascent chain and the PTC vary. As can be seen from the structures obtained already, whilst there seems to be a general consensus of interacting nucleotides, each stalling peptide appears to utilise a distinct message relay system to induce translation arrest.

1.2.6.2 Experimentally obtained stalling peptides

Due to the diversity of amino acid stalling sequences it is impossible to develop a bioinformatics program to efficiently identify potential arrest sequences from genomic libraries. As an alternative, researchers have instead sought to identify novel stalling sequences through experimental methods. Indeed through one such experimental screening of random libraries, the novel stalling sequence FxxYxIWPPP was identified (Tanner et al., 2009). Similarly to the method of SecM arrest, the final proline remains in the A site and is not incorporated into the nascent chain upon arrest. Unlike SecM

A.



B.

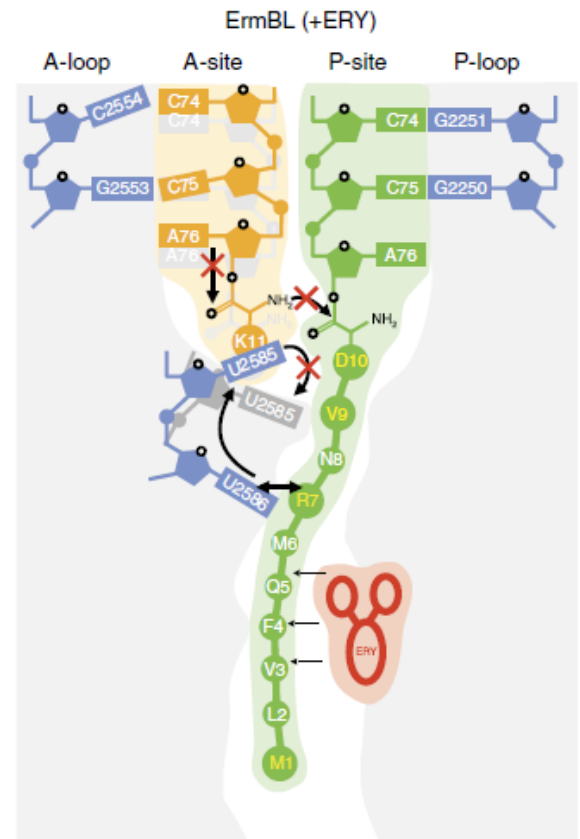


Figure 1.14 ErmBL in the ribosome exit tunnel. A. Schematic of the cryo-EM visualisation of ErmBL in the absence of erythromycin and B. in the presence of erythromycin, indicating the influence of erythromycin binding to the exit tunnel resulting in the alteration of the path of the nascent chain. This subsequently enables the formation of new, stable interactions of the nascent chain with the exit tunnel resulting in the induction of stalling. Diagram reproduced from Arenz et al., (2014).

however, tRNA-Asp and tRNA-Trp can substitute for the final proline and still undergo arrest. The results also indicate that the nascent chain undergoes a unique set of interactions with the ribosome exit tunnel as this novel peptide has differing responses to exit tunnel mutations in comparison to SecM or TnaC.

1.2.6.3 Mammalian uORFs encoding stalling peptides

There have been a small number of stalling peptides identified in mammalian cells that can undergo translation arrest. One such peptide is XBP1u, a mammalian translational arrest peptide that when activated encodes XBP1s, a transcription factor responsible for transcribing genes involved in the endoplasmic reticulum (ER) stress response (Pavitt and Ron, 2012). To be activated the XBP1u mRNA must be translocated to the ER membrane where a 26-nucleotide intron is spliced by the transmembrane endoribonuclease, Ire1 α , to generate XBP1s mRNA (Yoshida et al., 2001). Localization requires a hydrophobic region, HR2 (codons 186-208), a membrane-targeting signal that is only present in the XBP1u protein (total length - 261 codons) (Yanagitani et al., 2009). The purpose of translational stalling is to ensure that the peptide sequence, HR2, maintains localization of the mRNA at the ER membrane thus enabling efficient splicing of the XBP1u mRNA (Yanagitani et al., 2011). During translation arrest, Asn-261 is located in the ribosome A site (Ingolia et al., 2011), with serial truncation analysis demonstrating that the C-terminal region Lys-236 to Asn-261 constitutes the minimal sequence required for arrest, whilst alanine-scanning mutagenesis identified 14 specific amino acid residues as being essential for arrest (Yanagitani et al., 2011). The essential arrest motif was determined as 236-xxxxxYxPPxLxxWGxHQxSWKPLMN-261, whilst L246A and W256A mutations in particular were shown to strongly abolish translational stalling (Yanagitani et al., 2011). Translational stalling of XBP1u is fundamental to enable mRNA splicing and therefore enable translation of the active transcription factor XBP1s.

Another mammalian stalling peptide that has been identified is the uORF leader peptide of polyamine biosynthetic enzyme *S*-adenosyl-methionine decarboxylase (AdoMetDC). This uORF encodes a hexapeptide MAGDIS and is feedback repressed by polyamines, the exact mechanism of which still needs to be identified (Hill and Morris, 1993). Stalling occurs at the point of translation termination (Law et al., 2001), with Ser-tRNA situated in the ribosome P site, and prevents ribosomal scanning to the downstream initiation codon

(Raney et al., 2002). Mutational analysis of the sequence specificity indicates that the aspartic acid must be present at codon 4, whilst either isoleucine or valine can function at codon 5, meanwhile the identity of the other residues appears less stringent (Mize et al., 1998).

From these two examples alone the variation in mammalian stalling peptides is evident and further research is required to clearly define the abundance and determine the various mechanisms of action of stalling peptides in mammalian cells. Despite the relatively late evolutionary emergence of translational arrest peptides it is clear that they play important roles throughout all domains.

1.2.6.4 Summary of translation arrest peptides

This introduction has selected just a few relevant examples of translation arrest peptides and does not cover the large array of divergent stalling peptides that have so far been identified. From those featured it is clear that stalling peptides are diverse in both their amino acid sequences and their interactions with the ribosome. There are, however, some commonalities which can be observed, for instance, in the proximity of the PTC, 23S rRNA nucleotides A2062 and U2585 are common interaction points for many stalling peptides to relay arrest signals to the PTC. What is not known is whether the relay pathway back to the PTC that follows is always the same, and certainly the subsequent behaviour of the peptides within the PTC to implement stalling is different. For instance, SecM tRNA-Gly undergoes a ratcheting movement that moves it away from the A site tRNA-Pro and obstructs peptide bond formation, which is not seen in the other stalling peptides. Further down the length of the exit tunnel near the tunnel constriction point there are further common interactions with the ribosomal proteins L4 and L22 (L17) as well as 23S rRNA nucleotide A751, with interactions in this area appearing to have an important role in nascent chain conformation within the ribosome exit tunnel. These interactions have implications on stalling despite the distance from the PTC.

1.3 Project Aims

The aims of this project are to investigate the properties of translational arrest motifs and ribosome interactions with the nascent chain during translation. Chapter 3 of this project will examine the sequence specificity of the SecM translation arrest motif and the properties of the amino acids which are essential for their interaction with the ribosome exit tunnel. This will be done through analysis of systematic mutations of the key arrest motif residues of SecM to both alanine and conservative residues by CTABr precipitation assays (as detailed in Section 2.5.3), enabling direct analysis of the level of stalling of these mutant peptides in comparison to wild type SecM, to determine the effect of the mutations. It will also explore the influence of the structure of SecM by increasing the freedom of movement of the nascent chain within the exit tunnel, the importance of which was initially highlighted in previous studies by Woolhead et al., (2006). Following on from this Chapter 4 will explore the compaction of the SecM nascent chain within the exit tunnel upon stalling. This will be done through analysis of selected conservative mutations by pegylation assays (see Section 2.5.4) and will also be expanded further to investigate in-depth the effect of the flexibility of the nascent chain within the exit tunnel on translation arrest. Use of pegylation as a technique enables direct measurement of the level of compaction of the nascent chain within the full length of the ribosome exit tunnel as will be explained further in Chapter 4.

Chapter 5 will expand the scope of this thesis to investigate the specificity of translation arrest motifs of both prokaryotic and eukaryotic translation arrest peptides and explore the ability of these peptides to undergo stalling in ribosomes of alternative domains. This is an area in which past studies have yet to provide any conclusive answers. This study will draw clear conclusions through the use of two different assays, CTABr precipitation, as employed previously in Chapter 3, and a puromycin release assay (detailed in Section 2.5.5). Finally, Appendix 1 presents preliminary experimental evidence of SecM arrest sequence application, based on the knowledge gained from the study of SecM, to generate stable constructs containing proteins of interest attached to the N-terminus of the SecM arrest motif. These SecM arrest motifs will be modified and tested to identify alterations that result in prolonged translation arrest. The purpose of this is to create stable ribosome-nascent chain complexes that enable the timing and process of co-translational protein folding and exit from the ribosome tunnel of different proteins of interest to be investigated.

2 Materials and Methods

2.1 General reagents

Agilent Technologies UK Ltd., Wokingham, Berkshire, UK

PfuTurbo DNA Polymerase; QuikChange Multi Site-Directed Mutagenesis Kit;
QuikChange Site-Directed Mutagenesis Kit

BioRad Laboratories Ltd., Hemel Hempstead, Hampshire, UK

Agarose

Fisher Scientific UK Ltd., Loughborough, Leicestershire, UK

Ammonium persulphate (APS); Ethylenediaminetetraacetic acid (EDTA); Glucose;
Glycerol; Glycine; Methanol; Potassium hydroxide (KOH); Sucrose; Tris base

Formedium Ltd., Hunstanton, Norfolk, UK

Bacterial Agar; Tryptone; Yeast Extract Powder

Integrated DNA Technologies, Leuven, Belgium

Oligonucleotide primers

Invitrogen Ltd., Paisley, UK

PureLink PCR Purification Kit; SeeBlue Pre-stained Standard

Kodak, Hemel Hempstead, Hertfordshire, UK

X-ray film

Melford Laboratories Ltd., Chelworth, Ipswich, UK

Dithiothreitol (DTT); Isopropyl- β -D-thiogalactopyranoside (IPTG)

Merck Millipore, Billerica, MA, USA

Amicon Ultra 0.5 ml Centrifugal Filters (10K); Cetyltrimethylammonium bromide; di-Potassium hydrogen phosphate (K₂HPO₄)

New England Bioscience (UK) Ltd., Hitchin, Hertfordshire, UK

100 mM dNTPs (dATP, dCTP, dGTP, dTTP); 10x T4 DNA Ligase Buffer; T4 DNA Ligase; Prestained Protein Marker, Broad Range (7-175 kDa)

PerkinElmer, Cambridge, UK

EXPRESS Protein Labelling Mix (³⁵S Met)

Promega, Southampton, UK

1 kb DNA Ladder; 100 bp DNA Ladder; 100 mM rNTPs (rATP, rCTP, rGTP, rUTP); Bovine Serum Albumin (BSA); Dithiothreitol (DTT); *E. coli* S30 Extract System for Linear Templates; HindIII; KpnI; MfeI; Recombinant RNasin Ribonuclease Inhibitor; RNA Polymerase Transcription Buffer; SP6 RNA Polymerase; T7 RNA Polymerase; Wheat Germ Extract; XbaI

Qiagen Ltd., Crawley, West Sussex, UK

Nuclease-free Water; QIAquick Gel Extraction Kit; QIAprep Spin Miniprep Kit

Roche Diagnostic Ltd., Burgess Hill, UK

Creatine kinase; DpnI; tRNA from *E. coli* MRE 600

Severn Biotech Ltd., Kidderminster, Worcestershire, UK

30 % Acrylamide [Acrylamide: Bis-acrylamide ratio 37.5:1]

Sigma-Aldrich Ltd., Gillingham, Dorset, UK

Adenosine 3',5'-cyclic monophosphate (cAMP); Adenosine 5'-triphosphate (ATP);

Ammonium persulphate; Ampicillin; β -mercaptoethanol; Brilliant blue; Bromophenol blue; Calcium chloride (CaCl_2); Creatine phosphate; Ethidium bromide; Folinic acid; Hydrochloric acid; Isopropanol; L-Amino acids; L-Glutathione oxidised; Lysozyme; Magnesium acetate (MgOAc); Methoxypolyethylene glycol maleimide (PEG-mal); N,N,N',N'-Tetramethylethylenediamine (TEMED); PIPES; Phosphoenol pyruvate; Poly(ethylene glycol) MW 8000; Potassium Glutamate (KGlu); Puromycin; Pyruvate kinase from *Bacillus stearothermophilus*; Phenylmethylsulphonyl fluoride (PMSF); Ribonuclease A from bovine pancreas; Tricine

Takara Bio Europe, Saint-Germain-en-Laye, France

Ex Taq DNA Polymerase; Ex Taq DNA Polymerase Buffer

Thermo Fisher Scientific Inc., Waltham, Massachusetts, USA

Slide-A-Lyzer Dialysis Cassette 3,500 MWCO

VWR International Ltd., Lutterworth, Leicestershire, UK

Acetone; Ammonium acetate (NH_4OAc); Disodium hydrogen orthophosphate (Na_2HPO_4); Ethanol; Glacial acetic acid; 2-(4-(2-Hydroxyethyl)-1-piperazinyl)-ethanesulphonic acid (HEPES); Magnesium chloride (MgCl_2); Potassium acetate (KOAc); Potassium dihydrogen orthophosphate (KH_2PO_4); Potassium chloride (KCl); Sodium acetate (NaOAc); Sodium chloride (NaCl); Sodium dodecyl sulphate (SDS); Trichloroacetic acid (TCA)

2.2 General buffers and solutions

Competent cell buffer	60 mM CaCl ₂ , 15% (v/v) glycerol, 10 mM PIPES (pH 7).
Gel fixing solution	40% (v/v) methanol, 7% (v/v) Glacial acetic acid.
6x DNA loading buffer	30% (v/v) glycerol, 0.25% (w/v) bromophenol blue.
LB media	1% (w/v) tryptone, 0.5% (w/v) yeast extract, 1% (w/v) NaCl.
LB agar	1% (w/v) tryptone, 0.5% (w/v) yeast extract, 1% (w/v) NaCl, 1.5% (w/v) agar.
PEG buffer	20 mM HEPES (pH 7.2), 100 mM NaCl, 5 mM MgCl ₂ .
RNC (Ribosome Nascent Chain) buffer	20 mM HEPES (pH 7.5), 14 mM MgOAc, 100 mM KOAc.
Run-out premix	0.75 mM HEPES (pH 7.5), 7.5 mM DTT, 21.3 mM MgOAc, 75 μM each amino acid, 6 mM ATP, 20 mg/mL phosphoenol pyruvate, 0.14 mg/mL pyruvate kinase.
2x SDS PAGE Sample Buffer	125 mM Tris-HCL (pH 6.8), 20% (v/v) glycerol, 4% (w/v) SDS, 5% 2-mercaptoethanol, 0.04 % (w/v) bromophenol blue.
SDS-PAGE resolving gel solution	375 mM Tris (pH 8.8), 12.5% Acrylamide, 0.1% (w/v) SDS, 0.05% (v/v) ammonium persulphate, 0.005% (v/v) TEMED.

10x SDS-PAGE running buffer	0.25 M Tris, 1.92 M glycine, 1% (w/v) SDS.
SDS-PAGE stacking gel solution	125 mM Tris (pH 6.8), 6% Acrylamide, 0.1% (w/v) SDS, 0.05% (v/v) ammonium persulfate, 0.005% (v/v) TEMED.
S-30 extract Buffer 1	20 mM HEPES (pH 7.5), 14 mM MgOAc, 100 mM KCl, 6 mM β -mercaptoethanol, 0.5 mM PMSF.
S-30 extract Buffer 2	20 mM HEPES (pH 7.5), 14 mM MgOAc, 100 mM KCl, 1 mM DTT, 0.5 mM PMSF.
S-30 extract Buffer 3	20 mM HEPES (pH 7.5), 14 mM MgOAc, 100 mM KOAc, 1 mM DTT, 0.5 mM PMSF.
SOC media	2 % (w/v) Tryptone, 0.5 % (w/v) Yeast Extract, 0.05 % (w/v) NaCl, 10 mM MgCl ₂ , 10 mM MgSO ₄ , 20 mM Glucose.
50x TAE buffer	2 M Tris, 5.71 % (v/v) glacial acetic acid, 0.05 M EDTA (pH 8.0).
2.5x Translation premix	137.5 mM HEPES (pH 7.5), 520 mM KGlu, 68.75 mM NH ₄ OAc, 48.25 mM MgOAc, 4.25 mM DTT, 3 mM ATP, 2 mM each rNTPs, 625 μ g/mL creatine kinase, 200 mM creatine phosphate, 444 μ g/mL <i>E. coli</i> tRNA, 2 mM IPTG, 60 mg/mL PEG 8000, 170 μ M folinic acid, 1.6 mM cAMP.
10x Tricine gel Anode running buffer	1 M Tris, 1 M tricine, 1% (w/v) SDS.

10x Tricine gel Cathode running buffer	2 M Tris (pH 8.9).
Tricine separating gel solution	496 mM Tris (pH 8.45), 8.4% Acrylamide, 6.5% (v/v) glycerol, 0.07% (v/v) ammonium persulphate, 0.004% (v/v) TEMED.
Tricine spacer gel solution	1 M Tris (pH 8.45), 10% Acrylamide, 0.07% (v/v) ammonium persulphate, 0.004% (v/v) TEMED.
Tricine stacking gel solution	750 mM Tris (pH 8.45), 4% Acrylamide, 0.07% (v/v) ammonium persulphate, 0.004% (v/v) TEMED.

2.3 *Escherichia coli* strains and plasmid vectors

2.3.1 *Escherichia coli* strains

The following *E.coli* strains were used in this thesis:

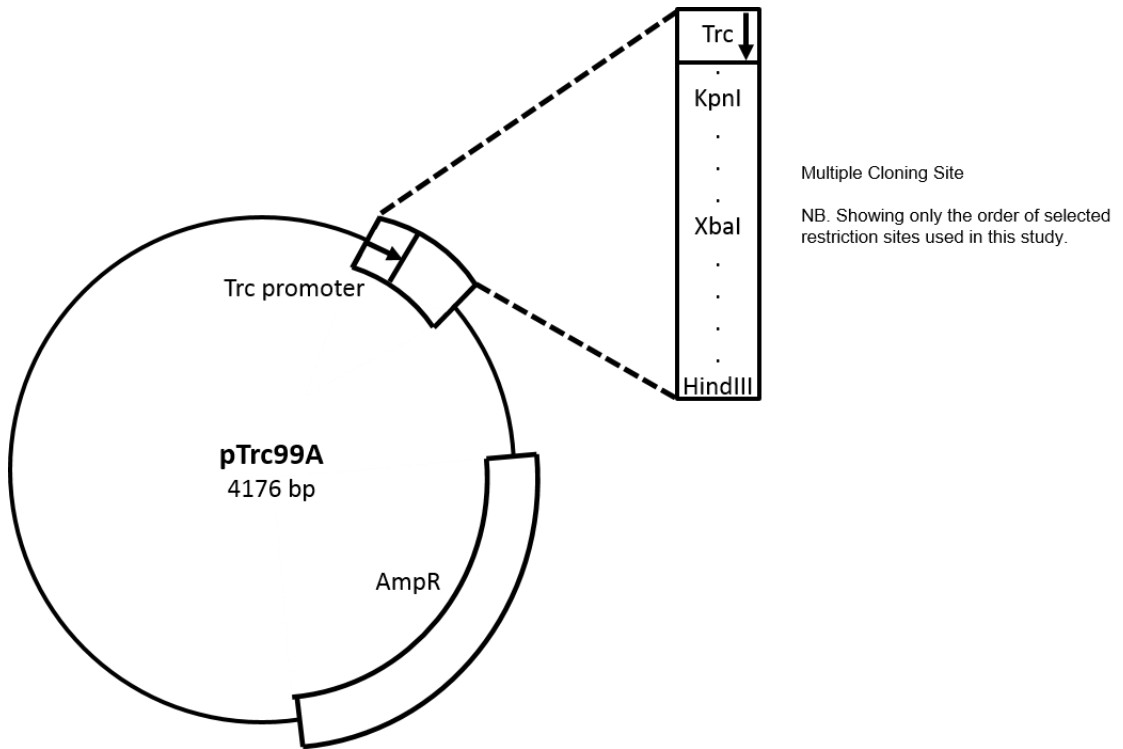
C41	F ⁻ <i>ompT hsdS_B (r_B⁻ m_B⁻) gal dcm</i> (DE3)
DH5- α	F ⁻ ϕ 80 <i>lacZ</i> Δ M15 Δ (<i>lacZYA-argF</i>)U169 <i>recA1 endA1 hsdR17</i> (r _k ⁻ , m _k ⁺) <i>phoA supE44 thi-1 gyrA96 relA1</i> λ -
MC4100	F ⁻ (<i>araD139</i>) Δ (<i>argF-lac</i>)169 λ - <i>e14- flhD5301</i> Δ (<i>fruK-yeiR</i>)725(<i>fruA25</i>) <i>relA1 rpsL150</i> (Str ^r) <i>rbsR22</i> Δ (<i>fimB-fimE</i>)632(:: <i>IS1</i>) <i>deoC1</i>
XL1-Blue	<i>recA1 endA1 gyrA96 thi-1 hsdR17 supE44 relA1 lac</i> [F' <i>proAB lacI^qZ</i> Δ M15 Tn10 (Tet ^r)]
XL10-Gold	Tet ^r Δ (<i>mcrA</i>)183 Δ (<i>mcrCB-hsdSMR-mrr</i>)173 <i>endA1 supE44 thi-1 recA1 gyrA96 relA1 lac</i> Hte [F' <i>proAB lacI^qZ</i> Δ M15 Tn10 (Tet ^r) Amy Cam ^r]

2.3.2 Plasmid vectors

Two plasmid vectors were used in the work detailed in this thesis, pTrc99A and pGEM-4Z. pTrc99A contains an inducible promoter that is chemically induced by isopropyl- β -D-thiogalactopyranoside (IPTG) whilst pGEM-4Z, depending on the orientation of the inserted gene of interest, is either SP6 or T7 polymerase dependant (Figure 2.1).

A full summary of all the constructs used in this study can be found in Appendix 2 whilst Appendix 3 contains a brief explanation of how the various SecM, AAP, TnaC and B2M constructs were designed and generated.

A.



B.

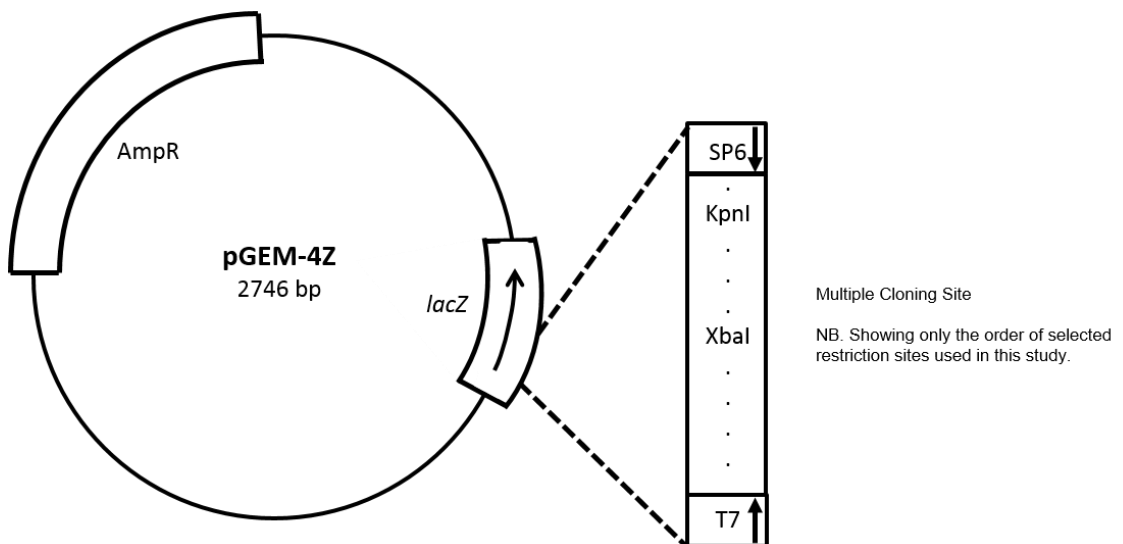


Figure 2.1 pTrc99A and pGEM-4Z plasmid maps. A. pTrc99A plasmid vector indicating KpnI, XbaI and HindIII restriction sites used in this study. B. pGEM-4Z plasmid vector indicating KpnI and XbaI restriction sites used in this study. All plasmid constructs used in this thesis were in the SP6 promoter orientation.

2.4 General Molecular Biology Methods

2.4.1 Preparation of LB plates

LB-agar was autoclaved and allowed to cool before ampicillin was added to a final concentration of 100 µg/mL, mixed well and then the plates poured under sterile conditions.

2.4.2 Preparation of competent bacterial cells

Bacterial strains, either XL1-Blue or DH5α, were streaked out on a LB plate in the absence of antibiotics and incubated overnight (~16 hours) at 37°C. Single colonies were picked and used to inoculate 5 mL LB broth which was then incubated overnight (~16 hours) in a shaking incubator at 37°C. 300 µL of this culture was then used to inoculate 50 mL of pre-autoclaved LB broth and incubated with moderate shaking (250 rpm) until the Optical Density (OD) reached 0.375 at 595 nm. Following this the culture was chilled on ice for 10 minutes, before being centrifuged in sterile falcon tubes at 2,500 rpm for 7 minutes at 4°C to pellet the bacteria. The supernatant was removed and the pellet re-suspended in 10 mL Competent cell buffer (see Section 2.1.2 for details) before being centrifuged again at 2500 rpm for 5 minutes at 4°C. Again the supernatant was discarded and the pellet was re-suspended in 10 mL Competent cell buffer, incubated on ice for 30 minutes and then centrifuged at 2,500 rpm for 5 minutes at 4°C. The pellet was then re-suspended in 2 mL Competent cell buffer and the cells then aliquoted into sterile eppendorf tubes, frozen on dry ice and stored at -80°C.

2.4.3 Transformation of competent bacteria

XL1-blue and XL10-Gold cells were used for site directed mutagenesis whilst DH5α cells were used for transformations of established plasmids for mini preps. An aliquot of competent cells was thawed on ice and 1 µL of the relevant plasmid DNA added. This was incubated on ice for 30 minutes before being heat shocked at 42°C for 2 minutes and returned to ice for 5 minutes. 1 mL of LB media was then added and incubated at 37°C for 1 hour with shaking. Following this it was then centrifuged at 7,000 rpm for 5 minutes at room temperature. 800 µL of the supernatant was then removed and discarded and the

remainder used to re-suspend the pellet. This was then transferred to an LB-ampicillin plate and incubated overnight (~16 hours) at 37°C.

2.4.4 Small-scale preparation of plasmid DNA (mini-prep)

From the bacterial transformation a single colony was picked and used to inoculate 5 mL LB broth containing 100 µg/mL of ampicillin which was then incubated overnight (~16 hours) in a shaking incubator at 37°C. Plasmid DNA was purified using Qiagen QIAprep Spin Miniprep kit. The overnight culture was centrifuged at 3,500 rpm for 10 minutes to pellet the cells. The pellet was re-suspended in 250 µL Buffer P1 and transferred to a sterile eppendorf tube. Cells were lysed by addition of 250 µL Buffer P2, which was then neutralised after 5 minutes by addition of 350 µL Buffer N3. The sample was then centrifuged at 13,400 rpm for 10 minutes and the supernatant transferred to a QIAprep spin column. The columns were centrifuged at 13,400 rpm for 1 minute, the flow-through discarded and the column washed with 750 µL Buffer PE and again centrifuged at 13,400 rpm for 1 minute. The flow-through was again discarded and the column spun again at 13,400 rpm for 2 minutes to remove residual wash buffer. The plasmid DNA was eluted into a sterile eppendorf by addition of 100 µL nuclease-free water to the column and centrifugation at 13,400 rpm for 1 minute. Plasmid DNA was then stored at -20°C.

2.4.5 Polymerase chain reaction

2.4.5.1 DNA amplification by Polymerase Chain Reaction (PCR)

Forward and reverse oligonucleotide primers were designed to amplify the DNA sequence of interest, including any appropriate restriction enzyme cut sites. All primers used in this study were synthesised by Integrated DNA Technologies. PCR reactions were set up in thin-walled PCR tubes on ice, using either plasmid or genomic DNA as a template. PCR reactions were set up using the following general protocol:

DNA template (~1 µg/µL)	1 µL
Forward primer (100 pMol)	1 µL
Reverse primer (100 pMol)	1 µL

10x DNA polymerase buffer	10 μ L
dNTP mix (2.5 mM each: dATP, dCTP, dGTP, dTTP)	8 μ L
Ex Taq DNA Polymerase	0.5 μ L
ddH ₂ O	78.5 μ L

PCR reactions were out in a thermocycler using the following standard conditions:

94°C (Initial denaturing)	1 minute	
94°C (Denaturing)	30 seconds	} 30 Cycles
56°C (Primer annealing)	30 – 60 seconds	
72°C (Elongation)	2 minutes/kb	
72°C (Final elongation)	8 minutes	
4°C	Hold	

This standard protocol could be adjusted to account for the melting temperatures of the primers being used. Generally the optimal annealing temperature is 5°C lower than the lowest melting temperature of the primers.

Once the PCR was complete the products were PCR purified (see Section 2.2.6) and run on an agarose gel (see Section 2.2.7) to confirm that a product of the correct size was obtained.

2.4.5.2 Site-directed mutagenesis PCR

2.4.5.2.1 Single point mutations

Single point mutations were inserted into constructs using the QuikChange Site-Directed Mutagenesis kit (Agilent). Forward and reverse primers were designed according to the

manufacturer's instructions to incorporate the desired mutation. PCR reactions were set up in thin-walled PCR tubes on ice as follows:

Plasmid DNA template (~1 µg/µL)	1 µL
Forward primer (100 pMol)	1 µL
Reverse primer (100 pMol)	1 µL
10x reaction buffer	5 µL
dNTP mix (10 mM each: dATP, dCTP, dGTP, dTTP)	1 µL
PfuTurbo DNA polymerase	1 µL
ddH ₂ O	41 µL

Once set up the PCR was performed in a thermocycler using the following program:

95°C (Initial denaturing)	30 seconds	
95°C (Denaturing)	30 seconds	} 18 Cycles
58°C (Primer annealing)	1 minute	
72°C (Elongation)	1 minute/kb	
72°C (Final elongation)	10 minutes	
4°C	Hold	

Once complete the PCR products were treated with 1 µL Dpn1 restriction enzyme and incubated for 1 hour at 37°C, to digest methylated parental DNA. 1 µL of reaction mix was then transformed into 50 µL competent XL-1 blue cells (see Section 2.2.3). Following incubation of agar plates overnight, single colonies were picked and grown in 5 mL LB-broth containing 100 µg/mL of ampicillin overnight (~16 hours) in a shaking 37°C incubator. The following day plasmids were isolated by small-scale DNA preparation (see

Section 2.2.4), before being sent for sequencing to confirm the correct mutation had been obtained (see Section 2.2.11).

2.4.5.2.2 Multiple point mutations

Multiple point mutations to the same construct were done simultaneously using the QuikChange Multi Site-Directed Mutagenesis kit (Agilent). Only forward primers were required and were designed according to the manufacturer's instructions to incorporate the desired mutation. PCR reactions were set up in thin-walled PCR tubes on ice as follows:

Plasmid DNA template (~1 µg/µL)	1 µL
Forward primer (100 ng 1-3 primers or 50 ng 4-5 primers)	1 µL of each
10x reaction buffer	2.5 µL
dNTP mix (10 mM each: dATP, dCTP, dGTP, dTTP)	1 µL
QuikChange Multi enzyme blend	1 µL
ddH ₂ O	Final volume of 25 µL

PCR was performed in a thermocycler using the following program:

95°C (Initial denaturing)	1 minute	
95°C (Denaturing)	1 minute	} 30 Cycles
58°C (Primer annealing)	1 minute	
72°C (Elongation)	2 minutes/kb	
4°C	Hold	

Once complete the PCR products were treated with 1 µL Dpn1 restriction enzyme and incubated for 1 hour at 37°C, to digest methylated parental DNA. 1 µL of reaction mix

was transformed into 50 μL competent XL-10 Gold ultracompetent cells (see Section 2.2.3). Single colonies were picked from the antibiotic LB-agar plates and grown in overnight cultures before plasmids were isolated the following day by small-scale DNA preparation (see Section 2.2.4). Following this they were sent for sequencing to confirm incorporation of the correct mutations (see Section 2.2.11).

2.4.6 Purification of PCR products

PCR products were purified using the PureLink PCR Purification Kit (Invitrogen). To bind DNA to the column 1 volume of PCR sample was mixed with 4 volumes of Binding Buffer (B2) in an eppendorf. This was then transferred to a PureLink Spin Column and centrifuged at 13,400 rpm for 1 minute. The flow-through was discarded and the column washed with 650 μL Wash Buffer and centrifuged at 13,400 rpm for 1 minute. Again the flow-through was discarded and the column centrifuged at 13,400 rpm for 2 minutes to remove any residual wash buffer. The collection tube was then transferred to a fresh eppendorf and the PCR product eluted by applying 50 μL ddH₂O to the column and centrifuging at 13,400 rpm for 1 minute. The PCR product was run on an agarose gel (see Section 2.2.7) to confirm the purification was successful and the correct size of PCR product had been produced.

2.4.7 DNA agarose gel electrophoresis

1% (w/v) agarose powder was dissolved in 1x TAE buffer (see Section 2.1.2 for details) by boiling in a microwave, and then allowed to cool before addition of 0.5 $\mu\text{g}/\text{mL}$ ethidium bromide. This was then poured into a sealed horizontal gel tank containing a loading comb and allowed to set before being immersed in 1x TAE buffer and the loading comb removed. DNA samples were prepared by addition of 6x Loading buffer before being loaded onto the gel and run beside either a 100 bp or 1 kb DNA ladder (Promega). Electrophoresis was carried out at 100 volts for ~30 minutes and the gel was visualised, and images recorded, using a BioRad Molecular Imager ChemiDoc XRS+ System.

2.4.8 DNA purification from agarose gels

DNA samples were separated by gel electrophoresis (see Section 2.2.7) and purified by gel extraction using the QIAquick Gel Extraction Kit (Qiagen). The gel was visualised on a UV light box and bands of the correct size were excised with a sharp scalpel and placed in sterile eppendorf tubes. 3 volumes of Buffer QG per 1 volume of gel was added and incubated at 50°C for 10 minutes or until the gel was completely dissolved. Once the gel was dissolved 1 volume of isopropanol was added and mixed before the solution was transferred to a 2 mL collection tube and centrifuged at 13,400 rpm for 1 minute. The flow-through was discarded and the column washed with 0.75 mL Buffer PE and centrifuged at 13,400 rpm for 1 minute. Again the flow-through was discarded and the column spun for an additional 2 minutes at 13,400 rpm to remove any residual wash buffer. The column was then transferred to a sterile eppendorf and the DNA eluted by addition of 30 µL of ddH₂O to the centre of the column and spinning at 13,400 rpm for 1 minute, before being stored at -20°C.

2.4.9 Restriction endonuclease digestion

Pairs of restriction enzymes were selectively chosen to cut plasmid DNA or PCR products at specific sites. Restriction digestions were set up as follows:

Plasmid DNA/PCR product (~1 µg/µL)	10 µL
Restriction enzyme buffer (as recommended by manufacturer)	1.5 µL
Restriction enzyme 1	0.5 µL
Restriction enzyme 2 (optional)	0.5 µL
10x BSA (as recommended by manufacturer)	1.5 µL
ddH ₂ O	Final volume 15 µL

Reactions were incubated at 37°C for 1 hour and then, depending on manufacturer's instructions, heat inactivated at 65°C for 20 minutes. Samples were then stored in the short-term at 4°C or for longer periods of time at -20°C.

2.4.10 Ligation of DNA

Plasmid vectors and PCR products cut using the same pair of restriction enzymes were run on an agarose gel and then purified by gel extraction (see Section 2.2.8) before being ligated as follows:

10x T4 DNA ligase buffer	2 μ L
T4 DNA ligase	1 μ L
Insert DNA - PCR product (~1 μ g/ μ L)	6 μ L
Vector DNA - Plasmid (~1 μ g/ μ L)	1 μ L
ddH ₂ O	10 μ L

Reactions were incubated at room temperature for 1 hour before being transformed into competent DH5 α cells as previously described in Section 2.2.3. The plasmid was isolated by small-scale DNA preparation as described earlier (see Section 2.2.4) and sent for sequencing (see Section 2.2.11) to confirm the ligation had been successful.

2.4.11 DNA sequencing

Plasmid DNA to be sequenced was mini-prepped and samples sent to the Sequencing Service at the School of Life Sciences, University of Dundee. Results were analysed by comparison to known nucleotide sequences using BLAST and the Swiss Institute of Bioinformatics (SIB) ExpASy translate online software.

2.4.12 In vitro transcription

RNA was transcribed from linear DNA as follows. The reactions were set up in thin-walled PCR tubes and incubated for 2 hours at 42°C:

Linear DNA (~1 μ g/ μ L)	5 μ L
5x Transcription buffer	10 μ L

1 M DTT	2 μ L
RNasin (20 units)	1 μ L
rNTP mix (25 mM each: rATP, rCTP, rGTP, rUTP)	6 μ L
SP6/T7 polymerase	2 μ L
ddH ₂ O	24 μ L

Synthesised RNA was precipitated by adding 0.1 volumes of 3M NaOAc (pH 5.2) and 3 volumes 100% ethanol and incubating on ice for 10 minutes. This was then centrifuged at 13,400 rpm for 10 minutes. The supernatant was discarded and the pellet washed with 250 μ L 70% ethanol and centrifuged for a further 10 minutes at 13,400 rpm. The supernatant was again discarded and the pellet was re-suspended in 50 μ L ddH₂O, which was then aliquoted and stored at -80°C. Small samples were removed and run on agarose gel (see Section 2.2.7) to confirm the RNA was the correct size.

2.5 *In vitro* translation methods

2.5.1 *S-30 bacterial cell extract preparation*

C41 cells from glycerol stocks were streaked out onto an antibiotic-free agar plate and incubated overnight (~16 hours) at 37°C. From this 2 individual colonies were picked and grown in separate 5 mL LB-broth cultures overnight (~16 hours). The next day these were used to inoculate separate 500 mL cultures of SOC media (see Section 2.1.2 for details of all the buffers used in this preparation). The cells were incubated at 37°C in a shaking incubator and grown until they reached mid-log phase, $A_{600} = 0.8$. Once this was reached the cultures were added to 1 litre of ice and then centrifuged at 7,000 rpm for 10 minutes at 4°C. The supernatant was then discarded and the pellet re-suspended in 100 mL of Buffer 1 and then centrifuged again at 7,000 rpm for 10 minutes at 4°C. The supernatant was discarded and the pellet re-suspended in 100 mL Buffer 1 and again centrifuged at 7,000 rpm for 10 minutes at 4°C. After removal of the supernatant the wet cell mass was weighed and the pellet was re-suspended in Buffer 2 at a concentration of 0.5 g/mL. Lysozyme was then added to a final concentration of 1 mg/mL and the cells then passed twice through a French Press at 8,000 psi. The extract was then centrifuged at 15,000 rpm for 30 minutes at 4°C before transferring the supernatant to a fresh tube and again centrifuging at 15,000 rpm for 30 minutes at 4°C. The supernatant was again retained and incubated at 26°C for 70 minutes with 0.15 volumes of Run-out premix. Following this the extract was dialysed 3 times in Buffer 3, for a minimum of 1 hour each, using a Slide-A-Lyzer Dialysis Cassette 3,500 MWCO. Following this the extract was centrifuged at 14,000 rpm for 10 minutes at 4°C and then aliquoted, snap frozen and stored at -80°C.

2.5.2 *Translation reactions*

2.5.2.1 *E.coli in vitro* transcription-translation reactions

Standard 25 μ L translation reactions were set up as follows, although volumes could be altered accordingly depending on the final volume. Note full radiation protection procedures were followed for all reactions containing 35 S-labelled methionine.

Linear DNA (~1 μ g/ μ L)

2.5 μ L

Translation premix	10 μ L
1 mM each L-amino acid (except methionine)	2.5 μ L
S-30 extract	7.5 μ L
[³⁵ S] methionine	10 μ Ci
5 μ g/ μ L anti-ssrA oligonucleotide	1 μ L
(5'-TTAAGCTGCTAAAGCGTAGTTTTTCGTCGTTTGCGACTA-3')	

Reactions were incubated at 37°C for 30 minutes and then chilled on ice for 5 minutes to stop translation. Translation products were then assayed as detailed in sections: 2.3.3 - 2.3.6.

2.5.2.2 Wheat Germ translation reactions

Wheat Germ translation reactions were carried out using the Promega Wheat Germ Extract kit. 50 μ L reactions were set up as follows, although larger translations could be performed by adjusting the volumes accordingly:

Wheat Germ Extract	25 μ L
1 mM each L-amino acids (except methionine)	4 μ L
RNA (~1 μ g/ μ L)	10 μ L
Potassium acetate	3.5 μ L
[³⁵ S] methionine	10 μ Ci
ddH ₂ O	Final volume 50 μ L

Standard reactions were incubated at 25°C for 60 minutes and then chilled on ice for 5 minutes to stop translation. As for the *E.coli* translation reactions, Wheat Germ translation products were then assayed as detailed in the following sections: 2.3.3 - 2.3.5.

2.5.3 CTABr precipitation assays

2.5.3.1 SecM constructs

After the 5 minute incubation on ice the translation products were mixed with 10 volumes of 2% (w/v) CTABr and 10 volumes of 0.5M NaOAc (pH 4.7) and incubated on ice for a further 15 minutes before being centrifuged at 13,400 rpm for 10 minutes at room temperature. Pellet and supernatant fractions were separated, the pellets were washed with 500 μ L cold acetone whilst the supernatant was incubated with 10% TCA on ice for 10 minutes before being centrifuged at 14,000 rpm for 10 minutes at 4°C. TCA pellets were then washed with 1 mL cold acetone and both pellets were then centrifuged at 14,000 rpm for 10 minutes at 4°C. The supernatants were then discarded and all pellets dried in a centrifugal evaporator at 14,000 rpm for 15 minutes. The pellets were then re-suspended in 2x sample buffer and analysed by SDS-PAGE (See section 2.4.1).

2.5.3.2 AAP and TnaC constructs

As above (Section 2.3.3.1) except following CTABr precipitation and centrifugation the pellet is re-suspended in 15 μ L 1 mg/mL RNaseA in ddH₂O and incubated at room temperature for 10 minutes. Following this 15 μ L 2x sample buffer is added and the sample analysed by resolving on tricine gels (see Section 2.4.1). The supernatant is treated the same as previously stated.

2.5.4 Pegylation assays

2.5.4.1 Pegylation assay as a test for nascent chain compaction in the exit tunnel

50 μ L *in vitro* transcription-translation reactions were carried out (see Section 2.3.2.1) with volumes altered accordingly. Once translation reactions were chilled on ice for 5 minutes they were then overlaid onto a 100 μ L sucrose cushion (0.5 M sucrose, RNC buffer) and centrifuged for 6 minutes at 100,000 rpm at 4°C using a Beckmann TLA-100 rotor. Pellets were then re-suspended on ice in 60 μ L PEG buffer before being divided in half. To one 30 μ L sample was added 30 μ L PEG buffer containing 2 mM PEG-mal (final PEG-mal concentration 1 mM) whilst to the control was added 30 μ L PEG buffer. These were then incubated on ice for 2 hours before the reaction was terminated by addition of 100 mM

DTT and incubation for 10 minutes. Samples were then CTABr precipitated by addition of 600 μL (10 volumes) 0.5 M NaOAc (pH 4.7) and 600 μL (10 volumes) 2% CTABr and incubated on ice for 15 minutes. They were then centrifuged at 13,400 rpm for 15 minutes, the supernatant was discarded and the pellet was re-suspended in 15 μL 1 mg/ml RNaseA in ddH₂O, followed by incubation at room temperature for 10 minutes. 15 μL 2x sample buffer was then added and samples were analysed by SDS-PAGE (see Section 2.4.1).

2.5.4.2 Pegylation RNaseA assay to test for nascent chain structure formation and cysteine protection.

100 μL *in vitro* transcription-translation reactions were carried out (see Section 2.3.2.1) with volumes altered accordingly. Translation reactions were chilled on ice for 5 minutes and then overlaid onto a 100 μL sucrose cushion (0.5 M sucrose, RNC buffer) and centrifuged for 6 minutes at 100,000 rpm at 4°C using a Beckmann TLA-100 rotor. Pellets were then re-suspended on ice in 60 μL PEG buffer before being divided in half. To one 30 μL sample was added 30 μL PEG buffer containing 1mg/ml RnaseA whilst to the other was added 30 μL PEG buffer. These samples were incubated at room temperature for 10 minutes before again being split in half. To one 30 μL sample was added 30 μL PEG buffer containing 2 mM PEG-mal (final PEG-mal concentration 1 mM) whilst to the control was added 30 μL PEG buffer. These were then incubated on ice for 2 hours before the reaction was terminated by addition of 100 mM DTT and incubation for 10 minutes. Samples were then CTABr precipitated by addition of 600 μL (10 volumes) 0.5 M NaOAc (pH 4.7) and 600 μL (10 volumes) 2% CTABr and incubated on ice for 15 minutes. They were then centrifuged at 13,400 rpm for 15 minutes and following this the pellet and supernatant fractions were split into separate eppendorf tubes. The pellets were washed with 500 μL cold acetone whilst the supernatant was incubated with 10% TCA on ice for 10 minutes before being centrifuged at 14,000 rpm for 10 minutes at 4°C. TCA pellets were then washed with 1 mL cold acetone and both pellets were then centrifuged at 14,000 rpm for 10 minutes at 4°C. The supernatants were then discarded and all pellets dried in a speedy vacuum at 14,000 rpm for 15 minutes. The pellets were then re-suspended in 2x sample buffer and analysed by SDS-PAGE (See section 2.4.1).

2.5.5 Puromycin release assays

Following translation (Sections 2.3.2.1 and 2.3.2.2) and incubation on ice for 5 minutes, the sample was divided in half, and to one was added puromycin to a final concentration of 1 mM whilst the other acted as a control. These were then incubated at 37°C for *E. coli* S-30 extracts or 25°C for Wheat Germ extracts for 15 minutes. Following incubation, they were placed on ice for 5 minutes before addition of an equal volume of 2x sample buffer and analysed by resolving on tricine gels (See section 2.4.1).

2.5.6 Ribosome nascent chain (RNC) stability assays

100µL translation reactions were performed as described previously in Sections 2.3.2.1 with volumes altered accordingly. The reactions were then stored at 4°C with aliquots taken at 0, 5, 24, 48 and 120 hours. Two assays were performed, samples were either overlaid onto 100 µL sucrose cushion (0.5 M sucrose, RNC buffer) and centrifuged for 6 minutes at 100,000 rpm at 4°C in a Beckmann TLA-100 rotor and pellets then re-suspended in 30 µL 2x sample buffer and analysed by SDS-PAGE (see Section 2.4.1). Alternatively the samples were precipitated by CTABr precipitation (see Section 2.3.4.1) and analysed by SDS-PAGE.

2.6 General biochemical methods and analysis

2.6.1 Gel Electrophoresis

Larger proteins (MW >15 kDa) were separated by mass on 12.5% SDS-PAGE gels whilst smaller proteins (MW <15 kDa) were resolved on tricine gels. Resolving and stacking solutions for SDS gels and separating, spacer and stacker solutions for tricine gels are outlined in Section 2.1. Following addition of 2x sample buffer the protein samples were heated at 95°C for 10 minutes. Samples were loaded alongside Pre-stained Protein Marker (New England Bioscience) on SDS gels or SeeBlue Pre-stained Standard (Invitrogen) on tricine gels. Gels were run at 100 volts for 20 minutes to allow proteins to pass through the stacking gel and then at 200 volts for the remainder until the proteins had separated sufficiently and the dye-front nearly reached the bottom of the gel. Once run, the gels were removed from the gel apparatus and soaked in destain solution (see Section 2.1.2) for 1 hour whilst shaking.

2.6.2 Autoradiography

Following gel electrophoresis and destaining, protein samples containing radiolabelled ³⁵S-methioine could be visualised by autoradiography. Gels were dried on a gel drier for approximately 1 hour at 65°C and then placed in a lightproof cassette, exposed to X-ray film for a period of time and then processed in a Kodak X-Omat processor.

2.6.3 Image J analysis

Following exposure of the gel to X-ray film, the processed films were scanned onto computer using a HP Scanjet 4850 scanner and the band intensity quantified using Image J software.

3 Sequence specificity of the SecM arrest motif

3.1 Introduction

Translational stalling peptides interact with the ribosome exit tunnel during synthesis and arrest their own translation, which in turn modulates the expression of downstream genes. It has been established that the interaction of the amino acids with the ribosome exit tunnel, and not the mRNA encoding it, which is responsible for arrest (Fang et al., 2000; Nakatogawa and Ito, 2002). The variability in the amino acid arrest sequences indicates that whilst achieving the same goal of ribosome stalling, methods of arrest and interaction within the exit tunnel differ for each peptide. Whilst there appears to be no overall sequence specificity there are some general similarities which can be seen in some, though not all, stalling peptides.

For instance, many stalling peptides such as SecM, AAP and TnaC contain a tryptophan residue 11-12 amino acids from the C-terminus that is essential for stalling (Freitag et al., 1996; Gong and Yanofsky, 2002; Nakatogawa and Ito, 2002). Upon translation arrest this residue is located close to the constriction point of the exit tunnel and is therefore thought to play an important role in communicating with the ribosome (Bhushan et al., 2011; Seidelt et al., 2009). Several peptides such as SecM and TnaC also contain a C-terminal proline residue which is located in the peptidyl transferase centre (PTC) upon stalling. A proline present in the ribosome A site upon arrest increases the stability of the peptidyl-tRNA complex (Woolhead et al., 2006), whilst the rigid nature and intrinsic properties of proline residues make formation of peptide bonds slower and would therefore further aid stalling (Pavlov et al., 2009). These patterns show that through the course of evolution there are some commonalities between stalling peptides, although they are not uniform, indicating that the combination of interactions that takes place between each peptide and the exit tunnel are unique. This chapter will specifically investigate the stalling sequence of SecM, a general introduction of which was given in Chapter 1.

Briefly, SecM is a 170 amino acid peptide which undergoes translation elongation arrest at Proline-166, 4 residues prior to the termination point. At this point tRNA-Pro166 is situated in the A site, however, a peptide bond does not form between Gly-165 and Pro-166 therefore the proline is not incorporated into the peptide (Muto et al., 2006). The

presence of the proline in the A site is still essential for translation arrest. The essential arrest motif of SecM is highlighted in Figure 3.1. Studies have shown that whilst the key arrest motif residues are critical for stalling *in vivo*, alterations to the arrest motif can be compensated for through multiple mutations of flanking residues *in vitro*, with Yap and Bernstein (2009) demonstrating that Arg-163 forms crucial interactions with the ribosomal exit tunnel that are required to induce stalling. This was supported by molecular-dynamics flexible fitting (MDFF) modelling data, which showed it is the key interaction of R163 with the ribosomal RNA (rRNA) nucleotide A2062 that is essential for stalling. This interaction results in a potential relay communication between the SecM nascent chain and the PTC to induce stalling, whilst the other key residues function to stabilise this interaction through positioning of the nascent chain within the exit tunnel (Gumbart et al., 2012).

The secondary interactions between SecM and the exit tunnel were shown by cryo-EM to include key interactions in the upper tunnel with 23S rRNA nucleotides A2062, U2585 and U2609 and in the mid-tunnel with A751 (Bhushan et al., 2011). Indeed insertion of an additional adenine residue within the 5 consecutive adenine residues A749-A753 abolished SecM stalling, highlighting that this area plays a function in nascent chain positioning (Nakatogawa and Ito, 2002). The path of the SecM nascent chain through the ribosome exit tunnel, and its position in relation to selected ribosomal proteins and rRNA residues, is shown in Figure 3.2.

The structure of the SecM nascent chain within the ribosome exit tunnel is critical to stalling as previous work has shown that compaction of the nascent chain upon arrest is essential for translation arrest (Woolhead et al., 2006). This paper also demonstrated that this movement of the nascent chain and its ability to adapt and interact with the exit tunnel is mediated by the amino acid sequence of the nascent chain as mutation of non-essential C-terminus residues S157, Q158 and Q160 to proline prevented compaction which in turn abolished stalling.



Figure 3.1 C-terminal 44 residues of SecM. Schematic diagram illustrating the portion of SecM required for optimal stalling, with the essential arrest motif residues highlighted in red. The arrest point at P166 is indicated by the arrow.

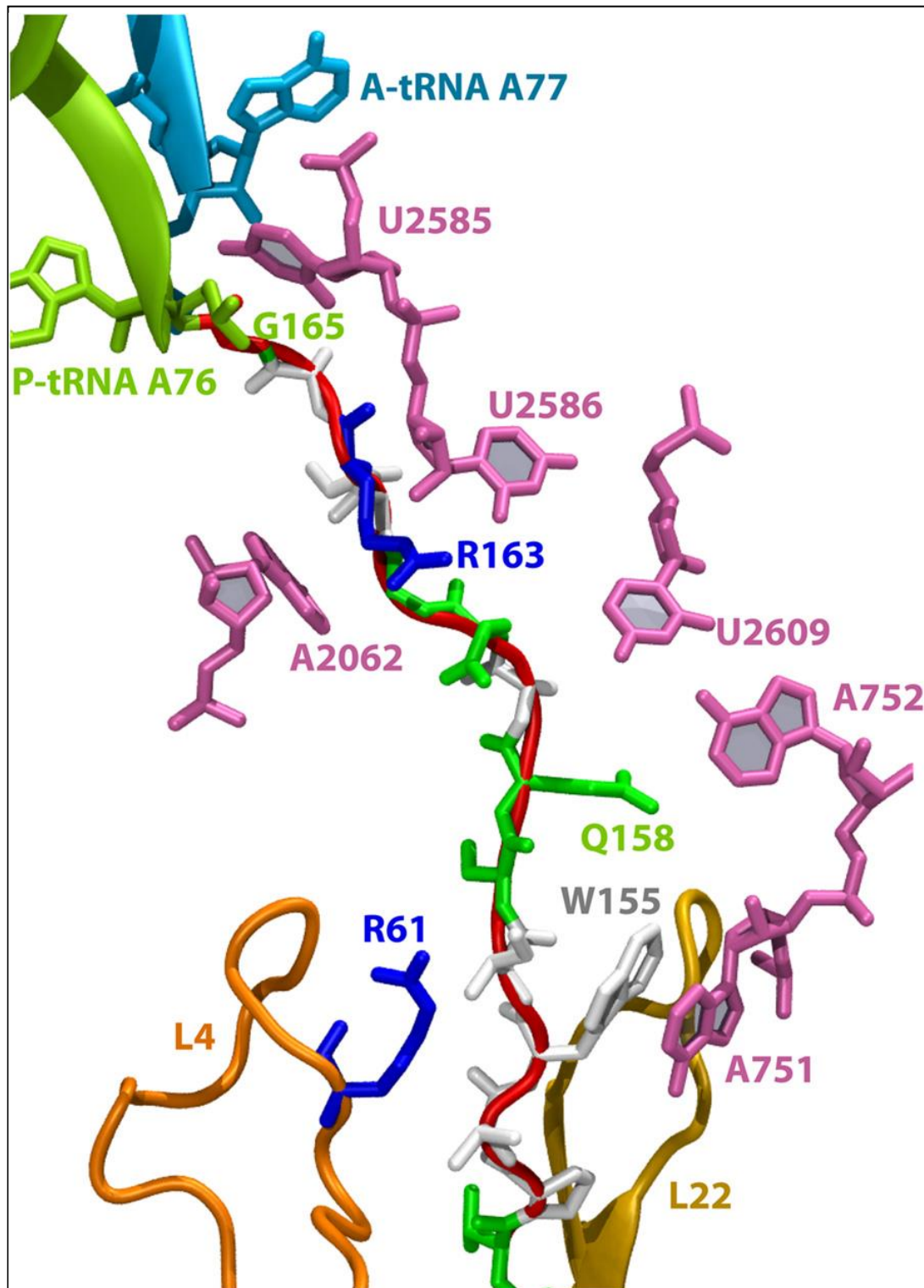


Figure 3.2 MDFF modelling of the SecM nascent chain indicating its path through the ribosome exit tunnel. SecM is shown in red cartoon with stick form overlaid (blue – basic residue; green – hydrophilic; and white – hydrophobic). Also shown are the key ribosomal rRNA nucleotides, L4/L22 proteins forming the constriction point and A- and P-tRNAs. Diagram reproduced from Gumbart et al., (2012).

Proline residues play an important role in the structure of the nascent chain as they restrict the flexibility of the nascent chain and therefore affect its movement within the exit tunnel (Schimmel and Flory, 1968). The P153A mutation is important because Proline-153 is a non-essential residue which upon stalling and compaction of the nascent chain is situated at a key site within the exit tunnel, close to the constriction point 20-35Å from the PTC (Bhushan et al., 2011). Whilst the cyclic structure of the proline side chain creates a rigid conformation, mutation to alanine, which has a small methyl side group (-CH₃), increases the flexibility of the nascent chain. Woolhead et al., (2006) demonstrated that whilst wild type SecM could not undergo translation arrest in mutant ribosomes possessing expanded exit tunnels (Δ 82-84 L22), incorporation of the P153A mutation recovered arrest of SecM peptides. The restoration of key interactions between the nascent chain and the ribosome exit tunnel re-enabled compaction of the nascent chain and subsequent translational stalling.

It has previously been shown that whilst SecM150-166 encompasses the essential arrest motif, when truncated constructs are translated SecM140-166 is more efficient at stalling than the shorter SecM150-166 minimum stalling sequence (Nakatogawa and Ito, 2002). This suggests that the residues further away from the C-terminus, whilst not forming essential interactions with the exit tunnel still play an important role in positioning the residues further up the nascent chain closer to the PTC, in particular Arg163. Therefore, it remained to be explored whether increased freedom of movement out with the essential arrest motif, could also influence positioning of the key residues at the C-terminus of the SecM nascent chain.

The purpose of this work is to further investigate the sequence specificity of the SecM arrest motif, in particular what properties of these amino acids are essential for their interaction with the exit tunnel to enable their role in positioning Arg-163. To do this the essential arrest residues were individually mutated to alanine and also to conservative amino acids (see Table 3.1 for structures) in order to determine what affect this has on translation arrest. Following this, in order to study the influence of nascent chain flexibility on stalling, double mutants containing alteration of a non-essential proline residue to alanine at positions within (P153A) and outwith (P146A) the key arrest motif were created and analysed.

Residue No.	Original residue	Alanine	Conservative
150	 Phenylalanine	 Alanine	 Tyrosine
155	 Tryptophan	 Alanine	 Tyrosine
156	 Isoleucine	 Alanine	 Leucine
161	 Glycine	 Alanine	 Serine
162	 Isoleucine	 Alanine	 Leucine
163	 Arginine	 Alanine	 Lysine
164	 Alanine		 Glycine
165	 Glycine	 Alanine	 Serine

Table 3.1 Molecular structures of the amino acid residues that were altered in the SecM mutant constructs.

3.2 Results

In this chapter the specificity of the SecM stalling sequence will be examined through analysis of SecM mutants by CTABr (Cetyltrimethylammonium bromide) precipitation. Details of the constructs and mutants used in this section can be found in Appendix 3. The expression and stalling of these constructs was analysed through *in vitro* coupled transcription-translation assays, containing radiolabelled methionine, followed by CTABr precipitation, see Section 2.3.3 for methods. CTABr binds to and precipitates RNA and by association, RNA-protein complexes. Therefore in these experiments CTABr precipitates SecM that is stalled on the ribosome, due to its covalent attachment to the tRNA-Gly, (Gilmore et al., 1991). By performing these assays containing a radiolabelled tracer amino acid, translation products can be purified, separated by SDS-PAGE and visualised by autoradiography, see Section 2.4.

Point mutations were introduced into the SecM constructs by site-directed mutagenesis, see Section 2.2.5.3.1, and were confirmed by DNA sequencing, see Section 2.2.11. The amino acid residues mutated to alanine are shown schematically in Figure 3.3A. To confirm the importance of these arrest motif residues, as identified by Nakatogawa and Ito (2002) by alanine scanning mutagenesis in an *in vivo* experimental system, initial CTABr precipitation experiments were carried out on SecM constructs containing single alanine mutations (Figure 3.3B). The results for wild type SecM are shown in Lanes 1 & 2, with the majority of the translation product in the pellet fraction. This represents the arrested SecM as it migrated further than the full-length SecM, of which there is a small amount present in both the pellet and supernatant fractions. The individual mutant SecM peptides had different translation capabilities, as seen by the varying total intensities on the gel (Figure 3.3B; Lanes 3-20), this is natural variation due to the efficiency of translation of each mutant construct.

The results shown in Figure 3.3B support the ability to reproduce the Nakatogawa and Ito (2002) findings *in vitro* by confirming the importance of the essential arrest motif residues, as only G165A was able to maintain any degree of stalling (Figure 3.3B; Lane 17). This residue is located in the ribosome P site upon stalling and therefore, unlike the other residues, which are located within the exit tunnel, may be able to accommodate the minor glycine to alanine mutation more effectively whilst still being an essential residue for

efficient stalling. The effect of the P153A mutation was also examined and it was confirmed that this mutation has no effect on stalling, with the levels of arrested peptide remaining the same as wild type SecM (Figure 3.3B; Lane 5).

The next step was to examine the effect of an increase in the freedom of movement of the SecM nascent chain to accommodate the mutation of essential residues. To do this the P153A mutation was introduced into the single alanine mutant constructs, to create constructs containing double mutations. The results of the CTABr experiments are shown in Figure 3.3C and all the results are summarised in Figure 3.4. The data indicate that, with the exception of R163A and G165A, increased flexibility of the nascent chain allowed alanine mutations of the essential arrest motif residues to be better accommodated. In particular the highest level of stalling was reintroduced when F150A or G161A mutations were coupled with P153A (Figure 3.3C; Lanes 3 & 9). These results indicate that residue 165, which is located in the ribosome P site is important for arrest but is not influenced by the positioning of the SecM nascent chain within the exit tunnel, as an increase in flexibility has no further increase in stalling (Figures 3.3B & C; Lanes 17 & 15 respectively). These results also highlight that the proximity of the alanine mutation to P153A is not a factor, with G161A/P153A (Figure 3.3C; Lane 9) having greater stalling than either W155A/P153A or I156A/P153A (Figure 3.3C; Lanes 5 & 7 respectively). The only alanine mutation that cannot be accommodated regardless of an increase in the flexibility of the nascent chain is R163A (Figures 3.3B & C; Lanes 15 & 13 respectively). This supports previous work by Yap and Bernstein (2009), which indicated that R163 is the sole essential residue with the other key arrest motif residues responsible for its correct positioning, enabling it to interact with rRNA nucleotide A2062 and initiate translation arrest.

These results are representative of multiple experiments and the double mutant I162A/P153A consistently ran at a higher molecular weight. For these calculations the higher top band was taken as the full length and the lower band as the arrested, despite it running at the same weight as the full length peptide in the other lanes. This higher molecular weight could be due to altered processing of the peptide causing it to run at a higher molecular weight. However, further tests such as mass spectrometry would need to be carried out to confirm this is the correct product that is present.

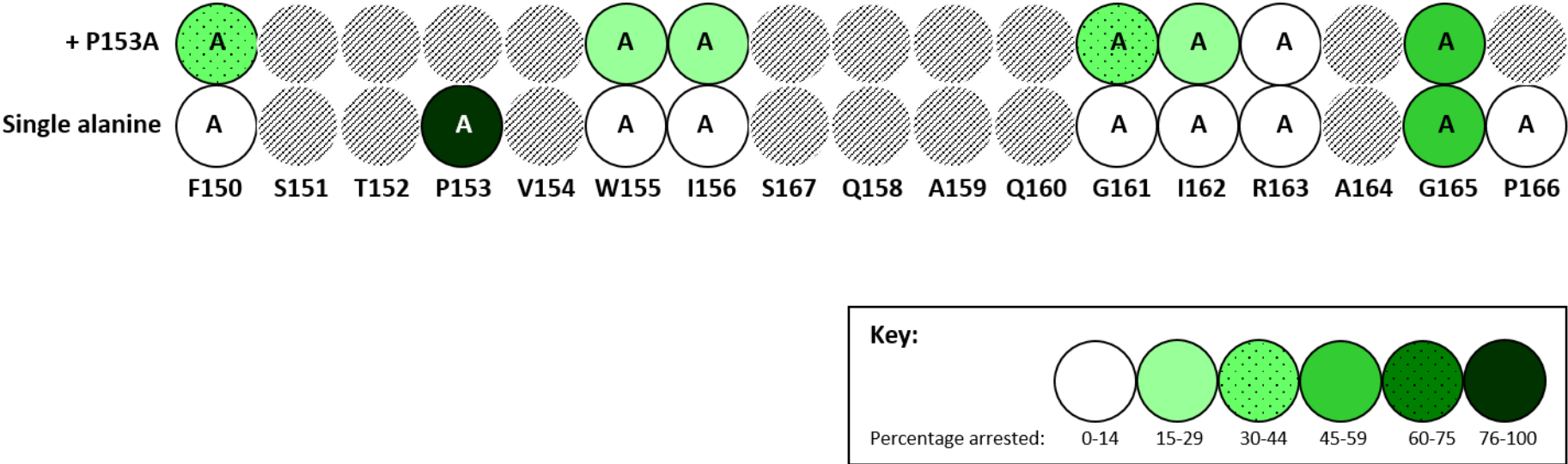


Figure 3.4 Summary of stalling of single and double SecM alanine mutants. Illustration of the effects of individual alanine mutations both on their own and in tandem with the P153A mutation based on the percentage stalling in the CTABr experiments shown in Figure 3.3B & C. Solid circles indicate the residues which were mutated and the key indicates the shading corresponding to the percentage arrested.

The key properties of the essential arrest motif amino acids were then investigated by individually mutating these residues to conservative amino acids, see Figure 3.5A, to identify whether the size or properties of the amino acid were critical to its involvement in translation arrest. The stalling capabilities of these mutants were analysed by CTABr precipitation as before (Figure 3.5B). Mutants of P166 were not made as it was previously shown by Nakatogawa and Ito (2002), and supported by the results in Figure 3.3B, that this proline is an essential residue required for stalling to occur. An illustration of the structures of the amino acids that were altered in these experiments are given in Table 3.1 for reference.

These results indicate that G165S retains levels of stalling analogous to wild type SecM (Figure 3.5B; Lane 17). This indicates that the properties of a serine residue can substitute for glycine and that despite having a larger side chain, this is not detrimental to stalling. F150Y and I156L (Figure 3.5B; Lanes 3 & 7) maintained levels of stalling of approximately 50% to that of wild type SecM (Figure 3.5B; Lane 1). When these residues are replaced with alanine, SecM stalling is abolished (Figure 3.3B; Lane 3 & 9), this suggests that the structure of these side chains is important for their function.

W155Y, G161S and A164G stalling is approximately 20% to that of wild type SecM (Figure 3.5B; Lanes 5, 9 & 15 respectively), whilst I162L and R163K have the lowest stalling capability (Figure 3.5B; Lanes 11 & 13 respectively), which is equivalent to that of their respective alanine mutants (Figure 3.3B; Lanes 13 & 15 respectively). These results support previous work that identified R163 as the key residue for translation arrest as both its presence and exact position were critical (Yap and Bernstein, 2009). In addition these results show that the residues surrounding R163 cannot tolerate mutation, even to conservative amino acids, as efficiently as residues further away.

Following this, the P153A mutation was incorporated into the single conservative mutant constructs to examine whether an increase in the freedom of movement at this region of the nascent chain could further accommodate the conservative mutations, thus allowing further examination of what properties of these amino acids are necessary for stalling. The results of these CTABr experiments are shown in Figure 3.5C and all results are summarised in Figure 3.6. The data show that increased flexibility in the lower region of the arrest motif

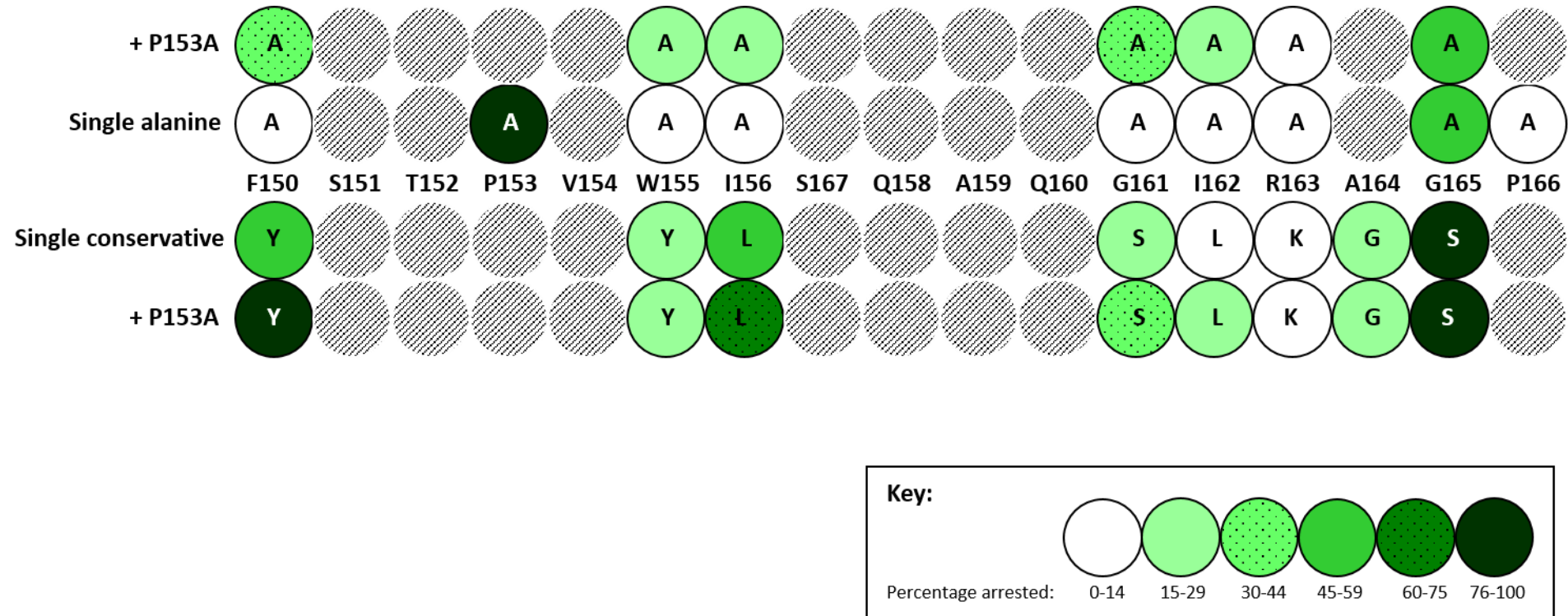


Figure 3.6 Summary of stalling of single and double SecM alanine and conservative mutants. Illustration of the effects of individual alanine and conservative mutations both on their own and in tandem with the P153A mutation based on the percentage stalling in the CTABr experiments shown in Figures 3.3B & C and 3.5B & C. Solid circles indicate the residues which were mutated and the key indicates the shading corresponding to the percentage arrested.

within the exit tunnel has no further effect on the level of stalling of the G165S construct (Figure 3.5C; Lane 17). Likewise for W155Y, R163K and A164G it did not result in significant changes in levels of arrest (Figure 3.5C; Lanes 5, 13 & 15 respectively). The constructs which did show an increase in arrest with the double mutation were F150Y, I156L, G161S and I162L (Figure 3.5C; Lanes 3, 7, 9 & 11 respectively). As can be seen in the schematic diagram in Figure 3.5A, these residues are spaced apart on the nascent chain and not necessarily close to the P153A mutation, indicating that it can have a far ranging influence.

These results establish the importance of increased flexibility of the nascent chain in allowing the arrest essential amino acid residues to re-position and interact with the exit tunnel and in turn compensate for the mutation of key residues. To further investigate this, the influence of increased freedom of movement in the nascent chain, outwith the arrest motif, was examined by mutating the proline residue at position 146 to alanine, as illustrated in Figure 3.7A. This residue is situated 4 amino acids upstream from the last residue of the arrest sequence, F150, and according to the study of Bhushan et al., (2011) is located beyond the exit tunnel constriction site upon compaction and stalling. CTABr precipitation assays show that, like the P153A mutation, the proline at position 146 can be mutated to alanine with no effect on the arrest efficiency of SecM (Figure 3.7B; Lane 3).

Coupled *in vitro* transcription-translation assays were then carried out using a ribosome extract derived from cells harbouring a deletion of residues 82-84 in the conserved β -hairpin of the L22 protein. This mutation results in ribosomes with expanded exit tunnels but has no significant effect on translation (Chittum and Champney, 1994; Gabashvili et al., 2001). Previous experiments examining SecM translation arrest in these mutant ribosomes have shown that arrest is severely impeded, however, when combined with the P153A mutation, arrest was restored (Woolhead et al., 2006). The increased flexibility of the nascent chain is believed to enable correct positioning of the key amino acid residues in the expanded ribosome exit tunnel. The results of CTABr experiments to observe the effect of the P146A mutation in these ribosomes are shown in Figure 3.7C. Whilst the P153A mutation restores stalling capability (Figure 3.7C; Lane 7), these experiments indicate that SecM P146A (Figure 3.7C; Lane 5) has equivalent levels of stalling to wild type SecM (Figure 3.7C; Lane 3) suggesting that an increase in flexibility further from the

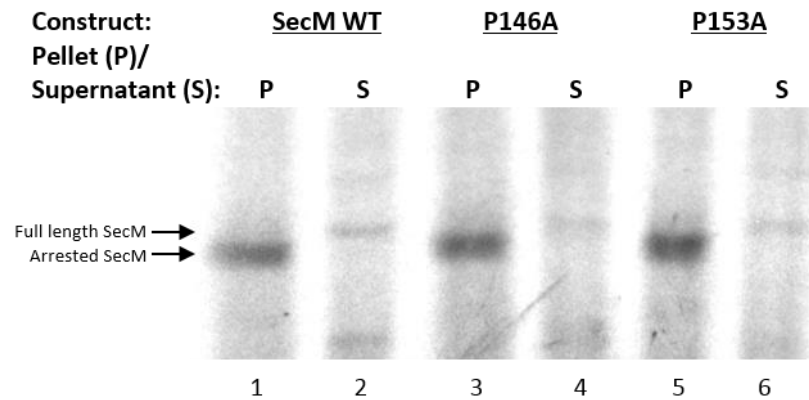
C-terminus and out with the arrest motif is unable to sufficiently influence the positioning of the residues within it.

To confirm this, further experiments were performed in which the P146A mutation was introduced into three of the conservative mutation constructs: F150Y, I156L and G161S, as well as into the double mutants: F150Y/P153A, I156L/P153A and G161S/P153A. These conservative mutants were selected as they have been shown to increase stalling when combined with the double mutation of P153A (Figure 3.5C; Lanes 3, 7 & 9 respectively). In addition to this a double mutant containing P146A/P153A was also created and tested and, as with the separate proline to alanine mutations, the level of stalling was analogous to wild type SecM (Figure 3.8; Lane 3). When the double P146A mutants were translated *in vitro* and CTABr precipitated the levels of stalling were lower than single conservative mutations (Figure 3.8; Lanes 5, 7 & 9). Whilst the F105Y and I156L reductions were not significant the G161S/P146A mutation appears to abolish stalling. Further experiments would need to be carried out to confirm why this occurs but it may be that freedom of movement in the 146 region of the nascent chain results in misplacement of the peptide chain further up the exit tunnel. When combined with P153A in a triple mutation (Figure 3.8; Lanes 11, 13 & 15) levels of stalling were comparable with that of the P153A double mutation (Figure 3.5; Lanes 3, 7 & 9) indicating that P153A can compensate and rescue stalling. The results are summarised in Figure 3.9 and they support the previous results of this chapter that show that increased flexibility out with the arrest motif does not enable repositioning of residues closer to the C-terminus and therefore cannot compensate for mutation of the key arrest motif residues.

A.



B.



C.

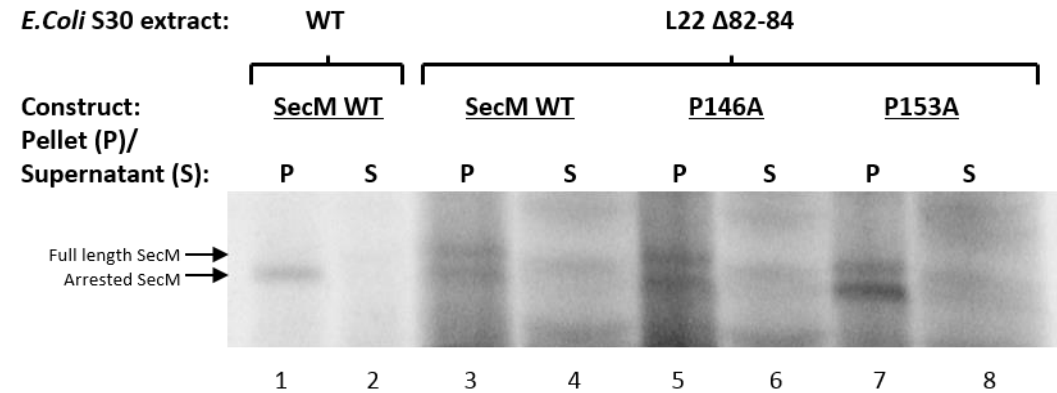


Figure 3.7 Stalling of selected SecM peptides in mutant ribosome exit tunnels. A. Schematic diagram indicating the position of the P146A and P153A mutations introduced into SecM constructs. The key arrest residues are highlighted in bold and underlined and the arrest point, Proline-166, is indicated by an arrow. B. SecM WT, P146A and P153A were translated *in vitro* and CTABr precipitated, separated into pellet (P) and supernatant (S) fractions and resolved by SDS-PAGE. C. The constructs indicated were translated in coupled *in vitro* transcription-translation assays containing wild type *E. coli* S30 cell extract or cell extract derived from *E. coli* strains containing ribosomal deletion mutations of residues 82-84 of the L22 protein, which results in an expanded exit tunnel. The reactions were precipitated by CTABr, separated into pellet (P) and supernatant (S) fractions and resolved by SDS-PAGE. All gels are representative of multiple experiments.

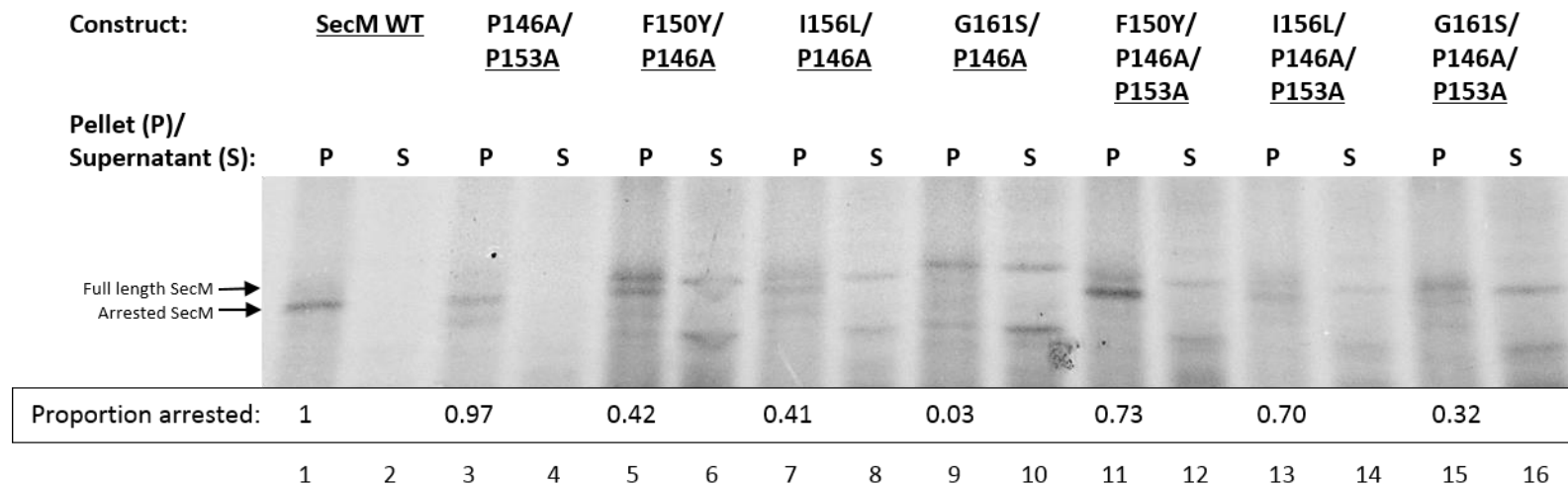


Figure 3.8 Stalling of double and triple SecM conservative mutants. SecM WT, P146A/P153A double mutant, double conservative mutations coupled with P146A and triple conservative mutations coupled with both P146A and P153A mutations were translated *in vitro* and CTABr precipitated, separated into pellet (P) and supernatant (S) fractions and resolved by SDS-PAGE. The percentage of arrested SecM was quantified by Image J software and calculated as a percentage of [Arrested/(Arrested + Total full length)], with each value adjusted for background. These values were then normalised to wild type SecM to calculate proportion arrested. All gels and percentages are representative of multiple experiments.

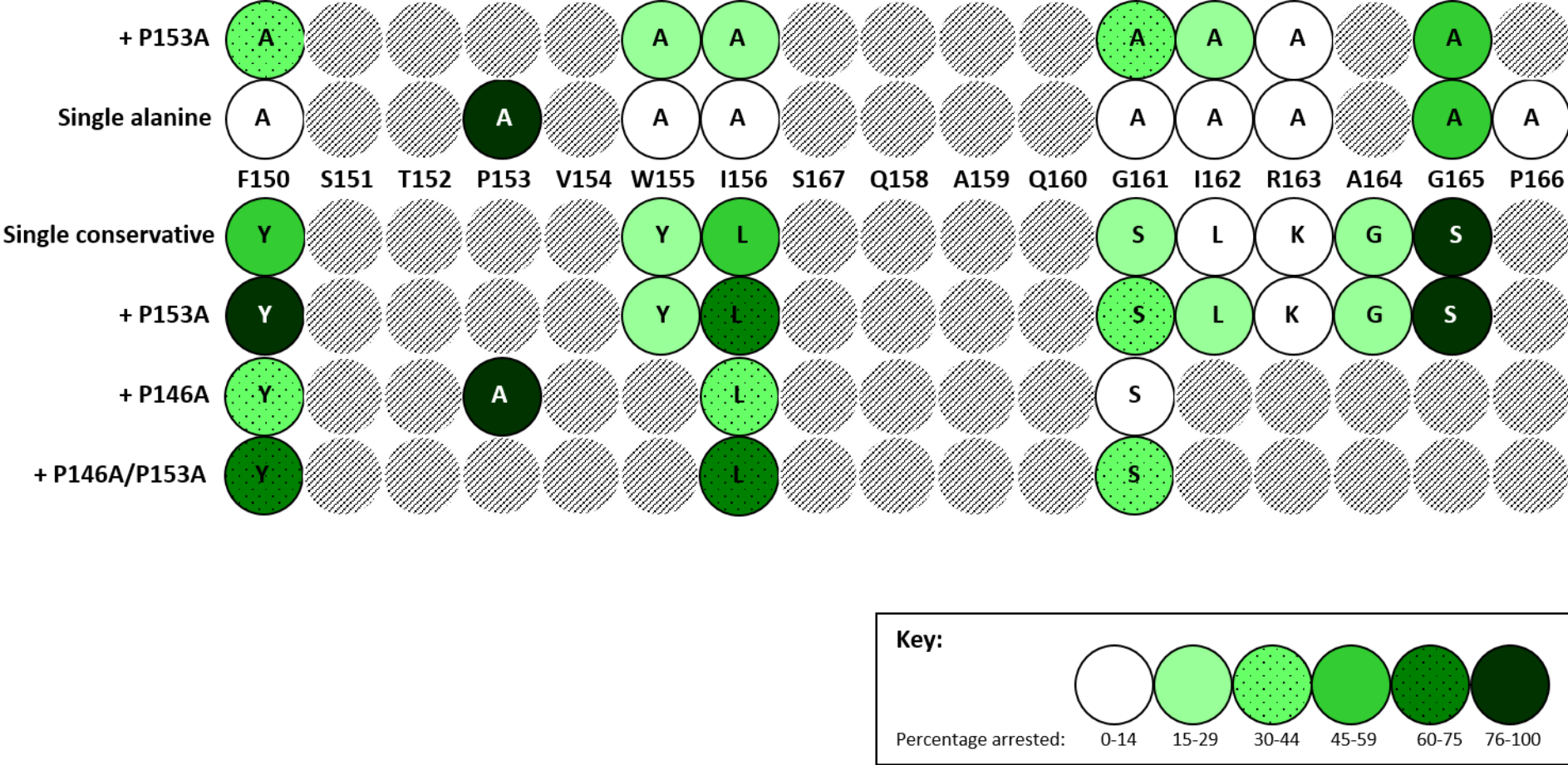


Figure 3.9 Full summary of the stalling results of all the SecM mutants in this study. Summary of the results of the CTABr precipitation experiments for all alanine and conservative mutations of the key arrest residues shown in Figures 3.3B & C, 3.5B & C and 3.8. Solid circles indicate the residues which were mutated and the key indicates the shading corresponding to the percentage arrested.

3.3 Conclusion

The results of the single alanine SecM mutants assayed in this study (Figure 3.3B) support the results of the alanine scanning mutagenesis conducted by Nakatogawa and Ito (2002), with some slight differences. Nakatogawa and Ito (2002) showed that Pro-166 and Arg-163 residues are essential; whilst Trp-155, Ile-156 and Gly-165 are important; and Phe-150, Gly-161, Ile-162 and Ala-164 are partially required for stalling. However, the results presented here show that G165A is the only alanine mutant able to maintain any degree of stalling, with nearly half the level of stalling relative to wild type SecM (Figure 3.3B; Lane 17). Both studies assayed SecM stalling by CTABr precipitation with the experiments presented here were carried out *in vitro* using *E.coli* cell extract whilst Nakatogawa and Ito (2002) conducted their experiments *in vivo* in *E.coli*. By performing the same assays but in coupled transcription-translation systems in the absence of any intrinsic factors, it appears to augment the effect of the mutations.

Upon stalling, interactions between the SecM nascent chain and the ribosome exit tunnel result in the P site tRNA adopting an altered conformation within the PTC; hindering peptide bond formation between Glycine-165 and Proline-166 in the A site (Bhushan et al., 2011). The ability of SecM to maintain a degree of stalling with the G165A mutation may be accounted for due to the fact that glycine (-H) to alanine (-CH₃) is a relatively simple exchange as there is no loss or gain of a major side chain. It could be speculated that in order to maintain stalling then the tRNA-Ala may also be capable of undergoing a similar ratcheting motion to tRNA-Gly, however, this cannot be confirmed from this study. The glycine residue also appears to be able to tolerate alteration more effectively in the PTC than when it is located in the exit tunnel at residue G161. In this situation the amino acid may be responsible for interacting with the tunnel wall or positioning the nascent chain within the tunnel, as the Glycine-161 to alanine modification has major implications on the stalling capability of the SecM peptide (Figure 3.3B; Lane 11). These results also indicate that when the SecM nascent chain is arrested residue 165, situated in the ribosome P site, is not influenced by the positioning of the nascent chain within the exit tunnel, as an increase in flexibility at P153A has no further increase in levels of stalling (Figures 3.3B & C; Lanes 17 & 15 respectively). As stated previously, the importance of G165 is in the shift the tRNA undertakes which prevents the formation a peptide bond with Proline-166 upon

stalling, this appears to be due to alterations within the PTC and cannot be optimised by the positioning of the nascent chain within the exit tunnel.

However, an increase in the flexibility of the nascent chain does increase stalling for some of the other SecM mutants, most notably, F150A and G161A. These residues are located apart on the arrest motif (see Figure 3.3A), upon stalling F150 is situated close to the L22 constriction site whilst G161 is positioned just below the rRNA nucleotide A2062, which forms important interactions with R163 (Bhushan et al., 2011). As noted previously, these residues are not concentrated in a small area of the nascent chain, indicating that this increased freedom of movement of P153A enables the repositioning of the essential amino arrest motif portion of the SecM nascent chain. There are, however, still some of the double mutants, W155A/P153A and I156A/P153A, which do not recover stalling effectively (Figure 3.3C; Lanes 5 & 7). These residues form an important contact with rRNA nucleotide A751 (Bhushan et al., 2011), which may require highly specific interactions with the wild type amino acids that in the case of the mutants cannot be compensated for by the ability to adapt the structure of the nascent chain.

The respite to stalling provided by the introduction of P153A is notable but the improvements are not complete as stalling is not restored to wild type levels, see Figure 3.4 for summary. This is likely to be because, despite the potential repositioning of the nascent chain provided by this increase in flexibility, the alanine in place of the key arrest residue is still lacking the vital properties required to interact with the exit tunnel and induce efficient stalling. To explore further what these properties might be, for example the shape or charge of the amino acid, the CTABr experiments were performed using SecM constructs with conservative mutations of the key arrest residues. The results of these experiments are shown in Figures 3.5B & C and summarised in Figure 3.6.

Despite the G165S mutation involving the addition of a larger serine side chain (-CH₂-OH), in place of the simple glycine (-H) side chain, this was the only construct capable of maintaining levels of translation arrest analogous to wild type SecM. There is genetic evidence for a serine residue at position 165 in SecM variants of other species, including *Mannheimia succiniciproducens*, which may account for its ability to maintain wild type levels of stalling in *E.coli* SecM. Also this P site tRNA undergoes a 2 Å shift in the ester

linkage upon stalling (Bhushan et al., 2011), therefore it is the ratcheting motion of the tRNA and impediment of peptide bond formation, as opposed to the direct properties of the amino acid side chain, which appear important for stalling at this position.

A164 is the last residue to be located in the exit tunnel upon stalling and translation arrest is reduced by ~75% in A164G SecM mutants in comparison to wild type SecM (Figure 3.5B; Lanes 15 & 1 respectively). Despite both alanine (-CH₃) and glycine (-H) having small side chains, the methyl group of the alanine residue must still have an important role in translation arrest and the communication of the stalling signal to the PTC. As might be expected, increased flexibility further down the tunnel at P153A has no effect on the stalling capability of this mutant (Figure 3.5C; Lane 15). A164 is located above the critical R163 in the exit tunnel and upstream alterations serve to position R163 correctly but do not appear to be able to compensate for alterations above this.

Alteration of R163 to another similar basic amino acid still abolishes stalling (Figure 3.5B; Lane 13) therefore it remains unknown what are the critical elements about arginine that are required to induce translation arrest. Interaction between arginine and the ribosome exit tunnel does not appear to be transient as it is so highly specific, instead it suggests that the arginine residue may bind within a specific rRNA pocket; interacting with rRNA nucleotide A2062, to induce structural changes that signal to the PTC leading to the ratcheting of the tRNA moiety and ultimately translational stalling (Bhushan et al., 2011). Having such a highly specific location and amino acid requirement is critical as this reduces the chances of similar peptides wrongly inducing translation arrest.

Interaction with A2062 has also been shown to be a key factor in translation arrest for several other stalling peptides such as the erythromycin resistance gene *ermC* (Vazquez-Laslop et al., 2010; Vazquez-Laslop et al., 2008). However, despite being conserved amongst SecM homologs, arginine is not conserved at this position in other stalling peptides. For instance the residue -2 from the PTC, and a critical factor for stalling in ErmAL1 and ErmCL, is alanine and phenylalanine respectively (Ramu et al., 2011). It is interesting to note that these inducible stalling peptides require the presence of erythromycin for stalling and the binding of this antibiotic occurs at this region and acts to bring the nascent chain in close proximity to the A2062 residue (Vazquez-Laslop et al.,

2008). Therefore other factors can enable different amino acids to function in this position and form the necessary interactions with A2062 to induce stalling.

The specificity of the nascent chain is complex as the same conservative mutations have different degrees of influence on stalling depending on where in the nascent chain they occur. For instance, I162, which is located beside the critical R163 and may also have subsidiary interactions with A2062 (Bhushan et al., 2011), does not tolerate conservative mutation to leucine and cannot be greatly compensated for by an increase in flexibility at P153A (Figures 3.5B & C; both Lane 11). However, further down the nascent chain I156L has relatively high levels of stalling for the same amino acid modification (Figures 3.5B & C; both Lane 7) and likewise G161S and G165S have greatly different effects (Figures 3.5B & C; Lanes 9 & 17 respectively). This illustrates the complex picture of interactions which take place within the exit tunnel and highlights that it is not necessarily the properties of the amino acids that are key but also where they are located within the exit tunnel; with those residues closer to R163 having higher specificity.

Both W155 and I156 have both been shown to make contact with the exit tunnel at rRNA nucleotide A751 (Bhushan et al., 2011) and insertion of additional nucleotides here also abolishes stalling (Nakatogawa and Ito, 2002). However, it is the tryptophan which appears to be the more essential residue, with low stalling when it is mutated to phenylalanine and no great increase in stalling with the additional P153A mutation (Figures 3.5B & C; both Lane 5) despite the close proximity of these residues to each other in the nascent chain (Figure 3.5A). I156 meanwhile still maintains approximately 50% stalling when mutated to leucine and this can be further enhanced by the increase in flexibility at P153A (Figures 3.5B & C; both Lane 7). This correlates with previous data which has shown that a tryptophan residue 11-12 amino acids from the PTC is an essential feature which is conserved amongst other stalling peptides such as TnaC (Gong and Yanofsky, 2002).

It is perhaps not surprising that the residue furthest from R163 has the greatest scope for alteration, with F150Y the most accommodating of the conservative mutations, with over 50% stalling compared to wild type SecM, which increases to ~80% with the P153A double mutation (Figures 3.5B & C; both Lane 3). This also highlights how

rearrangements in the lower part of the arrest motif can influence stalling despite this predominantly being based on the positioning of residues (R163) further up the exit tunnel near the PTC.

The recovery of stalling function enabled by the P153A mutation indicates this can compensate for the alteration of key arrest residues by improving the flexibility of the nascent chain and enabling it to reposition within the ribosome exit tunnel. The next step was to examine if an increase in flexibility further from the C-terminus, and outwith the arrest motif, could also influence the positioning of the essential amino acid arrest residues. The next proline residue in the SecM sequence is P146, but whilst removal of this restrictive proline residue for alanine had no detrimental effect on stalling (Figure 3.7B; Lane 3), it had no ability to recover stalling in SecM mutants (Figure 3.8). This is most likely due to the fact the P146 residue is located beyond the ribosome exit tunnel constriction point (Bhushan et al., 2011), which appears to null any ability to influence SecM nascent chain positioning closer to the PTC. Therefore an increase in flexibility of the nascent chain is only beneficial in the region within the arrest motif which is located in the upper tunnel upon arrest.

Finally, these results have shown that a combination of both nascent chain flexibility within the arrest motif, and amino acid specificity are required for SecM stalling. The SecM nascent chain is highly dynamic within the exit tunnel and is able accommodate mutations of essential residues to varying degrees. Some residues are more important than others in particular those located close to, and including, the essential R163 residue. Outwith R163, this work highlights that it is not necessarily how an individual residue behaves on its own, but how the C-terminus of SecM as a whole combines to position the key R163 residue. The ability of the P153A mutation to recover stalling of some mutants indicates that these SecM peptides must position themselves differently within the tunnel to allow the more effective communication of the stalling signal to reach the PTC. To confirm what repositioning each mutant undergoes it would be necessary to undertake cryo-EM for each mutant, this would be highly beneficial as it may reveal common rearrangements or exit tunnel connections to identify which of the contacts are key for the correct positioning of R163.

4. Compaction of the SecM nascent chain upon translation arrest

4.1 Introduction

With a length of approximately 100 Å from the peptidyl transferase centre (PTC) to the exit on the base of the large subunit, and a width ranging from 10-20 Å, the dimensions of the ribosome exit tunnel potentially allow attainment of a limited degree of secondary structure of the nascent chain during translation and passage through the large subunit (Ban et al., 2000; Nissen et al., 2000). In addition to this, the ribosome exit tunnel also provides a favourable environment for secondary structure formation as the conditions entropically stabilise alpha helix formation (Ziv et al., 2005). Indeed, studies have confirmed that the formation of alpha helices can occur at various points within the exit tunnel (Bhushan et al., 2010a; Lu and Deutsch, 2005a, b; Woolhead et al., 2004). However, formation of other secondary structure such as β -sheets, or more advanced tertiary structures, is restricted by the size constraints of the exit tunnel and has only been shown to occur at the distal end of the ribosome exit tunnel (Gilbert et al., 2004; Kosolapov and Deutsch, 2009; Robinson et al., 2006; Tu et al., 2014). Although the conditions are favourable, different peptides behave and interact uniquely within the exit tunnel and so not all peptides will form secondary structure. For instance, FRET-based experiments demonstrated that the transmembrane segment of a nascent membrane protein compacted within the ribosome exit tunnel whilst the secreted pre-prolactin protein (PPL) traversed the exit tunnel in an extended conformation (Woolhead et al., 2004).

Formation of secondary structure within the ribosome is relevant to translation arrest as studies have revealed that some stalling peptides, such as *E. coli* SecM and CGS1 in *Arabidopsis thaliana*, undergo compaction in the exit tunnel upon translation arrest (Onoue et al., 2011; Woolhead et al., 2006). This compaction acts to position key residues within the exit tunnel allowing interactions to take place between the nascent chain and the tunnel walls, thus enabling stalling signals to be transmitted to the PTC. For instance, in the case of SecM, the positioning of R163 is critical for translation arrest to occur (Gumbart et al., 2012; Woolhead et al., 2006; Yap and Bernstein, 2009). It is termed compaction as folding is not necessarily fully alpha helical and does not occur throughout the length of the nascent chain within the ribosome exit tunnel, (Woolhead et al., 2006). Only some stalling

peptides rely on compaction to achieve the correct positioning of key residues and this is not a uniform occurrence as some stalling peptides, such as *E.coli* TnaC and *N.crassa* AAP, have been shown to remain in an extended conformation upon stalling (Seidelt et al., 2009; Wu et al., 2012).

Previous studies by Woolhead et al., (2006) using FRET assays have revealed that the SecM peptide undergoes compaction at the C-terminus upon translation arrest and this compaction is essential for stalling. This arrest occurs through a series of reciprocal interactions between the nascent chain and the exit tunnel, which are triggered by the addition of Proline-166 to the PTC A site, and functions to correctly position the key arrest residues to enable translation stalling (Woolhead et al., 2006). Molecular-dynamics flexible fitting (MDFF) modelling has further refined this initial discovery to reveal that this compaction occurs between residues W155 and R163, shortening the distance between the two residues from the ~31 Å that would be expected if the peptide was in an fully extended conformation to 24 Å. This compaction was shown to locate and stabilise R163 in the vicinity of the 23S nucleotide A2062, the residue responsible for communicating stalling signals to the PTC (Gumbart et al., 2012).

Compaction of SecM upon translation arrest was further investigated in this study using a pegylation assay, a technique which has been modified from that previously described by Lu and Deutsch (2005a & b). These assays employ methoxy-polyethylene glycol maleimide (PEG-mal), which has a molecular weight of 5 kDa and binds covalently to the thiol groups of cysteine residues and results in an increase in the apparent molecular weight of the protein when separated on an SDS gel, see Figure 4.1A. These assays involve performing coupled *in vitro* transcription-translation, containing radiolabelled methionine, to produce stalled ribosome-nascent chain complexes. Exposed cysteine residues of the stalled nascent chains in these complexes are then mass-tagged with PEG-mal and detected by gel shift assay. PEG-mal is too large a molecule to enter the ribosome exit tunnel and therefore only cysteine residues on stalled nascent chains that are located outside of the ribosome exit tunnel will be exposed to pegylation (Lu and Deutsch, 2001), see Figure 4.1B. As SecM contains no native cysteine residues it can be selectively mutated to include single cysteine residues that are specifically located near to the end of the ribosome exit tunnel when the peptide stalls, see Figure 4.1C.

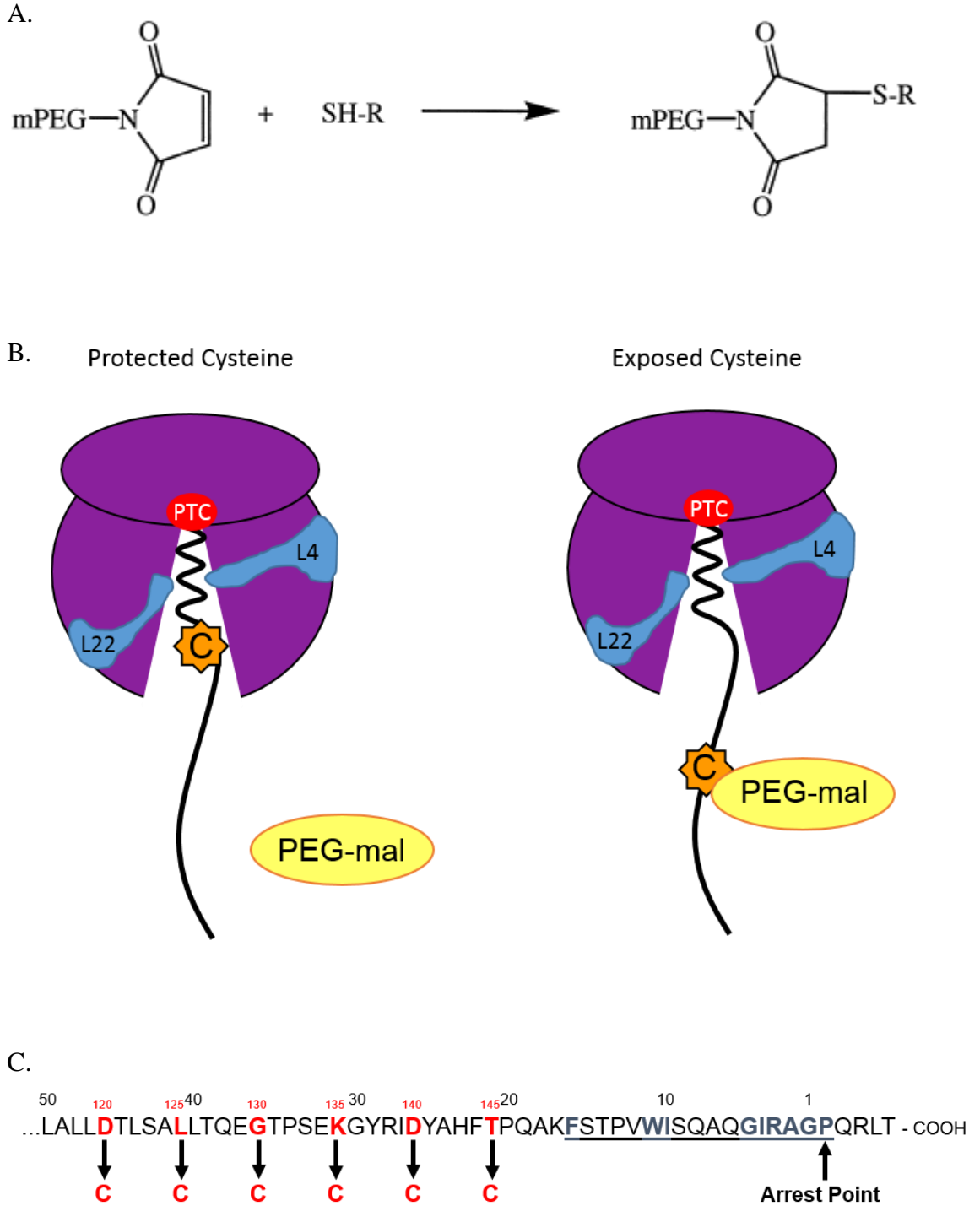


Figure 4.1 Pegylation as an assay for measuring nascent chain compaction within the ribosome exit tunnel. A. Structure of the PEG-mal functional group which covalently binds to the thiol group of cysteine. B. Diagrammatic representation illustrating the protection of cysteine residues located within the ribosome exit tunnel upon stalling in comparison to the pegylation of exposed cysteine residues located outside the ribosome exit tunnel. C. The sequence of the C-terminus of the SecM nascent chain highlighting the residues individually mutated to cysteine in red and the arrest motif underlined, with the essential residues highlighted in blue.

Based on the theory that a fully extended nascent chain would occupy 3.0-3.4 Å per amino acid residue, and an alpha helix would occupy 1.5 Å per amino acid residue, then it was hypothesised that a fully extended peptide would take ~28 residues to traverse the 100 Å length of the exit tunnel, whilst a partially alpha helical chain would take ~34-40 residues. This pegylation assay is ideal for measuring nascent chain compaction as the extent of pegylation is a representation of the length of peptide contained within the ribosome exit tunnel and therefore reflects the structure of the nascent peptide within the tunnel.

The aim of this chapter was to extend the initial discovery of SecM compaction upon translation arrest made by Woolhead et al., (2006) and analyse the compaction of 3 conservative SecM mutants selected from Chapter 3, both individually and in tandem with the additional P153A mutation. The results in Chapter 3 highlighted that it was not necessarily the properties of the amino acid that are important for translation arrest but also where they are located within the exit tunnel upon stalling. Therefore these experiments would reveal what influence these mutations had on compaction of the SecM nascent chain and how this is influenced by the increase in flexibility due to the additional P153A mutation. The mutants selected were F150Y, I156L and G161S as these retained the greatest degree of stalling in comparison to wild type SecM, which increased when combined with the double mutation of P153A (Figure 3.5B & C).

4.2 Results

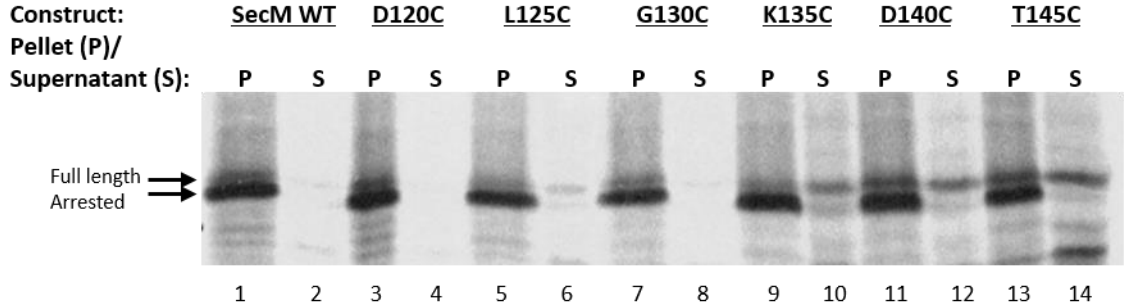
4.2.1 Pegylation as an assay to study SecM compaction upon translation arrest

As in the previous Chapter, SecM mutants were created by site-directed mutagenesis (see Section 2.2.5.3.1) and correct mutations were confirmed by DNA sequencing (see Section 2.2.11), these constructs are detailed in Appendix 3. The SecM residues for chosen for mutation to cysteine were selected as they cross the opening of the exit tunnel and ranged from SecM D120 to SecM T145. Upon ribosome stalling and SecM translation arrest, residue G165 is situated in the P-site of the PTC and therefore D120C will be located 46 amino acid residues from the PTC whilst T145C will be only 21 residues away. Based on these distances, upon stalling, D120C would be expected to have traversed the length of the large ribosome subunit and be exposed outside the exit tunnel, whilst T145C would still be contained within it.

These constructs were then analysed in coupled *in vitro* transcription-translation assays containing radiolabelled methionine, followed by CTABr precipitation (see Section 2.3.3 for details). The results are shown in Figure 4.2 and indicate that all the single cysteine SecM constructs translated efficiently, retaining levels similar to wild type SecM. In terms of translation arrest, SecM D120C, L125C and G130C constructs maintained levels analogous to wild type SecM (Figure 4.2A; Lanes 1-8), whilst a small proportion of SecM K135C, D140C and T145C appears to be released as full length peptide (Figure 4.2A; Lanes 9-14, upper bands). Despite this all the SecM peptides created were suitable for assaying in pegylation experiments as translation levels were high and the protocol was designed to isolate only the stalled ribosome-nascent chain complexes by centrifuging the translation products at high velocity through a sucrose cushion and obtaining the pellet.

To demonstrate the suitability of PEG-mal for these experiments, and ensure it labelled only exposed cysteine residues and not those contained within the ribosome exit tunnel, two constructs, SecM D120C and SecM T145C were first tested. Of the six SecM cysteine mutant constructs created these two constructs contain cysteine residues located furthest apart on the nascent chain and are separated by 25 amino acids (Figure 4.1C). Constructs were first translated *in vitro* as described previously and then assayed for nascent chain compaction by pegylation (see Section 2.3.4.1). The products were then separated by SDS

A.



B.

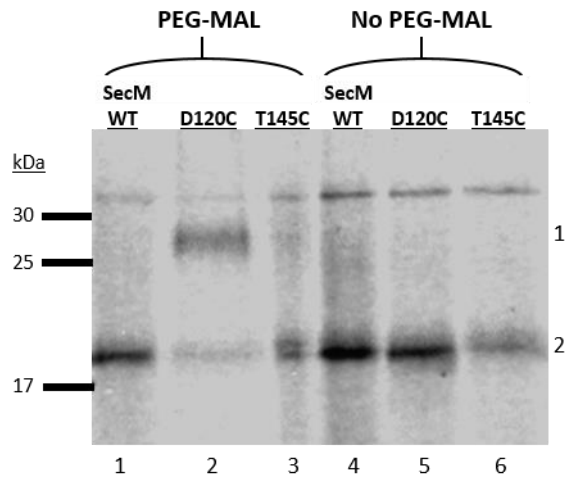


Figure 4.2 SecM cysteine mutants analysed by CTABr precipitation and initial test pegylation assay. A. SecM peptides indicated were translated *in vitro*, CTABr precipitated and separated into pellet (P) and supernatant (S) fractions and separated by SDS-PAGE. Wild type SecM is shown in Lanes 1 & 2 and all cysteine modified SecM peptides are shown in comparison (Lanes 3-14). B. SecM WT, D120C and T145C were translated *in vitro* and stalled ribosome-nascent chain complexes were isolated by ultracentrifugation through a 0.5 M sucrose cushion, divided in two and then incubated with 1mM PEG-mal (Lanes 1-3) or without (Lanes 4-6). Pegylation of cysteine residues is indicated by a mass shift (1) of ~10 kDa in comparison to unpegylated translation product (2). Gels are representative of multiple experiments.

gel electrophoresis and visualised by autoradiography (see Section 2.4). These results confirmed that the exposed D120C residues were stably tagged with PEG-mal and resulted in a ~10 kDa shift when the products were separated by SDS-PAGE (Figure 4.2B; Lane 2). However, if there was no cysteine present, as in wild type SecM, or the cysteine residue was still protected inside the ribosome exit tunnel, as in SecM T145C, then no pegylation occurred and there was no mass shift (Figure 4.2B; Lanes 1 & 3 respectively).

An additional control was performed to determine the degree of cysteine pegylation achieved in the absence of the ribosome and associated factors. This was done by incubating the translation product with 1mg/ml RNaseA prior to incubation with PEG-mal to degrade any RNA present, thereby releasing the nascent chain from the ribosome (see Section 2.3.4.2 for details). Two constructs were analysed, SecM G130C and D140C were selected as results in Figure 4.5B, which have yet to be discussed, show that these two peptides traverse the opening of the ribosome exit tunnel, with G130C (Figure 4.5B; Lane 4) located outside the ribosome and therefore accessible to pegylation, and D140C (Figure 4.5B; Lane 6) remaining protected within the exit tunnel and therefore shielded from pegylation. The results of this RNaseA control experiment also serve to highlight the importance of the CTABr precipitation step in the isolation of the synthesised peptide as the presence of pegylated protein in the supernatant fraction indicates that a portion of stalled peptide is released from the ribosome during the time frame of the PEG-mal incubation (Figure 4.3; Lanes 2 & 4). If not separated and removed from the final product these released peptides would give a false result as to the level of pegylated stalled peptide bound to the ribosome. These results indicate that, under the normal pegylation protocol, 30.9% of translation arrested SecM G130C undergoes pegylation (Figure 4.3; Lane 1); whilst of the released SecM G130C in the supernatant fraction 42.6% is pegylated (Figure 4.3; Lane 2). Meanwhile stalled SecM D140C in the pellet fraction, which is still contained within the ribosome exit tunnel, only undergoes 3.8% pegylation (Figure 4.3; Lane 3) whilst released SecM D140C peptide isolated in the supernatant fraction undergoes 33.8% pegylation (Figure 4.3; Lane 4).

When treated with 1mg/ml RNaseA prior to incubation with PEG-mal, to degrade any RNA present and therefore release all peptides from the ribosome, all the translation product is recovered in the supernatant fraction following CTABr precipitation, as no tRNA is present to precipitate any attached peptide, (Figure 4.3; Lanes 10, 12, 14 & 16).

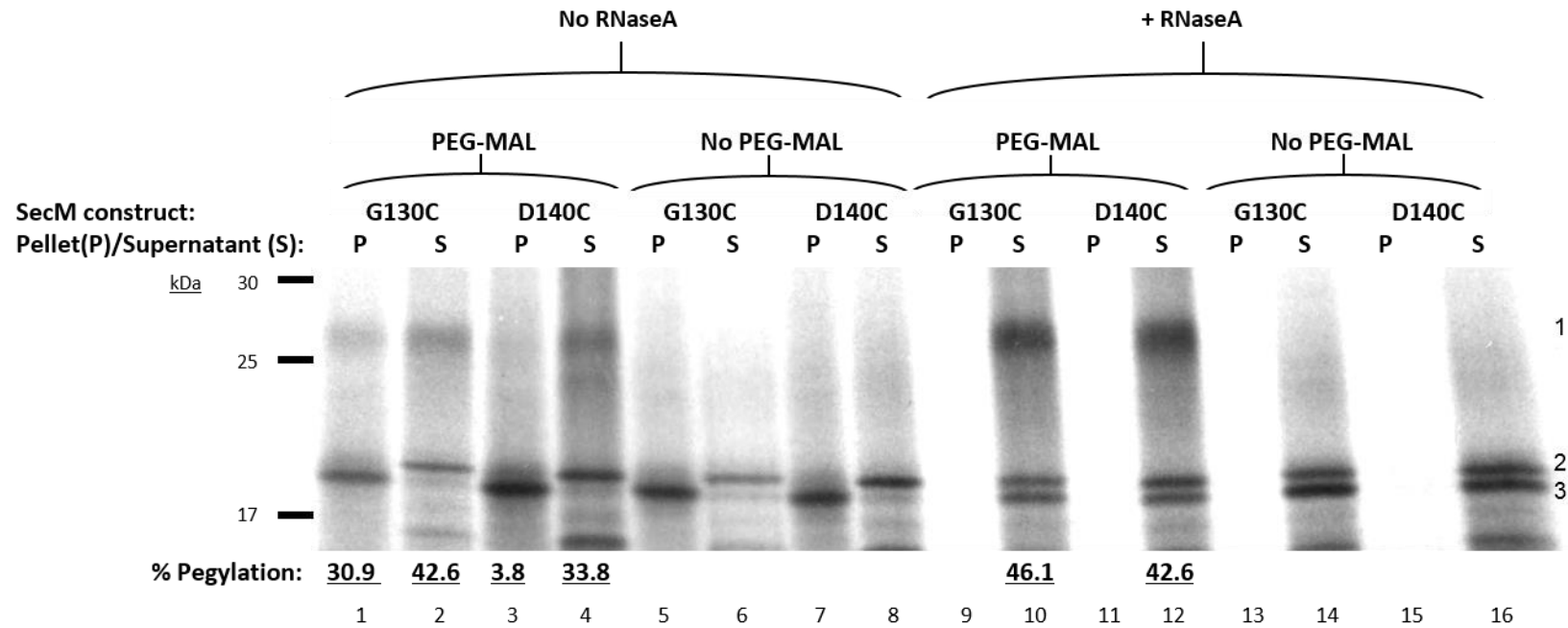


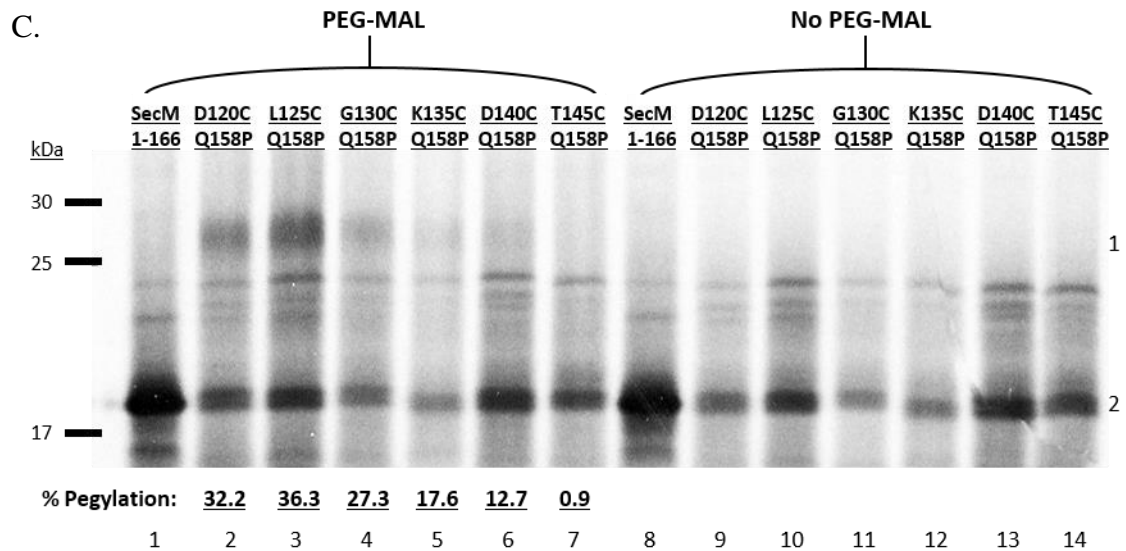
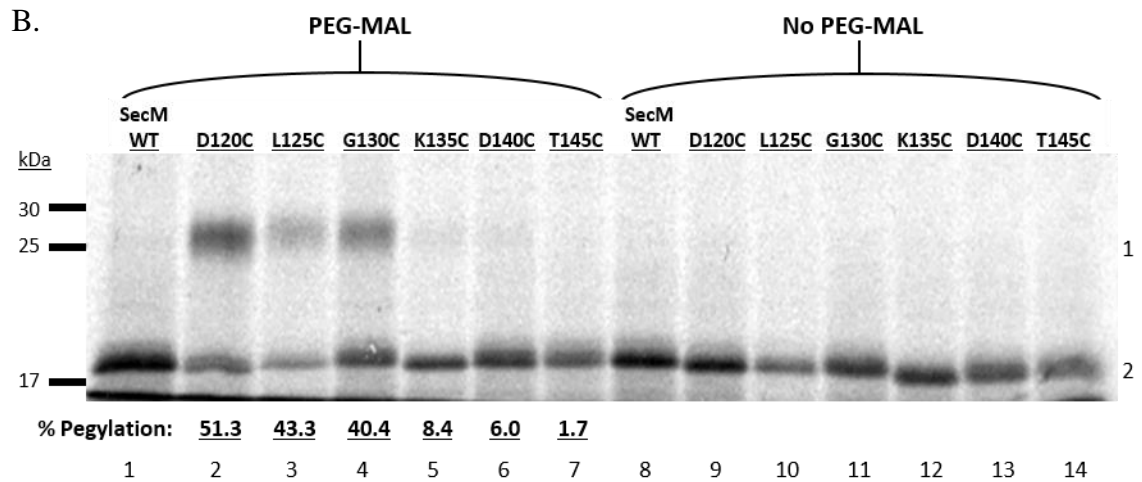
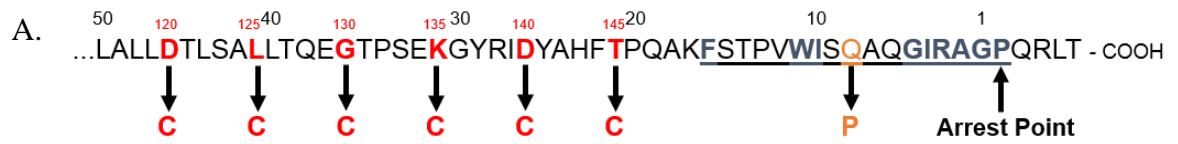
Figure 4.3 RNaseA nascent chain release control. Prior to incubation with 1mM PEG-mal, SecM G130C and D104C were translated *in vitro* and half of the sample incubated in the absence of RNaseA (Lanes 1-8) and the other half incubated with 1mg/ml RNaseA (Lanes 9-16). Samples were halved again, with half incubated with 1 mM PEG-mal (Lanes 1-4 and 9-12) and the other half acting as a control without (Lanes 5-8 and 13-16). Final products were isolated by CTABr precipitation and separated into pellet (P) and supernatant (S) fractions and resolved by SDS-PAGE. Pegylation of cysteine residues is indicated by a mass shift of ~10 kDa (1) in comparison to unpegylated full length (2) and arrested (3) translation product. % pegylation was calculated as a percentage of [pegylated/(unpegylated+pegylated)] adjusted for background.

The results indicate that in the absence of the ribosome and any associated factors, 100% pegylation of the nascent chain is still not achieved with SecM G130C undergoing 46.1% pegylation (Figure 4.3; Lane 10) and SecM D140C undergoing 42.6% pegylation (Figure 4.3; Lane 12). This indicates that the cysteine residues are being protected from PEG-mal modification, most likely due to folding of the peptide into secondary or possibly tertiary structure, however, it is unknown from these assays whether this is a structured or disordered folding of the nascent chain outside the exit tunnel. Disordered folding is likely as a result of hydrophobic amino acid residues seeking to avoid contact with water molecules by shielding within the nascent chain but as there are no chaperones to assist this process it may not have a determined structure.

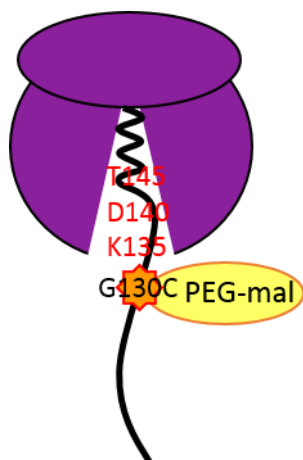
4.2.2 Pegylation of compacted and extended SecM peptides stalled on the ribosome

The next step was to assay all SecM cysteine mutants (D120C-T145C) to define at which point the stalled nascent chain is exposed from the ribosome exit tunnel by determining the degree of pegylation across multiple points. Figure 4.4A illustrates the position of the cysteine mutations made to individual SecM constructs, also indicating their distance away from the PTC. As seen in the previous experiment (Figure 4.2B; Lane 1), wild type SecM does not undergo pegylation as it does not contain any native cysteine residues to bind PEG-mal (Figure 4.4B; Lane 1), whilst SecM cysteine mutants D120C, L125C and G130C undergo pegylation of ~40-50% (Figure 4.4B; Lanes 2-4 respectively). There is a dramatic reduction in pegylation at K135C to 8.4% and this continues to decrease the nearer the cysteine residue is situated to the C-terminus, with 6.0% pegylation at D140C and only 1.7% at T145C (Figure 4.4B; Lanes 5-7 respectively). These results indicate that residues K135C, D140C and T145C are still contained within the ribosome exit tunnel upon stalling and compaction of the SecM nascent chain and is summarised diagrammatically in Figure 4.4D.

To enable comparisons to be drawn between compacted and extended SecM nascent chains, the SecM Q158P mutation was utilised. Residue Q158 is a non-essential amino acid located within the arrest motif and situated close to the essential R163 residue (see Figure 4.4A). Whilst not an essential amino acid for arrest it has been shown to interact the 23S rRNA nucleotide A752 (Gumbart et al., 2012). Due to the restrictive nature of proline, mutation to this residue prevents compaction and results in a loss of translation



D. SecM WT



E. SecM Q158P

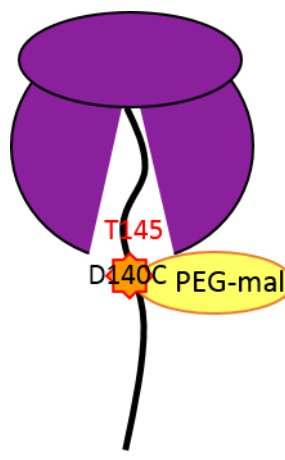


Figure 4.4 Pegylation assays of wild type SecM and SecM Q158P.

A. Schematic diagram of the mutations made to individual SecM constructs. Mutated cysteine residues are shown in red; Q158P in orange; and the arrest motif is underlined with the essential residues shown in blue. B. Wild type SecM and C. SecM Q158P containing single cysteine mutations were translated *in vitro* and divided in half, with one half a control and the other incubated with 1 mM PEG-mal before being CTABr precipitated and resolved by SDS-PAGE. Pegylation of cysteine residues is indicated by a mass shift of ~10 kDa (1) in comparison to unpegylated translation

product (2). % pegylation was calculated as a percentage of [pegylated/(unpegylated+pegylated)] adjusted for background. Results are representative of multiple experiments. D & E. Schematic diagram of pegylation results for D. wild type SecM and E. SecM Q158P, indicating the first exposed cysteine residue which undergoes pegylation, G130C and D140C respectively.

stalling (Woolhead et al., 2006). As this peptide no longer undergoes translation arrest, to obtain stalled ribosome-nascent chain complexes it was necessary to use truncated linear DNA lacking a stop codon and containing Proline-166 as the terminal residue, in the *in vitro* transcription-translation assays. In the absence of a stop codon mRNA remains associated with the ribosome, as there is no signal to initiate termination, allowing stalled ribosome-nascent chain complexes to be obtained.

These results indicate that the extended SecM Q158P undergoes pegylation at residues D120C – D140C (Figure 4.4C; Lanes 2-6), whilst T145C remains unpegylated (Figure 4.4C; Lane 7), indicating only residue T145C remains within the ribosome exit tunnel upon stalling, see Figure 4.4E for summary. The overall percentage of pegylation is reduced in comparison to wild type SecM with the highest level of pegylation being 51.3% in wild type SecM (Figure 4.4B; Lane 2), compared to 36.3% in SecM Q158P (Figure 4.4C; Lane 3). This is most likely due to differences in the secondary or tertiary structure of the nascent chain outside the exit tunnel, which in the case of SecM Q158P results in the cysteine residue being more protected and therefore consequently decreasing the accessibility of PEG-mal, resulting in a reduced overall rate of pegylation. Despite this there is still a clear segregation in the level of pegylation between residues outside of the exit tunnel and those protected within it, as pegylation of SecM Q158P at residue T145C reduces to only 0.9% (Figure 4.4C; Lane 7).

Hypothetically, an extended nascent chain has 3.5 Å per amino acid and would therefore require ~28 residues to traverse the 100 Å length of the ribosome tunnel (Figure 4.5A), whilst a fully alpha helical nascent chain has 1.5 Å per amino acid and would therefore require ~67 residues to traverse the ribosome exit tunnel (Figure 4.5D) (Lu and Deutsch, 2005a). However, previous studies have shown that nascent chains traversing the exit tunnel do not form complete alpha helices throughout its full length, with certain parts of the exit tunnel more favourable to secondary structure formation than others (Bhushan et al., 2010a; Lu and Deutsch, 2005a; Woolhead et al., 2006). Therefore it is hypothesised that a partially alpha helical chain with 10 amino acids forming an alpha helix, with the remainder fully extended, would require ~34 residues to traverse the exit tunnel (Figure 4.5B1), whilst a partially alpha helical chain with 20 amino acids in the helix with the remainder fully extended would require ~40 residues to traverse the exit tunnel (Figure 4.5C). The previous studies indicated that compaction occurred within defined areas of the

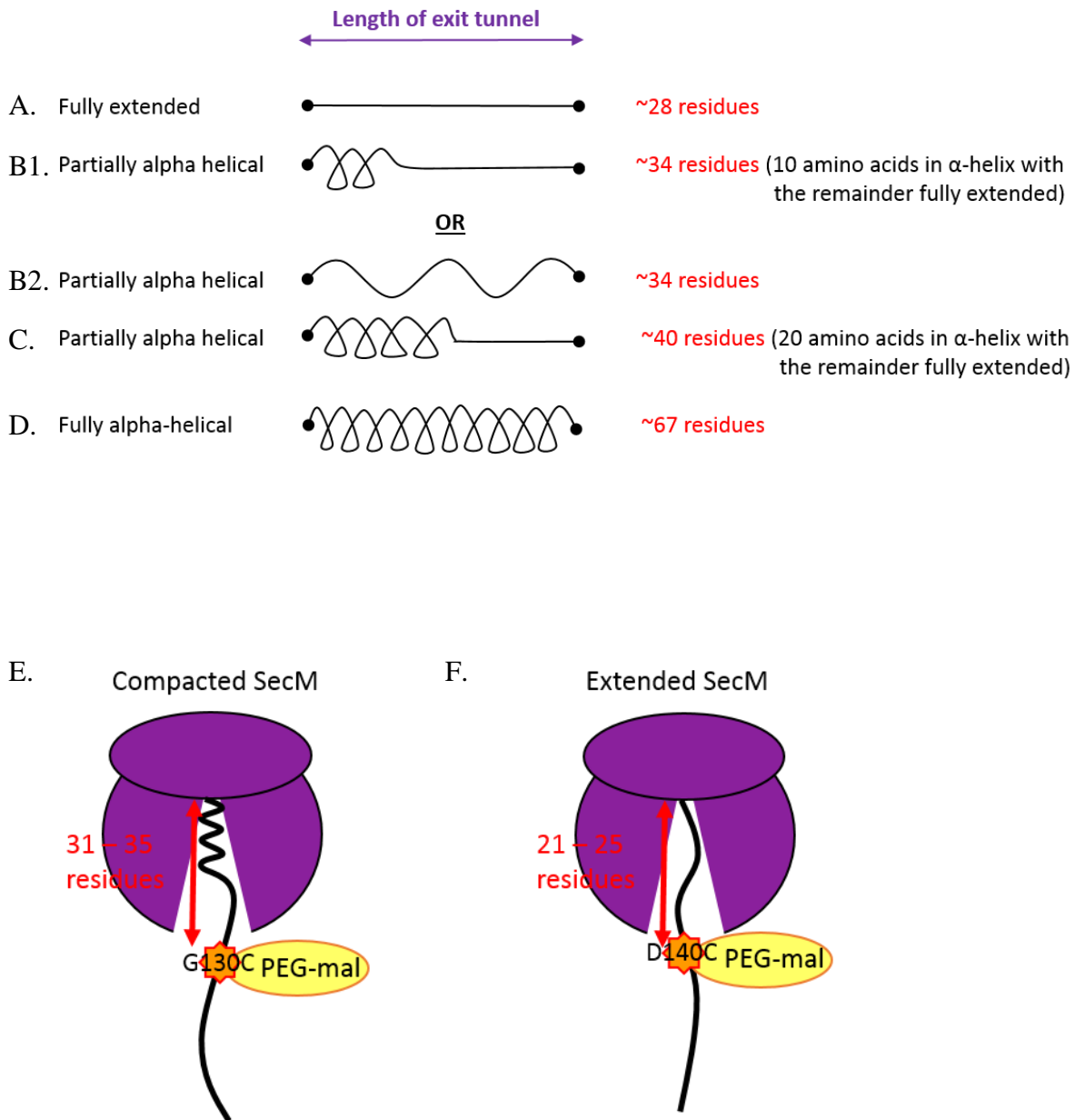


Figure 4.5 Length of nascent chain contained within the ribosome exit tunnel dependant on the level of compaction. A. A fully extended nascent chain. B1. Partially alpha helical nascent chain tightly compacted within a 10 amino acid region or B2. Loosely compacted along the length of the nascent chain. C. Partially alpha helical nascent chain tightly compacted within a 20 amino acid region. D. Fully alpha-helical nascent chain throughout the length of the ribosome exit tunnel. E. Compacted wild type SecM is initially pegylated at G130C indicating that 31-35 residues are contained within the exit tunnel. F. Extended SecM mutants are first pegylated at D140C indicating that only 21-25 residues are contained within the ribosome exit tunnel.

exit tunnel, however, the pegylation assay does not discriminate between a tight compaction in one area of the nascent chain and an overall looser compaction of the full nascent chain throughout the length of the exit tunnel (Figure 4.5B1 & B2 respectively).

These results indicate that wild type SecM has between 31 and 35 residues contained within the exit tunnel upon stalling and compaction, whilst the extended SecM Q158P peptide has between 21 and 25 residues protected by the exit tunnel, a difference of ~10 amino acids (Figure 4.5E & F). These values are close to the hypothesised values which estimate that a fully extended peptide would require ~28 residues to traverse the exit tunnel whilst a partially alpha helical chain would take ~34-40 residues. The slight differences may be due to PEG-mal being able to access and pegylate residues at the very end of the exit tunnel where it widens slightly, however, these results still indicate that the difference in pegylation between extended and compacted SecM is representative of a partially alpha helix compaction of the SecM nascent chain upon stalling.

The compaction of truncated SecM constructs has previously been assayed through FRET analysis by Woolhead et al., (2006), in which they established that SecM does not undergo compaction until the full arrest motif including Proline-166 has been synthesised. To further explore the pegylation rates of extended and compacted SecM peptides additional pegylation assays were performed using truncated SecM 1-166 and 1-165 single cysteine constructs, the results of which are shown Figures 4.6A & B respectively. The pegylation of SecM 1-166 is analogous to wild type SecM, with these results indicating that the percentage pegylation of SecM 1-166 is between 40.2-31.0% at residues D120C, L125C and G130C (Figure 4.6A; Lanes 2-4 respectively), with a sudden decrease to 5.8% pegylation at K135C (Figure 4.6B; Lane 5). This further decreases to 2.2 and 0.5% at D140C and T145C respectively (Figure 4.6B; Lanes 6 & 7 respectively). These results again indicate that when SecM compacts upon stalling the nascent chain crosses the opening of the exit tunnel between residues G130C and K135C. In contrast, the extended SecM peptide is protected within the exit tunnel only at residue T145C, with only 2.9% of the peptide undergoing pegylation (Figure 4.6B; Lane 7), and the other peptides, D120C – D140C undergoing between 24.4 and 17.2% pegylation (Figure 4.6B; Lanes 2-6 respectively). These results support the previous data in Figure 4.4B & C that compacted SecM has between 31 and 35 residues contained within the exit tunnel upon stalling and compaction, whilst extended SecM has between 21 and 25 residues. These results are

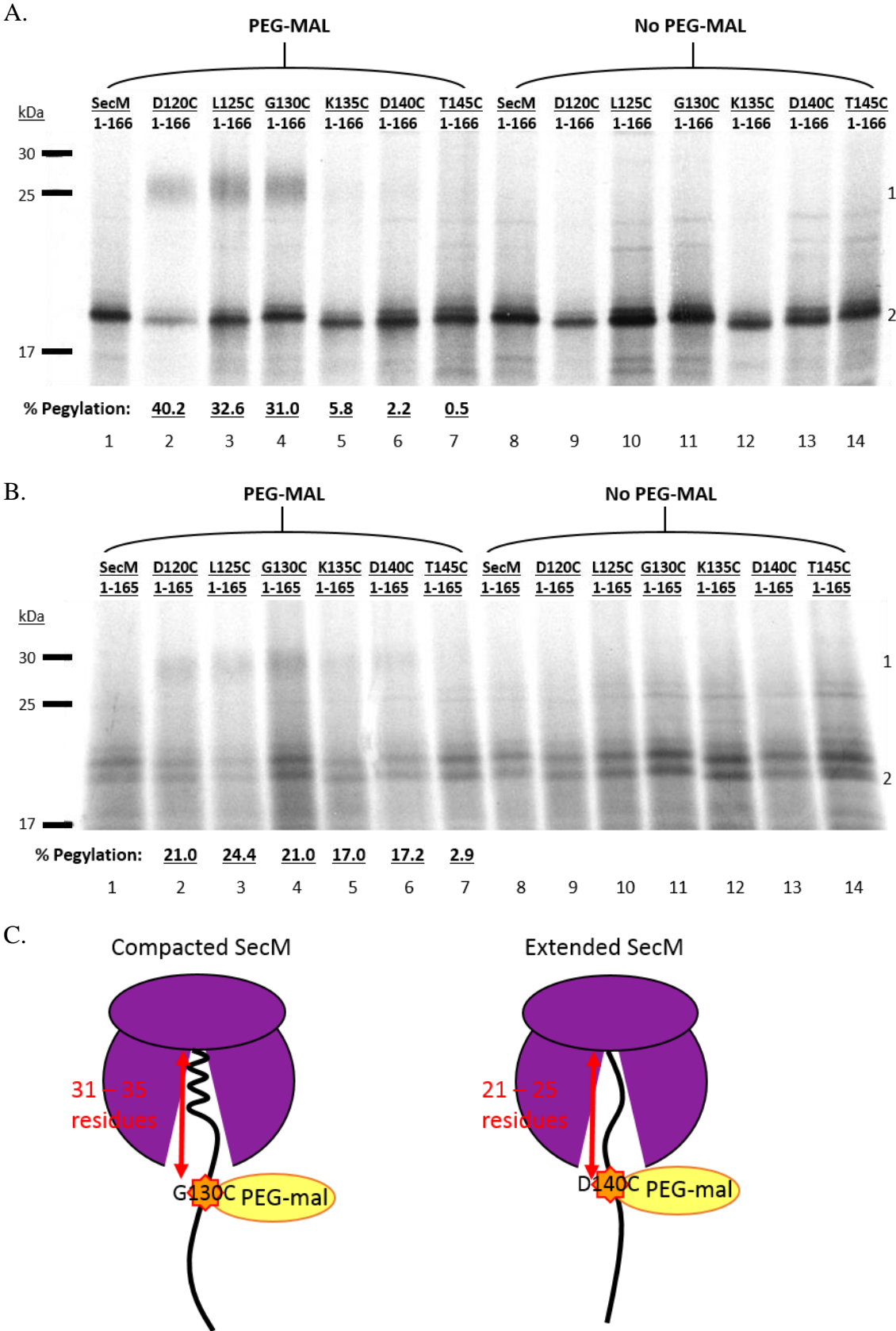


Figure 4.6. Pegylation assays of truncated SecM constructs. A. SecM 1-166 and B. SecM 1-165 single cysteine constructs were translated *in vitro* as previously described, divided in half, with one half a control and the other incubated with 1 mM PEG-mal before being CTABr precipitated and resolved by SDS-PAGE. Pegylation of cysteine residues is indicated by a mass shift of ~10kDa (1) in comparison to unpegylated translation product (2). % pegylation was calculated as a percentage of [pegylated/(unpegylated+pegylated)] adjusted for background. Results are representative of multiple experiments. C. Summary of the pegylation results of compacted SecM (WT and 1-166) and extended SecM (Q158P and 1-165) indicating the number of residues contained within the ribosome exit tunnel upon stalling.

summarised diagrammatically in Figure 4.6C. The results of the truncated SecM 1-165 constructs in Figure 4.6B also highlight that reduced pegylation of the exposed residues in extended SecM peptides in comparison to those of compacted SecM is a recurring commonality. This supports the theory that extended SecM peptides adopt secondary or tertiary structure outside the exit tunnel, which results in a more protected cysteine residues and therefore lower degrees of pegylation.

4.2.3 Analysis of compaction of selected single SecM mutants

From these initial experiments the next step was to assay the compaction of several selected SecM mutants to identify the effect of altering key arrest motif residues on the ability of the SecM nascent chain to undergo compaction upon translation arrest. The first SecM mutant to be assayed was SecM P153A, as work in the previous chapter had shown that this alteration of the restrictive proline residue for an alanine plays an important role in the ability of SecM mutants to regain stalling ability. This recovery of stalling function is thought to be due to the ability of the SecM nascent chain to reposition the key R163 residue and the work in this chapter further expands on this to examine what role compaction of the nascent chain has in this process. Previous work has shown that the P153A mutation does not affect stalling (Figure 3.3B; Lane 5) and additionally, Woolhead et al., (2006) employed a FRET assay to show that compaction between the two FRET probes at residues 135 and 159 of the SecM nascent chain was unaffected by this mutation.

Therefore, initial pegylation experiments were carried out to confirm the overall degree of compaction of SecM P153A within the full-length of the ribosome exit tunnel in comparison to wild type SecM. The assay focused on the 3 cysteine mutants G130C, K135C and D140C as from the previous results, these have been identified as the residues spanning the opening of the exit tunnel (Figure 4.4 and 4.6). The results of SecM P153A compaction and pegylation are shown in Figure 4.7A and indicate that this mutation has no effect on nascent chain compaction upon stalling in comparison to wild type SecM. G130C undergoes an average of 31.2% pegylation (Figure 4.7A; Lane 1) which reduces to an average of 6.5% and 5.0% at K135C and D140C respectively (Figure 4.7A; Lanes 2 and 3) indicating that, like wild type SecM, the nascent chain compacts and protects residues K135C and D140C within the ribosome exit tunnel. The graph in Figure 4.7B summarises these results, highlighting the differences in the pegylation of residues G130C, K135C and

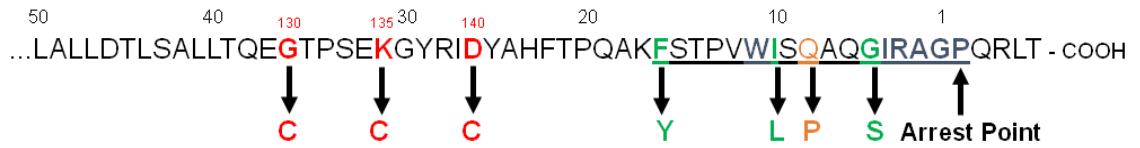
D140C, in extended SecM Q158P and 1-165 in comparison to wild type SecM and SecM P153A which undergo compaction.

Following this, the compaction and stalling of 3 conservative SecM mutations: F150Y, I156L and G161S were assayed. These constructs have been shown in Chapter 3 to maintain the highest level of stalling of the conservative mutations studied with ~50% stalling in F150Y and I156L and ~25% stalling in G161S (Figure 3.5B; Lanes 3, 7 & 9 respectively). The work in this chapter examined what effect these mutations had on the compaction of the SecM nascent chain and whether this is linked to the level of translation arrest undergone by the peptide.

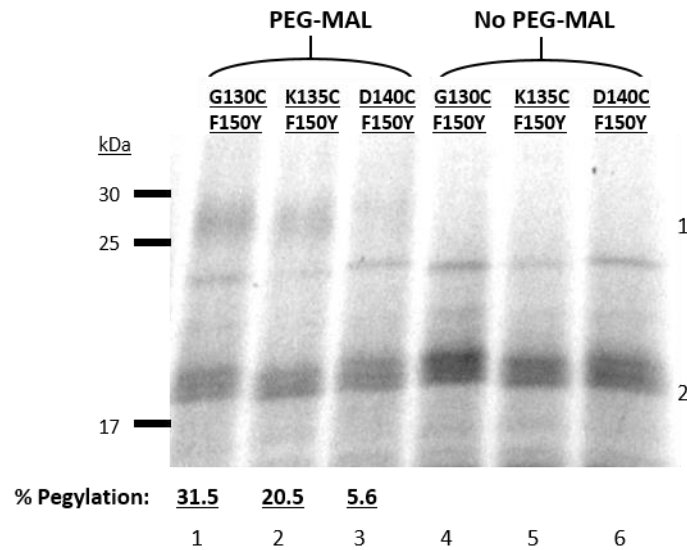
Whilst the average pegylation rates of residues G130C and D140C of SecM F150Y (Figure 4.8A; Lanes 1 & 3) remain relatively similar to that of wild type SecM (Figure 4.4B; Lanes 4 & 6), the increased pegylation of SecM F150Y at residue K135C (Figure 4.8A; Lane 2) in comparison to wild type (Figure 4.4B; Lane 5) indicates that this peptide adopts a less compact structure within the exit tunnel upon stalling, resulting in increased exposure of K135C from the exit tunnel and hence increased pegylation. These results indicate that only 26-30 residues of SecM F150Y are contained within the ribosome exit tunnel upon stalling, in comparison to 31-35 residues of wild type SecM. This suggests that there is still partial folding or helix formation as a fully extended SecM had only 21-25 residues contained within the exit tunnel (see Figure 4.6C). SecM G161S undergoes a similar degree of compaction as SecM F150Y with residue D140C (Figure 4.9B; Lane 3) remaining protected by the ribosome exit tunnel whilst increased pegylation of K135C indicates increased exposure of the residue from the exit tunnel again implying a more extended conformation of this SecM mutant upon stalling (Figure 4.9B; Lane 2).

Of the three conservative mutants, I156L adopts the most extended conformation upon stalling, comparable to a fully extended SecM peptide (Figure 4.9A; Lanes 1-3) with pegylation present at all 3 cysteine residues (G130C – D140C) indicating all 3 residues are exposed and only 21-25 residues remain within the exit tunnel. Also, as seen with the extended peptides, SecM Q158P and truncated SecM 1-165, the overall rates of pegylation are lower than wild type SecM, with SecM I156L having a highest average pegylation at G130C of 24.5% (Figure 4.9A) in comparison to wild type SecM which has 40.4% (Figure

A.



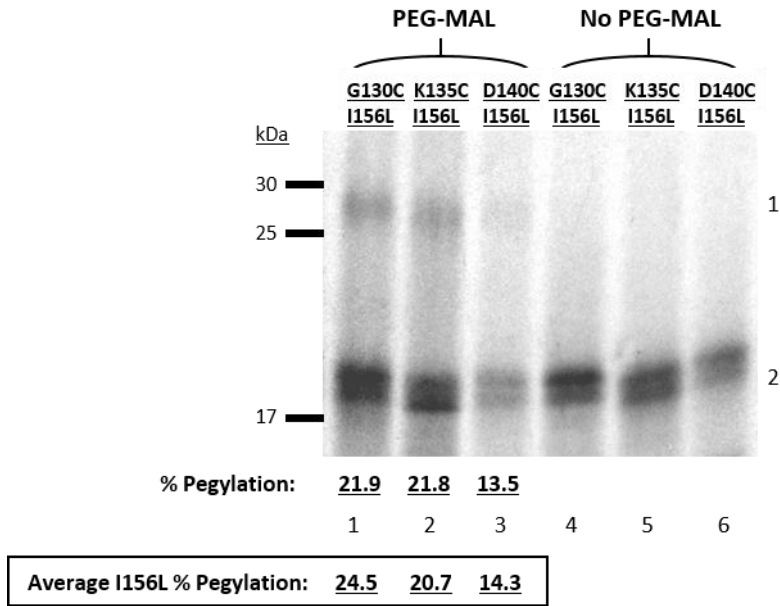
B.



Average F150Y % Pegylation:	34.7	23.1	6.8
-----------------------------	------	------	-----

Figure 4.8 Pegylation of conservative SecM F150Y mutant. A. Schematic diagram of the C-terminus of SecM, the conservative mutations made to separate SecM constructs are highlighted in green. Additional mutations were made to these constructs as described in the text including: G130C, K135C and D140C mutations which are shown in red. The Q158P mutation is indicated in orange. The arrest motif is underlined with the essential residues shown in blue. B. Pegylation results for SecM F150Y single cysteine constructs G130C, K135C and D140C. These peptides were translated *in vitro* as previously described, divided in half, with one half a control and the other incubated with 1 mM PEG-mal before being CTABr precipitated and resolved by SDS-PAGE. Pegylation of cysteine residues is indicated by a mass shift of ~10 kDa (1) in comparison to unpegylated translation product (2). % pegylation was calculated as a percentage of [pegylated/(unpegylated+pegylated)] adjusted for background. Average percentage pegylation is calculated from an n of 3.

A.



B.

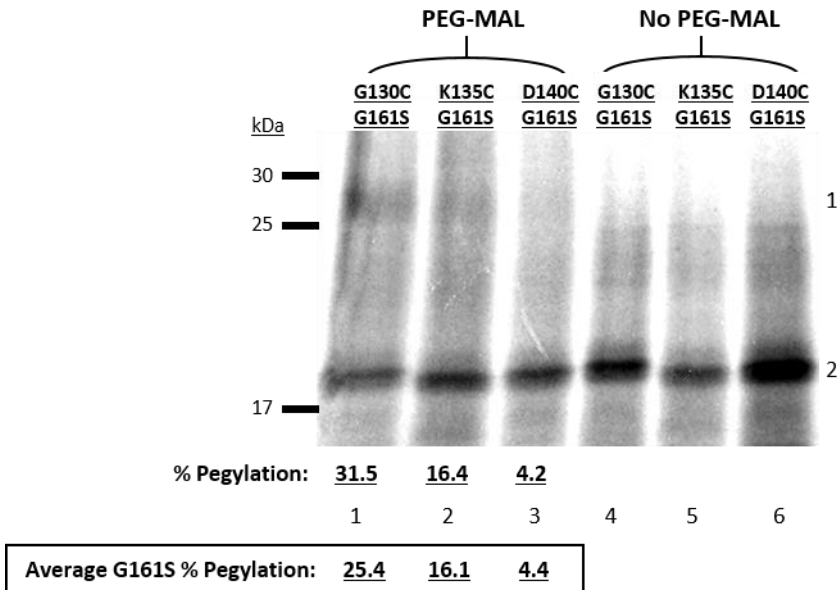


Figure 4.9 Pegylation of conservative SecM I156L and G161S mutants. Pegylation results for A. SecM I156L and B. SecM G161S single cysteine constructs G130C, K135C and D140C. These peptides were translated *in vitro* as previously described, divided in half, with one half a control and the other incubated with 1 mM PEG-mal before being CTABr precipitated and resolved by SDS-PAGE. Pegylation of cysteine residues is indicated by a mass shift of ~10 kDa (1) in comparison to unpegylated translation product (2). % pegylation was calculated as a percentage of [pegylated/(unpegylated+pegylated)] adjusted for background. Average percentage pegylation is calculated from an n of 3.

4.4B; Lane 4). This indicates that I156L also undergoes similar secondary or tertiary structure outside the exit tunnel as the other extended peptides SecM Q158P and SecM 1-165, reducing access of PEG-mal to the cysteine residues of the extended peptide.

4.2.4 Analysis of compaction of selected conservative SecM mutations coupled with P153A

Work in Chapter 3 showed that introduction of the P153A mutation into the conservative SecM mutants resulted in a recovery of translation arrest (see Figure 3.5C). This increase in stalling was attributed to the increased flexibility of the nascent chain provided by the removal of the restrictive proline residue, resulting in more efficient placing of the nascent chain to position R163 correctly to initiate stalling. Further to this, the next aim of these experiments was to examine what effect this increased flexibility had on the compaction of the SecM nascent chain, to explore what influence this has on the recovery of stalling.

The results of compaction of the SecM F150Y/P153A double mutant are shown in Figure 4.10A and indicate that incorporation of the P153A mutation results in increased compaction of the nascent chain. Whilst G130C pegylation remains high at an average of 30.5% indicating it is positioned outside the exit tunnel and exposed to PEG-mal binding (Figure 4.10A; Lane 1), average pegylation of K135C decreases from 23.1% in SecM F150Y (Figure 4.8B; Lane 2) to an average of 10.0% when combined with the P153A mutation (Figure 4.10A; Lane 2). Meanwhile D140C remains protected by the exit tunnel and undergoes an average of 8.1% pegylation (Figure 4.10A; Lane 3). This indicates that compaction of the nascent chain is restored when combined with the P153A mutation, indicated by the withdrawing of the K135C residue further into the exit tunnel protecting it from PEG-mal binding. The pegylation of SecM F150Y and F150Y/P153A mutants are compared to wild type SecM and extended SecM Q158P in Figure 4.10B, with this graph illustrating that the presence of the P153A mutation returns compaction to levels analogous to wild type, restoring the 31-35 residues contained within the exit tunnel.

Of the three SecM mutants examined the I156L single mutant has been shown to be the most extended upon stalling (Figure 4.9A), with levels of pegylation analogous to extended SecM Q158P (Figure 4.4C), however, incorporation of the P153A mutation

restores compaction of the SecM nascent chain (see Figure 4.11A). Pegylation of the exposed G130C residue of the SecM I156L/P153A double mutant increased to an average of 36.2% (Figure 4.11A; Lane 1) which is analogous to wild type SecM which undergoes 40.4% pegylation (Figure 4.4C; Lane 4). In addition to this average pegylation of K135C and D140C reduced to 13.1% and 8.7% respectively (Figure 4.11A; Lanes 2 & 3 respectively) indicating that these residues are now protected within the exit tunnel upon stalling and compaction. These results are summarised in Figure 4.11B which highlights the difference in overall pegylation between the extended and compacted SecM nascent chains. These results also further indicate that there must be a difference in secondary or tertiary structure formation of the extended peptide outside the exit tunnel to account for the lower rates of pegylation of these peptides.

The final SecM mutation examined was G161S, which of the 3 conservative mutations had the lowest recovery of stalling from ~20% (Figure 3.5B; Lane 9) to ~40% when combined with the P153A mutation (Figure 3.5C; Lane 9). The results of the pegylation assays of the G161S/P153A double mutant show that G130C had an average of 23.4% pegylation (Figure 4.12A; Lane 1) which, although lower than wild type SecM at 40.4% (Figure 4.4; Lane 4), indicated that this residue was located outside the exit tunnel upon stalling. Meanwhile pegylation at residues K135C and D140C reduced to an average of 5.9% and 2.1% respectively (Figure 4.12A; Lanes 2 & 3 respectively), indicating these residues are protected within the ribosome exit tunnel (see Figure 4.12B for summary). These results show that whilst the single mutant had a more extended conformation upon stalling with only 26-30 residues contained within the exit tunnel, in combination with the P153A double mutation, partial alpha helix structure of the nascent chain was again restored, with 21-25 residues contained within the exit tunnel upon stalling and compaction.

These results indicate that conservative mutations of the key amino acid arrest residues affect compaction of the SecM nascent chain upon stalling to differing degrees, which does not correlate with the level of translation arrest that these mutants attain. For instance, SecM I156L maintains a greater degree of stalling than SecM G161S with ~50% of the peptide arrested in comparison to ~20% (Figure 3.5B; Lanes 7 & 9 respectively), however, pegylation results reveal that it is in a more extended conformation upon stalling (Figure 4.9A & B respectively). Increased freedom of movement of the nascent chain by mutation of the restrictive Proline-153 to alanine results in restoration of compaction to levels

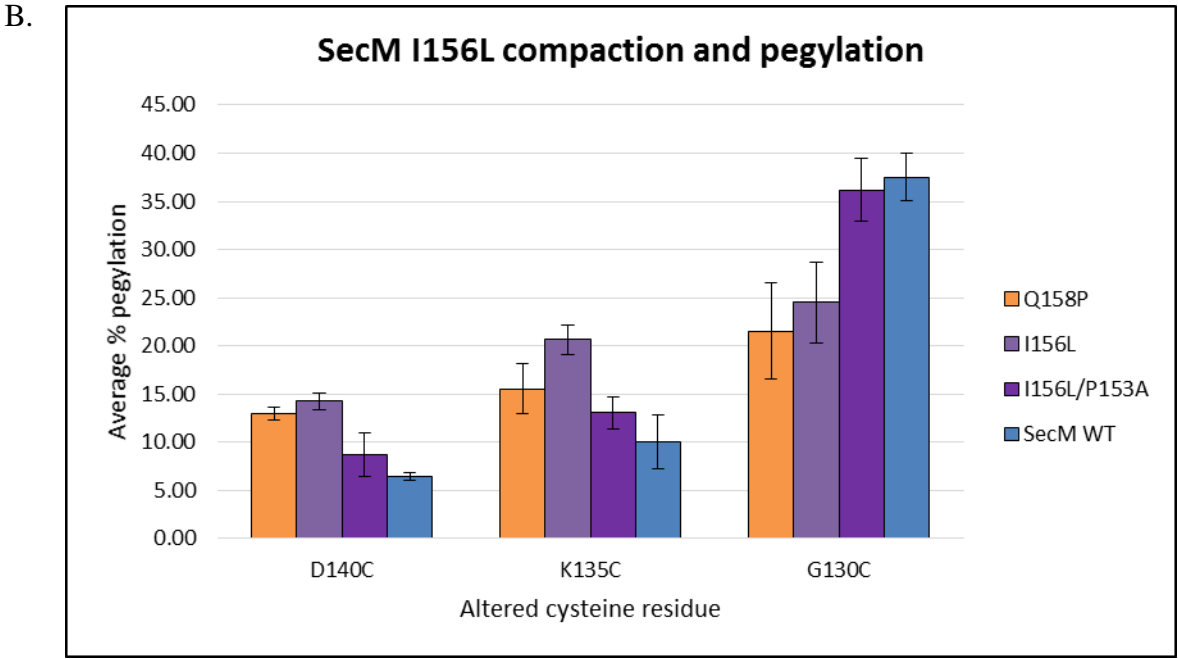
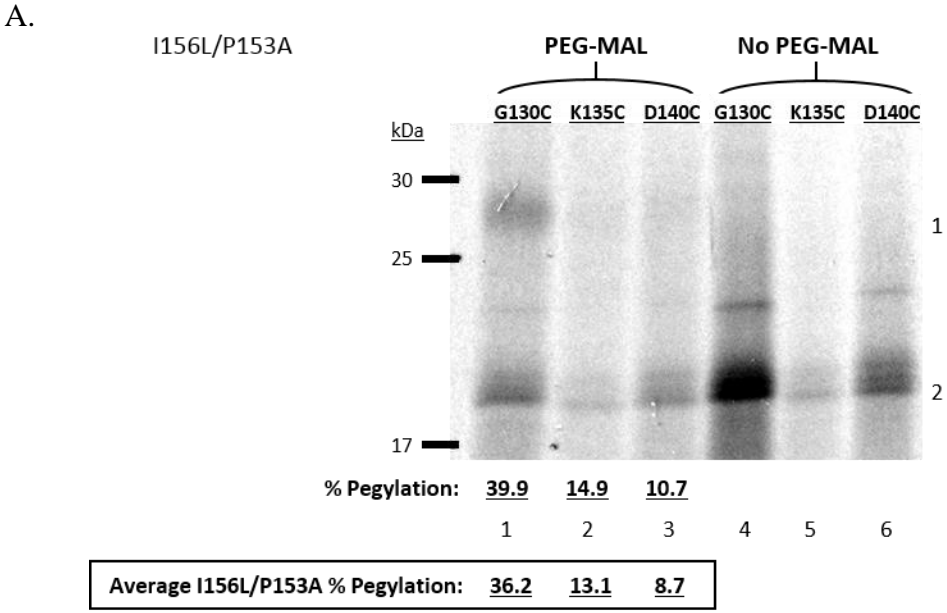


Figure 4.11 Analysis of pegylation and compaction of SecM I156L and SecM I156L/P153A mutants.
A. SecM I156L/P153A single cysteine constructs G130C, K135C and D140C were translated *in vitro* and divided with one half a control and the other half incubated with 1 mM PEG-mal before being CTABr precipitated and resolved by SDS-PAGE. Pegylation of the cysteine residue is indicated by a mass shift of ~10 kDa (1) in comparison to unpegylated translation product (2). B. Average percentage pegylation of SecM I156L and SecM I156L/P153A constructs at G130C, K135C and D140C in comparison to SecM WT and extended mutant SecM Q158P. All % pegylation values were calculated as a percentage of [pegylated/(unpegylated + pegylated)] adjusted for background. Average percentage pegylation is calculated from an n of 3. Error bars indicate standard deviation.

analogous to wild type SecM for all three conservative mutant constructs studied (see Figures 4.10, 4.11 & 4.12). The increase in the levels of translation arrest are due to the increased freedom of movement of the nascent chain within the exit tunnel which enables the repositioning of key amino acid arrest residues. The resulting increase in translation arrest indicates that the interactions between the nascent chain and the ribosome exit tunnel are a key mediator in the level of translation arrest. However, although the additional P153A mutation increases the level of stalling of the F150Y, I156L and G161S mutants, these results indicate that recovery of full compaction of the SecM nascent chain does not result in a full recovery of translation arrest, see Figure 4.13 for an overall summary of the results.

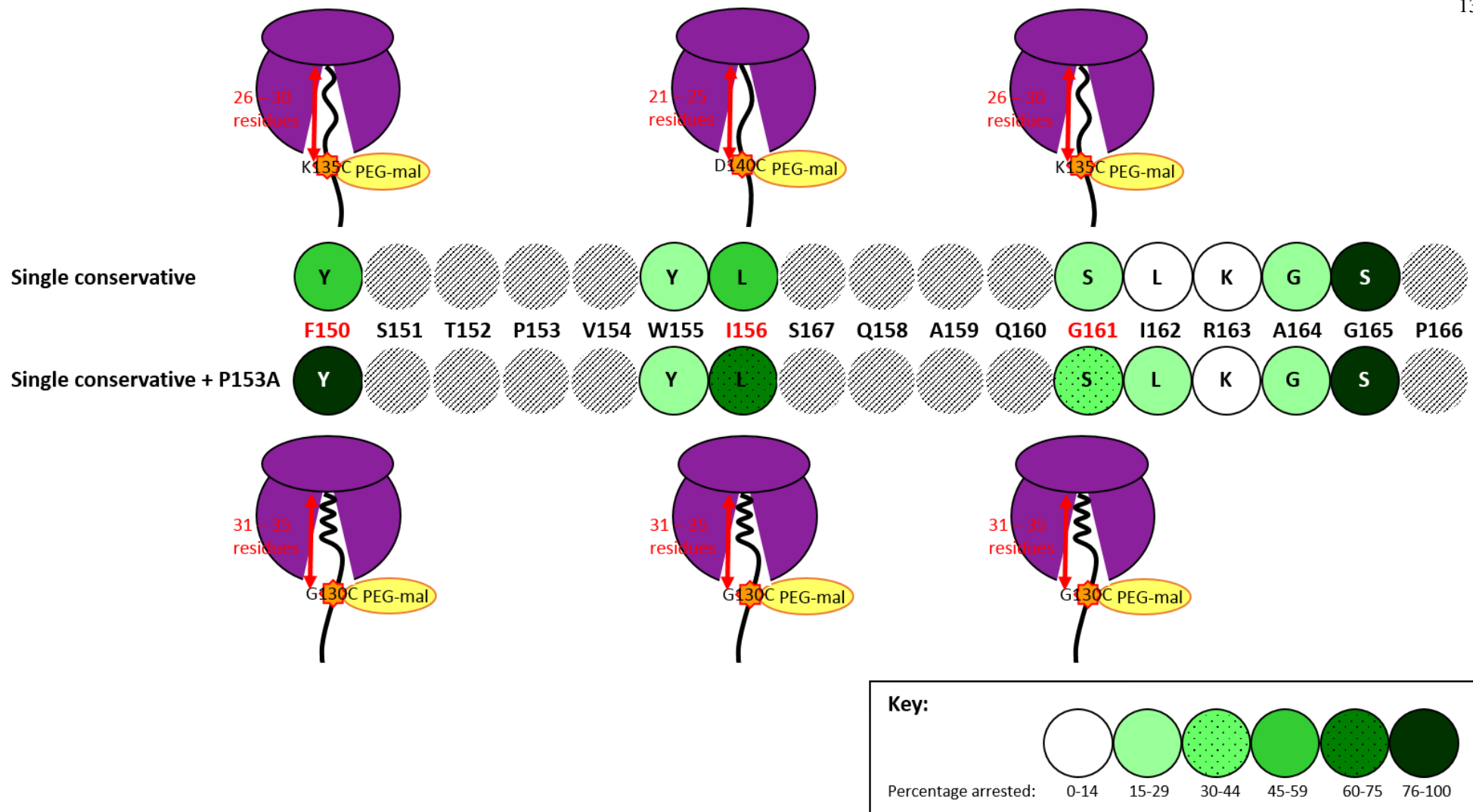


Figure 4.13 Combined summary of translation arrest and degree of compaction for the selected conservative SecM mutants studied. Highlighted in red are the three conservative SecM mutations which were investigated in the pegylation assay to determine number of residues contained within the ribosome exit tunnel, and therefore the degree of compaction of the SecM nascent chain upon translation arrest.

4.3 Conclusion

4.3.1 Analysing SecM stalling and compaction by cysteine pegylation

Cysteine modification by PEG-maleimide is a technique that has previously been exploited to detect nascent peptide conformation within the ribosome exit tunnel and this technique has been utilised here to assay the level of SecM compaction upon translation arrest. SecM compaction had previously been established by Woolhead et al., (2006) through use of a FRET assay, however, it was only possible to define the extent of folding between the position of the two FRET probes at residues 135 and 159 due to the limitations of having to place the probes at these positions so as not to affect the essential arrest motif amino acids. The pegylation assay described here is advantageous as it allowed the full degree of compaction within the whole length of the ribosome exit tunnel to be measured, and from this, comparisons to be drawn between wild type SecM and several SecM mutants.

To determine if exposed cysteine residues outside of the ribosome exit tunnel undergo complete pegylation, SecM nascent chain release was induced by RNaseA degradation of the ribosome prior to incubation with PEG-mal (see Figure 4.3). In the absence of the ribosome and associated factors the SecM peptide does not achieve complete pegylation, with the results showing that less than 50% pegylation is achieved (Figure 4.3; Lanes 10 & 12). This indicates that the inability to undergo complete pegylation cannot be accounted for by any protection provided by the ribosome or associated factors but instead could be due to folding of the SecM nascent chain resulting in a shielding of the cysteine residue. This appears to be evident in all the extended SecM peptides in this study, with the overall percentage of pegylation seen with both the extended control peptides, SecM Q158P and 1-165, and also the extended SecM I156L peptide when stalled on the ribosome, reduced in comparison to wild type SecM. As this was not an isolated occurrence and all extended SecM peptides examined showed a similar pattern of lower pegylation, it is most likely accounted for due to differences in secondary or tertiary structure outside the ribosome exit tunnel, resulting in protection of the cysteine residue and therefore a reduction in the overall rate of pegylation.

Although not necessary for the scope of these experiments, it may be possible to confirm this theory by using NMR spectroscopy to examine the structure of stalled SecM attached

to the ribosome. The structure of proteins attached to the ribosome has previously been studied using by NMR analysis by using the SecM C-terminus to anchor other proteins to the ribosome (Cabrita et al., 2009; Hsu et al., 2007). Therefore, using these established techniques it would be possible to study the folding of the full-length SecM nascent chain of both wild type SecM, and an extended SecM peptide, whilst stalled on the ribosome.

4.3.2 Influence of single conservative mutations on compaction of SecM nascent chain

The structure of the SecM nascent chain within the exit tunnel appears to be dynamic and mutations of key arrest motif residues can be compensated for by increased freedom of movement of the nascent chain, as this enables re-positioning of the nascent chain upon stalling thus enabling accommodation of mutations of key amino acid residues, see Chapter 3 for details. The focus of this chapter was to examine SecM compaction by studying selected mutations of key arrest motif residues and also to examine the influence of a further P153A mutation in the restoration of stalling capability of these peptides. As stated previously the 3 conservative mutations studied in this Chapter were selected due to their ability to retain the greatest degree of stalling which is further increased when combined with the additional P153A mutation. The results in this chapter reveal that of the three conservative SecM mutants studied, F150Y and G161S underwent only slight compaction upon stalling, not equivalent to the partially alpha helical structure of wild type SecM, whilst SecM I156L remained in an extended conformation. Despite this loss of compaction SecM F150Y and I156L maintain stalling capability of ~ 55% whilst SecM G161S is ~20%, see Figure 4.13 for a summary of these results.

The timing of compaction was shown to occur once the synthesis of the arrest motif was complete, with the SecM nascent chain remaining in an extended conformation until this time (Woolhead et al., 2006). Molecular-dynamics flexible fitting (MDFF) modelling revealed that compaction of the SecM nascent chain upon stalling occurs between residues W155 and R163, and results in a shortening of the distance between these residues from ~31 Å in a fully extended conformation to 24 Å (Gumbart et al., 2012). Loss of compaction will therefore affect the positioning of the residues downstream from R163, and although this residue will remain in the vicinity of rRNA nucleotide A2062 (Bhushan et al., 2011) it is still dependant on downstream contacts with the ribosome exit tunnel to position it correctly to ensure correct interaction with A2062 and initiate stalling.

Previous experiments using truncated constructs to generate ribosome-nascent chain complexes have shown that the SecM nascent chain still underwent compaction when selected key arrest motif amino acid residues were mutated to alanine, despite these mutations resulting in stalling being abolished in full-length constructs (Woolhead et al., 2006). This is believed to be due to the importance of these residues and their function in interacting with the ribosome exit tunnel and the subsequent positioning of residue R163, to enable it to interact correctly with the rRNA nucleotide A2062. The question remains what are these key interactions between the SecM nascent chain and the ribosome exit tunnel, and how do they vary between different stalling peptides? It has already been established that different stalling peptides have little amino acid sequence similarity suggesting that each one forms different interactions with the exit tunnel to induce translation arrest (Ito et al., 2010). Evidence here indicates that different interactions can be formed by mutants of the same stalling peptide, as the mutated SecM nascent chains compact differently from wild type SecM yet are still able to maintain a degree of stalling. This suggests that in order to achieve this the SecM nascent chain must utilise the time taken between synthesis of the arrest motif and ratcheting of the glycine-tRNA in the P site to achieve a conformation which enables translation arrest to be maintained, through correct positioning of R163 with rRNA nucleotide A2062. Although some mutants achieve this, not all peptides of the same mutant are successful, hence why stalling is not 100% effective, and in these instances the SecM nascent chain continues to be synthesised and is released.

Previous evidence showed that constriction of the nascent chain backbone by mutation of non-essential residues 157-160 to proline prevented compaction and in doing so abolished arrest (Woolhead et al., 2006). However, in these experiments SecM I156L has shown that an extended SecM nascent chain can still undergo arrest, see Figure 4.13 for summary. This indicates that a SecM peptide that is extended but not constrained is still able to utilise its movement within the exit tunnel to shift and potentially allow it to sample a range of structures to find one capable of forming suitable interactions that enable stalling. It must do so through potentially forming new interactions or by alternative residues being able to form these key interactions with the ribosome exit tunnel as the loss of compaction resulting in an extended nascent chain upon stalling would result in different positioning of the key arrest amino acids upstream from R163.

As stated previously, the main interaction between the SecM nascent chain and the ribosome exit tunnel that is responsible for translation arrest occurs at rRNA nucleotide A2062, however, there are other interactions between the nascent chain and exit tunnel which occur near the L4/L22 constriction point that are also important but appear less essential (Gumbart et al., 2012). In particular in this region residue W155 of SecM has been shown to base stack with nucleotide A751 of 23S rRNA. As I156L is directly beside W155 and this SecM mutant remains in an extended conformation, this suggests that mutation of this residue to Leucine prevents base stacking between W155 and A751, resulting in the extended conformation of SecM I156L upon stalling. The loss of base stacking at A751 due to the proximity of the I156L mutation would explain why F150Y and G161S mutations, which are further away, affect compaction to a lesser degree. Despite this the level of extension or compaction, does not correlate with the level of stalling, as SecM I156L has the highest level of translation arrest out of the three conservative mutations studied. This suggests that compaction of the SecM nascent chain does not directly determine the stalling capability of the peptide, instead stalling appears to be based on a more refined ability of the nascent chain to position the key R163 residue correctly within the ribosome exit tunnel. For wild type SecM this is achieved through compaction of the nascent chain, however, these results show that SecM mutants can be accommodated by alternative positioning and interactions of the nascent chain within in the exit tunnel. In turn, this accounts for the high level of variation in the sequence and behaviour of other stalling peptides which do not rely on nascent chain compaction to achieve translation arrest, such as AAP (Wu et al., 2012).

Of the 3 conservative mutations examined SecM I156L would be the most interesting to examine further as it maintains the highest rate of stalling at ~55% (Figure 3.5B; Lane 7) yet this peptide is in the most extended conformation upon translation arrest (Figure 4.10B). In wild type SecM, I156 is located near the L4/L22 constriction point and both I156 and W155 make contact with the exit tunnel at rRNA nucleotide A751 (Bhushan et al., 2011). W155 is a highly conserved residue and as stated previously many stalling peptides such as SecM, AAP and TnaC contain a tryptophan residue 11-12 amino acids from the C-terminus which is essential for stalling (Freitag et al., 1996; Gong and Yanofsky, 2002; Nakatogawa and Ito, 2002). Closer examination of the positioning of the SecM I156L nascent chain within the ribosome exit tunnel would need to be performed, potentially through cryo-EM, to examine the structure of this stalled peptide and observe

how it overcomes the loss of these key interactions and indeed to examine what new interactions it forms that can compensate for this.

4.3.3 Influence of additional flexibility of the nascent chain resulting from P153A mutation on compaction of SecM mutants

Mutation of P153A alone does not affect the efficiency of SecM stalling in comparison to wild type (Figure 3.3B; Lane 5), neither does it have any effect on the overall compaction of SecM upon stalling (Figure 4.7). However, when combined with single conservative mutations it resulted in a return of nascent chain compaction to levels analogous to that of wild type SecM, for all 3 conservative mutations studied. This also correlated with an increase in translation arrest, however, unlike nascent chain compaction, the levels of translation arrest do not return to that of wild type SecM, see Figure 4.13 for an overall summary. Although not possible to conclude from these experiments, the close proximity of P153A to the W155 residue may account for the observed recovery of stalling in the peptides containing the additional P153A mutation. The increased flexibility of the SecM nascent chain adjacent to the base stacking of W155 with rRNA nucleotide A751 appears to enable accommodation of the conservative mutations and return compaction of the nascent chain to that of wild type levels. However, although the results indicate that the increased flexibility of the SecM nascent chain restores the levels of compaction to that of wild type SecM, it is unable to completely compensate for the loss of the essential amino acid residues, despite their mutation to closely related conservative amino acids. The restoration of compaction in these conservative mutants when provided with increased nascent chain flexibility, reinforces again that compaction of SecM upon stalling provides the optimum positioning of R163.

The P146A mutation that was examined in Chapter 3 (see Figure 3.8) which, unlike the P153A, resulted in no improvement to the rate of translation arrest is most likely due to this mutation being unable to restore compaction, as the distance between P146A and W155 is too great to provide effective alternative positioning of the SecM nascent chain at this critical point to accommodate the conservative mutations and enable restoration of base stacking. These conclusions would need to be confirmed by further experiments which would be hypothesised to show that the additional P146A mutation had no effect on nascent chain compaction.

4.4.4 Overall conclusions and scope for future investigations

This study has utilised a cysteine pegylation assay to establish the length of the SecM nascent chain contained within the ribosome exit tunnel when both extended and compacted upon translation arrest. Furthermore it has identified differences in compaction of the SecM nascent chain with selected conservative mutations, and also the influence of an increase in the flexibility of the nascent chain on this compaction. The work here has shown that whilst compaction is not reliant on the detection of a completely accurate arrest motif complete stalling capability is.

In terms of the importance of individual residues, of the 3 conservative mutations studied in this chapter it appears that G161 forms the most important interactions as it has the least toleration for mutation most likely due to its close proximity to the essential R163 residue (see Figure 4.13). Conversely F150Y, appears to be the most tolerated mutation as this residue is furthest away from R163, and also outside of the compaction zone between W155 and R163, as identified by Gumbart et al., (2012). These results have shown that increased flexibility of the SecM nascent chain results in recovery of the compaction of SecM mutants. However, whilst the P153A mutation is sufficient to return SecM compaction to wild type levels the pegylation assay does not reveal any details on the exact structure adopted by the SecM nascent chain within the exit tunnel, and how it may be individually adapted so as to position the R163 residue most effectively. Therefore, future routes of study could involve the cryo-EM analysis of these mutants as this, combined with the knowledge of their stalling abilities, could identify the key interactions required for positioning of R163 and translation arrest.

5. Specificity of translation arrest motifs in non-native ribosomes (prokaryotic vs. eukaryotic)

5.1 Introduction

Peptides capable of undergoing translation arrest, and subsequent control of the expression of downstream genes, occur in both prokaryotic and eukaryotes, however, these peptides share little homology in both length and amino acid stalling sequence, indicating that each has a relatively unique arrest mechanism (Ito et al., 2010). Previous work has shown variations in the species dependency of stalling sequences, with some showing stricter requirements for native ribosomes than others. Non-specific examples include the fungal arginine attenuator peptide (AAP) which undergoes stalling in fungi, plants and animals (Fang et al., 2004) and human cytomegalovirus (hCMV) gp48 upstream open reading frame 2 (uORF2) which can undergo stalling in Wheat Germ ribosomes (Bhushan et al., 2010b). Meanwhile, prokaryotic stalling peptides *E.coli* SecM and *Bacillus subtilis* MifM appear to be species-specific (Chiba et al., 2011), however, this is not universal for all bacterial stalling peptides, with others such as the *Proteus vulgaris* TnaC peptide capable of undergoing stalling in *E.coli* ribosomes (Cruz-Vera et al., 2009). In addition, as discussed in previous chapters, amino acid stalling sequences can be modified extensively and still function (Yap and Bernstein, 2009). It was therefore sought to firmly establish whether stalling peptides could instigate translation arrest in ribosome systems from different domains, for example whether a prokaryotic stalling peptide can stall translation of a eukaryotic ribosome and vice versa.

Eukaryotic cytoplasmic ribosomes are composed of a large 60S subunit (50S in prokaryotes) and a small 40S subunit (30S in prokaryotes) which combine to form the complete 80S ribosome (70S in prokaryotes) upon translation initiation. This is composed of 80 ribosomal proteins (79 in yeast) and four rRNA chains (25S, 5.8S, and 5S in the large subunit and 18S in the small subunit) (Wilson and Cate, 2012). Of these ribosomal proteins, 46 are eukaryote-specific (18 in the 40S subunit and 28 in the 60S subunit) and have no bacterial homologs, whilst in the prokaryotic 70S ribosome, 20 ribosomal proteins are bacteria-specific (6 in the 30S subunit and 14 in the 50S subunit) (Melnikov et al., 2012). Despite these differences genetic data and structural models of prokaryotic and eukaryotic ribosomes indicate that they share a common core structure containing

evolutionarily conserved protein and ribosomal RNA. In addition to this core structure, eukaryotic ribosomes contain eukaryotic-specific extensions to conserved proteins and additional proteins which account for it being ~40% larger than prokaryotic ribosomes. Those proteins that are unique to either domain tend to be located on the surface of the ribosome, enabling them to be accessible to interacting factors such as translation factors and chaperones which may act to regulate translation allosterically (Ben-Shem et al., 2011). Meanwhile studies have shown that the ribosomal interface between the large and small subunits, the area around the mRNA entry site and the ribosome exit tunnel, are highly conserved, with structural studies revealing that the length and dimensions of the exit tunnel are universal between prokaryotes and eukaryotes (Ban et al., 2000; Ben-Shem et al., 2011; Klinge et al., 2011; Nissen et al., 2000). Both eukaryotic and prokaryotic ribosome exit tunnels contain a constriction site approximately 20 Å from the PTC formed by the L4 and L22 (formally named L17 in eukaryotes) proteins, although due to insertions in the L4 protein in eukaryotes this constriction is slightly narrower (Klinge et al., 2011). In addition to the L4 and L22 proteins the bacterial ribosome exit tunnel contains bacteria-specific extensions of L23, whilst in eukaryotes these contributions are replaced by L39e (Ban et al., 2000; Ben-Shem et al., 2011; Klinge et al., 2011). Also, in comparison to prokaryotic ribosomes, eukaryotic ribosomes contain additional inter-subunit bridges formed predominantly by eukaryotic-specific proteins. These bridges appear to aid in the rotation of the head domain of the small subunit during translation which aids translocation of mRNA and tRNA through the ribosome (Ben-Shem et al., 2010). The diagram in Figure 5.1 provides a comparison of prokaryotic and eukaryotic ribosomes and highlights the proteins involved in lining the exit tunnel.

Despite the relative conservation between prokaryotic and eukaryotic ribosomes the variation in size and complexity between the two systems also correlates with a difference in the speed of translation. Prokaryotic ribosomes translate at a 10-fold faster rate than eukaryotes, with prokaryotic ribosomes capable of synthesising peptides 15-20 amino acids per second whilst eukaryotes synthesise at a rate of 2 amino acids per second (Lafontaine and Tollervey, 2001; Netzer and Hartl, 1997). Despite this, and whilst the translation initiation process in eukaryotes is more complex than prokaryotes, the conservation of the PTC between all domains suggests that the process of elongation is relatively conserved (Klinge et al., 2011).

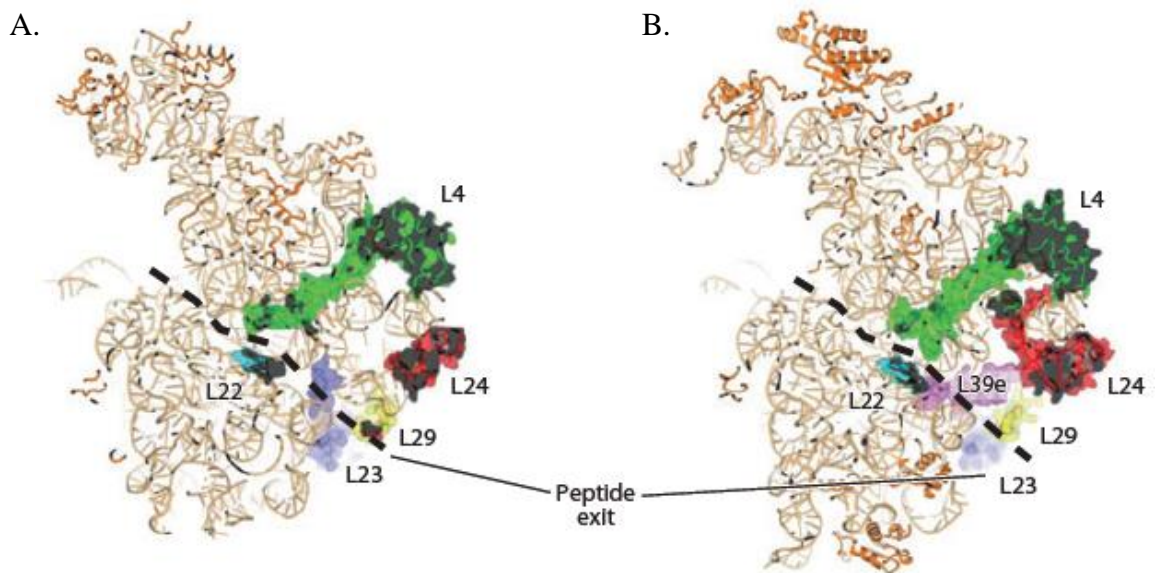


Figure 5.1 Molecular structures of prokaryotic and eukaryotic large ribosomal subunits indicating the path of the exit tunnel. A. Prokaryotic and B. Eukaryotic ribosomes with the path of exit tunnel through the large subunit shown by a dashed line. Diagram reproduced from Yusupova and Yusupov (2014).

To explore the specificity of translation arrest motifs in ribosomes of different domains, the *in vitro* stalling capabilities of selected stalling peptides were examined in two different systems, prokaryotic *E.coli* cell extract systems and eukaryotic Wheat Germ cell-free systems. Three stalling peptides were selected for study: prokaryotic *E.coli* SecM, leader peptide of the SecA operon; prokaryotic *E.coli* TnaC, leader peptide of the tryptophanase operon; and eukaryotic upstream open reading frame (uORF) fungal *N.crassa* arginine attenuator peptide (AAP). These stalling peptides were selected to give a broad representation of different arrest mechanisms with SecM being an intrinsic stalling peptide whilst TnaC and AAP are inducible, only undergoing stalling in the presence of high concentrations of their signal molecules tryptophan and arginine respectively. These signal molecules are believed to bind to the ribosome near the PTC site, with tryptophan believed to induce arrest of TnaC by causing conformational alterations to the ribosome resulting in the inability to complete translation termination (Cruz-Vera et al., 2006; Wu et al., 2012) whilst arginine has been shown to induce a conformational change in AAP within the ribosome exit tunnel resulting in prevention of translation termination (Wu et al., 2012). Additionally SecM is a translation elongation stalling peptide and undergoes arrest 4 amino acids from the stop codon, whilst AAP and TnaC are both translation termination stalling peptides, undergoing arrest when the stop codon is located in the ribosome P site. The essential amino acid stalling motifs of these peptides are compared in Table 5.1. Whilst there are some shared amino acid residues this comparison highlights the lack of any strong sequence similarity between stalling peptides either within the same domain or across different domains.

Intrinsic																				P site	A site	
[1] SecM <i>E.coli</i>	...	Q	A	K	E	S	T	P	V	W	I	S	Q	A	Q	G	I	R	A	G	P	
[2] TnaC <i>E.coli</i>	...	I	C	V	T	S	K	W	F	N	I	D	N	K	I	V	D	H	R	P	*	+ Tryptophan
[3] AAP <i>N.crassa</i>	...	S	V	F	T	S	Q	D	Y	L	S	D	H	L	W	R	A	L	N	A	*	+ Arginine
Distance from ribosome P site	-19	-18	-17	-16	-15	-14	-13	-12	-11	-10	-9	-8	-7	-6	-5	-4	-3	-2	-1	0	+1	

Table 5.1. Comparison of the C-terminus amino acid sequences of the translational stalling peptides SecM, TnaC and AAP. Essential stalling residues are highlighted in red and bold with non-essential residues in black. Residues shaded green are conserved between the stalling peptides as indicated whilst those highlighted in orange are similar but non-identical residues. Residues occupying the ribosome A and P sites are shown on the right of the table. An asterisk (*) is used where peptides stall with the stop codon in the ribosome A site. Arrest sequences from [1] Nakatogawa and Ito (2002); [2] Cruz-Vera et al., (2008); and [3] Spevak et al., (2010).

To obtain optimal translation it was necessary to take into account the different translation initiation systems present in both prokaryotes and eukaryotes, therefore separate constructs were made for each system with Shine-Dalgarno sequences engineered into the prokaryote specific constructs and Kozak sequences in the eukaryotic constructs. Details of the plasmids and constructs used in this study can be found in Appendix 3. This removes any issues of ineffective peptide translation and places the focus on the peptides' ability to interact with the ribosome exit tunnel and undergo translation arrest. As both *E. coli* TnaC and *N. crassa* AAP are only 24 amino acids in length, considerably shorter than SecM which is 170 amino acids, adapted constructs were created in order to study these stalling peptides effectively. To clearly visualise these peptides on a gel, modified constructs were created by attaching these peptides at the C-terminus of the 62 N-terminal residues of SecM (see Figure 5.2A). The constructs were additionally point-mutated within the SecM region to include a further 3 methionine residues as the original constructs produced too weak a signal in initial experiments. The N-terminus of SecM is responsible for peptide targeting to the membrane and has no role in translation arrest (Chiba et al., 2011), therefore it can be employed in these constructs without effecting the results of these assays. Whilst other unrelated proteins could have been selected to serve as an N-terminus attachment to these constructs, further studies would have been required to establish that any folding of these additional peptides outside of the ribosome exit tunnel did not result in a pull on the nascent chain which could artificially release stalling.

In addition to SecM-AAP and SecM-TnaC, constructs were also made containing the last 4 amino acids of SecM (QRLT) at the C-terminus of both AAP and TnaC, to establish whether truncated TnaC or AAP functions efficiently or if an additional mRNA 'tail' has a role in providing stability within the ribosome beyond the translation pause site, Figure 5.2B. Finally an additional control AAP construct was created containing the D12N mutation which has previously been shown to eliminate arginine specific regulation of AAP thus preventing stalling *in vitro* (Freitag et al., 1996; Wang and Sachs, 1997), Figure 5.2C. A full list of the constructs used in this chapter, including details of how they were generated, can be found in Appendix 3.

AAP and TnaC undergo translation arrest in the presence of high concentrations of inducer molecule, arginine and tryptophan respectively. Although the location of inducer molecule was unable to be visualised by cryo-EM (Bhushan et al., 2010b; Seidelt et al., 2009), the

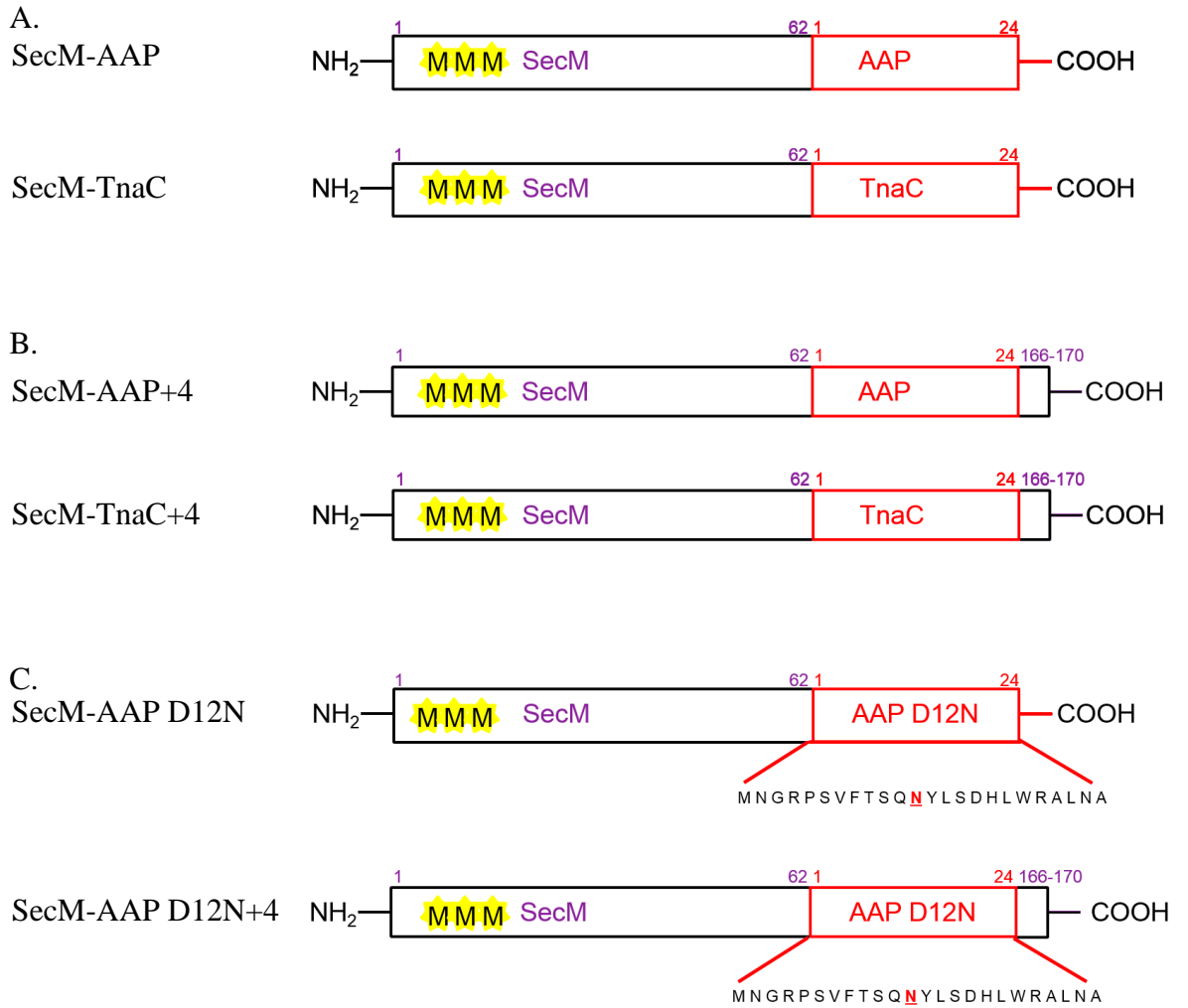


Figure 5.2 The generated AAP and TnaC constructs employed in this chapter. A. SecM-AAP and SecM-TnaC constructs, B. SecM-AAP and SecM-TnaC constructs containing the additional 4 C-terminal residues of SecM (QRLT) and C. Control SecM-AAP D12N and SecM-AAP D12N+4 construct. Note the three additional methionine residues introduced into the SecM portion of each of the above constructs by point mutation to provide a stronger signal when labelled with radio-labelled methionine.

inducer molecule is believed to bind close to the PTC to induce stalling (Cruz-Vera et al., 2006). Therefore the AAP and TnaC constructs were synthesised in *in vitro* prokaryotic *E.coli* cell extract systems and eukaryotic Wheat Germ cell-free systems in both the presence of high inducing concentrations (1 mM or 2 mM) or low non-inducing concentrations (0.01 mM) of their respective inducer molecules. Two assays were then implemented to investigate peptide stalling, the previously described CTABr precipitation and also a Puromycin release assay. Puromycin is an aminonucleoside antibiotic with part of it analogous to the 3' end of tyrosyl-tRNA (Yarmolinsky and de la Haba, 1961) (see Figure 5.3A & B). Due to this structural similarity, puromycin is able to enter the ribosome A site and covalently attach to the carboxyl terminus of the polypeptide chain, preventing further chain elongation and resulting in premature release of the peptide from the ribosome (Figure 5.3C). This assay has previously been utilised to illustrate that, when arrested, stalling peptides undergo alterations within the PTC which results in them no longer being susceptible to release by puromycin (Gong et al., 2001; Wei et al., 2012; Woolhead et al., 2006). Therefore, by using truncated mRNA to artificially stall peptides on the ribosome at the point of the proposed arrest, only those which have undergone changes in the PTC induced by actual translation arrest will remain bound in the presence of puromycin, whilst those peptides attached to the ribosome solely through the use of truncated mRNA will be released (see Figure 5.3 D). This is detected when the translation products are resolved on a gel, by the presence or absence of the higher molecular weight band of the stalled tRNA-peptide.

Each of the stalling peptides SecM, TnaC and AAP have been visualised by cryo-EM, which shows that they appear to undergo separate interactions within the ribosome exit tunnel upon translation arrest (Bhushan et al., 2010b; Gumbart et al., 2012; Seidelt et al., 2009). Chapter 1 contains a comprehensive summary, briefly however, due to the similarities between prokaryotic and eukaryotic ribosome exit tunnels the nascent peptides appear to interact within similar areas of the exit tunnel including ribosomal RNA nucleotides U2585, A2062, A2058 and A751, and the extensions of ribosomal proteins L4 and L22 (L17). This suggests it may be feasible for eukaryotic stalling peptides to arrest in prokaryotic ribosomes and vice versa and therefore investigating the specificity of arrest sequences will be the focus of this chapter.

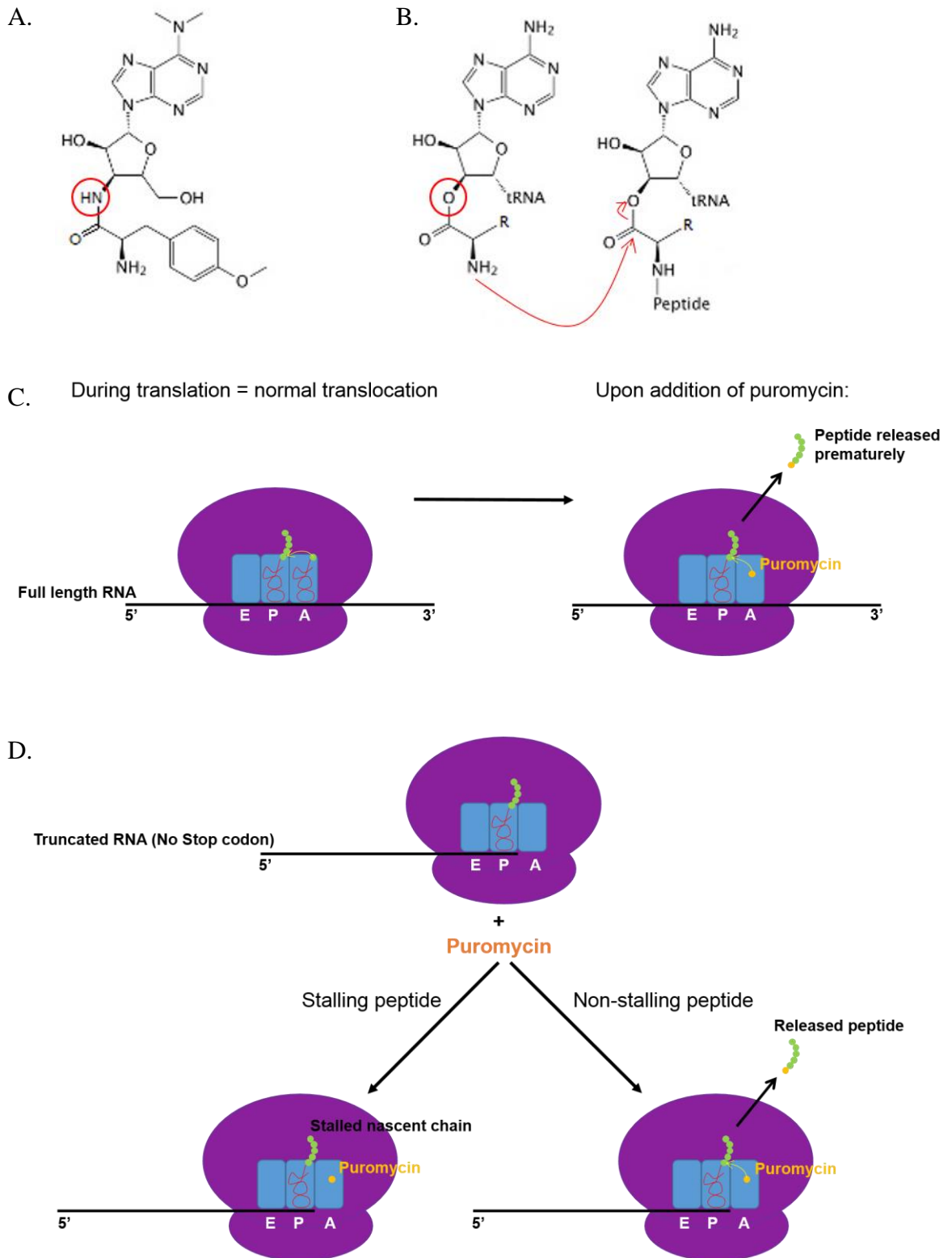


Figure 5.3 Summary of puromycin release assay. A. Chemical structure of puromycin, which resembles the 3' end of tyrosyl-tRNA. Circled in red is the amide group which differs from the ester group of tRNA (circled in B.) and is responsible for the prevention of further chain elongation. B. Under normal circumstances aminoacyl-tRNA attacks the peptidyl-tRNA as indicated by the curly arrows, resulting in chain elongation. C. Diagrammatic representation of chain elongation during translation, transfer of amino acid to the growing nascent chain occurs under normal conditions, however, in the presence of puromycin, this molecule is incorporated into the nascent chain resulting in translation termination and premature release of the peptide from the ribosome. D. In the puromycin release assay, truncated mRNA is used to artificially stall ribosomes, however, only those containing fully arrested peptides will remain bound to the ribosome in the presence of puromycin, whilst artificially arrested, non-stalling peptides will be released from the ribosome by the addition of puromycin.

5.2 Results

5.2.1 SecM

To examine the ability of stalling peptides to undergo translation arrest in alternative ribosome systems initial CTABr experiments were conducted on *E. coli* SecM to examine the ability of this peptide to undergo stalling in eukaryotic ribosomes. SecM is an ideal model stalling peptide for *in vitro* studies in eukaryotic translation systems as the results can be compared to the robust stalling ability of this peptide in its native prokaryotic *E. coli* system. SecM undergoes a high level of arrest in *E. coli*, with the majority of the peptide isolated as the shorter (166 amino acids) translation elongation-arrested peptide in the CTABr pellet fraction (Figure 5.4; Lane 1), and only a small amount of full length peptide is released and isolated in the CTABr supernatant fraction (Figure 5.4; Lane 2). Although the SecM peptide is sufficiently well translated in eukaryotic Wheat Germ ribosomes, stalling does not occur, as the majority of the peptide is full-length (170 amino acids) and recovered in the CTABr supernatant fraction (Figure 5.4; Lane 4). There is no lower band present in the pellet fraction indicating an absence of stalled peptide (Figure 5.4; Lane 3).

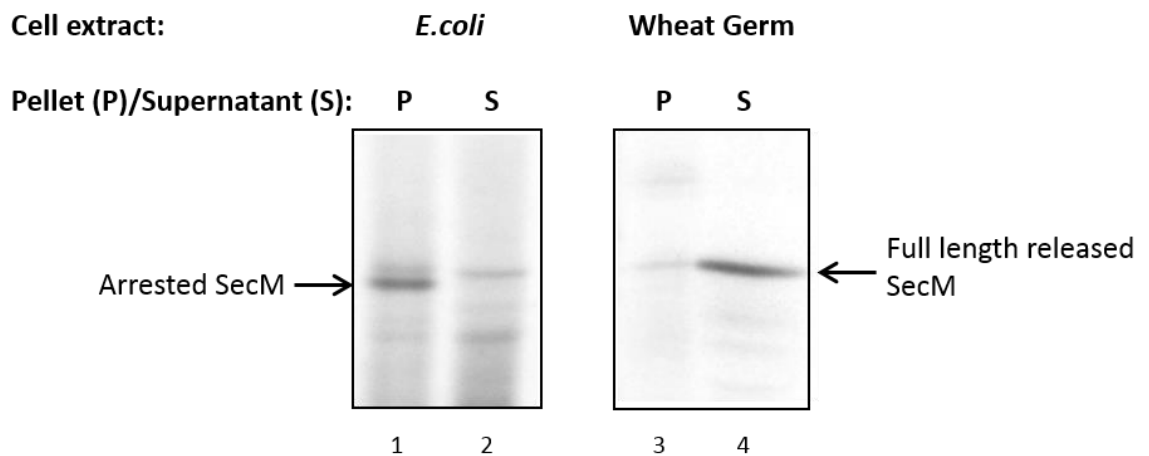


Figure 5.4 Stalling of *E. coli* SecM in prokaryotic *E. coli* and eukaryotic Wheat Germ translation systems. SecM WT was translated *in vitro* in both *E. coli* cell extract and a Wheat Germ cell-free translation system before being CTABr precipitated, separated into pellet (P) and supernatant (S) fractions and resolved by SDS-PAGE. Results are representative of multiple experiments.

5.2.2 *TnaC* and *TnaC+4*

5.2.2.1 *TnaC* and *TnaC+4* stalling in prokaryotic *E.coli* ribosomes

Following this, *E.coli* *TnaC* was synthesised *in vitro* using *E.coli* cell extract in the presence of several different tryptophan concentrations (initially: 0.01, 1 and 2 mM) with stalling expected to occur only in the presence of high concentrations of inducer molecule. The two constructs, SecM-*TnaC* and SecM-*TnaC+4*, were synthesised and the results are shown in Figure 5.5. In comparison to wild type SecM stalling in *E.coli* cell extract, *TnaC* undergoes a lower level of overall stalling even at high tryptophan concentrations, resulting in a strong band present in the supernatant fraction of all the samples indicating released peptide (Figure 5.5A; even numbered lanes). This lower level of stalling of *TnaC* in comparison to SecM is not believed to be due to lack of inducer molecule, as previous studies have established the optimum levels of tryptophan for efficient stalling (Gong et al., 2001; Gong and Yanofsky, 2001). Instead this difference may be due to the inefficiency of tryptophan binding and therefore inducible stalling in this *in vitro* translation system. Also, affecting interpretation of these results is the presence of a higher band at ~40 kDa in the pellet fraction (Figure 5.5A; denoted by asterix *), which previous studies have identified as being SecM-*TnaC*-tRNA^{Pro} (Gong and Yanofsky, 2001). Removal of this band was achieved by incubation with RNaseA prior to separating on a tricene gel, concentrating the stalled peptides within the one lower band in the CTABr pellet fraction (Figure 5.5 B). This enabled calculation of the percentage of translation arrest of *TnaC* at different tryptophan concentrations, with the results indicating that there appeared to be a basal level of *TnaC* stalling even at low concentrations of tryptophan inducer (Figure 5.6A; Lane 1). Interestingly this basal level of stalling was higher for *TnaC+4* peptides (Figure 5.6A; Lane 7). Both peptides displayed increasing levels of arrest with increasing tryptophan concentrations (Figure 5.6A; Lanes 3 & 9), with *TnaC+4* also achieving a higher maximum overall percentage of arrest (Figure 5.6A; Lane 11) in comparison to *TnaC* (Figure 5.6A; Lane 5).

The average percentage of arrest for the *TnaC* and *TnaC+4* peptides are shown in Figure 5.6B. This graph highlights that although the *TnaC+4* construct had an overall greater level of stalling at high concentrations of inducer (2 mM tryptophan) this was countered by a higher initial level of stalling at low tryptophan concentrations (0.01 mM). It appears

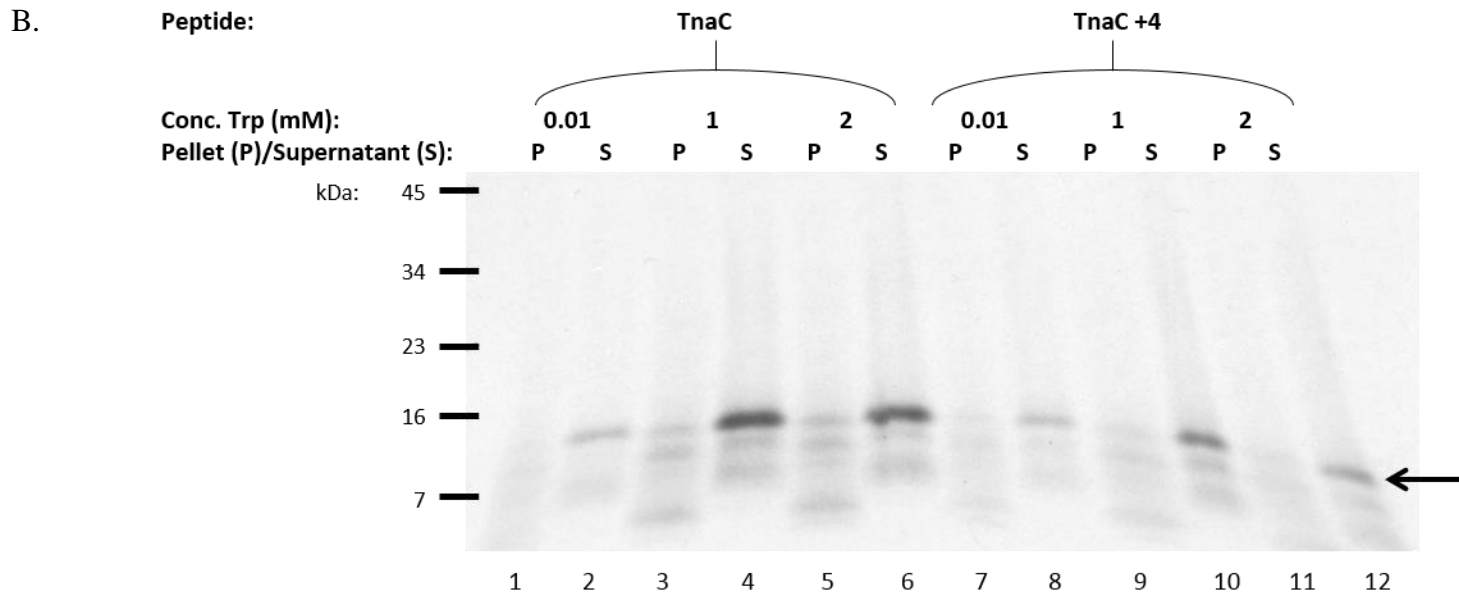
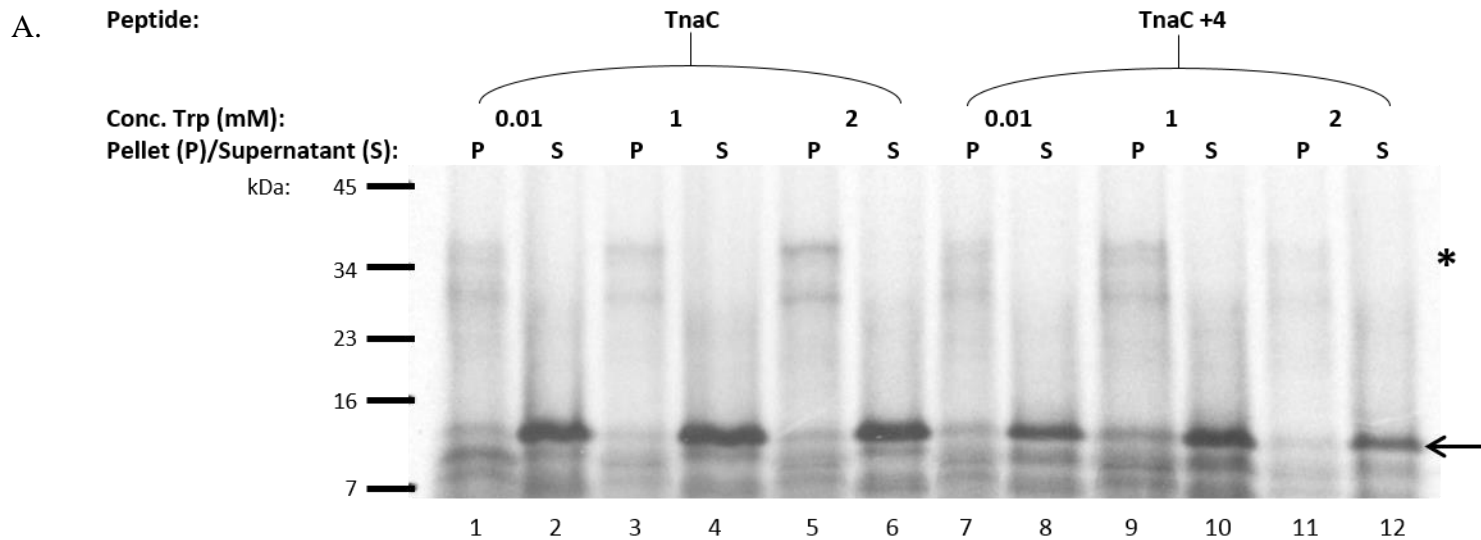
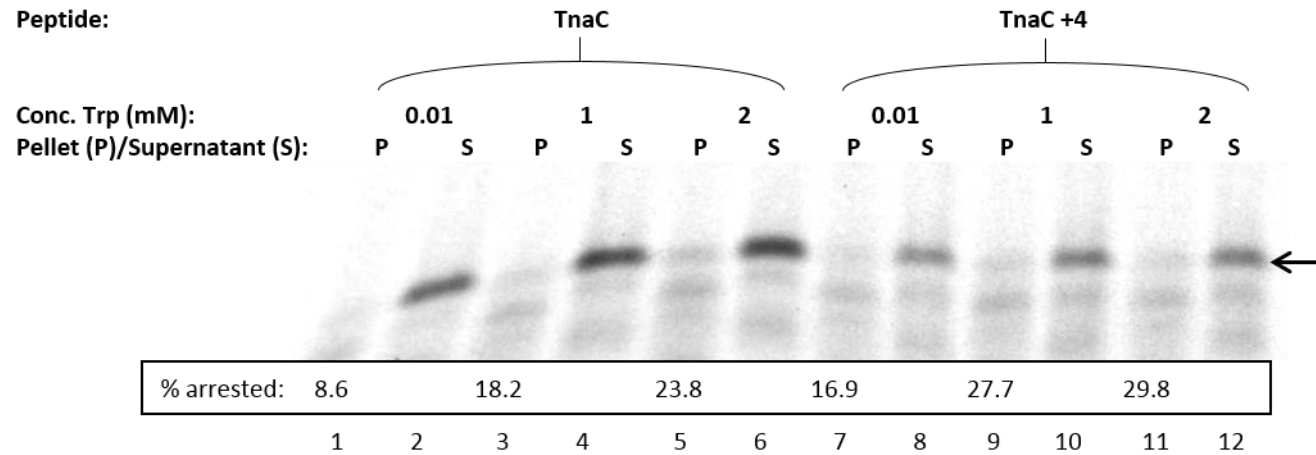


Figure 5.5 Stalling of SecM-TnaC and SecM-TnaC+4 in a prokaryotic *E.coli* translation system. A. SecM-TnaC and SecM-TnaC+4 were synthesised in *E.coli* cell extract *in vitro* transcription-translation assays containing 0.01 mM, 1 mM or 2 mM tryptophan (inducer molecule). Products were CTABr precipitated, separated into pellet (P) and supernatant (S) fractions and resolved on tricine gels. An asterix (*) indicates SecM-TnaC-tRNA^{Pro} whilst the arrow indicates the band representing the TnaC peptide. B. SecM-TnaC and SecM-TnaC+4 were synthesised as previously with an additional incubation with 1 mg/ml RNaseA, prior to separating on tricine gels. RNaseA treatment removes tRNA^{Pro} resulting in one band representing total translated TnaC peptide and indicated on the gel by arrow. All gels are representative of multiple experiments.

A.



B.

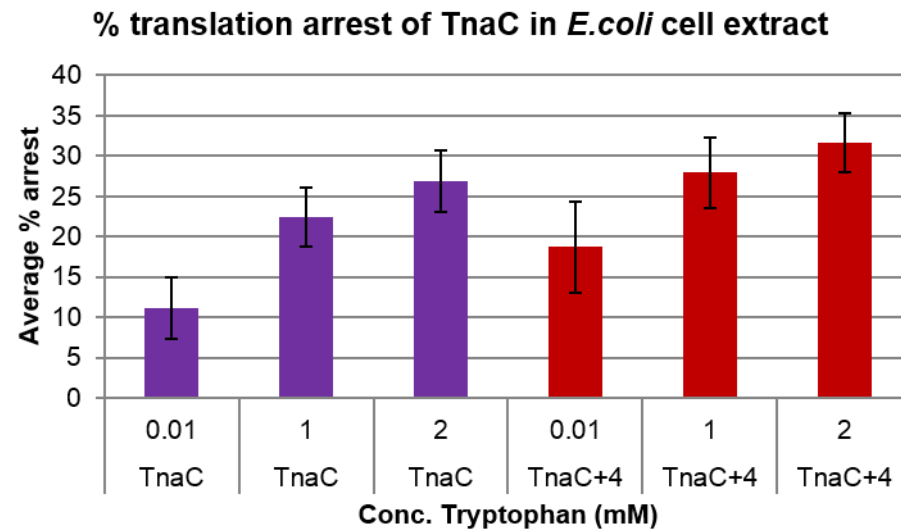


Figure 5.6 Stalling of SecM-TnaC and SecM-TnaC+4 in an *E. coli* translation system with RNaseA incubation. A. SecM-TnaC and SecM-TnaC+4 were synthesised in *E. coli* cell extract *in vitro* transcription-translation assays containing 0.01 mM, 1 mM or 2 mM tryptophan (inducer molecule). Translation products were CTABr precipitated, separated into pellet (P) and supernatant (S) fractions and incubated with 1 mg/ml RNaseA prior to being resolved on tricine gels. The arrow indicates total translated TnaC peptide. The percentage of arrested TnaC was quantified by Image J software and calculated as a percentage of $[\text{Arrested}/(\text{Arrested} + \text{Released})]$, with each value adjusted for background. Gel is representative of multiple experiments. B. Average percentage arrest of SecM-TnaC and SecM-TnaC+4 peptides at 0.01 mM, 1 mM and 2 mM tryptophan concentrations. Average is calculated from an n of 3. Error bars indicate standard deviation.

that the additional 4 residues at the C-terminus of TnaC+4 does have a role in aiding arrest and more will be discussed on this later with relation to the AAP+4 construct.

5.2.2.2 TnaC and TnaC+4 stalling in eukaryotic Wheat Germ ribosomes

After establishing the level of TnaC translation arrest in native *E.coli* ribosomes the stalling capabilities of these peptides were then tested in eukaryotic Wheat Germ ribosomes. Similar to the results in the prokaryotic system, there was a higher level of basal stalling for TnaC+4 (Figure 5.7; Lane 5) than TnaC (Figure 5.7; Lane 1) at low tryptophan concentrations (0.01 mM). These levels of basal stalling were similar to that seen in *E.coli* ribosomes at the same concentrations of tryptophan (0.01 mM) with ~8% for TnaC (Figure 5.6A & 5.7; both Lane 1) and ~16% for TnaC+4 (Figure 5.6A & 5.7; Lane 7 and 5 respectively). However, unlike in the prokaryotic system, there was no further increase in the level of arrest at high concentrations of inducer molecule (2 mM tryptophan) for either TnaC (Figure 5.7; Lane 3) or TnaC+4 (Figure 5.7; Lane 7). This indicates that the TnaC peptide is only able to undergo increased levels of induced stalling in native *E.coli* ribosome systems.

To confirm these results, further experiments were carried out to examine translation arrest using the puromycin release assay. Truncated mRNA was used for these assays to artificially stall the nascent chain on the ribosome therefore only SecM-TnaC, and not SecM-TnaC+4, could be investigated using this assay. Stalled TnaC peptidyl-tRNA^{Pro} is indicated by the presence of the higher molecular weight band (Gong et al., 2001) which in the absence of puromycin is seen at both low (0.01 mM) and high (2 mM) concentrations of tryptophan in both *E.coli* (Figure 5.8, Lanes 1 & 2) and Wheat Germ systems (Figure 5.8, Lanes 5 & 6). Addition of puromycin results in the loss of artificially induced stalling caused by the use truncated mRNA constructs, which is indicated by the absence of the higher weight molecular band. These results show that in *E.coli* cell extract, at low tryptophan concentrations (0.01 mM) addition of puromycin relieves the artificial stalling induced by truncated mRNA (Figure 5.8, Lane 3). However, arrest is maintained after the addition of puromycin in the presence of high concentrations (2 mM) of tryptophan (Figure 5.8, Lane 4). This stalling is not reflected in eukaryotic ribosome systems with the abolishment of the higher molecular weight peptidyl-tRNA^{Pro} band at both low (0.01 mM) and high (2 mM) tryptophan concentrations in the presence of puromycin (Figure 5.8, Lane

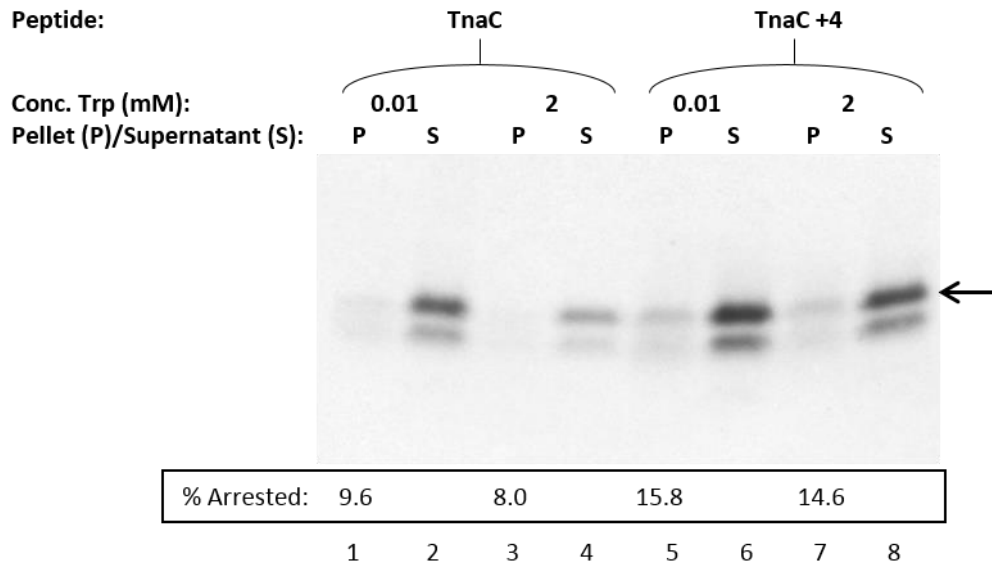


Figure 5.7 Stalling of SecM-TnaC and SecM-TnaC+4 in eukaryotic Wheat Germ cell-free translation system with RNaseA incubation. SecM-TnaC and SecM-TnaC+4 were synthesised in Wheat Germ cell extract *in vitro* translation assays containing 0.01 mM or 2 mM tryptophan (inducer molecule). Translation products were CTABr precipitated, separated into pellet (P) and supernatant (S) fractions and incubated with 1 mg/ml RNaseA prior to being resolved on tricine gels. The percentage of arrested TnaC was quantified by Image J software and calculated as a percentage of [Arrested/(Arrested + Released)], with each value adjusted for background. Arrow indicates translated TnaC peptide. Gel is representative of multiple experiments.

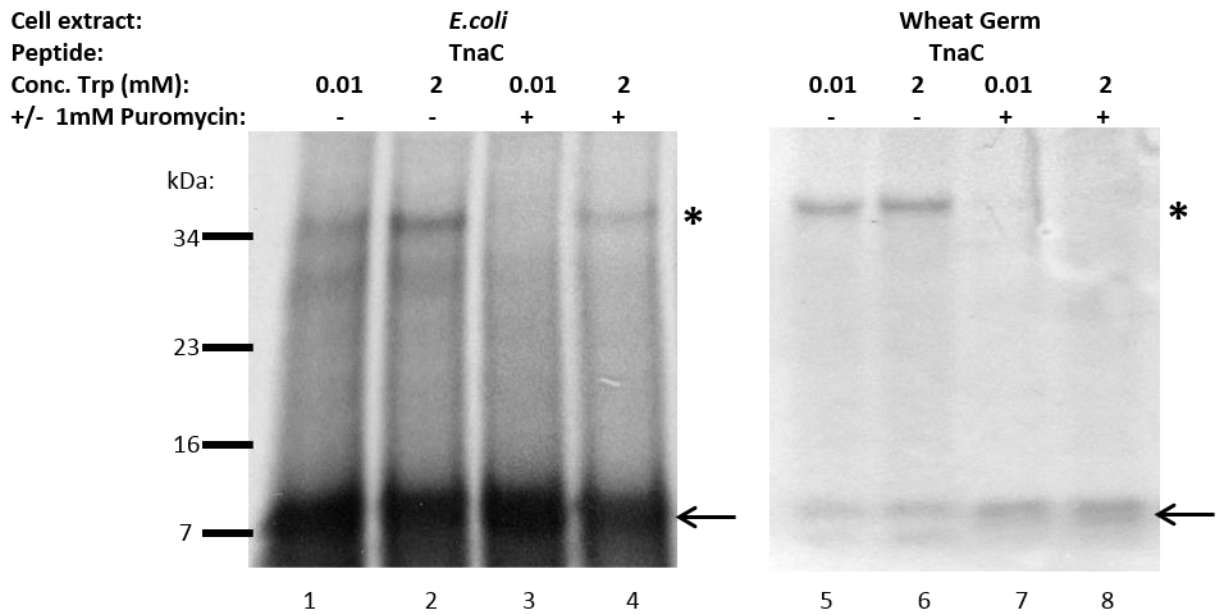


Figure 5.8 SecM-TnaC stalling in prokaryotic *E. coli* and eukaryotic Wheat Germ translation system detected by Puromycin release assay. Truncated SecM-TnaC mRNA lacking a stop codon was translated *in vitro* in *E. coli* and Wheat Germ cell extract, in the presence of either 0.01 mM or 2 mM tryptophan (inducer molecule). Reactions were divided in half with 1 mM puromycin added to one whilst the other served as a control. After incubation the products were resolved on tricine gels. The asterix (*) indicates TnaC peptidyl-tRNA^{Pro} whilst the arrow indicates released SecM-TnaC peptide. Gel is representative of multiple experiments.

7 & 8). This confirms the previous CTABr precipitation results which indicated that TnaC undergoes stalling at high inducer concentrations in native *E.coli* ribosomes but is not able to emulate this stalling in eukaryotic Wheat Germ ribosomes. Instead the basal stalling seen in the CTABr precipitation assays at low inducer concentrations in the *E.coli* cell extract system (Figure 5.6A; Lanes 1 and 7) and both low and high inducer concentrations in eukaryotic Wheat Germ ribosomes (Figure 5.7; Lanes 1, 3, 5 and 7) is indicative of the peptide undergoing a translational pause without obtaining full translational arrest. The significance of this will be discussed further in Section 5.3.

5.2.3 AAP and AAP+4

5.2.3.1 AAP and AAP+4 stalling in eukaryotic Wheat Germ ribosomes

CTABr precipitation assays were carried out to assess the stalling capability of the eukaryotic *N.crassa* stalling peptide AAP, in both eukaryotic Wheat Germ and prokaryotic *E.coli* translation systems. Previous work has shown that this peptide has the ability to stall in fungal, plant and animal ribosomes (Fang et al., 2004), therefore it was first sought to establish the stalling of these SecM-AAP and SecM-AAP+4 peptides in eukaryotic Wheat Germ ribosome systems. The results indicate that at low arginine concentration (0.01 mM) there is minimal basal stalling of wild type AAP (Figure 5.9A; Lane 1), whilst high arginine concentrations (2 mM) activated AAP stalling (Figure 5.9A; Lane 3). This is similar to AAP+4, however, as with TnaC+4, the basal rate of stalling was slightly higher (Figure 5.9A; Lane 5) and in turn the stalling under inducing arginine concentrations was also higher (Figure 5.9A; Lane 7). There is a noticeable difference in the lengths of the stalled AAP+4 peptides in the pellet fraction (Figure 5.9A; Lane 7) to the released peptides isolated in the supernatant fraction (Figure 5.9A; Lane 8) due to the stalled peptide not having translated the additional 4 C-terminal residues at the point of arrest. Also of note was that the basal level of AAP+4 stalling was higher than that seen for the AAP D12N+4 peptide (Figure 5.9A; Lane 13). As expected neither of the mutant AAP D12N peptides underwent stalling at low (0.01 mM) or high (2 mM) arginine inducer concentrations (Figure 5.9A; Lanes 11 & 15).

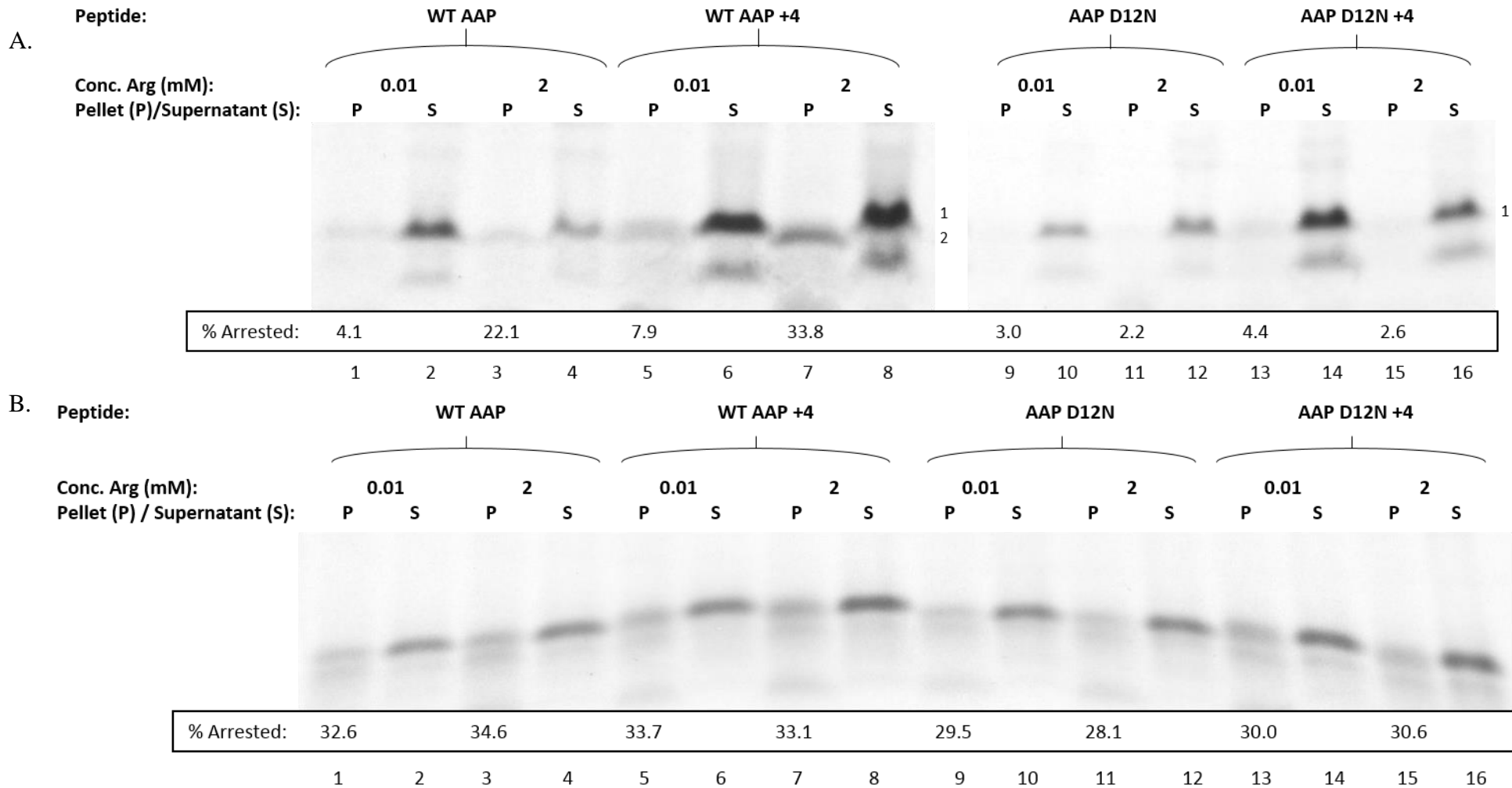


Figure 5.9 AAP stalling in eukaryotic Wheat Germ and prokaryotic *E.coli* translation systems. Peptides were synthesised in A. Wheat Germ and B. *E.coli* *in vitro* transcription-translation assays containing 0.01 mM or 2 mM arginine (inducer molecule). Products were CTABr precipitated, separated into pellet (P) and supernatant (S) fractions and incubated with 1 mg/ml RNaseA prior to being resolved on tricine gels. The percentage of arrested AAP was quantified by Image J software and calculated as a percentage of [Arrested/(Arrested + Released)], with each value adjusted for background. 1. Released (full length) and 2. Stalled AAP peptide. Gels are representative of multiple experiments.

5.2.3.2 AAP and AAP+4 stalling in prokaryotic *E.coli* ribosomes

Further to this, the stalling of AAP in prokaryotic *E.coli* ribosomes was then investigated, with the results showing that both AAP and AAP+4 undergo a high level of basal stalling at low (0.01 mM) arginine inducer concentrations (Figure 5.9B; Lanes 1 & 5). This stalling is far greater than the level observed in the eukaryotic translation system and is more analogous to the induced arrested state seen in Wheat Germ ribosomes at high (2 mM) arginine inducer concentrations (Figure 5.9A; Lane 7). However, stalling remained at this level in the *E.coli* translation system and did not increase at high (2 mM) concentrations of the arginine inducer molecule (Figure 5.9B; Lane 3). There was also no difference seen with the presence of the four additional (QRLT) SecM C-terminus residues (Figure 5.9B; Lane 7). Similarly the AAP D12N and AAP D12N+4 mutants also had a high level of stalling in low (0.01 mM) arginine inducer conditions (Figure 5.9B; Lanes 9 & 13 respectively) which did not increase any further even in the presence of high (2 mM) concentrations of arginine (Figure 5.9B; Lanes 11 & 15 respectively). Although in the *E.coli* ribosome system the AAP D12N mutation no longer completely abolished stalling, there was still a slight influence with stalling of this mutant overall slightly decreased compared to wild type AAP (Figure 5.9B).

To enable better interpretation of these results, puromycin release assays were also performed on the AAP peptide in the prokaryotic *E.coli* ribosome system. As previously, truncated mRNA constructs were used to obtain artificially stalled ribosomes, if translation arrest has occurred then these peptides will be resistant to puromycin whilst simulated stalled peptides will be released from the ribosome. The results indicate that in the absence of puromycin, truncated mRNA results in a population of the peptides stalled as peptidyl-tRNA^{Ala} for both AAP WT and AAP D12N peptides at both low (0.01 mM) and high (2 mM) arginine concentrations (Figure 5.10; Lanes 1-2 & 5-6). However, the addition of puromycin causes stalling to be released for both AAP WT and AAP D12N, as indicated by the absence of the higher molecular weight band of peptidyl-tRNA^{Ala}, regardless of the presence of high concentrations of arginine inducer molecule (Figure 5.10; Lanes 3-4 & 7-8). This indicates that these peptides are only stalled on the ribosome initially because of the truncated mRNA lacking a stop codon and AAP and AAP D12N do not undergo functional translation arrest in prokaryotic *E.coli* ribosomes.

This makes the interpretation of the CTABr precipitation results in Figure 5.9B very interesting as the high level of basal stalling does not correspond to stably arrested peptide and instead, similar to the TnaC peptide, suggests that the AAP peptide undergoes a translational pausing which is independent of the small molecule inducer arginine. This will be discussed further in Section 5.3.

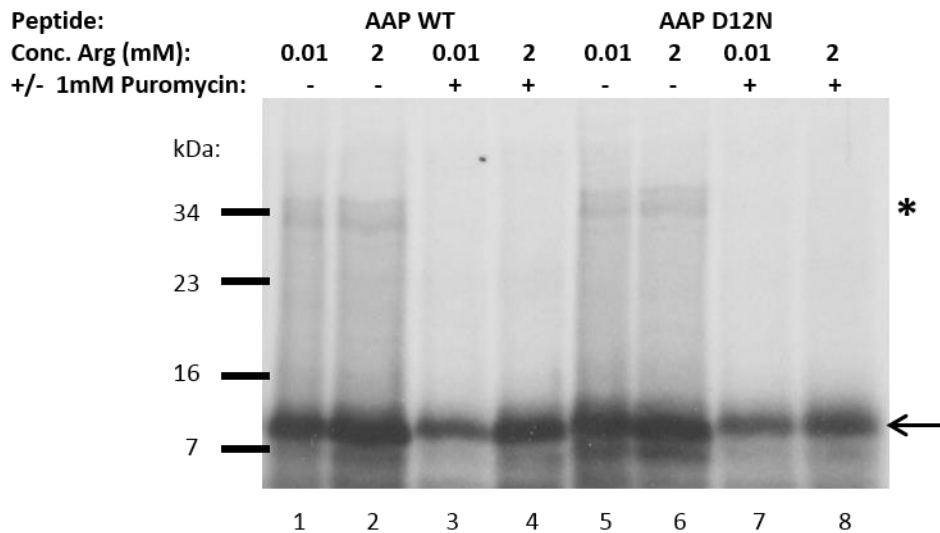


Figure 5.10 Stalling of SecM-AAP and SecM-AAP D12N in prokaryotic *E.coli* translation system detected by puromycin release assay. Truncated SecM-AAP and SecM-AAP D12N constructs lacking a stop codon were synthesised in *E.coli* cell extract *in vitro* transcription-translation assays containing 0.01 mM or 2 mM arginine (inducer molecule). Reactions were divided in half with 1 mM puromycin added to one whilst the other served as a control. After incubation the products were resolved on tricine gels. The asterisk (*) indicates AAP peptidyl-tRNA^{Ala} whilst the arrow indicates released SecM-AAP/SecM-AAP D12N peptide. Gel is representative of multiple experiments.

5.2.4 Summary

The overall results of this chapter are summarised in Table 5.2 and indicate that prokaryotic *E.coli* stalling peptides SecM and TnaC can only undergo full translation arrest in prokaryotic ribosome systems and vice versa for eukaryotic stalling peptide *N.crassa* AAP. There does, however, appear to be a degree of translational pausing which can be undergone by the inducible stalling peptides TnaC and AAP in the absence of inducer molecule in their native systems and also independently of their inducer molecules in the alternative ribosome systems. The lack of full arrest of stalling peptides in alternative ribosome systems highlights the complexity of the ribosome and the uniqueness of the interactions which occur to induce stalling of different translation arrest peptides.

Stalling peptide (P – prokaryotic, E – eukaryotic)	Prokaryotic ribosomes	Eukaryotic ribosomes
SecM (P)	Arrest	No arrest
TnaC (P)	Arrest	No arrest - Pausing
AAP (E)	No arrest - Pausing	Arrest

Table 5.2 Summary of SecM, TnaC and AAP stalling in alternative ribosome systems. The combined results from both CTABr and puromycin release assays for the three stalling peptides SecM, TnaC and AAP in both prokaryotic and eukaryotic ribosome systems.

5.3 Conclusion

5.3.1 Inducible translation arrest peptides can undergo translational pausing, but not arrest, in alternative ribosome systems

Firstly, from these results translation arrest of the inducible stalling peptides AAP and TnaC appears to be less efficient than the intrinsically stalling SecM peptide, as both undergo lower levels of arrest. However, it should be noted that this may be a result of the *in vitro* translation system and may not reflect the *in vivo* levels of stalling achieved by these peptides. This is because whilst SecM stalling continues *in vivo* until the stalled nascent chain is subject to a pulling force from the translocon resulting in its release (Butkus et al., 2003), AAP and TnaC stalling is controlled by the presence of the bound inducer molecule, arginine and tryptophan respectively. The stability of the inducer molecule binding is experimentally undetermined, as is how this binding is affected *in vitro*, and therefore it is possible that potential instability of inducer molecule *in vitro* may result in a more transient stalling process than occurs *in vivo*. In addition, previous studies have shown that when multiple AAP arrest sequences are engineered in tandem into the same construct, whilst stalling occurs temporarily, at some point translation arrest is overcome and translation continues along the transcript resulting in multiple stalled intermediates and full length peptides (Fang et al., 2004). Therefore the stalling rates of ~30% obtained for AAP and TnaC in these assays at high (2 mM) inducer concentrations (Figure 5.9 and 5.6 respectively) appears to be consistent in comparison to published *in vitro* translation systems.

These results are very interesting as the cross-domain stalling of TnaC and AAP in alternative ribosome systems, indicated by the results of the CTABr precipitation assays (Figure 5.7 & 5.9B respectively), does not withstand puromycin addition (Figure 5.8 & 5.10 respectively). The release of this stalling by puromycin indicates that the results of the CTABr experiments are not reflective of full stalling, but instead that these peptides must be undergoing a translational pausing. Translational pausing is a well-documented occurrence which has been under research for some time (Wolin and Walter, 1988), it can serve several regulatory functions, examples include aiding the co-translational folding of nascent peptides on the ribosome (Thanaraj and Argos, 1996; Zhang et al., 2009), and also to delay completion of translation to allow correct cellular localisation of the peptide upon release (Yanagitani et al., 2011). TnaC also appears to undergo a similar pausing in native

E.coli ribosomes at low tryptophan inducer concentrations (Figure 5.6; Lane 1), which is also abolished by puromycin addition (Figure 5.8; Lane 3). The results indicate that translational pausing occurs in the absence of inducer molecule and is therefore dependent upon synthesis of the arrest motif residues and the subsequent interactions of the nascent chain within the exit tunnel. To increase the efficiency of inducer molecule binding to the ribosome it is logical that inducible peptides may undergo a pause after the translation of the arrest motif. The peptide can then undergo full stalling only if the inducer molecule binds correctly and promotes the necessary changes within the ribosome. Indeed previous studies have shown that arginine can bind after the synthesis of the peptide and still induce a change in the PTC to induce stalling (Wei et al., 2012), supporting the theory that pausing provides additional time to enable the efficient binding of the inducer.

Whilst pausing of the TnaC peptide in eukaryotic Wheat Germ ribosomes was equivalent to un-induced levels in native *E.coli* ribosomes, in contrast, AAP pausing in *E.coli* ribosomes was equivalent to induced levels of stalling of AAP+4 in eukaryotic Wheat Germ ribosome systems. In the prokaryotic *E.coli* system AAP and AAP+4 peptides underwent ~32-34% arrest (Figure 5.9; Lanes 1-7), whilst even the AAP D12N mutant, which abolishes arrest in native eukaryotic ribosomes had only slightly reduced the levels of pausing in prokaryotic *E.coli* ribosomes compared to wild type AAP at ~28-30% (Figure 5.9; Lanes 9-16). The high level of translational pausing of the D12N mutants in the prokaryotic *E.coli* ribosome system indicate that this residue is no longer critical to AAP stalling. These results are striking as they reveal that arginine-independent translational pausing in the prokaryotic ribosome system is equivalent to the levels of full translation arrest observed in native eukaryotic ribosome system, however, despite this the AAP peptide is missing an essential impetus required to achieve full arrest. This will be discussed further in the following section 5.3.2.

In contrast, no stalling of SecM was observed in eukaryotic ribosomes (Figure 5.4, Lane 4), this is most likely due to differences in the properties of intrinsic and inducible stalling peptides. Intrinsic arrest peptides do not require any external influences and are dictated by their interactions within the ribosomal exit tunnel and the PTC. It appears that in cross-domain translation if these do not occur efficiently, then stalling will not occur. Meanwhile inducible stalling peptides that rely on both the presence of an inducer molecule and interactions within the ribosome exit tunnel are able to undergo translational

pausing which may be part of a natural two-step process on the way to complete translation arrest, however, due to the cross-domain differences are unable to undergo full translation arrest.

5.3.2 Translation arrest in alternative ribosome systems

There is a range of evidence present that illustrates that stalling peptides maintain the ability to arrest outwith their native species, for example, as stated previously, AAP is capable of undergoing stalling in a range of eukaryotic ribosomes including fungi, plants and animals (Fang et al., 2004) whilst *Proteus vulgaris* TnaC peptide is capable of arresting in *E.coli* ribosomes (Cruz-Vera et al., 2009). Also due to the conservation between prokaryotic and eukaryotic ribosome exit tunnels, stalling peptides appear to interact within similar areas of the exit tunnel, including ribosomal RNA nucleotides U2585, A2062, A2058, A751 and the protein extensions L4 and L22 (L17) (Bhushan et al., 2010b; Gumbart et al., 2012; Seidelt et al., 2009). Therefore, in theory, it would be reasonable to suggest that full translation arrest of prokaryotic peptides may be able to occur in eukaryotic systems and vice versa.

However, the results in this chapter show that cross-stalling over different domains does not occur. SecM is unable to undergo translation arrest in eukaryotic ribosomes as shown by the CTABr precipitation assays in which only full-length SecM peptide was produced (Figure 5.4; Lane 4). Likewise, TnaC and AAP peptides are unable to undergo full translation arrest in their alternative eukaryotic and prokaryotic ribosome systems respectively, as confirmed by puromycin release assays (Figures 5.8 and 5.10 respectively). A potential explanation for this could be that, despite the conservation in the ribosome exit tunnels, x-ray crystallography studies show that the head domain of the eukaryotic ribosome small subunit goes through global conformational changes during translation. This large-scale rotation of the head domain of the small subunit serves to enable translocation of the tRNA and mRNA along the large and small ribosome subunit interface (Ben-Shem et al., 2011). This is enhanced by the fact that eukaryotic ribosomes contain additional intersubunit bridges at the large and small subunit interface, which nearly double the surface area between them in comparison to prokaryotic ribosomes and play an important function in the rotation of the subunits (Yusupova and Yusupov, 2014). Studies also indicate that there is a difference in tRNA positioning during translocation

between prokaryotes and eukaryotes with the elbow domains of A and P site tRNAs 10 Å further apart in eukaryotic ribosomes than prokaryotic ribosomes, whilst the P and E site ribosomes are 16 Å closer in eukaryotes (Budkevich et al., 2011), see Figure 5.11 for an overview.

These differences in structure will have a considerable impact on the process of translation arrest of stalling peptides, for instance, interactions of the SecM nascent chain with the exit tunnel cause it to arrest due to a subsequent shift in the position of the peptidyl-tRNA^{Gly}, with this ratcheting preventing the nucleophilic attack of the aminoacyl-tRNA^{Pro} thus resulting in a stalled nascent chain (Bhushan et al., 2011). A large scale movement of the small subunit upon translocation and the difference in tRNA-positioning within the A and P sites in eukaryotic ribosomes may negate this relatively subtle shift causing the loss of translation arrest and resulting in complete translation of the SecM peptide. Conversely for AAP stalling, whilst the peptide is able to interact with the exit tunnel of prokaryotic ribosomes sufficiently to undergo a translational pause, the difference in subunit movement and tRNA positioning upon translocation may account for the loss of full translation arrest of this peptide even in the presence of high concentrations of arginine inducer molecule. This would explain how *N.crassa* AAP is not specific within eukaryotic ribosomes and can maintain stalling function in fungal, plant and animal ribosomes (Fang et al., 2004) but does not, as shown in this study, undergo full translation arrest in prokaryotic ribosomes.

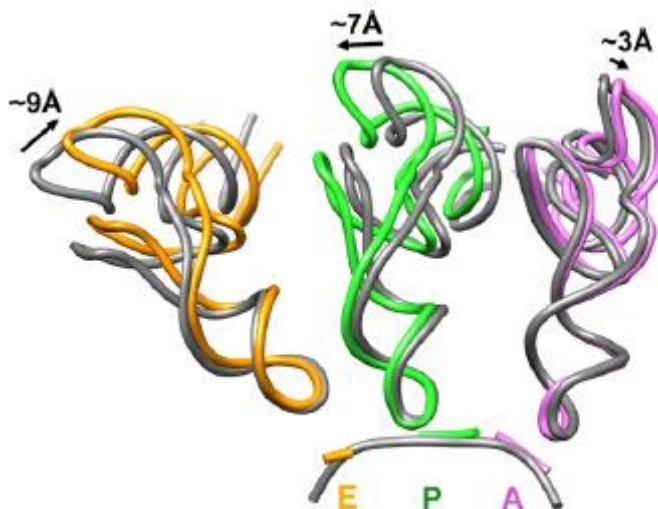


Figure 5.11 Comparison of tRNA positions within the PTC of prokaryotic and eukaryotic ribosomes. The differences in tRNA positioning are highlighted with the eukaryotic A, P and E site tRNAs shown in pink, green and yellow respectively whilst prokaryotic tRNA positioning is shown in grey. Figure reproduced from Budkevich et al., (2011).

It is not possible to determine from these experiments if the interactions within the exit tunnel have been maintained across prokaryotic and eukaryotic domains. However, if so then this highlights that whilst the interactions within the exit tunnel may be important for initiating translation arrest and relaying messages to the PTC to induce stalling, the subsequent interactions within the PTC are vital to uphold stalling. In addition to this, whilst intrinsic stalling peptides rely on their interactions within the exit tunnel to initiate stalling, correct inducer molecule binding in alternative ribosomes may also be a factor for inducible peptide stalling, however, this is unable to be determined from these experiments.

5.3.3 Influence of additional +4 C-terminus residues

As the open reading frame (ORF) for stalling peptides are located upstream on the mRNA from their downstream cistrons, SecM-AAP and SecM-TnaC constructs containing an additional four C-terminal residues (QRLT) were created to determine whether additional mRNA beyond the stop codon had a role in providing stabilisation of the mRNA within the PTC and therefore influencing levels of translation arrest. These residues were selected as they are the four C-terminal residues of SecM beyond the Proline-166 translation arrest point and are known to enable stalling to occur without causing any interference. The results indicated that the additional residues had a dual effect, resulting in higher basal translational pausing at low inducer concentrations (0.01 mM) of both AAP (Figure 5.8A) and TnaC (Figure 5.5A) in their native eukaryotic and prokaryotic ribosome systems respectively, and subsequently increased levels of stalling in the presence of high concentrations (2 mM) of the relevant inducer molecule. In ribosome systems of the opposite domain the effect of the +4 residues in AAP was negated (Figure 5.8B) whilst the effect on TnaC was the same as in the prokaryotic system (Figure 5.6).

Prokaryotes contain an inbuilt rescue system, transfer-messenger RNA (tm-RNA), to alleviate stalled ribosomes by tagging the C-terminus of stalled peptides and in doing so marking them for destruction by cellular proteases (Keiler et al., 1996). The additional four C-terminal residues would result in occupancy of the ribosome A site thus preventing the identification of the stalled ribosome by tm-RNA, however, the observed results are not likely to be due to delaying cellular recycling of stalled ribosomes by tm-RNA as the coupled *in vitro* transcription-translation systems employed in these assays were

purposefully designed to include anti-ssrA oligonucleotide to bind and sequester tm-RNA to prevent this issue. Therefore the increased level of translational pausing and stalling seen in the peptides with the additional mRNA tail is most likely due to stabilising the mRNA within the ribosome PTC and delaying mRNA drop off.

5.3.4 Overall conclusions

The ribosome is a hugely complex processing system responsible for the synthesis of all cellular proteins, which must then in turn leave through the ribosome exit tunnel. Despite the increasing number of stalling peptides which have been identified, their high specificity explains how ribosomes are able to support stalling peptides by making their interactions niche so that multiple factors must be correct to induce full translation arrest thereby minimising the occurrence of aberrant, and subsequently detrimental, ribosome stalling.

6 Final Discussion

6.1 Stalling peptide nascent chain interactions with the ribosome exit tunnel

The aim of this thesis was to investigate the interactions between stalled translation arrest peptides and the ribosome exit tunnel. This work sheds light on the key interactions that occur during translation arrest that are responsible for enabling this small niche of peptides to stall on the ribosome, a process that, if it were to occur aberrantly, would be highly detrimental to the cell. Initially this work focussed on one particular stalling peptide, SecM, an ideal protein of interest as much research has already been carried out on elucidating its method of stalling and identifying the important contacts it makes within the ribosome exit tunnel. Through the study of selected SecM mutants this thesis has revealed further insights into the interactions of the SecM nascent chain with the ribosome exit tunnel and also the influence of these interactions in the compaction of the SecM nascent chain upon translation arrest. In particular highlighting the importance of the flexibility of the SecM nascent chain to enable positioning of the key interactions required for efficient translation arrest.

As discussed earlier, Nakatogawa and Ito (2002) identified the key amino acids that are essential for SecM stalling, and it was these particular residues that were the focus of the first part of thesis. In particular, determining what the key properties of these amino acids are for promoting translation arrest and what alterations they can undergo whilst still functioning to maintain stalling. It was previously identified by Yap and Bernstein (2009) that Arg-163 was the sole essential residue required for SecM translation arrest, whilst the function of the other key arrest amino acids is to position this residue correctly within the ribosome exit tunnel. Subsequent visualisation of the stalled SecM nascent chain within the ribosome exit tunnel by cryo-EM supported this, as Arg-163 appears to form the essential communication network with rRNA nucleotide A2062 to enable signalling to the PTC to induce stalling (Bhushan et al., 2011; Gumbart et al., 2012). From the work in this thesis it has been established that the ability of the SecM peptide to tolerate mutation of the other key arrest residues to conservative amino acids is dependent on their distance from R163. It appears that, with the exception of W155, the further away from residue R163 the greater the adaptability to mutation appears to be. The lower tolerance of residue W155 to

mutation is most likely due to its location at the constriction site of the ribosome exit tunnel upon stalling (Bhushan et al., 2011).

As Gly-165 is located in the P site of the ribosome upon stalling, the important role of this residue in SecM arrest is mediated through the movement of the tRNA-Gly in preventing peptide bond formation upon translation arrest (Bhushan et al., 2011), and not the properties of the amino acid itself. Therefore of the key arrest motif residues, it is able to withstand mutation most effectively and can be mutated to serine without impacting stalling, with the peptide maintaining levels of arrest analogous to wild type SecM (refer to Figure 3.9 for reference). I162 which is situated just below R163 in the exit tunnel is the least tolerant to mutation as it is in closest proximity to this key residue. Meanwhile one residue further down at G161 has slightly more adaption to mutation which is improved with increased flexibility of the nascent chain provided by the P153A mutation. Indeed, the greater the distance from R163, the more effectively mutations can be tolerated, with increased flexibility of the SecM nascent chain further counter acting the loss of stalling caused by the initial mutation. This indicates the highly accurate nature of the placement of residue R163 with the rRNA nucleotide A2062, and indicates how accidental stalling is kept to a minimum as the interactions at this point are so specific.

Further to this, it appears that the properties of specific amino acids have differing importance depending on where they are positioned within the SecM nascent chain, again the closer to the essential R163 the less tolerance there is for alteration. For instance, an isoleucine to leucine mutation at residue 156 can be tolerated more effectively than one at position 162. Likewise, glycine to serine, when located at residue 165 at the ribosome P site upon stalling, has far greater scope for modification than the same mutation at position 161 which is located within the exit tunnel.

As discussed previously, increased flexibility of the SecM nascent chain by mutation of a restrictive proline residue to an alanine at residue 153, provided improved ability to adapt to mutation of the key arrest motif amino acid residues. This is believed to be because it enables the repositioning of the SecM nascent chain within the ribosome exit tunnel allowing it to compensate for mutations to varying extents, except R163 as previously stated. This better flexibility must come from within the essential arrest motif, as

increased movement provided by mutation of another proline residue outwith the essential motif, at P146, had no effect on improving stalling of SecM mutants. The P146 residue is located beyond the constriction point of the ribosome exit tunnel (Bhushan et al., 2011), indicating that to influence SecM nascent chain positioning improvements in flexibility must be able to influence the residues in the upper portion of the exit tunnel where the key interactions take place.

Another feature of SecM stalling that was investigated in this thesis was the compaction of the nascent chain upon translation arrest, a process that has previously been established as being required for SecM arrest (Woolhead et al., 2006). These results expand this work further to reveal that conservative mutations of key arrest motif residues affect SecM nascent chain compaction but do not completely abolish stalling (see Figure 4.13 for summary). This is in contrast to the effect of alanine mutations to key arrest residues which have previously been shown, by FRET assays, to maintain compaction but abolish stalling (Woolhead et al., 2006). This indicates that whilst conservative mutations affect the placement of SecM within the exit tunnel, resulting in a more extended conformation, the nascent chain can adapt to these mutations by forming new interactions which enable the correct positioning of the key R163 residue, maintaining a degree of stalling. Tolerance to mutation can be further enhanced through increased flexibility of the SecM nascent chain provided by the P153A mutation. This mutation results in recovery of the compaction of SecM mutants to levels analogous to wild type SecM, correlating with a further increase in the levels of translation arrest obtained by the peptide. Despite this, the levels of arrest do not reach that of wild type SecM, indicating that whilst compaction is not reliant on the detection of a completely accurate arrest motif, complete stalling capability is.

Further work in this area would ideally involve the elucidation of the specific interactions occurring within the ribosome exit tunnel of a range of these SecM mutants, particularly SecM I162L, which has an extended conformation yet can maintain a relatively high level of stalling. It would be highly interesting to discover if these mutants undergo different interactions with the ribosome exit tunnel to enable initiation of stalling and how these compensate for the loss of the original connections. Also, these studies could explore whether enabling the SecM conservative mutants additional freedom through mutation of P153A enables the nascent chain to revert back to the original interactions or if they also

form an altered compacted structure. Cryo-EM would be an ideal method to study this as it would enable direct visualisation of the SecM nascent chain within the ribosome exit tunnel. Additionally photo-crosslinking would be a suitable alternative or as a supplementary analysis, by enabling the use of crosslinkers to biochemically map the interactions of the SecM nascent chain within the ribosome exit tunnel. Although in comparison to cryo-EM, which can map the full path of the nascent chain through the exit tunnel, crosslinking only provides a snap-shot of the interactions at the location selected for the placement of the crosslinking probes within the nascent chain. However, photo-crosslinking is advantageous as it does not depend on long term RNC stability, as experiments are able to be completed as soon as the stalled nascent chain complexes are generated, by light activation of the crosslinker, these products themselves are then also relatively stable with the chemical crosslinks permanently formed. This removes any issues as to whether the time course of the experiment has altered the structure of the nascent chain within the exit tunnel as is a consideration with cryo-EM. Also with cryo-EM protocols it may be necessary to add additional proteins to the N-terminus of the protein of interest to enable pure samples to be obtained by affinity purification. These are all factors which need to be taken into consideration when planning the best experimental course of action.

6.2 Specificity of translation arrest peptides in non-native ribosomes

This thesis also sought to establish the specificity of translation arrest of prokaryotic and eukaryotic stalling peptides in non-native ribosomes of other domains. This study has revealed that whilst translation arrest peptides are unable to commit to full translational stalling in ribosomes from non-native domains, most likely due to the differences in the architecture of prokaryotic and eukaryotic ribosome exit tunnels, it has identified their ability to undergo translational pausing. This step appears to only occur during stalling of inducible translation arrest peptides, which would benefit from a pause after synthesis of the arrest motif to allow efficient binding of the inducer molecule, thereby enabling instigation of full translation arrest. It was not identified directly in native ribosome stalling systems of AAP and TnaC as nascent chain/ribosome compatibility results in attainment of full arrest. The translational pause is likely to occur after recognition of the stalling sequence of the nascent chain, prior to binding by the inducer molecule. The cryo-

EM structures of the stalled ribosome-nascent chain complexes of AAP and TnaC currently available are in the absence of inducer molecule, yet they show the peptides forming distinct conformations within the exit tunnel, influencing the position of the key 23S rRNA nucleotides, such as A2062 (Bhushan et al., 2010b; Seidelt et al., 2009). From the results established in this study it can therefore be hypothesised that interaction of the nascent chain with the exit tunnel induces a structural change within the ribosome to establish ribosome pausing. The purpose of the translational pause is to provide a reasonable time frame to allow for the binding of inducer molecule to occur (Figure 6.1C). If binding does not occur due to low concentrations of inducer molecule, then pausing will be released and full translation arrest will not be achieved (Figure 6.1D). Conversely, this translational pause is not necessary in intrinsic stalling peptides, which do not rely on external stimuli for stalling, and therefore would not benefit from undergoing a translational pause prior to initiation of full translation arrest.

This study was restricted in that it only assessed three stalling peptides, one intrinsic and two inducible, therefore to further validate if the occurrence of translational pausing occurs for all inducible peptides it would be necessary to assess a wider range of translation arrest peptides. In addition, this would also enable determination of whether similar patterns hold true for all prokaryotic and eukaryotic stalling peptides. For instance in this study, the prokaryotic peptide TnaC appeared to undergo translational pausing in eukaryotic Wheat Germ ribosomes at levels equivalent to un-induced levels of translational stalling in native *E.coli* ribosomes, whilst in contrast, eukaryotic AAP pausing in *E.coli* ribosomes was equivalent to induced levels of stalling in eukaryotic Wheat Germ ribosome systems. Further analysis on a wider range of peptides is required to assess if this occurrence was uniform across all prokaryotic and eukaryotic stalling peptides or varied for individual peptides.

Although prokaryotic and eukaryotic ribosomes share a core structure, this work concludes that cross-domain stalling does not occur, however, it remains to be established how indiscriminating stalling peptides can be within their own domains. At the moment there exists conflicting reports of the capability of stalling peptides to undergo translation arrest within the ribosomes of different species within the same domain, for instance as discussed previously, the AAP peptide is able to undergo stalling in fungi, plants and animals (Fang et al., 2004), whilst on the other hand *E.coli* SecM and *Bacillus subtilis* MifM appear to be

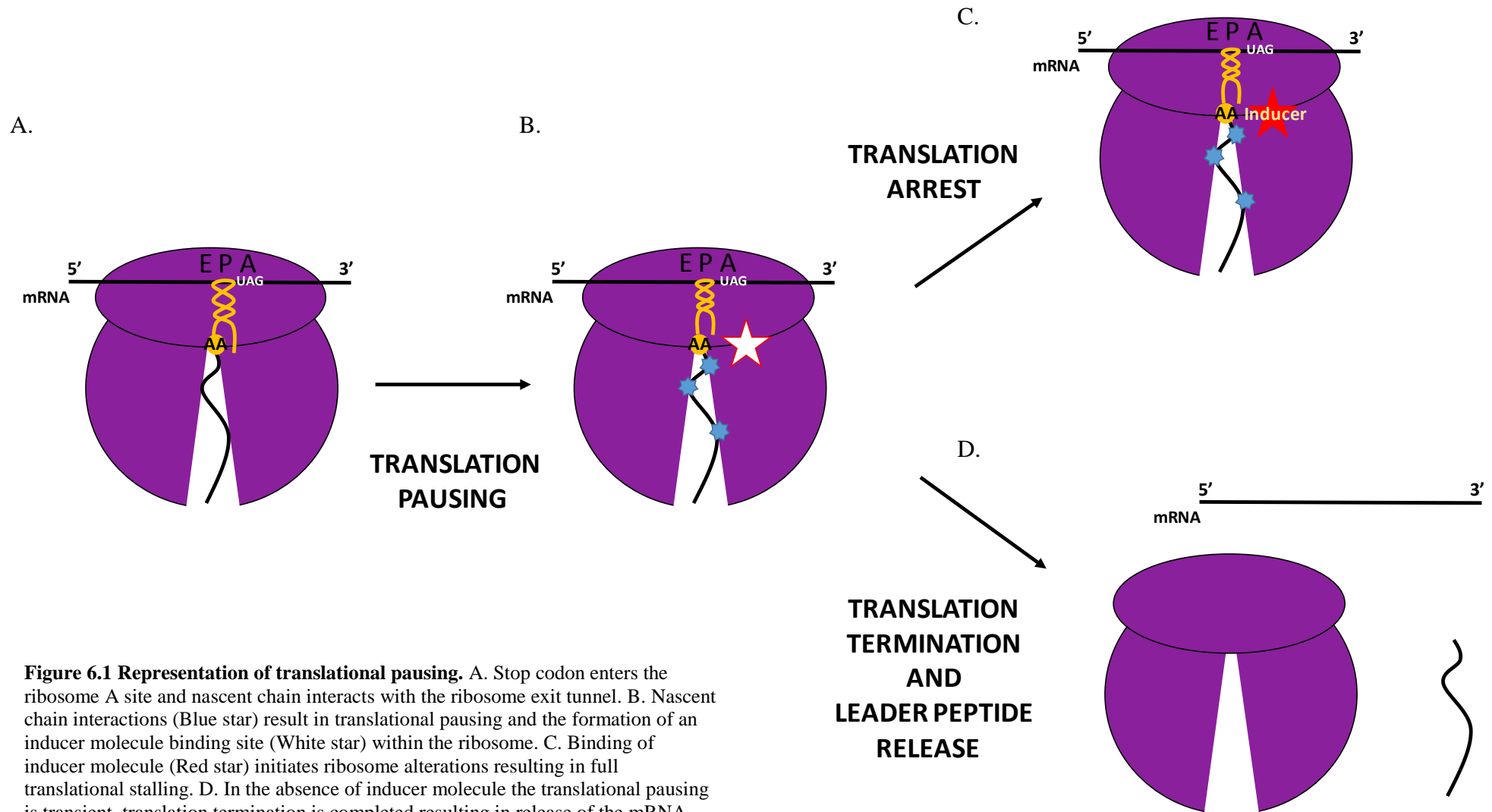


Figure 6.1 Representation of translational pausing. A. Stop codon enters the ribosome A site and nascent chain interacts with the ribosome exit tunnel. B. Nascent chain interactions (Blue star) result in translational pausing and the formation of an inducer molecule binding site (White star) within the ribosome. C. Binding of inducer molecule (Red star) initiates ribosome alterations resulting in full translational stalling. D. In the absence of inducer molecule the translational pausing is transient, translation termination is completed resulting in release of the mRNA and leader peptide and subsequent recycling of the ribosome.

species-specific (Chiba et al., 2011). However, not all SecM variants appear to be species-specific, with distantly related SecM homologs from *Haemophilus influenzae* and *Mannheimia succiniciproducens* able to efficiently stall translation in *E.coli* ribosomes (Yap and Bernstein, 2011). Perhaps, it may be that within the same domain, the ability of peptides to undergo stalling in foreign ribosomes varies on an individual peptide basis, dependant on the particular peptide and ribosomes being analysed and the interactions made within the ribosome exit tunnel.

These conflicting reports of SecM stalling in alternative ribosomes indicate that this may be an area requiring further study. Investigating the stalling ability of different SecM homologs within ribosomes of alternative bacterial species would reveal if there were specific shared features of the ribosome exit tunnel that enable cross-species stalling or whether certain SecM variants could adapt to maintain stalling function in different species. If the individual SecM species can undergo adaptations to stall in different species of bacterial ribosome then establishing how that is achieved would be crucial to a better understanding of SecM stalling. The investigation could also be expanded to examine the role of the mRNA sequence or potential auxiliary factors in mediating this cross species stalling.

In addition, pegylation assays similar to those performed in this thesis would determine if all SecM homologs compact, and if so to what degree does this correspond between different species. This in turn can be expanded to explore if compaction of a SecM peptide remains the same when translated in a different species or does it alter to provide adaptation to the foreign exit tunnel and enable stalling to proceed in the different ribosomes. This will provide a fascinating insight into how adaptable stalling peptides are to sense their environment and explore the interactions required to undergo translation arrest.

6.3 Future directions

The work presented in this thesis has further increased our knowledge on translation arrest peptides and their interactions within the ribosome exit tunnel upon stalling. Following on from this work, several paths of future research can be pursued. Firstly, there is still much to discover regarding the interactions of stalling peptides with the ribosome exit tunnel, in

particular how the signal to undergo translation arrest is transferred from these interactions to the PTC where stalling is induced and maintained. Previous studies have suggested that ribosomal proteins and specific rRNA nucleotides are responsible for conveying signals to the PTC to induce subtle structural rearrangements within the PTC to induce stalling. However, it remains to be firmly established how this stalling signal is conveyed to PTC and if all stalling peptides communicate from the exit tunnel to the PTC through the same pathway. With increasing refinement of cryo-EM techniques greater clarity can be gained into the stalling peptides interactions within the exit tunnel upon translation which may help to provide a better understanding of this process. By comparing the structures of empty ribosomes and stalled ribosome-nascent chain complexes (RNCs) it will be possible to further assess the process undergone during translation arrest, providing molecular level detail. Whilst various cryo-EM structures of translation arrest peptides have already been defined, drawbacks of the current structures for the inducible peptides TnaC and AAP are that both have been visualised in the absence of their respective inducer molecules tryptophan and arginine (Bhushan et al., 2010b; Seidelt et al., 2009). It is critically important that structures are obtained with the inducer molecule present as this would ascertain that the current data from these previous studies is correct and also allow definitive establishment of the binding site of the inducer molecule and analysis of how it influences induction of stalling. There is the distinct possibility that structures with the inducer molecule bound could reveal differences in either conformation of the peptide within the exit tunnel or alterations in the structure of the translation arrested ribosome.

In addition to this path of research, it is also possible to take the knowledge that has been gathered from the study of translation arrest peptides and utilise it to generate hyper stable stalled-RNC complexes, using modified SecM stalling sequences that have been altered by selective mutation to gain increased stability. Previous studies have attached the wild type SecM arrest motif at the C terminus of proteins of interest to create constructs capable of translating peptides that can stall on the ribosome (Cabrita et al., 2009; Evans et al., 2005; Schaffitzel and Ban, 2007), however, this can be further refined and Appendix 1 provides the ground work of such a study. These high-stability constructs are highly beneficial for use in time-intensive experiments such as FRET, NMR, cryo-EM and X-ray crystallography.

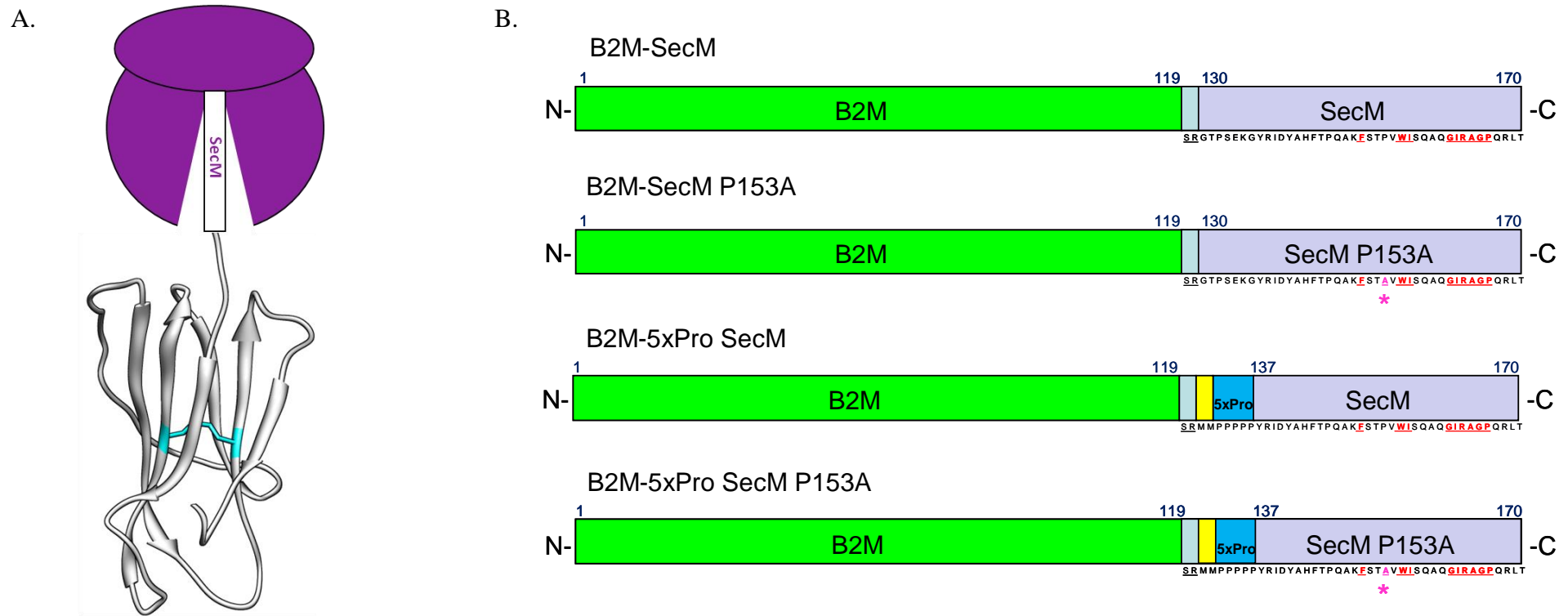
This thesis focussed on the interactions of stalling peptides, in particular SecM, within the ribosome exit tunnel, however, little is known about the role of these peptides beyond the exit tunnel. It is already known that the fate of SecM is to be rapidly degraded by tail-specific proteases upon translocation to the periplasm (Nakatogawa and Ito, 2001), however, studies are now starting to explore if there are roles for the remainder of the SecM peptide in addition to its C-terminal arrest motif and N-terminal signal sequence. Indeed recently a role for residues 100-109 in export-coupled arrest release was discovered (Nakamori et al., 2014), which leaves the question of whether there are additional functions for the remainder of the SecM peptide.

The study and further understanding of stalling peptides is crucial as they perform important functions in gene and protein expression through the regulation of transcription and translation of downstream genes on the same operon. Additionally, as indicated in Appendix 1, a better understanding of stalling peptides enables them to be exploited more efficiently for uses in molecular biology techniques through the generation of hyper stable, stalled-ribosome nascent chain complexes of alternative proteins. This enables the investigation of the behaviour and processes undertaken by natively non-stalling peptides whilst they are being translated by the ribosome to be examined.

Appendix 1: Applying SecM stalling to generate ribosome-nascent chain complexes to study the folding of proteins of interest arrested on the ribosome

Further to the work already presented in this thesis, the knowledge gathered from the study of SecM stalling can be utilised to create constructs containing proteins of interest attached to the N-terminus of the SecM arrest motif, which are therefore capable of stalling on the ribosome. The generation of these stable, stalled ribosome-nascent chain (RNC) complexes enables the timing and process of co-translational protein folding and exit from the ribosome exit tunnel to be studied. Previous studies have employed the wild type SecM stalling sequence to obtain RNCs of proteins of interest stalled on the ribosome (Cabrita et al., 2009; Evans et al., 2005), however, whilst SecM stalling *in vivo* is strong it is not permanent, as this would be detrimental to the cell to have ribosomes sequestered too long. Therefore, the results presented here expand this concept further to identify variants of the SecM arrest motif which can be exploited to obtain the most stable long-term ribosome stalling. The potential number of proteins that can be studied whilst stalled on the ribosome by attaching SecM is vast, however, for the purpose of this study, human beta-2 microglobulin (B2M) a component of MHC class 1 molecules was selected. The human B2M is 119 amino acids in length and has been selected as it is a small, soluble protein with a known structure (Figure A1.1A). It contains a single disulphide bond between Cys45 – Cys100 which connects the two β -sheets and stabilises the molecule.

Several B2M constructs were created containing the SecM stalling sequence at the C terminus, to enable stalled ribosome-nascent chains displaying the B2M protein to be obtained for structural studies (Figure A1.1B). Four test constructs were created to analyse the stability of the SecM arrest sequence with the B2M protein attached. Each construct is 161 amino acids in length and contains full length B2M at the N-terminus, 2 spacer residues (Ser, Arg) and the C-terminal 40 residues of SecM (or a variation of the SecM C-terminus). The length of the SecM portion of these constructs has been designed based on the pegylation data in Chapter 4 (Figure 4.4B), so that upon compaction of the SecM nascent chain during translation arrest, the C-terminus of the B2M protein will be positioned at the opening of the exit tunnel. The constructs contain either wild type SecM



C.

MSRSVALAVLALLSLSGLEAIQRTPKIQVYSRHPAENGKSNFLN **C**YVSGFHPSDIEVDLLKNGERIEKVEHSDLSFSKDW SFY
 LLYYTEFTPTTEKDEYA **C**RVNHVTLSQPKIVKWDRDM Stop

Figure A1.1 Structure of B2M and B2M-SecM constructs. A. Structure of human beta-2 microglobulin (PDB: 1a1m) attached to the SecM C-terminus stalled on the ribosome, note diagram not to scale. Shown in cyan are residues Cys 45 and 100 which form a disulphide bond. B. Schematic diagrams of the 4 B2M-SecM constructs created: B2M-SecM, B2M-SecM P153A, B2M-Pro5x SecM and B2M-Pro5x SecM P153A. C. Full wild type Beta-2 microglobulin amino acid sequence, highlighted in cyan are Cys-45 and 100 which form a disulphide bond in the folded protein.

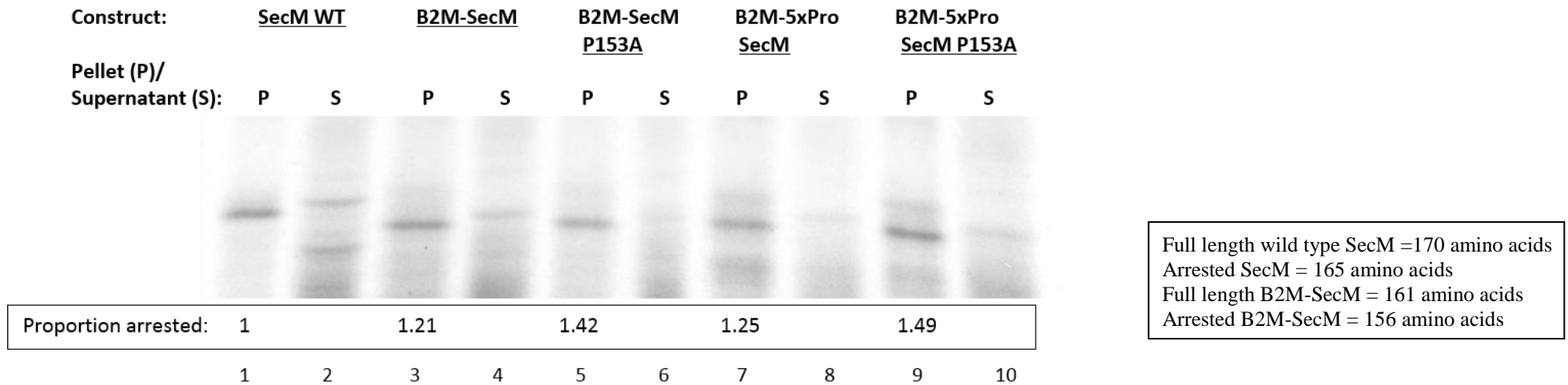


Figure A1.2 B2M-SecM test translations. SecM WT, B2M-SecM, B2M-SecM P153A, B2M-Pro5x SecM and B2M-Pro5x SecM P153A were translated in coupled *in vitro* transcription-translation assays before being CTABr precipitated, separated into pellet (P) and supernatant (S) fractions and resolved by SDS-PAGE. The percentage of arrested peptide was quantified by Image J software and calculated as a percentage of [Arrested/(Arrested + Total full length)], with each value adjusted for background, and then taken as a proportion of wild type SecM. Results are representative of multiple experiments.

or SecM P153A and in addition to this two of the constructs also contain a 5x proline repeat (Figure A1.1B). Previous work has shown that a 5x proline repeat contained within the ribosome exit tunnel upon arrest increases the stability of ribosome-SecM nascent chain complexes (Woolhead, unpublished data). A proline repeat forms a rigid helix structure (Cowan and McGavin, 1955) which, in this instance, will serve to promote the stability of the interactions between the SecM portion of the nascent chain and the ribosome exit tunnel. The SecM P153A mutant was selected as it has been hypothesised from the work in Chapter 3 of this thesis that increased flexibility of the nascent chain within the ribosome exit tunnel, due to the mutation of a restrictive proline residue to alanine, could enable the nascent chain increased adaptability to gain the correct interactions within the exit tunnel. It is thought that this will increase the stability of the stalled RNC over a longer time frame.

Initial experiments were carried out to ensure the addition of B2M at the N-terminus did not impede SecM translation or arrest. The results indicated that the additional B2M portion did not hinder translation and in fact resulted in all constructs having improved levels of arrest in comparison to wild type SecM (Figure A1.2). Even B2M-SecM had an increased level of stalling in comparison to wild type SecM (Figure A1.2; Lane 3), this is possibly due to folded B2M outside the ribosome acting to stabilise the ribosome-nascent chain complex. The additional P153A mutation further increased levels of arrest (Figure A1.2; Lane 5) with the 5x proline repeat further increasing it slightly more so (Figure A1.2; Lane 9).

Following this, the longer term stability of the ribosome bound nascent chain complexes was assessed over a 120 hour period (Figure A1.3 and A1.4). The constructs were synthesised in coupled *in vitro* transcription-translation assays for 30 minutes at 37°C before being stored at 4°C and aliquots were then taken at the time points 0, 5, 24, 48 and 120 hours. To assess the stability of the peptidyl-tRNA the samples were either centrifuged through a sucrose cushion to pellet the ribosome-nascent chain complexes (Figure A1.3) or CTABr precipitated (Figure A1.4). The results indicated that at 24 hours all wild type SecM was released from the ribosome (Figure A1.3A; Lane 3 and A1.4A; Lane 5) whilst in comparison at 48 hours all of the B2M constructs still had some level of stalling (Figure A1.3A & B and A1.4B & C). Similar to the test translation results, this

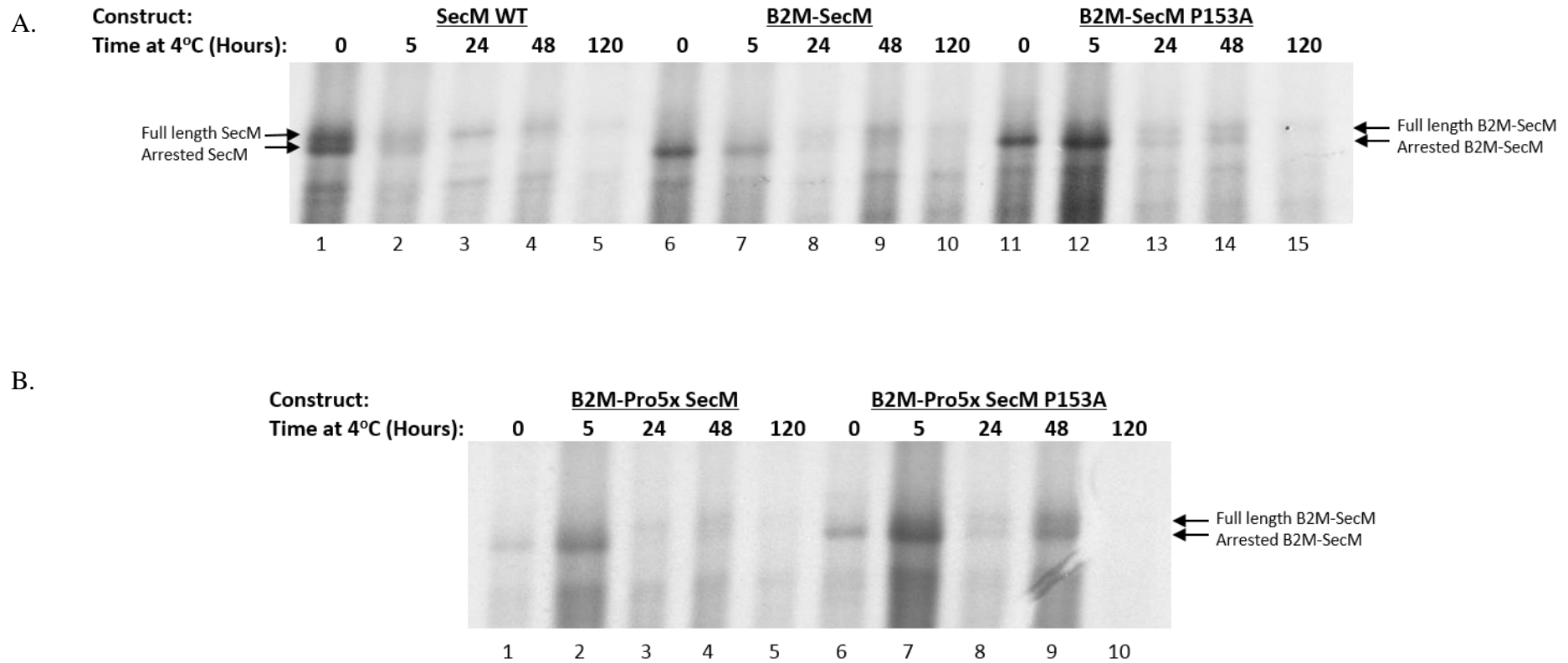


Figure A1.3 B2M-SecM stability time course with sucrose cushion assay. A. SecM WT, B2M-SecM, B2M-SecM P153A and B. B2M-Pro5x SecM and B2M-Pro5x SecM P153A were translated in coupled *in vitro* transcription-translation assays before being stored at 4°C with aliquots taken at time points: 0, 5, 24, 48 and 120 hours. These were then centrifuged through a sucrose cushion and the pellet resuspended in sample buffer and separated on an SDS gel. Results are representative of multiple experiments.

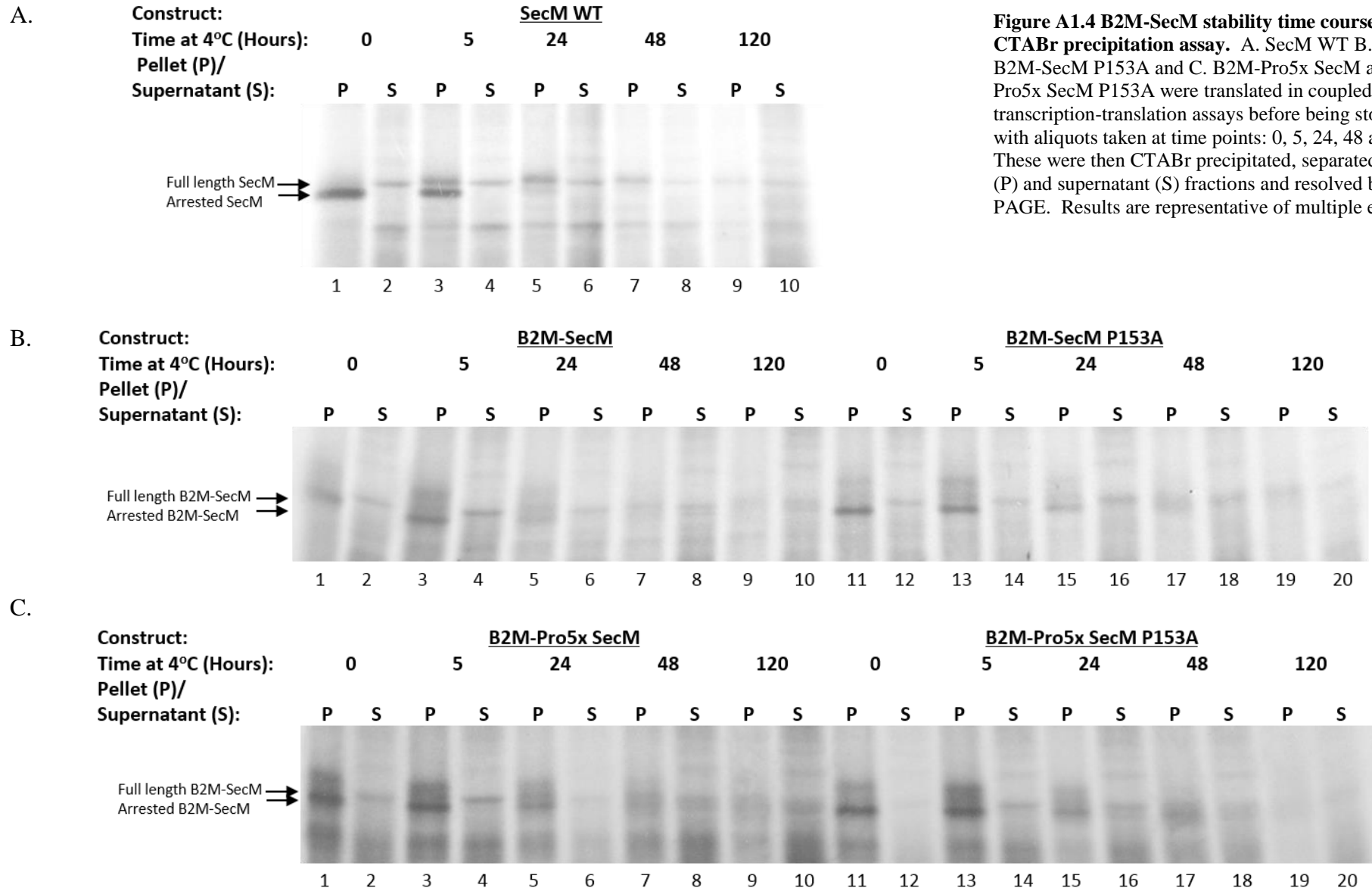


Figure A1.4 B2M-SecM stability time course with CTABr precipitation assay. A. SecM WT B. B2M-SecM, B2M-SecM P153A and C. B2M-Pro5x SecM and B2M-Pro5x SecM P153A were translated in coupled *in vitro* transcription-translation assays before being stored at 4°C with aliquots taken at time points: 0, 5, 24, 48 and 120 hours. These were then CTABr precipitated, separated into pellet (P) and supernatant (S) fractions and resolved by SDS-PAGE. Results are representative of multiple experiments.

stalling was further improved by the P153A mutation (Figure A1.3A; Lane 14 and A1.4B; Lane 17) and Pro5x repeat (Figure A1.3B; Lane 9 and A1.4C; Lane 17).

Both stability assay methods identify B2M-Pro5x SecM P153A as the most stable stalled construct and this will therefore be taken forward for future work. This work will include engineering the B2M portion of the construct to study various features such as protein folding during translation through methods including fluorescence resonance energy transfer (FRET) and pegylation assays. Additionally, by maintaining the SecM stalling sequence but truncating or extending the length of the C-terminus of B2M it would be possible to study the timing of the folding of the peptide as it exits the ribosome tunnel. These assays require long term stable ribosome stalling to generate the highest possible yields of RNCs and therefore can be carried out more efficiently using the higher stability constructs identified in this study. Indeed the optimisation of the SecM stalling sequence established in this study will be useful to any researchers carrying out time-intensive structural studies such as NMR, cryo-EM and X-ray crystallography where long term maintenance of the RNC complexes would increase experimental efficiency.

Appendix 2: Table of constructs

A2.1 Chapter 3 constructs

All constructs used in this chapter are in the pTrc99A plasmid

Construct	Original nucleotide sequence	Mutated nucleotide sequence
SecM F150A	TTC	GCC
SecM P153A	CCC	GCC
SecM W155A	TGG	GCG
SecM I156A	ATA	GCA
SecM G161A	GGC	GCC
SecM I162A	ATC	GCC
SecM R163A	CGT	GCT
SecM G165A	GGC	GCC
SecM P166A	CCT	GCT

Table A2.1 SecM single alanine mutants

Construct	Original nucleotide sequence	Mutated nucleotide sequence
SecM F150A/ P153A	See Table A3.1	For individual mutations
SecM W155A/P153A		
SecM I156A/P153A		
SecM G161A/P153A		
SecM I162A/P153A		
SecM R163A/P153A		
SecM G165A/P153A		

Table A2.2 SecM alanine mutants with P153A double mutation

Construct	Original nucleotide sequence	Mutated nucleotide sequence
SecM F150Y	TTC	TAC
SecM W155Y	TGG	TAC
SecM I156L	ATA	CTA
SecM G161S	GGC	AGC
SecM I162L	ATC	CTC
SecM R163K	CGT	AAA
SecM A164G	GCT	GGT
SecM G165S	GGC	AGC

Table A2.3 SecM single conservative mutants

Construct	Original nucleotide sequence	Mutated nucleotide sequence
SecM F150Y/P153A	See Tables A3.1 and A3.3	For individual mutations
SecM W155Y/P153A		
SecM I156L/P153A		
SecM G161S/P153A		
SecM I162L/P153A		
SecM R163K/P153A		
SecM A164G/P153A		
SecM G165S/P153A		

Table A2.4 SecM conservative mutants with P153A double mutation

Construct	Original nucleotide sequence	Mutated nucleotide sequence
SecM P146A	CCA	GCA
SecM P146A/P153A	See above and Tables A3.1 and A3.3	For individual mutations
SecM F150Y/P146A		
SecM I156L/P146A		
SecM G161S/P146A		
SecM F150Y/P146A/P153A		
SecM I156L/P146A/P153A		
SecM G161S/P146A/P153A		

Table A2.5 SecM conservative mutants with P146A and P153A double and triple mutations

A2.2 Chapter 4 constructs

All constructs used in this chapter are in the pTrc99A plasmid

Construct	Original nucleotide sequence	Mutated nucleotide sequence
SecM D120C	GAT	TGT
SecM L125C	CTG	TGC
SecM G130C	GGC	TGC
SecM K135C	AAG	TGC
SecM D140C	GAT	TGT
SecM T145C	ACC	TGC

Table A2.6 SecM single cysteine mutants

Construct	Original nucleotide sequence	Mutated nucleotide sequence
SecM Q158P	CAG	CCG
SecM D120C/Q158P	See above and Table A3.6	For individual mutations
SecM L125C/Q158P		
SecM G130C/Q158P		
SecM K135C/Q158P		
SecM D140C/Q158P		
SecM T145C/Q158P		

Table A2.7 SecM cysteine mutants with Q158P mutations

Construct	Original nucleotide sequence	Mutated nucleotide sequence
SecM P153A/G130C	See Tables A3.1, A3.3 and A3.6	For individual mutations
SecM P153A/K135C		
SecM P153A/D140C		
SecM F150Y/G130C		
SecM F150Y/K135C		
SecM F150Y/D140C		
SecM I156L/G130C		
SecM I156L/K135C		
SecM I156L/D140C		
SecM G161S/G130C		
SecM G161S/K135C		
SecM G161S/D140C		

Table A2.8 SecM P153A and conservative mutants with cysteine mutations

Construct	Original nucleotide sequence	Mutated nucleotide sequence
SecM F150Y/P153A/G130C	See Tables A3.1, A3.3 and A3.6	For individual mutations
SecM F150Y/P153A/K135C		
SecM F150Y/P153A/D140C		
SecM I156L/P153A/G130C		
SecM I156L/P153A/K135C		
SecM I156L/P153A/D140C		
SecM G161S/P153A/G130C		
SecM G161S/P153A/K135C		
SecM G161S/P153A/D140C		

Table A2.9 SecM conservative/P153A double mutants with cysteine mutations

A2.3 Chapter 5 constructs

All pGEM-4Z plasmid constructs used in this study are in SP6 promoter orientation

pTrc-SecM WT

pGEM-SecM WT

pTrc-SecM-AAP WT

pTrc-SecM-AAP WT+4

pTrc-SecM-AAP D12N

pTrc-SecM-AAP D12N+4

pGEM-SecM-AAP WT *

pGEM-SecM-AAP WT+4 *

pGEM-SecM-AAP D12N *

pGEM-SecM-AAP D12N+4 *

pTrc-SecM-TnaC

pTrc-SecM-TnaC+4

pGEM-SecM-TnaC *

pGEM-SecM-TnaC+4 *

* Asterix indicates constructs which have the following additional methionine mutations:

Residue	Original nucleotide sequence	Mutated nucleotide sequence
SecM V25M	GTT	ATG
SecM A26M	GCG	ATG
SecM A27M	GCG	ATG

Table A2.10 SecM methionine mutations

A2.4 Appendix 1 constructs

pTrc-B2M-SecM

pTrc-B2M-SecM P153A

pTrc-B2M-5xPro SecM

pTrc-B2M-5xPro SecM P153A

Appendix 3: Generation of plasmid constructs

A3.1 pTrc-SecM

pTrc-SecM was created by Dr Cheryl Woolhead as described in Woolhead et al., (2006).

A3.2 pGEM-SecM

SecM was cut from pTrc-SecM using Kpn1 and Xba1 restriction enzymes and transferred to empty pGEM-4Z plasmid vector also cut with Kpn1 and Xba1, this positioned SecM in the SP6 promoter orientation.

A3.3 pTrc-SecM-AAP and pTrc-SecM-AAP+4

AAP and AAP D12N constructs were originally obtained from Mathew Sachs laboratory (Texas A&M University). These were PCR amplified using the oligonucleotide primers: 5'-CATGGTACCGGCAGGAAACAGACCATGATGATGATGATG-3' and 5'-GTATCTAGAGTATTATTACACGGCGATCTTTCCGCCCTTC-3' and cloned into separate pTrc99a plasmids using restriction sites Kpn1 and Xba1, to create pTrc-AAP WT and pTrc-AAP D12N. From these constructs, AAP WT and AAP D12N were again PCR amplified using the following oligonucleotide primers:

5'-CATCAATTGATGAACGGTCGCCCCGTCAGTCTTCACTAGTC-3' and 5'-GTATCTAGAGTATTATTACGCGTTAAGGGCTCTCCACAGATGG-3' (or 5'-GTATCTAGAGTATTATTAGGTGAGGCGTTGCGCGTTAAGGGCTCTCCACAGATGG-3' to create +4 constructs) and separately cloned into pTrc-SecM using Mfe1 and Xba1 restriction sites to produce pTrc-SecM-AAP WT and pTrc-SecM-AAP D12N (and similarly pTrc-SecM-AAP WT+4 and pTrc-SecM-AAP D12N+4) constructs. Note, SecM contains a native Mfe1 restriction site, therefore cutting the pTrc-SecM construct with Mfe1 and Xba1 restriction enzymes removes residues 63-170.

A3.4 pGEM-SecM-AAP and pGEM-SecM-AAP+4

Both wild type and D12N mutant pTrc-SecM-AAP and pTrc-SecM-AAP+4 constructs were cut with Xba1 and Kpn1 restriction enzymes and transferred to separate empty

pGEM-4Z plasmid vectors also cut with these restriction enzymes, positioning these genes in the SP6 promoter orientation. Three additional methionine residues were introduced in each construct at SecM V25, A26 and A27 by consecutive rounds of site-directed mutagenesis (see Section 2.2.5.3.1 for method).

A3.5 pTrc-SecM-TnaC and pTrc-SecM-TnaC+4

The *tnaC* gene was PCR amplified from the genomic DNA of *E.coli* strain MC4100 using the oligonucleotide primers:

5'-CATCAATTGATGAATATCTTACATATATGTGTGACC-3' and 5'-GTATCTAGAGTATTATCAAGGGCGGTGATCGACAATTTTG-3' (or 5'-GTATCTAGAGTATTATTAGGTGAGGCGTTGAGGGCGGTGATCGACAATTTTG-3' to create +4 constructs). These were separately cloned into pTrc-SecM using MfeI and XbaI restriction sites to produce pTrc-SecM-TnaC and pTrc-SecM-TnaC+4 constructs.

A3.6 pGEM-SecM-TnaC and pGEM-SecM-TnaC+4

SecM-TnaC and SecM-TnaC+4 were cut from the pTrc99a plasmids using XbaI and KpnI restriction enzymes and inserted into empty pGEM-4Z vector cut with the same restriction enzymes. This created pGEM-SecM-TnaC and pGEM-SecM-TnaC+4 constructs in the SP6 promoter orientation. Three additional methionine residues were introduced in these constructs at SecM V25, A26 and A27 by consecutive rounds of site directed mutagenesis (see Section 2.2.5.3.1 for method).

A3.7 pTrc-B2M-SecM constructs

pBluescript-B2M plasmid was kindly provided by Prof. Neil Bulleid (University of Glasgow). From this the *B2M* gene was PCR amplified using the following oligonucleotide primers:

5'-CATGGTACCGGCAGGAAACAGACCATGTCTCGCTCCGTGGCC-3' and 5'-GTATCTAGACATGTCTCGATCCCCTTA ACTATCTTGGG-3'. This was then cloned into empty pTrc99a plasmid vector at KpnI and XbaI cut sites to create pTrc-B2M. The C-terminal portion of SecM was then amplified from the pTrc-SecM plasmid using the oligonucleotide primers: 5'-CATTCTAGAGGCACGCCGTCTGAAAAGGGTTATCGC-

3' (or 5'-CATTCTAGAATGATGCCGCCGCCGCCGCGTATCGCATTG-3' for 5xPro SecM) and 5'-GTAAAGCTTGTATTATTAGGTGAGGCGTTGAGGGCCAGC-3'. These were then cloned into pTrc-B2M at XbaI and HindIII restriction sites to create pTrc-B2M-SecM and pTrc-B2M-5xPro SecM. This was also repeated with the same oligonucleotide primers but using pTrc-SecM P153A as the template to obtain pTrc-B2M-SecM P153A and pTrc-B2M-5xPro SecM P153A constructs. See Appendix 1, Figure A1.1B for a summary diagram of these four constructs.

References

- Agirrezabala, X., Lei, J., Brunelle, J.L., Ortiz-Meoz, R.F., Green, R., and Frank, J. (2008). Visualization of the Hybrid State of tRNA Binding Promoted by Spontaneous Ratcheting of the Ribosome. *Molecular Cell* 32, 190-197.
- Alkalaeva, E.Z., Pisarev, A.V., Frolova, L.Y., Kisselev, L.L., and Pestova, T.V. (2006). In vitro reconstitution of eukaryotic translation reveals cooperativity between release factors eRF1 and eRF3. *Cell* 125, 1125-1136.
- Amunts, A., Brown, A., Bai, X.-c., Llacer, J.L., Hussain, T., Emsley, P., Long, F., Murshudov, G., Scheres, S.H.W., and Ramakrishnan, V. (2014). Structure of the Yeast Mitochondrial Large Ribosomal Subunit. *Science* 343, 1485-1489.
- Antoun, A., Pavlov, M.Y., Lovmar, M., and Ehrenberg, M. (2006). How initiation factors tune the rate of initiation of protein synthesis in bacteria. *Embo Journal* 25, 2539-2550.
- Arenz, S., Ramu, H., Gupta, P., Berninghausen, O., Beckmann, R., Vazquez-Laslop, N., Mankin, A.S., and Wilson, D.N. (2014). Molecular basis for erythromycin-dependent ribosome stalling during translation of the ErmBL leader peptide. *Nature Communications* 5.
- Baek, J.M., and Kenerley, C.M. (1998). The *arg2* gene of *Trichoderma virens*: Cloning and development of a homologous transformation system. *Fungal Genetics and Biology* 23, 34-44.
- Ban, N., Nissen, P., Hansen, J., Moore, P.B., and Steitz, T.A. (2000). The complete atomic structure of the large ribosomal subunit at 2.4 angstrom resolution. *Science* 289, 905-920.
- Becker, T., Bhushan, S., Jarasch, A., Armache, J.-P., Funes, S., Jossinet, F., Gumbart, J., Mielke, T., Berninghausen, O., Schulten, K., *et al.* (2009). Structure of Monomeric Yeast and Mammalian Sec61 Complexes Interacting with the Translating Ribosome. *Science* 326, 1369-1373.
- Belew, A.T., Meskauskas, A., Musalgaonkar, S., Advani, V.M., Sulima, S.O., Kasprzak, W.K., Shapiro, B.A., and Dinman, J.D. (2014). Ribosomal frameshifting in the CCR5 mRNA is regulated by miRNAs and the NMD pathway. *Nature* 512, 265-269.
- Ben-Shem, A., de Loubresse, N.G., Melnikov, S., Jenner, L., Yusupova, G., and Yusupov, M. (2011). The Structure of the Eukaryotic Ribosome at 3.0 angstrom Resolution. *Science* 334, 1524-1529.
- Ben-Shem, A., Jenner, L., Yusupova, G., and Yusupov, M. (2010). Crystal Structure of the Eukaryotic Ribosome. *Science* 330, 1203-1209.
- Bengtson, M.H., and Joazeiro, C.A.P. (2010). Role of a ribosome-associated E3 ubiquitin ligase in protein quality control. *Nature* 467, 470-473.
- Beringer, M., Bruell, C., Xiong, L.Q., Pfister, P., Bieling, P., Katunin, V.I., Mankin, A.S., Bottger, E.C., and Rodnina, M.V. (2005). Essential mechanisms in the catalysis of peptide bond formation on the ribosome. *Journal of Biological Chemistry* 280, 36065-36072.
- Bernabeu, C., and Lake, J.A. (1982). Nascent polypeptide-chains emerge from the exit domain of the large ribosomal-subunit - Immune mapping of the nascent chain. *Proceedings of the National Academy of Sciences of the United States of America-Biological Sciences* 79, 3111-3115.
- Bhushan, S., Gartmann, M., Halic, M., Armache, J.-P., Jarasch, A., Mielke, T., Berninghausen, O., Wilson, D.N., and Beckmann, R. (2010a). alpha-Helical nascent

polypeptide chains visualized within distinct regions of the ribosomal exit tunnel. *Nature Structural & Molecular Biology* *17*, 313-318.

Bhushan, S., Hoffmann, T., Seidelt, B., Frauenfeld, J., Mielke, T., Berninghausen, O., Wilson, D.N., and Beckmann, R. (2011). SecM-Stalled Ribosomes Adopt an Altered Geometry at the Peptidyl Transferase Center. *Plos Biology* *9*.

Bhushan, S., Meyer, H., Starosta, A.L., Becker, T., Mielke, T., Berninghausen, O., Sattler, M., Wilson, D.N., and Beckmann, R. (2010b). Structural Basis for Translational Stalling by Human Cytomegalovirus and Fungal Arginine Attenuator Peptide. *Molecular Cell* *40*, 138-146.

Blanchard, S.C., Kim, H.D., Gonzalez, R.L., Puglisi, J.D., and Chu, S. (2004). tRNA dynamics on the ribosome during translation. *Proceedings of the National Academy of Sciences of the United States of America* *101*, 12893-12898.

Bornemann, T., Joeckel, J., Rodnina, M.V., and Wintermeyer, W. (2008). Signal sequence-independent membrane targeting of ribosomes containing short nascent peptides within the exit tunnel. *Nature Structural & Molecular Biology* *15*, 494-499.

Budkevich, T., Giesebrecht, J., Altman, R.B., Munro, J.B., Mielke, T., Nierhaus, K.H., Blanchard, S.C., and Spahn, C.M.T. (2011). Structure and Dynamics of the Mammalian Ribosomal Pretranslocation Complex. *Molecular Cell* *44*, 214-224.

Butkus, M.E., Prundeanu, L.B., and Oliver, D.B. (2003). Translocon "Pulling" of nascent SecM controls the duration of its translational pause and secretion-responsive secA regulation. *Journal of Bacteriology* *185*, 6719-6722.

Cabrita, L.D., Hsu, S.-T.D., Launay, H., Dobson, C.M., and Christodoulou, J. (2009). Probing ribosome-nascent chain complexes produced in vivo by NMR spectroscopy. *Proceedings of the National Academy of Sciences of the United States of America* *106*, 22239-22244.

Carter, A.P., Clemons, W.M., Brodersen, D.E., Morgan-Warren, R.J., Hartsch, T., Wimberly, B.T., and Ramakrishnan, V. (2001). Crystal structure of an initiation factor bound to the 30S ribosomal subunit. *Science* *291*, 498-501.

Chadani, Y., Ito, K., Kutsukake, K., and Abo, T. (2012). ArfA recruits release factor 2 to rescue stalled ribosomes by peptidyl-tRNA hydrolysis in *Escherichia coli*. *Molecular Microbiology* *86*, 37-50.

Chadani, Y., Ono, K., Kutsukake, K., and Abo, T. (2011). *Escherichia coli* YaeJ protein mediates a novel ribosome-rescue pathway distinct from SsrA- and ArfA-mediated pathways. *Molecular Microbiology* *80*, 772-785.

Chiba, S., and Ito, K. (2012). Multisite Ribosomal Stalling: A Unique Mode of Regulatory Nascent Chain Action Revealed for MifM. *Molecular Cell* *47*, 863-872.

Chiba, S., Kanamori, T., Ueda, T., Akiyama, Y., Pogliano, K., and Ito, K. (2011). Recruitment of a species-specific translational arrest module to monitor different cellular processes. *Proceedings of the National Academy of Sciences of the United States of America* *108*, 6073-6078.

Chiba, S., Lamsa, A., and Pogliano, K. (2009). A ribosome-nascent chain sensor of membrane protein biogenesis in *Bacillus subtilis*. *Embo Journal* *28*, 3461-3475.

Chittum, H.S., and Champney, W.S. (1994). Ribosomal-protein gene sequence changes in erythromycin-resistant mutants of *Escherichia coli*. *Journal of Bacteriology* *176*, 6192-6198.

- Cigan, A.M., Feng, L., and Donahue, T.F. (1988). Transfer RNA(imet) functions in directing the scanning ribosome to the start site of translation. *Science* 242, 93-97.
- Cornish, P.V., Ermolenko, D.N., Noller, H.F., and Ha, T. (2008). Spontaneous intersubunit rotation in single ribosomes. *Molecular Cell* 30, 578-588.
- Cowan, P.M., and McGavin, S. (1955). Structure of poly-L-proline. *Nature* 176, 501-503.
- Craigen, W.J., and Caskey, C.T. (1986). Expression of peptide-chain release factor-II requires high-efficiency frameshift. *Nature* 322, 273-275.
- Cruz-Vera, L.R., Gong, M., and Yanofsky, C. (2006). Changes produced by bound tryptophan in the ribosome peptidyl transferase center in to TnaC, a nascent leader peptide. *Proceedings of the National Academy of Sciences of the United States of America* 103, 3598-3603.
- Cruz-Vera, L.R., Rajagopal, S., Squires, C., and Yanofsky, C. (2005). Features of ribosome-peptidyl-tRNA interactions essential for tryptophan induction of tna operon expression. *Molecular Cell* 19, 333-343.
- Cruz-Vera, L.R., Yang, R., and Yanofsky, C. (2009). Tryptophan Inhibits Proteus vulgaris TnaC Leader Peptide Elongation, Activating tna Operon Expression. *Journal of Bacteriology* 191, 7001-7006.
- Cruz-Vera, L.R., and Yanofsky, C. (2008). Conserved residues Asp16 and Pro24 of TnaC-tRNA(Pro) participate in tryptophan induction of tna operon expression. *Journal of Bacteriology* 190, 4791-4797.
- Dallas, A., and Noller, H.F. (2001). Interaction of translation initiation factor 3 with the 30S ribosomal subunit. *Molecular Cell* 8, 855-864.
- Doronina, V.A., Wu, C., de Felipe, P., Sachs, M.S., Ryan, M.D., and Brown, J.D. (2008). Site-specific release of nascent chains from ribosomes at a sense codon. *Molecular and Cellular Biology* 28, 4227-4239.
- Evans, M.S., Ugrinov, K.G., Frese, M.A., and Clark, P.L. (2005). Homogeneous stalled ribosome nascent chain complexes produced in vivo or in vitro. *Nature Methods* 2, 757-762.
- Fang, P., Spevak, C.C., Wu, C., and Sachs, M.S. (2004). A nascent polypeptide domain that can regulate translation elongation. *Proceedings of the National Academy of Sciences of the United States of America* 101, 4059-4064.
- Fang, P., Wang, Z., and Sachs, M.S. (2000). Evolutionarily conserved features of the arginine attenuator peptide provide the necessary requirements for its function in translational regulation. *Journal of Biological Chemistry* 275, 26710-26719.
- Frank, J., and Agrawal, R.K. (2000). A ratchet-like inter-subunit reorganization of the ribosome during translocation. *Nature* 406, 318-322.
- Frank, J., Gao, H., Sengupta, J., Gao, N., and Taylor, D.J. (2007). The process of mRNA-tRNA translocation. *Proceedings of the National Academy of Sciences of the United States of America* 104, 19671-19678.
- Frank, J., Zhu, J., Penczek, P., Li, Y.H., Srivastava, S., Verschoor, A., Radermacher, M., Grassucci, R., Lata, R.K., and Agrawal, R.K. (1995). A model of protein-synthesis based on cryoelectron microscopy of the e-coli ribosome. *Nature* 376, 441-444.
- Freistoffer, D.V., Pavlov, M.Y., MacDougall, J., Buckingham, R.H., and Ehrenberg, M. (1997). Release factor RF3 in E-coli accelerates the dissociation of release factors RF1 and RF2 from the ribosome in a GTP-dependent manner. *Embo Journal* 16, 4126-4133.

- Freitag, M., Dighde, N., and Sachs, M.S. (1996). A UV-Induced mutation in neurospora that affects translational regulation in response to arginine. *Genetics* 142, 117-127.
- Fulle, S., and Gohlke, H. (2009). Statics of the Ribosomal Exit Tunnel: Implications for Cotranslational Peptide Folding, Elongation Regulation, and Antibiotics Binding. *Journal of Molecular Biology* 387, 502-517.
- Gaba, A., Wang, Z., Krishnamoorthy, T., Hinnebusch, A.G., and Sachs, M.S. (2001). Physical evidence for distinct mechanisms of translational control by upstream open reading frames. *Embo Journal* 20, 6453-6463.
- Gabashvili, I.S., Gregory, S.T., Valle, M., Grassucci, R., Worbs, M., Wahl, M.C., Dahlberg, A.E., and Frank, J. (2001). The polypeptide tunnel system in the ribosome and its gating in erythromycin resistance mutants of L4 and L22. *Molecular Cell* 8, 181-188.
- Gagnon, M.G., Seetharaman, S.V., Bulkley, D., and Steitz, T.A. (2012). Structural Basis for the Rescue of Stalled Ribosomes: Structure of YaeJ Bound to the Ribosome. *Science* 335, 1370-1372.
- Gallie, D.R. (1991). The cap and Poly(A) tail function synergistically to regulate messenger-RNA translational efficiency. *Genes & Development* 5, 2108-2116.
- Garza-Sanchez, F., Janssen, B.D., and Hayes, C.S. (2006). Prolyl-tRNA(Pro) in the A-site of SecM-arrested ribosomes inhibits the recruitment of transfer-messenger RNA. *Journal of Biological Chemistry* 281, 34258-34268.
- Gesteland, R.F., Weiss, R.B., and Atkins, J.F. (1992). Recoding - reprogrammed genetic decoding. *Science* 257, 1640-1641.
- Gilbert, R.J.C., Fucini, P., Connell, S., Fuller, S.D., Nierhaus, K.H., Robinson, C.V., Dobson, C.M., and Stuart, D.I. (2004). Three-dimensional structures of translating ribosomes by cryo-EM. *Molecular Cell* 14, 57-66.
- Gilmore, R., Collins, P., Johnson, J., Kellaris, K., and Rapiejko, P. (1991). Transcription of full-length and truncated messenger-RNA transcripts to study protein translocation across the endoplasmic reticulum. *Methods in Cell Biology* 34, 223-239.
- Gong, F., Ito, K., Nakamura, Y., and Yanofsky, C. (2001). The mechanism of tryptophan induction of tryptophanase operon expression: Tryptophan inhibits release factor-mediated cleavage of TnaC-peptidyl-tRNA(Pro). *Proceedings of the National Academy of Sciences of the United States of America* 98, 8997-9001.
- Gong, F., and Yanofsky, C. (2001). Reproducing tna operon regulation in vitro in an S-30 system - Tryptophan induction inhibits cleavage of TnaC peptidyl-RNA? *Journal of Biological Chemistry* 276, 1974-1983.
- Gong, F., and Yanofsky, C. (2002). Instruction of translating ribosome by nascent peptide. *Science* 297, 1864-1867.
- Gong, M., Cruz-Vera, L.R., and Yanofsky, C. (2007). Ribosome recycling factor and release factor 3 action promotes TnaC-peptidyl-tRNA dropoff and relieves ribosome stalling during tryptophan induction of tna operon expression in *Escherichia coli*. *Journal of Bacteriology* 189, 3147-3155.
- Gong, M., Gong, F., and Yanofsky, C. (2006). Overexpression of tnaC of *Escherichia coli* inhibits growth by depleting tRNA(2)(Pro) availability. *Journal of Bacteriology* 188, 1892-1898.
- Gray, M.W. (1993). Origin and evolution of organelle genomes. *Current opinion in genetics & development* 3, 884-890.

- Greber, B.J., Boehringer, D., Leitner, A., Bieri, P., Voigts-Hoffmann, F., Erzberger, J.P., Leibundgut, M., Aebersold, R., and Ban, N. (2014). Architecture of the large subunit of the mammalian mitochondrial ribosome. *Nature* 505, 515-519.
- Grigoriadou, C., Marzi, S., Kirillov, S., Gualerzi, C.O., and Cooperman, B.S. (2007). A quantitative kinetic scheme for 70 S translation initiation complex formation. *Journal of Molecular Biology* 373, 562-572.
- Gryczan, T.J., Grandi, G., Hahn, J., Grandi, R., and Dubnau, D. (1980). Conformational alteration of messenger-RNA structure and the posttranscriptional regulation of erythromycin-induced drug resistance. *Nucleic Acids Research* 8, 6081-6097.
- Guillemaut, P., and Weil, J.H. (1975). Aminoacylation of phaseolus-vulgaris cytoplasmic, chloroplastic and mitochondrial transfer-RNAs met and of Escherichia coli transfer RNAs met by homologous and heterologous enzymes. *Biochimica Et Biophysica Acta* 407, 240-248.
- Guillon, J.M., Meinnel, T., Mechulam, Y., Lazennec, C., Blanquet, S., and Fayat, G. (1992). Nucleotides of transfer-RNA governing the specificity of Escherichia coli methionyl-transfer RNA(met)f formyltransferase. *Journal of Molecular Biology* 224, 359-367.
- Gumbart, J., Schreiner, E., Wilson, D.N., Beckmann, R., and Schulten, K. (2012). Mechanisms of SecM-Mediated Stalling in the Ribosome. *Biophysical Journal* 103, 331-341.
- Guth, E.C., and Francklyn, C.S. (2007). Kinetic discrimination of tRNA identity by the conserved motif 2 loop of a class II aminoacyl-tRNA synthetase. *Molecular Cell* 25, 531-542.
- Han, Y., Gao, X., Liu, B., Wan, J., Zhang, X., and Qian, S.-B. (2014). Ribosome profiling reveals sequence-independent post-initiation pausing as a signature of translation. *Cell research* 24, 842-851.
- Harms, J., Schluenzen, F., Zarivach, R., Bashan, A., Gat, S., Agmon, I., Bartels, H., Franceschi, F., and Yonath, A. (2001). High resolution structure of the large ribosomal subunit from a mesophilic Eubacterium. *Cell* 107, 679-688.
- Hartz, D., Binkley, J., Hollingsworth, T., and Gold, L. (1990). Domains of initiator transfer-RNA and initiation codon crucial for initiator transfer-RNA selection by Escherichia coli IF3. *Genes & Development* 4, 1790-1800.
- Herbst, K.L., Nichols, L.M., Gesteland, R.F., and Weiss, R.B. (1994). A mutation in ribosomal protein-L9 affects ribosomal hopping during translation of gene-60 from bacteriophage-T4. *Proceedings of the National Academy of Sciences of the United States of America* 91, 12525-12529.
- Herr, A.J., Gesteland, R.F., and Atkins, J.F. (2000). One protein from two open reading frames: mechanism of a 50 nt translational bypass. *Embo Journal* 19, 2671-2680.
- Hill, J.R., and Morris, D.R. (1993). Cell-specific translational regulation of S-adenosylmethionine decarboxylase messenger-RNA - dependence on translation and coding capacity of the cis-acting upstream open reading frame. *Journal of Biological Chemistry* 268, 726-731.
- Hood, H.M., Spevak, C.C., and Sachs, M.S. (2007). Evolutionar changes in the fungal carbamoyl-phosphate synthetase small subunit gene and its associated upstream open reading frame. *Fungal Genetics and Biology* 44, 93-104.

- Horinouchi, S., and Weisblum, B. (1980). Posttranscriptional modification of messenger-RNA conformation - mechanism that regulates erythromycin-induced resistance. *Proceedings of the National Academy of Sciences of the United States of America-Biological Sciences* 77, 7079-7083.
- Houben, E.N.G., Zarivach, R., Oudega, B., and Luirink, J. (2005). Early encounters of a nascent membrane protein: specificity and timing of contacts inside and outside the ribosome. *Journal of Cell Biology* 170, 27-35.
- Hsu, S.-T.D., Fucini, P., Cabrita, L.D., Launay, H., Dobson, C.M., and Christodoulou, J. (2007). Structure and dynamics of a ribosome-bound nascent chain by NMR spectroscopy. *Proceedings of the National Academy of Sciences of the United States of America* 104, 16516-16521.
- Huang, W.M., Ao, S.Z., Casjens, S., Orlandi, R., Zeikus, R., Weiss, R., Winge, D., and Fang, M. (1988). A persistent untranslated sequence within bacteriophage-T4 DNA topoisomerase gene-60. *Science* 239, 1005-1012.
- Ibba, M., and Soll, D. (2000). Aminoacyl-tRNA synthesis. *Annual Review of Biochemistry* 69, 617-650.
- Ingolia, N.T., Lareau, L.F., and Weissman, J.S. (2011). Ribosome Profiling of Mouse Embryonic Stem Cells Reveals the Complexity and Dynamics of Mammalian Proteomes. *Cell* 147, 789-802.
- Ito, K., and Chiba, S. (2013). Arrest Peptides: Cis-Acting Modulators of Translation. *Annual Review of Biochemistry*, Vol 82 82, 171-202.
- Ito, K., Chiba, S., and Pogliano, K. (2010). Divergent stalling sequences sense and control cellular physiology. *Biochemical and Biophysical Research Communications* 393, 1-5.
- Jackson, R.J., Hellen, C.U.T., and Pestova, T.V. (2010). The mechanism of eukaryotic translation initiation and principles of its regulation. *Nature Reviews Molecular Cell Biology* 11, 113-127.
- Janssen, B.D., and Hayes, C.S. (2012). The tmRNA ribosome-rescue system. *Advances in Protein Chemistry and Structural Biology*, Vol 86: Fidelity and Quality Control in Gene Expression 86, 151-191.
- Julian, P., Konevega, A.L., Scheres, S.H.W., Lazaro, M., Gil, D., Wintermeyer, W., Rodnina, M.V., and Valle, M. (2008). Structure of ratcheted ribosomes with tRNAs in hybrid states. *Proceedings of the National Academy of Sciences of the United States of America* 105, 16924-16927.
- Kaushal, P.S., Sharma, M.R., Booth, T.M., Haque, E.M., Tung, C.-S., Sanbonmatsu, K.Y., Spremulli, L.L., and Agrawal, R.K. (2014). Cryo-EM structure of the small subunit of the mammalian mitochondrial ribosome. *Proceedings of the National Academy of Sciences of the United States of America* 111, 7284-7289.
- Keiler, K.C., Waller, P.R.H., and Sauer, R.T. (1996). Role of a peptide tagging system in degradation of proteins synthesized from damaged messenger RNA. *Science* 271, 990-993.
- Klinge, S., Voigts-Hoffmann, F., Leibundgut, M., Arpagaus, S., and Ban, N. (2011). Crystal Structure of the Eukaryotic 60S Ribosomal Subunit in Complex with Initiation Factor 6. *Science* 334, 941-948.
- Kontos, H., Naphine, S., and Brierley, I. (2001). Ribosomal pausing at a frameshifter RNA pseudoknot is sensitive to reading phase but shows little correlation with frameshift efficiency. *Molecular and Cellular Biology* 21, 8657-8670.

- Kosolapov, A., and Deutsch, C. (2009). Tertiary interactions within the ribosomal exit tunnel. *Nature Structural & Molecular Biology* 16, 405-411.
- Kozak, M. (1986). Point mutations define a sequence flanking the AUG initiator codon that modulates translation by eukaryotic ribosomes. *Cell* 44, 283-292.
- Kozak, M. (1987). An analysis of 5'-noncoding sequences from 699 vertebrate messenger-RNAs. *Nucleic Acids Research* 15, 8125-8148.
- Lafontaine, D.L.J., and Tollervey, D. (2001). The function and synthesis of ribosomes. *Nature Reviews Molecular Cell Biology* 2, 514-520.
- Laurberg, M., Asahara, H., Korostelev, A., Zhu, J., Trakhanov, S., and Noller, H.F. (2008). Structural basis for translation termination on the 70S ribosome. *Nature* 454, 852-857.
- Laursen, B.S., Sorensen, H.P., Mortensen, K.K., and Sperling-Petersen, H.U. (2005). Initiation of protein synthesis in bacteria. *Microbiology and Molecular Biology Reviews* 69, 101-123.
- Law, G.L., Raney, A., Heusner, C., and Morris, D.R. (2001). Polyamine regulation of ribosome pausing at the upstream open reading frame of S-adenosylmethionine decarboxylase. *Journal of Biological Chemistry* 276, 38036-38043.
- Lecompte, O., Ripp, R., Thierry, J.C., Moras, D., and Poch, O. (2002). Comparative analysis of ribosomal proteins in complete genomes: an example of reductive evolution at the domain scale. *Nucleic Acids Research* 30, 5382-5390.
- Lee, C.P., Seong, B.L., and Rajbhandary, U.L. (1991). Structural and sequence elements important for recognition of Escherichia coli formylmethionine transfer-RNA by methionyl-transfer RNA transformylase are clustered in the acceptor stem. *Journal of Biological Chemistry* 266, 18012-18017.
- Liao, S.R., Lin, J.L., Do, H., and Johnson, A.E. (1997). Both luminal and cytosolic gating of the aqueous ER translocon pore are regulated from inside the ribosome during membrane protein integration. *Cell* 90, 31-41.
- Lockwood, A.H., Chakraborty, P.R., and Maitra, U. (1971). Complex between initiation factor IF2, guanosine triphosphate and fMet-transfer RNA - intermediate in initiation complex formation. *Proceedings of the National Academy of Sciences of the United States of America* 68, 3122-3126.
- Lu, J., and Deutsch, C. (2008). Electrostatics in the Ribosomal Tunnel Modulate Chain Elongation Rates. *Journal of Molecular Biology* 384, 73-86.
- Lu, J.L., and Deutsch, C. (2001). Pegylation: A method for assessing topological accessibilities in Kv1.3. *Biochemistry* 40, 13288-13301.
- Lu, J.L., and Deutsch, C. (2005a). Folding zones inside the ribosomal exit tunnel. *Nature Structural & Molecular Biology* 12, 1123-1129.
- Lu, J.L., and Deutsch, C. (2005b). Secondary structure formation of a transmembrane segment in Kv channels. *Biochemistry* 44, 8230-8243.
- Luke, G.A., de Felipe, P., Lukashev, A., Kallioinen, S.E., Bruno, E.A., and Ryan, M.D. (2008). Occurrence, function and evolutionary origins of '2A-like' sequences in virus genomes. *Journal of General Virology* 89, 1036-1042.
- Malkin, L.I., and Rich, A. (1967). Partial resistance of nascent polypeptide chains to proteolytic digestion due to ribosomal shielding. *Journal of Molecular Biology* 26, 329-346.

- Martinez, A.K., Gordon, E., Sengupta, A., Shirole, N., Klepacki, D., Martinez-Garriga, B., Brown, L.M., Benedik, M.J., Yanofsky, C., Mankin, A.S., *et al.* (2014). Interactions of the TnaC nascent peptide with rRNA in the exit tunnel enable the ribosome to respond to free tryptophan. *Nucleic Acids Research* *42*, 1245-1256.
- Matsufuji, S., Matsufuji, T., Miyazaki, Y., Murakami, Y., Atkins, J.F., Gesteland, R.F., and Hayashi, S. (1995). Autoregulatory frameshifting in decoding mammalian ornithine decarboxylase antizyme. *Cell* *80*, 51-60.
- Mayford, M., and Weisblum, B. (1989). ErmC leader peptide - amino acid sequence critical for induction by translational attenuation. *Journal of Molecular Biology* *206*, 69-79.
- McNicholas, P., Salavati, R., and Oliver, D. (1997). Dual regulation of *Escherichia coli* secA translation by distinct upstream elements. *Journal of Molecular Biology* *265*, 128-141.
- Melnikov, S., Ben-Shem, A., de Loubresse, N.G., Jenner, L., Yusupova, G., and Yusupov, M. (2012). One core, two shells: bacterial and eukaryotic ribosomes. *Nature Structural & Molecular Biology* *19*, 560-567.
- Menninger, J.R. (1985). Functional consequences of binding macrolides to ribosomes. *Journal of Antimicrobial Chemotherapy* *16*, 23-34.
- Miller, W.A., Brown, C.M., and Wang, S.P. (1997). New punctuation for the genetic code: Luteovirus gene expression. *Seminars in Virology* *8*, 3-13.
- Mize, G.J., Ruan, H.J., Low, J.J., and Morris, D.R. (1998). The inhibitory upstream open reading frame from mammalian S-adenosylmethionine decarboxylase mRNA has a strict sequence specificity in critical positions. *Journal of Biological Chemistry* *273*, 32500-32505.
- Moazed, D., and Noller, H.F. (1989). Intermediate states in the movement of transfer-RNA in the ribosome. *Nature* *342*, 142-148.
- Munro, J.B., Altman, R.B., O'Connor, N., and Blanchard, S.C. (2007). Identification of two distinct hybrid state intermediates on the ribosome. *Molecular Cell* *25*, 505-517.
- Muto, H., Nakatogawa, H., and Ito, K. (2006). Genetically encoded but nonpolypeptide Prolyl-tRNA functions in the A site for SecM-mediated ribosomal stall. *Molecular Cell* *22*, 545-552.
- Nakamori, K., Chiba, S., and Ito, K. (2014). Identification of a SecM segment required for export-coupled release from elongation arrest. *FEBS letters* *588*, 3098-3103.
- Nakatogawa, H., and Ito, K. (2001). Secretion monitor, SecM, undergoes self-translation arrest in the cytosol. *Molecular Cell* *7*, 185-192.
- Nakatogawa, H., and Ito, K. (2002). The ribosomal exit tunnel functions as a discriminating gate. *Cell* *108*, 629-636.
- Nakatogawa, H., Murakanti, A., Mori, H., and Ito, K. (2005). SecM facilitates translocase function of SecA by localizing its biosynthesis. *Genes & Development* *19*, 436-444.
- Namy, O., Rousset, J.P., Naphine, S., and Brierley, I. (2004). Reprogrammed genetic decoding in cellular gene expression. *Molecular Cell* *13*, 157-168.
- Netzer, W.J., and Hartl, F.U. (1997). Recombination of protein domains facilitated by co-translational folding in eukaryotes. *Nature* *388*, 343-349.
- Nissen, P., Hansen, J., Ban, N., Moore, P.B., and Steitz, T.A. (2000). The structural basis of ribosome activity in peptide bond synthesis. *Science* *289*, 920-930.

Nissen, P., Kjeldgaard, M., Thirup, S., Polekhina, G., Reshetnikova, L., Clark, B.F.C., and Nyborg, J. (1995). Crystal structure of the ternary complex of Phe-tRNA(Phe), EF-TU and a GTP analog. *Science* 270, 1464-1472.

Noller, H.F., Hoffarth, V., and Zimniak, L. (1992). Unusual resistance of peptidyl transferase to protein extraction procedures. *Science* 256, 1416-1419.

O'Brien, E.P., Hsu, S.-T.D., Christodoulou, J., Vendruscolo, M., and Dobson, C.M. (2010). Transient Tertiary Structure Formation within the Ribosome Exit Port. *Journal of the American Chemical Society* 132, 16928-16937.

Ogle, J.M., Brodersen, D.E., Clemons, W.M., Tarry, M.J., Carter, A.P., and Ramakrishnan, V. (2001). Recognition of cognate transfer RNA by the 30S ribosomal subunit. *Science* 292, 897-902.

Onouchi, H., Nagami, Y., Haraguchi, Y., Nakamoto, M., Nishimura, Y., Sakurai, R., Nagao, N., Kawasaki, D., Kadokura, Y., and Naito, S. (2005). Nascent peptide-mediated translation elongation arrest coupled with mRNA degradation in the CGS1 gene of Arabidopsis. *Genes & Development* 19, 1799-1810.

Onoue, N., Yamashita, Y., Nagao, N., Goto, D.B., Onouchi, H., and Naito, S. (2011). S-Adenosyl-L-methionine Induces Compaction of Nascent Peptide Chain inside the Ribosomal Exit Tunnel upon Translation Arrest in the Arabidopsis CGS1 Gene. *Journal of Biological Chemistry* 286, 14903-14912.

Pan, D., Kirillov, S.V., and Cooperman, B.S. (2007). Kinetically competent intermediates in the translocation step of protein synthesis. *Molecular Cell* 25, 519-529.

Panse, V.G., and Johnson, A.W. (2010). Maturation of eukaryotic ribosomes: acquisition of functionality. *Trends in Biochemical Sciences* 35, 260-266.

Pape, T., Wintermeyer, W., and Rodnina, M.V. (1998). Complete kinetic mechanism of elongation factor Tu-dependent binding of aminoacyl-tRNA to the A site of the E-coli ribosome. *Embo Journal* 17, 7490-7497.

Pavitt, G.D., and Ron, D. (2012). New Insights into Translational Regulation in the Endoplasmic Reticulum Unfolded Protein Response. *Cold Spring Harbor Perspectives in Biology* 4.

Pavlov, M.Y., Watts, R.E., Tan, Z., Cornish, V.W., Ehrenberg, M., and Forster, A.C. (2009). Slow peptide bond formation by proline and other N-alkylamino acids in translation. *Proceedings of the National Academy of Sciences of the United States of America* 106, 50-54.

Peske, F., Rodnina, M.V., and Wintermeyer, W. (2005). Sequence of steps in ribosome recycling as defined by kinetic analysis. *Molecular Cell* 18, 403-412.

Pestova, T.V., and Kolupaeva, V.G. (2002). The roles of individual eukaryotic translation initiation factors in ribosomal scanning and initiation codon selection. *Genes & Development* 16, 2906-2922.

Pestova, T.V., Lomakin, I.B., Lee, J.H., Choi, S.K., Dever, T.E., and Hellen, C.U.T. (2000). The joining of ribosomal subunits in eukaryotes requires eIF5B. *Nature* 403, 332-335.

Pisarev, A.V., Hellen, C.U.T., and Pestova, T.V. (2007). Recycling of eukaryotic posttermination ribosomal complexes. *Cell* 131, 286-299.

Pisarev, A.V., Skabkin, M.A., Pisareva, V.P., Skabkina, O.V., Rakotondrafara, A.M., Hentze, M.W., Hellen, C.U.T., and Pestova, T.V. (2010). The Role of ABCE1 in Eukaryotic Posttermination Ribosomal Recycling. *Molecular Cell* 37, 196-210.

- Plant, E.P., Jacobs, K.L.M., Harger, J.W., Meskauskas, A., Jacobs, J.L., Baxter, J.L., Petrov, A.N., and Dinman, J.D. (2003). The 9-angstrom solution: How mRNA pseudoknots promote efficient programmed -1 ribosomal frameshifting. *Rna-a Publication of the Rna Society* 9, 168-174.
- Polacek, N., Gomez, M.J., Ito, K., Xiong, L.Q., Nakamura, Y., and Mankin, A. (2003). The critical role of the universally conserved A2602 of 23S ribosomal RNA in the release of the nascent peptide during translation termination. *Molecular Cell* 11, 103-112.
- Ramakrishnan, V. (2002). Ribosome structure and the mechanism of translation. *Cell* 108, 557-572.
- Ramu, H., Mankin, A., and Vazquez-Laslop, N. (2009). Programmed drug-dependent ribosome stalling. *Molecular Microbiology* 71, 811-824.
- Ramu, H., Vazquez-Laslop, N., Klepacki, D., Dai, Q., Piccirilli, J., Micura, R., and Mankin, A.S. (2011). Nascent Peptide in the Ribosome Exit Tunnel Affects Functional Properties of the A-Site of the Peptidyl Transferase Center. *Molecular Cell* 41, 321-330.
- Raney, A., Law, G.L., Mize, G.J., and Morris, D.R. (2002). Regulated translation termination at the upstream open reading frame in S-adenosylmethionine decarboxylase mRNA. *Journal of Biological Chemistry* 277, 5988-5994.
- Robinson, J.M., Kosolapov, A., and Deutsch, C. (2006). Tertiary and quaternary structure formation of voltage-gated potassium channels. In *Methods in Molecular Biology*, J.D. Stockand, and M.S. Shapiro, eds., pp. 41-52.
- Robinson, P.J., Findlay, J.E., and Woolhead, C.A. (2012). Compaction of a Prokaryotic Signal-Anchor Transmembrane Domain Begins within the Ribosome Tunnel and Is Stabilized by SRP during Targeting. *Journal of Molecular Biology* 423, 600-612.
- Rodnina, M.V., Fricke, R., Kuhn, L., and Wintermeyer, W. (1995). Codon-dependent conformational change of elongation-factor TU preceding GTP hydrolysis on the ribosome. *Embo Journal* 14, 2613-2619.
- Rodnina, M.V., Pape, T., Fricke, R., Kuhn, L., and Wintermeyer, W. (1996). Initial binding of the elongation factor Tu center dot GTP center dot aminoacyl-tRNA complex preceding codon recognition on the ribosome. *Journal of Biological Chemistry* 271, 646-652.
- Samatova, E., Konevega, A.L., Wills, N.M., Atkins, J.F., and Rodnina, M.V. (2014). High-efficiency translational bypassing of non-coding nucleotides specified by mRNA structure and nascent peptide. *Nature Communications* 5.
- Schaffitzel, C., and Ban, N. (2007). Generation of ribosome nascent chain complexes for structural and functional studies (vol 158, pg 463, 2007). *Journal of Structural Biology* 159, 302-310.
- Schimmel, P.R., and Flory, P.J. (1968). Conformational energies and configurational statistics of copolypeptides containing L-proline. *Journal of Molecular Biology* 34, 105-120.
- Schmeing, T.M., Huang, K.S., Strobel, S.A., and Steitz, T.A. (2005). An induced-fit mechanism to promote peptide bond formation and exclude hydrolysis of peptidyl-tRNA. *Nature* 438, 520-524.
- Schuwirth, B.S., Borovinskaya, M.A., Hau, C.W., Zhang, W., Vila-Sanjurjo, A., Holton, J.M., and Cate, J.H.D. (2005). Structures of the bacterial ribosome at 3.5 angstrom resolution. *Science* 310, 827-834.

- Scolnick, E., Tompkins, R., Caskey, T., and Nirenber.M (1968). Release factors differing in specificity for terminator codons. *Proceedings of the National Academy of Sciences of the United States of America* *61*, 768-774.
- Seidelt, B., Innis, C.A., Wilson, D.N., Gartmann, M., Armache, J.-P., Villa, E., Trabuco, L.G., Becker, T., Mielke, T., Schulten, K., *et al.* (2009). Structural Insight into Nascent Polypeptide Chain-Mediated Translational Stalling. *Science* *326*, 1412-1415.
- Selmer, M., Dunham, C.M., Murphy, F.V., Weixlbaumer, A., Petry, S., Kelley, A.C., Weir, J.R., and Ramakrishnan, V. (2006). Structure of the 70S ribosome complexed with mRNA and tRNA. *Science* *313*, 1935-1942.
- Seong, B.L., and Rajbhandary, U.L. (1987a). Escherichia coli formylmethionine transfer RNA - mutations in GGG-CCC sequence conserved in anticodon stem of initiator transfer-RNAs affect initiation of protein synthesis and conformation of anticodon loop. *Proceedings of the National Academy of Sciences of the United States of America* *84*, 334-338.
- Seong, B.L., and Rajbhandary, U.L. (1987b). Mutants of Escherichia coli formylmethionine transfer RNA - a single base change enables initiator transfer-RNA to act as an elongator in vitro. *Proceedings of the National Academy of Sciences of the United States of America* *84*, 8859-8863.
- Shajani, Z., Sykes, M.T., and Williamson, J.R. (2011). Assembly of Bacterial Ribosomes. *Annual Review of Biochemistry*, Vol 80 *80*, 501-526.
- Sharma, M.R., Wilson, D.N., Datta, P.P., Barat, C., Schluenzen, F., Fucini, P., and Agrawal, R.K. (2007). Cryo-EM study of the spinach chloroplast ribosome reveals the structural and functional roles of plastid-specific ribosomal proteins. *Proceedings of the National Academy of Sciences of the United States of America* *104*, 19315-19320.
- Sharma, P., Yan, F., Doronina, V.A., Escuin-Ordinas, H., Ryan, M.D., and Brown, J.D. (2012). 2A peptides provide distinct solutions to driving stop-carry on translational recoding. *Nucleic Acids Research* *40*, 3143-3151.
- Shatkin, A.J. (1976). Capping of eukaryotic messenger RNAs. *Cell* *9*, 645-653.
- Sheets, M.D., and Wickens, M. (1989). 2 phases in the addition of a poly(A) tail. *Genes & Development* *3*, 1401-1412.
- Shen, W.C., and Ebbole, D.J. (1997). Cross-pathway and pathway-specific control of amino acid biosynthesis in *Magnaporthe grisea*. *Fungal Genetics and Biology* *21*, 40-49.
- Shine, J., and Dalgarno, L. (1974). The 3-prime terminal sequence of Escherichia coli 16S ribosomal RNA complementarity to nonsense triplets and ribosome binding sites. *Proceedings of the National Academy of Sciences of the United States of America* *71*, 1342-1346.
- Shoemaker, C.J., and Green, R. (2012). Translation drives mRNA quality control. *Nature Structural & Molecular Biology* *19*, 594-601.
- Sievers, A., Beringer, M., Rodnina, M.V., and Wolfenden, R. (2004). The ribosome as an entropy trap. *Proceedings of the National Academy of Sciences of the United States of America* *101*, 7897-7901.
- Simonetti, A., Marzi, S., Myasnikov, A.G., Fabbretti, A., Yusupov, M., Gualerzi, C.O., and Klaholz, B.P. (2008). Structure of the 30S translation initiation complex. *Nature* *455*, 416-420.

- Simonovic, M., and Steitz, T.A. (2009). A structural view on the mechanism of the ribosome-catalyzed peptide bond formation. *Biochimica Et Biophysica Acta- Gene Regulatory Mechanisms* 1789, 612-623.
- Skinner, R., Cundliffe, E., and Schmidt, F.J. (1983). Site of action of a ribosomal RNA methylase responsible for resistance to erythromycin and other antibiotics. *Journal of Biological Chemistry* 258, 2702-2706.
- Smith, A.E., and Marcker, K.A. (1968). N-formylmethionyl transfer RNA in mitochondria from yeast and rat liver. *Journal of Molecular Biology* 38, 241-243.
- Snell, E.E. (1975). Tryptophanase - Structure, catalytic activities and mechanism of action. *Advances in Enzymology and Related Areas of Molecular Biology* 42, 287-333.
- Sonenberg, N., and Hinnebusch, A.G. (2009). Regulation of Translation Initiation in Eukaryotes: Mechanisms and Biological Targets. *Cell* 136, 731-745.
- Sothiselvam, S., Liu, B., Han, W., Ramu, H., Klepacki, D., Atkinson, G.C., Brauer, A., Remm, M., Tenson, T., Schulten, K., *et al.* (2014). Macrolide antibiotics allosterically predispose the ribosome for translation arrest. *Proceedings of the National Academy of Sciences of the United States of America* 111, 9804-9809.
- Spahn, C.M.T., Beckmann, R., Eswar, N., Penczek, P.A., Sali, A., Blobel, G., and Frank, J. (2001). Structure of the 80S ribosome from *Saccharomyces cerevisiae* - tRNA-ribosome and subunit-subunit interactions. *Cell* 107, 373-386.
- Spevak, C.C., Ivanov, I.P., and Sachs, M.S. (2010). Sequence Requirements for Ribosome Stalling by the Arginine Attenuator Peptide. *Journal of Biological Chemistry* 285, 40933-40942.
- Stewart, V., Landick, R., and Yanofsky, C. (1986). Rho-dependent transcription termination in the tryptophanase operon leader region of *Escherichia coli* K-12. *Journal of Bacteriology* 166, 217-223.
- Subramanian, A.R., and Davis, B.D. (1970). Activity of initiation factor-IF3 in dissociating *Escherichia coli* ribosomes. *Nature* 228, 1273-1275.
- Tanner, D.R., Cariello, D.A., Woolstenhulme, C.J., Broadbent, M.A., and Buskirk, A.R. (2009). Genetic Identification of Nascent Peptides That Induce Ribosome Stalling. *Journal of Biological Chemistry* 284, 34809-34818.
- Tenson, T., Lovmar, M., and Ehrenberg, M. (2003). The mechanism of action of macrolides, lincosamides and streptogramin B reveals the nascent peptide exit path in the ribosome. *Journal of Molecular Biology* 330, 1005-1014.
- Thanaraj, T.A., and Argos, P. (1996). Ribosome-mediated translational pause and protein domain organization. *Protein Science* 5, 1594-1612.
- Tiller, N., and Bock, R. (2014). The translational apparatus of plastids and its role in plant development. *Molecular Plant* 7, 1105-1120.
- Trabuco, L.G., Villa, E., Mitra, K., Frank, J., and Schulten, K. (2008). Flexible fitting of atomic structures into electron microscopy maps using molecular dynamics. *Structure* 16, 673-683.
- Tu, L., Khanna, P., and Deutsch, C. (2014). Transmembrane Segments Form Tertiary Hairpins in the Folding Vestibule of the Ribosome. *Journal of Molecular Biology* 426, 185-198.
- Tu, L.W., and Deutsch, C. (2010). A Folding Zone in the Ribosomal Exit Tunnel for Kv1.3 Helix Formation. *Journal of Molecular Biology* 396, 1346-1360.

van der Sluis, E.O., and Driessen, A.J.M. (2006). Stepwise evolution of the Sec machinery in Proteobacteria. *Trends in Microbiology* *14*, 105-108.

Vazquez-Laslop, N., Klepacki, D., Mulhearn, D.C., Ramu, H., Krasnykh, O., Franzblau, S., and Mankin, A.S. (2011). Role of antibiotic ligand in nascent peptide-dependent ribosome stalling. *Proceedings of the National Academy of Sciences of the United States of America* *108*, 10496-10501.

Vazquez-Laslop, N., Ramu, H., Klepacki, D., Kannan, K., and Mankin, A.S. (2010). The key function of a conserved and modified rRNA residue in the ribosomal response to the nascent peptide. *Embo Journal* *29*, 3108-3117.

Vazquez-Laslop, N., Thum, C., and Mankin, A.S. (2008). Molecular mechanism of drug-dependent ribosome stalling. *Molecular Cell* *30*, 190-202.

Voss, N.R., Gerstein, M., Steitz, T.A., and Moore, P.B. (2006). The geometry of the ribosomal polypeptide exit tunnel. *Journal of Molecular Biology* *360*, 893-906.

Wang, Z., Fang, P., and Sachs, M.S. (1998). The evolutionarily conserved eukaryotic arginine attenuator peptide regulates the movement of ribosomes that have translated it. *Molecular and Cellular Biology* *18*, 7528-7536.

Wang, Z., and Sachs, M.S. (1997). Ribosome stalling is responsible for arginine-specific translational attenuation in *Neurospora crassa*. *Molecular and Cellular Biology* *17*, 4904-4913.

Wei, J., Wu, C., and Sachs, M.S. (2012). The Arginine Attenuator Peptide Interferes with the Ribosome Peptidyl Transferase Center. *Molecular and Cellular Biology* *32*, 2396-2406.

Weinger, J.S., Parnell, K.M., Dorner, S., Green, R., and Strobel, S.A. (2004). Substrate-assisted catalysis of peptide bond formation by the ribosome. *Nature Structural & Molecular Biology* *11*, 1101-1106.

Weixlbaumer, A., Jin, H., Neubauer, C., Voorhees, R.M., Petry, S., Kelley, A.C., and Ramakrishnan, V. (2008). Insights into Translational Termination from the Structure of RF2 Bound to the Ribosome. *Science* *322*, 953-956.

Wells, S.E., Hillner, P.E., Vale, R.D., and Sachs, A.B. (1998). Circularization of mRNA by eukaryotic translation initiation factors. *Molecular Cell* *2*, 135-140.

Werner, M., Feller, A., Messenguy, F., and Pierard, A. (1987). The leader peptide of yeast gene-CPA1 is essential for the translational repression of its expression. *Cell* *49*, 805-813.

Werner, M., Feller, A., and Pierard, A. (1985). Nucleotide sequence of yeast gene CPA1 encoding the small subunit of arginine pathway carboamoyl phosphate synthetase - Homology of the deduced amino acid sequence to other glutamine amidotransferases. *European Journal of Biochemistry* *146*, 371-381.

Wills, N.M., O'Connor, M., Nelson, C.C., Rettberg, C.C., Huang, W.M., Gesteland, R.F., and Atkins, J.F. (2008). Translational bypassing without peptidyl-tRNA anticodon scanning of coding gap mRNA. *Embo Journal* *27*, 2533-2544.

Wilson, D.N., and Cate, J.H.D. (2012). The Structure and Function of the Eukaryotic Ribosome. *Cold Spring Harbor Perspectives in Biology* *4*.

Wilson, K.S., and Noller, H.F. (1998). Molecular movement inside the translational engine. *Cell* *92*, 337-349.

Wolin, S.L., and Walter, P. (1988). Ribosome pausing and stacking during translation of a eukaryotic messenger RNA. *Embo Journal* *7*, 3559-3569.

- Woolhead, C.A., Johnson, A.E., and Bernstein, H.D. (2006). Translation arrest requires two-way communication between a nascent polypeptide and the ribosome. *Mol Cell* 22, 587-598.
- Woolhead, C.A., McCormick, P.J., and Johnson, A.E. (2004). Nascent membrane and secretory proteins differ in FRET-detected folding far inside the ribosome and in their exposure to ribosomal proteins. *Cell* 116, 725-736.
- Wu, C., Wei, J., Lin, P.-J., Tu, L., Deutsch, C., Johnson, A.E., and Sachs, M.S. (2012). Arginine Changes the Conformation of the Arginine Attenuator Peptide Relative to the Ribosome Tunnel. *Journal of Molecular Biology* 416, 518-533.
- Yanagitani, K., Imagawa, Y., Iwawaki, T., Hosoda, A., Saito, M., Kimata, Y., and Kohno, K. (2009). Cotranslational Targeting of XBP1 Protein to the Membrane Promotes Cytoplasmic Splicing of Its Own mRNA. *Molecular Cell* 34, 191-200.
- Yanagitani, K., Kimata, Y., Kadokura, H., and Kohno, K. (2011). Translational Pausing Ensures Membrane Targeting and Cytoplasmic Splicing of XBP1u mRNA. *Science* 331, 586-589.
- Yang, R., Cruz-Vera, L.R., and Yanofsky, C. (2009). 23S rRNA Nucleotides in the Peptidyl Transferase Center Are Essential for Tryptophanase Operon Induction. *Journal of Bacteriology* 191, 3445-3450.
- Yap, M.-N., and Bernstein, H.D. (2009). The Plasticity of a Translation Arrest Motif Yields Insights into Nascent Polypeptide Recognition inside the Ribosome Tunnel. *Molecular Cell* 34, 201-211.
- Yap, M.-N., and Bernstein, H.D. (2011). The translational regulatory function of SecM requires the precise timing of membrane targeting. *Molecular Microbiology* 81, 540-553.
- Yarmolinsky, M.B., and de la Haba, G.L. (1961). Inhibition by puromycin of amino acid incorporation into protein. Gray, Tabenkin and Bradley, Editors *Antimicrobial Agents Annual 1960*, 320-327.
- Yoshida, H., Matsui, T., Yamamoto, A., Okada, T., and Mori, K. (2001). XBP1 mRNA is induced by ATF6 and spliced by IRE1 in response to ER stress to produce a highly active transcription factor. *Cell* 107, 881-891.
- Youngman, E.M., Brunelle, J.L., Kochaniak, A.B., and Green, R. (2004). The active site of the ribosome is composed of two layers of conserved nucleotides with distinct roles in peptide bond formation and peptide release. *Cell* 117, 589-599.
- Yusupova, G., and Yusupov, M. (2014). High-Resolution Structure of the Eukaryotic 80S Ribosome. *Annual review of biochemistry* 83, 467-486.
- Yusupova, G.Z., Yusupov, M.M., Cate, J.H.D., and Noller, H.F. (2001). The path of messenger RNA through the ribosome. *Cell* 106, 233-241.
- Zavialov, A.V., Buckingham, R.H., and Ehrenberg, M. (2001). A posttermination ribosomal complex is the guanine nucleotide exchange factor for peptide release factor RF3. *Cell* 107, 115-124.
- Zavialov, A.V., Hauryliuk, V.V., and Ehrenberg, M. (2005). Splitting of the posttermination ribosome into subunits by the concerted action of RRF and EF-G. *Molecular Cell* 18, 675-686.
- Zhang, G., Hubalewska, M., and Ignatova, Z. (2009). Transient ribosomal attenuation coordinates protein synthesis and co-translational folding. *Nature Structural & Molecular Biology* 16, 274-280.

Zhouravleva, G., Frolova, L., Legoff, X., Leguellec, R., Ingevechtomov, S., Kisselev, L., and Philippe, M. (1995). Termination of translation in eukaryotes is governed by 2 interacting polypeptide chain release factors ERF1 and ERF3. *Embo Journal* 14, 4065-4072.

Ziv, G., Haran, G., and Thirumalai, D. (2005). Ribosome exit tunnel can entropically stabilize alpha-helices. *Proceedings of the National Academy of Sciences of the United States of America* 102, 18956-18961.

Zucker, F.H., and Hershey, J.W.B. (1986). Binding of *Escherichia coli* protein synthesis initiation factor-IF1 to 30S ribosomal subunits measured by fluorescence polarization. *Biochemistry* 25, 3682-3690.